Title	
Author(s)	Ahmed, Sana
Citation	
Issue Date	2017-06
Type	Thesis or Dissertation
Text version	ETD
URL	http://hdl.handle.net/10119/14750
Rights	
Description	Supervisor:　　　　　, ,

Japan Advanced Institute of Science and Technology

Enhanced Cytoplasmic Internalization of Biomacromolecules by Freeze Concentration

SANA AHMED

Japan Advanced Institute of Science and Technology

Doctoral Dissertation

Enhanced Cytoplasmic Internalization of Biomacromolecules by Freeze Concentration

Sana Ahmed

Supervisor: Assoc. Prof. Kazuaki Matsumura

School of Materials Science

Japan Advanced Institute of Science and Technology

June 2017

Referee-in-chief: Associate Professor Dr. Kazuaki Matsumura

Japan Advanced Institute of Science and Technology

Referees: **Professor Dr. Takahiro Hohsaka**

Japan Advanced Institute of Science and Technology

Professor Dr. Shinya Maenosono

Japan Advanced Institute of Science and Technology

Associate Professor Dr. Tsutomu Hamada

Japan Advanced Institute of Science and Technology

Professor Dr. Yasuhiko Iwasaki

Kansai University

Preface

Recently, the growing interest in nanotechnology which involves the creation, manipulation is considered to be having enormous potential in medicines. The tremendous development in the field of nanoscience and nanotechnology has led to a new discipline called nanomedicines. Nanomedicine is the bio-medical application of nanotechnology. This technology has been broadly used for the process of diagnosing, treating, preserving and improving health, treating and preventing from diseases. Nanomedicines seek to uses macromolecules such as proteins or drug molecules that are packaged into nanoscale system for delivery inside the body to achieve its desired therapeutic effect. However, the efficient delivery of macromolecules into cells is a major challenge in drug delivery applications. Various physical methods have been developed such as electroporation, ultrasonication but many of them showed toxicity and cell damage. Hence, the development of new, safe and versatile method is needed to prevent the intracellular barrier that impedes the penetration of macromolecules with no toxicity.

Therefore, the main purpose of this study was to developed new freeze concentration strategy for macromolecule delivery to overcome the hurdles and to apply them for different therapeutic applications.

The first chapter deals with the general background in regards to the work for the thesis are presented and the latter part of this chapter explains the detailed research objective of the thesis.

The second chapter is dedicated to the development of novel freeze concentration in the delivery of model proteins. Preliminary investigation of freeze concentration method for effective cytoplasmic delivery has been carried out and discussed in this chapter.

The third chapter deals with the development of new polyampholyte-modified liposomes as a non-toxic carrier. The mechanistic studies were also investigated to find out the deep understanding of internalization and cytosolic delivery of proteins after using freeze concentration.

The fourth chapter discusses the utilization of freeze concentration strategy in immunotherapy based applications. The expression of cell surface proteins and cytokines were also investigated using freeze concentration strategy.

Further, fifth chapter presents the effective use of freeze concentration method for gene therapy. Non-toxic polyampholyte nanoparticles were developed to carry genetic materials inside the cells. Furthermore, mechanistic studies were also carried out to explore the enhanced gene transfection using freezing approach.

The final chapter presents the summary and also discusses the possible future impact of this thesis.

In conclusion, this thesis demonstrates the feasibility and versatility of freeze concentration approach for delivery of variety of macromolecules and its applications in immunotherapy and gene therapy.

To the best of my knowledge, the presented work is original and I stand solely responsible for any lapses that might have occurred in carrying out and in presentation of this work, despite all the precautions taken to the best of my ability.

Sana Ahmed

Table of Contents

Chapter 1
General Introduction

1.1 Medical Nanotechnology: Nanomedicine

Recently, new opportunities have been recognized in the area of nanotechnology which is not limited to only electronics, nanomotors, and intelligent nanoscale materials but also included medicines and biology.[1] The increase of attention in the medical nanotechnology was improving by the great advancement in medical resources and practice, therefore the concept of nanomedicine was taking into shape.[2] Nanomedicine is the medical application of nanotechnology, which applies nanotechnology to highly specific medical interventions for prevention, diagnosis and treatment of various severe diseases.[3] Numerous diseases such as cancer, infectious diseases have been identified and nanotechnology approaches promised to circumvent these problems for future application.[4] Also, nanomedicine makes use of nanomaterials and nanoelectronic biosensors.[5] The medical area of nanotechnology has been projected benefits and potentially valuable for mankind. Medical technologies can make use of smaller device and can possibly used to be implanted and transport inside the body.[3] Nanomedicines is uses for drug delivery which is based on nanoscale particles that can improve drug bioavailability.[6] The nanoengineered materials and strategies are being developed for effectively used for treatment of diseases such as cancer. Therefore, the use of nanomedicines and more specifically drug delivery is set to spread rapidly.

1.2 Delivery system of bio-macromolecules

Biomacromolecules are the macromolecules of biological origin from which all life on earth actually depends on are carbohydrates, proteins and genetic materials such as nucleic acids. These bioactive macromolecules possess many desirable characteristics as they provide unique feature to treat human diseases such as cancer, neurodegenerative diseases or infectious diseases. Macromolecular therapeutics are rapidly gaining interest in the area of nanomedicine to serve as alternatives to traditional drug regimens.[7] Various classes of bio-macromolecules such as peptides, proteins[8], DNA,[9] synthetic oligonucleotides[10] are developed and used to deliver inside our body to treat certain diseases. Among macromolecules, proteins and nucleic acids are the two popular macromolecules have been possessing biological activity that makes them highly effective, desirable and specific as a therapeutic agent.[11]

In my doctoral research, I used two type of bio macromolecules i.e. proteins and nucleic acids as model therapeutics for delivery system.

Protein therapeutics

In the early 1980s proteins have emerged as a major role in pharmaceuticals that are included as therapeutics and small number of vaccines.[12] Proteins are the large macromolecules consisting of long chain of amino acids. They are engine of life that regulates various functions inside the cells such as enzyme catalysis and signal transduction. Many proteins and peptides possess biological activity that makes them potent therapeutics.[13] Protein therapeutics has deliberately increased in number since the first introduction of recombinant protein therapeutics as human insulin-25 year ago.[14] Later, insulin is one of the popular among drugs which is used as therapeutics. However, the alteration in the functions of intracellular proteins gives rise to many diseases. To date, 100 different functional proteins have been transported into cells in various animal models.[15, 16] Several studies have been done to show the use of protein based therapeutics is effective for biomedical applications. The intracellular delivery of active form of proteins is essential for the treatment of cancer, inflammatory diseases, diabetes, vaccination and regenerative medicines.[17]

Nucleic acid therapeutics

Modern drug research aims to use biological active molecules which are responsible for treatment of severe diseases. So far, numerous genetic based human diseases have been known.[18] Gene therapy is an alternative of the therapeutic delivery of nucleic acid into cells to treat diseases Nucleic acids are the large bio-molecules which includes DNA (deoxyribonucleic acid) or RNA (ribonucleic acid) and has shown great potential for specific control of gene expression. In 1977, Paterson et al. demonstrated the use of nucleic acids in regulating gene expression.[19] Plasmids, oligonucleotides, aptamers are the few DNA based therapeutics are used for gene related diseases.[20] Plasmids are the high molecular weight, double stranded DNA construct transgenes which encodes specific proteins. Plasmids can be used as DNA vaccines for genetic immunization.[21] Oligonucelotides are the short single stranded DNA that used for antisense and antigen applications.[22] DNA aptamers are double stranded nucleic acids that interferes molecular function of diseases implicated proteins in the transcription and translational process.[23] In general, particular therapeutic genes would provide therapeutic replacement of missing, dysfunctional or poorly expressed proteins.

One of the most important strategies employed in nanomedicine for medical applications are nanocarriers. An important advance in nanomedicine was the development of nanocarriers which able to respond physical and chemical stimuli to enhance the efficacy of therapeutics

and delivered at the target site.[24] These nanocarriers collectively called as nanomedicines that can delivered therapeutic molecules to disease site to exert clinical benefit.

1.3 Carrier System

A variety of carriers have been studied for their applicability as a delivery system. The carrier system is included Liposome, micelles, Inorganic nanomaterials and cell penetrating peptides (**Figure 1.1**).
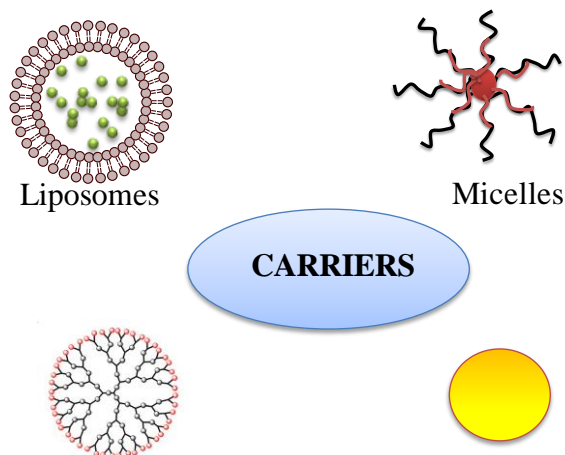
Figure 1.1 Schematic depiction of different carriers has been developed for drug delivery.

Liposome

Liposomes were first produced in England in 1961 by Alec D. Bangham. This carrier has been considered as promising drug carriers for over two decades.[25] Liposome are composed of artificial lipid bilayers separating an aqueous internal compartment from the bulk aqueous phase of varying diameters from 50 to 1000 nm, which can load various macromolecules. Additionally, liposomes are able to carry both hydrophobic and hydrophilic molecules.[26, 27] Several studies have been carried out the applicability of liposomes as a carrier for cancer therapy and immunotherapy applications.[28] The precise mechanisms of their action in the body are under study, in which to target them to specific diseased tissues.

Inorganic particles

Inorganic nanoparticles such as gold have generally possessed versatile properties for cellular delivery.[29] These nanoparticles are exhibited rich functionality, good biocompatibility for targeted delivery system.[30] Nanoparticles have comparatively large surface which is able to bind, adsorbed and carry various molecules such as drugs proteins.[30] Recently, the use of various inorganic materials as gene delivery carriers were effectively demonstrated.[31] There are large number of inorganic nanoparticles have been studied as carriers for cellular delivery of various drugs including genes and proteins.[32] Among nanoparticles, gold nanoparticles have shown number of biomedical applications such as drug, gene delivery or biological imaging.[33] However, at very small size, gold nanoparticles are exhibited to induce cytotoxicity.[34] In chemotherapy based applications, some drugs are relatively non-specific and induced side effect in healthy tissue. In order to overcome this problem, magnetic

nanocarriers are the alternatives to delivered drugs at target site. The magnetization of drug carrier can guided to the target site with the help of external magnetic field. The role of magnetic nanoparticles (Fe_3O_4) as a carrier has shown the effectiveness in chemotherapy applications.[35]

Cell penetrating peptides

Cell penetrating peptides (CPPs), also known as protein transduction domains (PTDs). These peptides contain short sequence of peptides that are able to enter inside the cells and deliver a wide variety of cargos such as oligonucleotides, therapeutic drugs and proteins into the cytoplasm.[36] CPPs are positively charged due to abundance of arginine and lysine residues.[37] CPPs are known to exhibit a functional versatility which shows ability to delivered various macromolecular cargo complex.[38] Arginine-rich cell penetrating peptides are most widely studied for carrying molecules to target site.[39]

Dendrimers

Dendrimers are three dimensional well organized nanoscopic macromolecules which displayed an effective role in nanomedicine.[40] The unique properties such as uniform size, water solubility, well defined molecular weight makes them attractive for drug delivery applications.[41] There are various application of dendrimers in various fields such as photodynamic therapy (PDT), boron neutron capture therapy and bio imaging applications.[40] Dendrimers are often used in gene, ocular, oral, transdermal and pulmonary delivery applications.[42]

Drawbacks of current carriers are

These carriers have been shown promising strategy in drug delivery system. Unfortunately, the potential uses of such carriers are still limited in delivery system.

1. In various reports, it has been shown that dendrimers[43] and CPPs[44] exhibited high cytotoxicity towards the cells. Cationic carriers, more specifically CPPs and dendrimers are well known to interact with negative biological membrane that results in their destabilization and causes cell lysis.[40] This is because the cationic surface groups tend to interact with lipid bilayer which increases the permeability and decreases the integrity of biological membrane.

2. Gold nanoparticles have been used as a carrier and also acting as a useful sensor particles. But smaller size of nanoparticles showed high toxicity which leads to highly undesirable.[45]

Similarly, superparamagnetic iron oxides are used as efficient agent in magnetic resonance and used as chemotherapeutics. However, at high doses, this particle promotes intense oxidative stress.[46]

The low efficiency of release of drugs, high toxicity, instability and low efficiency are still major issues in carrier system. With all these disadvantages associated with them must be overcome in order to find safe and efficient system for therapeutic applications as well as clinical trial progress. With the advancement of nanotechnology, polymeric nanoparticles have been attracted and studied because of their unique shape, size and physical properties.[47]

Polymeric nanoparticles

Recently, researchers are more interested to prepare such carriers for delivery systems which show several advantages over existed carriers to delivered therapeutic molecules safely and precisely. Polymeric nanoparticles are one of the carriers which already been applied in drug delivery system with a great success. The nano-size particles formation in polymers are usually formed by physically or chemically cross linked across polymer network.[48] Polymeric nanoparticles provide massive advantages regarding drug targeting, delivery and release emerges as one of the major tools in nanomedicine.[49] Previously, many studies were focused on preparation of nanosized polymeric nanoparticles. In one report, poly (ethyleneoxide)-block-poly (aspartic acid) (PEO-PAA)-Adriamycin drug conjugate was shown to self assemble in aqueous media and were used in biomedical applications.[50] The polymeric nanoparticles are relatively superior to other system as its controlled, sustained drug release at the target site. Moreover, the biocompatibility and biodegradability are quite good. Also, it exhibited relatively low toxicity compared to other carriers. In addition, polymeric nanoparticles have better stability for over a week. Polymeric micelles are one of the examples of polymeric nanoparticles. Micelles are formed by the self assembly of monolayer of amphiphilic block copolymers in aqueous solutions which ranging their size around 5-50 nm and are of great interest in drug delivery system.[51] The molecules are tending to arrange themselves in such a way which indicated that inner core are hydrophobic and outer layer are hydrophilic.[52] However, micelles can carry transport only insoluble hydrophobic molecules.[52] The micellar property of polymers enhances the drug-loading capacity, tumor-specific uptake as well as anticancer effect.[53] Moreover, polymeric micelles have been extensively used as versatile and effective delivery system for cancer therapy. These polymeric systems have been proved as a promising carrier in drug delivery system. However, their extreme smaller

size compared to larger carrier such as liposome restricts to carry specific therapeutic molecules. Moreover, in micelles, there is a high risk in premature releasing of drugs by reaching to the target site.[54]

Currently, a variety of polymeric nanoparticles have been designed in both preclinical and clinical studies. These all characteristics made polymeric nanoparticles considered to be attractive carrier for several medicinal purposes.

Development of polyampholyte nanoparticles as a carrier

Polyampholytes are the charged polymers which contains both positive and negative charged groups on the polymer chain[55]. The popular examples of polyampholytes are proteins such as gelatin, bovine serum albumin.[56] In polyampholytes, the charge of polymeric backbone can be easily tuned or changed by changing the ratio of composition of monomers or substitution of charged functional group. Therefore, in polyampholytes one charge can dominate and the net charge of the polymer may be either positive, negative or zero. Several polyampholytes such as polypeptides and polysaccharides have been synthesized and characterized for various types of biomaterial applications such as tissue engineering, [57] non-fouling agents[58] etc. Akiyoshi and co-workers have demonstrated the small size nanogel formation in aqueous medium by self aggregation using pullulan, PNIPAM, hydrophobic polysaccharides and hydrophobic pullulan by physical interactions.[59] These nanogels have shown the ability to formed complex with proteins, drugs and DNA. In another study, Shen and co workers have demonstrated the use of polyamino acids based polyampholyte nanoparticles. Polyampholyte nanoparticles were prepared by grafting cationic amino acid (L-Arg) to γ-PGA by inter/ intra-molecular electrostatic interactions when the polymer dispersed into water.[60] The properties of polyampholyte nanoparticles are similar to those of nanogels which are aggregated through intermolecular forces to some extent. Various self assembled nanocarriers are still being developed based on the interaction of amino acid residues.[61, 62] There are various advantages of polyampholyte nanoparticles as it shows good biocompatibility, excellent stability and show high drug absorbance.[63] These carriers are easy to modify and ability to delivered drugs at target site. These unique characteristics of polyampholyte nanoparticles showed great potential as a carrier in future.

1.4 Intracellular delivery

The major objectives for targeted drug delivery are enhancing therapeutic molecules accumulation at a target site. Intracellular delivery is the transfer of macromolecules including proteins, enzymes and antibodies need to deliver inside the cells to achieve a desired therapeutic effect inside cytoplasm or onto nucleus or other specific organelles such as lysosomes, mitochondria or endoplasmic reticulum (**Figure 1.2**).[64] The intracellular delivery process has been used in biomedical studies such as in gene therapy or protein therapy. Recently, enormous research has been attributed for intracellular delivery of macromolecules in the field of drug delivery for modulating therapeutic applications. Cells possess a variety of active internalization mechanism to accommodate cellular entry of large molecular complex. The cell membrane involves invagination to engulf molecules that will subsequently traffic through the cells via endocytosis.[65]
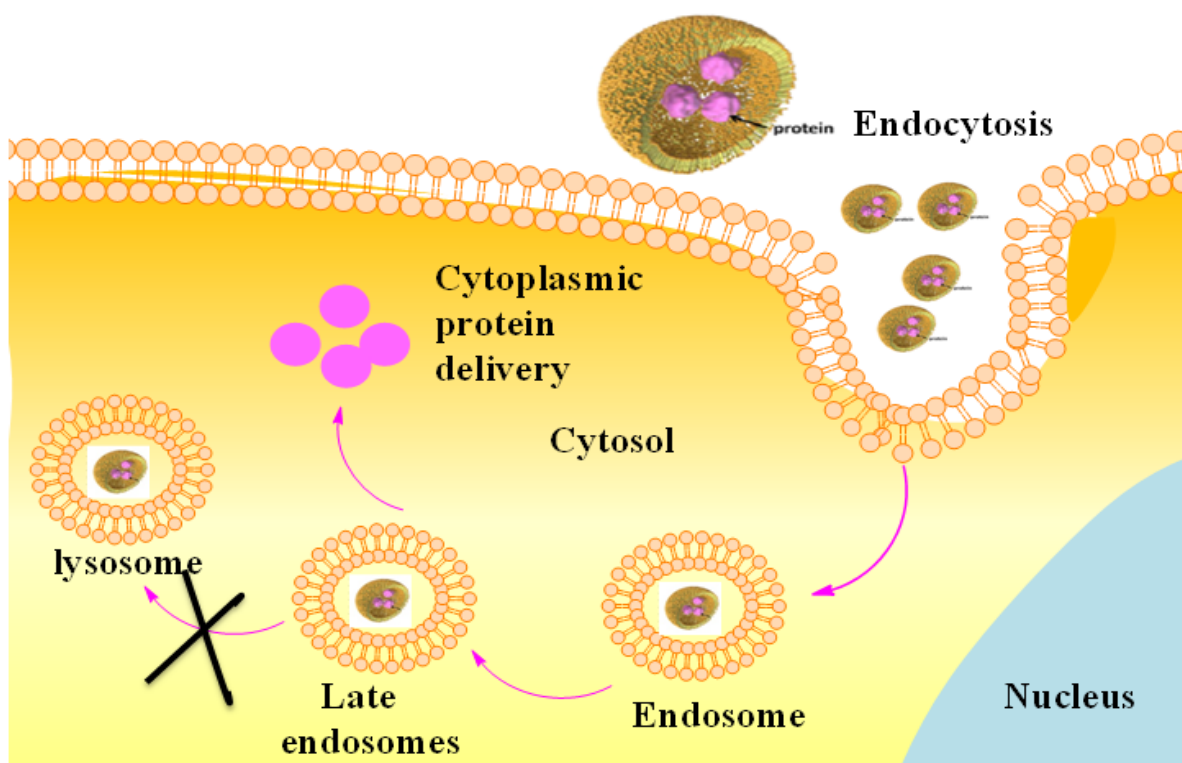
Figure 1.2 Schematic representation of ideal endocytic pathway of model protein loaded nanocarriers internalized inside the cells through endocytic pathway. Protein loaded nanocarrier are internalized and entered to endosomes, trafficked to late endosomes and released protein cargo to the cytosol of the cells without reaching to lysosomes (lytic and hydrolytic enzymes are present).[64]

Endocytic Uptake

Most of the molecules or particles are entered to the cells via endocytic pathway. Endocytosis pathways are the transportation of macromolecules into the cells by engulfing them through energy process.[66] Materials such as protein and carbohydrates interacted with the cell membrane where it can directly interact with the membrane embedded receptors or associated with the lipid bilayer. Depending on their size, shape and surface chemistry, nanoparticles loaded therapeutics are internalized by the target cells through endocytic pathways.[67]

Endocytosis process are divided into two parts

1. **Phagocytosis**

   Phagocytosis is the process in which large size microparticles are engulf as large as 20 µm. The vesicles are formed by the evagination of the membrane around the food particles. This process specifically found in macrophages, neutrophils, dendritic cells.[68] The phagocytic pathway consists of three steps after cellular entry. Firstly, recognition of particles in the bloodstream. Secondly, adhesion of particles onto the cell membrane. Last, the particles were ingested by the cells in phagocytosis. Previous studies have shown that several factors such as size, surface charge plays an important role of selecting phagocytic pathway.[69] In one study, polymethylmethacrylate (PMMA) exhibited higher uptake when their size increased around 200 nm to several microns.[70]

2. **Pinocytosis**

   Pinocytosis also known as cell drinking, fluid endocytosis is the process in which small particles are brought into the cells. The vesicles are formed by invagination of the plasma membrane.[71] Pinocytosis are further classified as clathrin dependent endocytosis, caveolae mediated endocytosis, macropinocytosis (**Figure 1.3**).

   (a) **Clathrin mediated or Receptor mediated endocytosis**

   Clathrin or receptor mediated endocytosis is the uptake of materials into the cells via clathrin coated pits. It shared the pathway for the internalization of different ligand receptor complexes. This mode of endocytosis is not only for ligands but also for viruses. The endocytosis occurs in a membrane specifically enriched in clathrin which is cytosolic coated protein. The coated pit forms due to

polymerization of a cytosolic protein called clathrin-1which required proteins like AP 180 and AP-2. The assembled vesicles are pinched off from the plasma membrane by GTPase dynamin.[72] Polymeric nanoparticles such as D,L poly-lactic-co-glycolic (PLGA) was relatively large in size around 300 nm, negatively charged and predominantly entered via clathrin mediated endocytosis.[73]

(b) Caveolae mediated endocytosis

This particular endocytosis are specifically occurred which exhibit size generally reported around 50-100 nm range. The particles are interacted by caveolin which is dimeric protein, enriched in cholesterol and sphingolipids. When particles approached and bind to the cell surface, the particles across the plasma membrane to caveolae invagination like flask-shaped membrane. Then the vesicles can be detached from the membrane by GTPase dynamin.[74] The example of caveolae mediated endocytosis is amphiphillic self assembled nanoparticles (100 nm) of poly (3-aminopropyl) siloxane (PAPS) modified with stearic acid residues and galactose were selectively target caveolae in human aortic endothelial cells.[75]

(c) Macropinocytosis

Macropinocytosis is a special pathway of clathrin and caveolae endocytosis. They can simply melt with the cell membrane or form an intracellular vacuole, termed as macropinosomes. The macropinosomes are larger (0.5-10 μm) and distinct from other vesicles formed during pinocytosis.[76] It can internalize the larger particles and greater sizes in cells, which lack phagocytosis. Many particles such as bacteria, viruses can internalize via macropinosomes.[72]
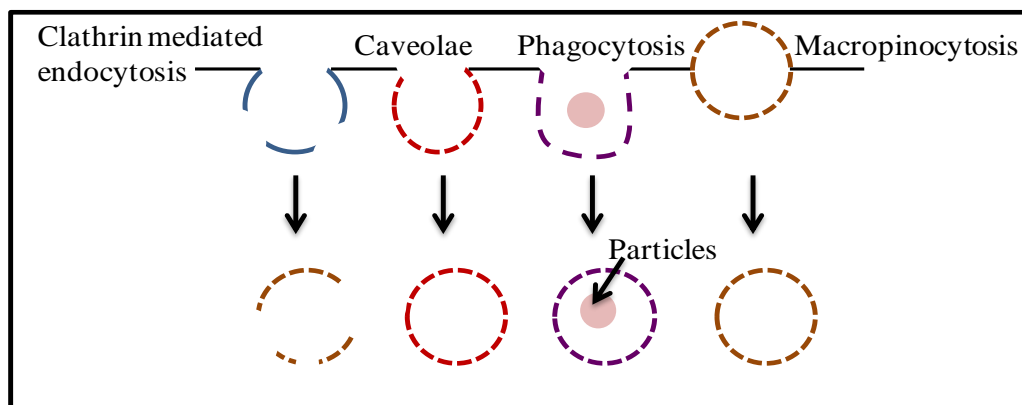
Figure 1.3 Different intracellular uptake pathways after internalization of particles [77]

Endosome organelle: Intracellular Barrier

After endocytic internalization, the macromolecules are tended to entrap in endosomes organelles. The pathway is composed of vesicles known as endosomes with internal pH around 5. Endosomes are defined as acidic, prelysosomal intracellular compartment which contains endocytosed materials and delivered internalized materials from the Golgi to the lysosomes or vacuole.[78] The maturation of endosomes takes place from early endosomes to late endosomes. However, the serious problem is that every molecule which is entered into endosomes that eventually end into lysosomes, where active degradation process takes place because of lytic and hydrolytic enzymes is present through it.[79] After endocytosis, therapeutic macromolecules are needed to be released from endosomes. Therefore several approaches have been examined to facilitate the early release of therapeutic materials from the endosomal pathway into cytosol of the cells.[80]

Recent strategies and hypothesis for mechanism of endosomal escape

The entrapment of nanocarriers in endosome vesicles and lysosome degradation are major barrier for effective cytoplasmic delivery. Intracellular hydrolases degrade all type of biological polymers, proteins, polysaccharides, lipid, DNA. Therefore, for effective delivery of therapeutic materials, it is important that materials should be released from endosomes.[81] Endosomal release can be mediated by pore formation in the endosomal membrane, pH buffering effect, fusogenic mechanism or photochemical disruption of the endosome membrane.

1. Pore formation in the endosomal membrane

Pore formation in endosomes by certain materials also found for intracellular delivery (**Figure1.4**). Certain peptides have the ability to induce pore formation which facilitates the escaping of materials from the endosomes. Generally, pore formation is based on the interplay between a membrane tension that enlarges the pore and line tension that close the pores.[82] Cationic peptides and cationic amphiphilic materials has the ability to bind lipid bilayer which leads to tensed or provide internal membrane tension that can responsible to create strong pores in lipid bilayers.[83] These pore formation leads to destabilize the endosome membrane by creating the internal membrane tension through peptides. In one example, presence of the cholesterol-GALA peptide on the liposomal membrane effective enhances the endosomal release of the liposomal contents. The

presence of peptides undergoes conformational changes at low pH in endosomes to interact with and perturb endosomal membrane.[84]
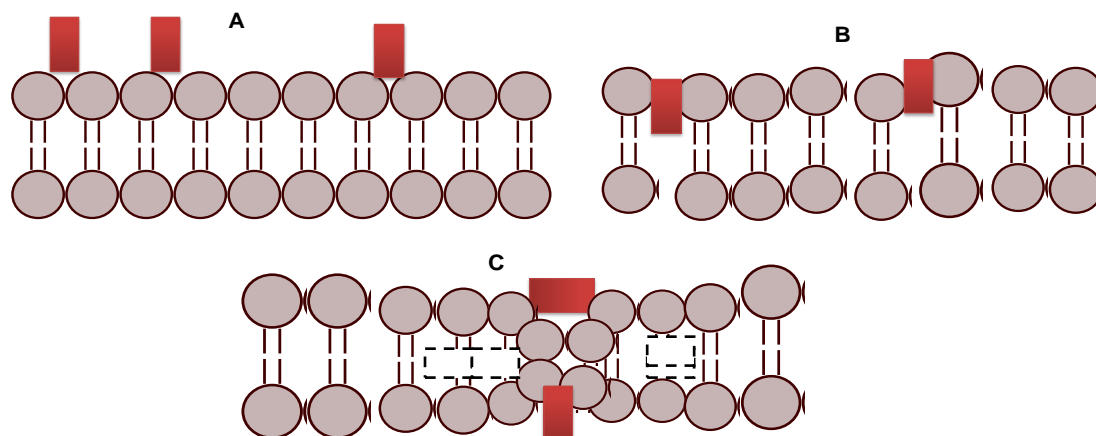
Figure 1.4 The proposed interactions between cell penetrating peptides and lipid bilayer. (a) High affinity of CPPs for binding to the lipid bilayer. (b) Insertion of peptides inside the membrane which created internal membrane tension. (c) The internal membrane tension factor is responsible to bind through edges of the pores which subsequently destabilized the endosomal membrane.[82]

2. Photochemical interference on the endosomal membrane

Photochemical effect is also responsible for disruption of endosomes vesicles. The materials which contain photosensitizer are able to produce reactive oxygen species upon excitation with light and release the contents to the cytosol of the cells.[85] The most commonly photo-sensitizers including sulfonated tetraphenylporphyrins (TPPS$_{2a}$, TPPS$_4$), dendrimer based sensitizers are used to localized in the endosomal membrane. The reactive singlet oxygen was formed after the exposure of light that has short life time eventually destroys endosmal/lysosomal membrane, where the contents are delivered to cytosol of the cells efficiently (**Figure 1.5**). In various systems photostimulation has been applied for endosomal release of therapeutic material.[87]
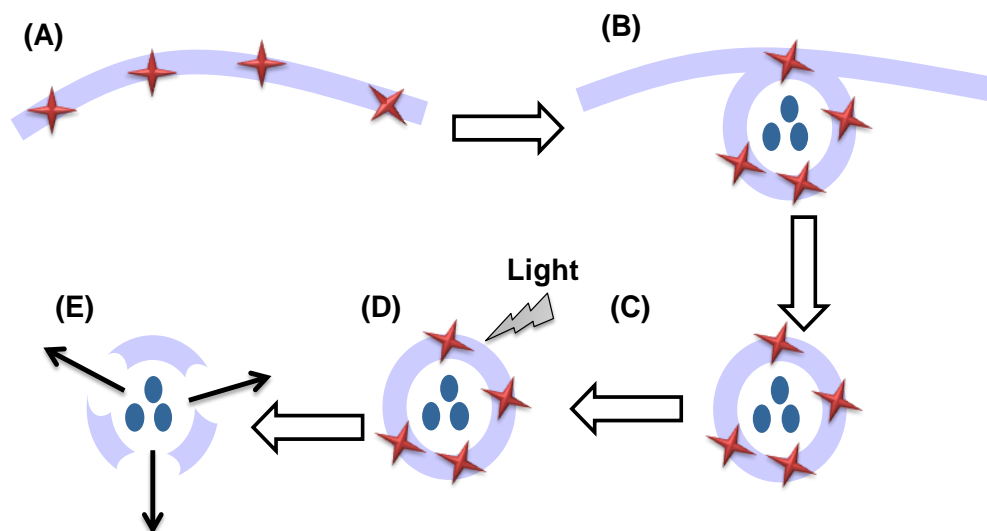
Figure 1.5 Photochemical induced endosomal escape of materials. (A) Sensitizer localize to cell membrane (B) sensitizer can internalized through endocytosis (C) photosensitizer are entered to endosomal membrane and remain inactive. (D) Sensitizers are activated and formation of reactive oxygen species by illumination (E) destabilization of endosomal/ lysosomal membrane is transported to cytosol of the cells.[87]

3. Proton-Sponge effect

Another mechanism for endosomal escape is the proton sponge effect or pH buffering effect. It is an osmotic effect that attributed to extensive buffering capacity which shows various characteristics such as inhibition of lysosomal nuclease and change in osmolarity of endosomes vesicles leads to rupture and damage.[88] The generalized mechanism for proton sponge has been hypothesized as after maturation of endosomal membrane, the ATPase proton pump actively transfer protons from the cytosol to endosomal membrane, that leads to acidified endosomal membrane and activated hydrolytic enzymes. The polymers which have buffering property will become protonated and inhibit acidification.[89] Cationic polymers such as polyethyleneimine (PEI) and cationic dendrimers containing an excess of uncharged amines that shows high buffering capacity are inhibit the endosomal acidification by absorbing the protons that are pumped inside.[87] Because of inhibition from polymers, the

accumulation of more protons will continuously pumped into the endosomes to try to lower down the pH. By the time, extensive proton pumping action is followed by the entry of chloride ions that increases the ionic concentration and leads to water influx. The osmotic pressure in the endosomes leads to swelled, rupture the endosomes ultimately release contents to cytosol of the cells. This approach has been used by many researchers to enhance pH buffering capacity to promote cytosolic delivery by endosomal escape (**Figure 1.6**).
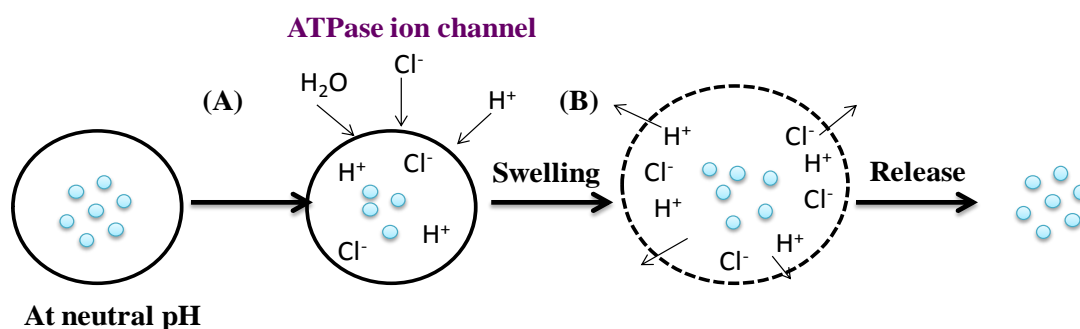

Figure 1.6. Illustration of proton sponge effect (pH-buffering hypothesis). Polymer-DNA complex are entered via endocytosis (A) After endocytosis, polymer -DNA complex are trapped into ATPase proton pump which transported protons inside the endosomes. Polymer become protonated and tries to inhibit the acidification of endosomes. (C) Passive entry of chloride ions leads to increase the ionic concentration causes the rupture of endosomes, releasing their contents into cytosol of the cells.[90]

4. Fusion in the endosomal membrane

Destabilization of endosome membrane by fusogenic lipid and peptides are extensively used in many studies. Various viruses which have single peptides undergo conformational changes upon changing in pH.[91] This phenomenon was found in various lipids. In previous study, it was found that the incorporation of neutral lipids such as dipoleoylphosphatidylethanolamine (DOPE) enhances the cytosolic delivery.[92] In one study, Farhood et al. showed that use of a certain amount of DOPE incorporated to cationic liposome achieved endosomal membrane destabilization. DOPE lipid act as a helper lipid which attributes endosomolytic activity.[93] DOPE lipid contains ethanolamine head group which have a tendency to form inverted hexagonal phase at acidic pH. Therefore, the presence of fusogenic lipids in the liposome composition as DOPE has the ability to change the conformation which is required for facilitating the cargo release from endosomes (**Figure 1.7**).[94] There is various successful application of pH sensitive

liposome which demonstrated in delivery of variety of bio-macromolecules such as protein, DNA, drugs etc.

Destabilization of endosomal membrane
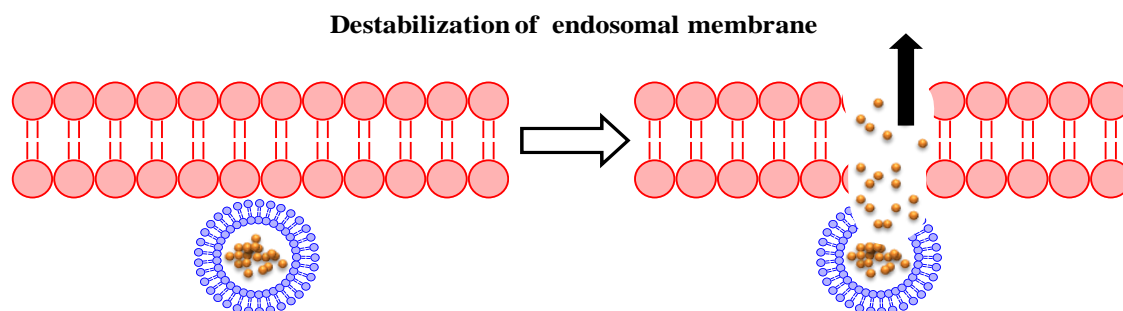
Figure 1.7 Endosomal escape of macromolecules by the use of pH-sensitive liposome. pH sensitive lipsoomes (fusogenic liposome) interacting with endosomal membrane and destabilization occurs.[64]

In the above sections, I discussed about the recent development in delivery system and intracellular trafficking and mechanism of nanomaterials. Despite many improvements in delivery system, there are still major issues for the internalization and penetration of nanomaterials inside the cells. In the next section, I will highlight the physical methods which have been developed so far for penetration of biological materials inside the cells.

1.5 Development of Recent physical approaches for delivery of macromolecules

A major intracellular barrier is the cell membrane barrier that restricts the penetration of hydrophilic macromolecules. The plasma membranes separate extracellular molecules from materials within the cell. Most hydrophilic macromolecules cannot pass plasma membrane because plasma membrane is hydrophobic in nature.[95] Crossing plasma membrane is the major hurdles for macromolecules that can limit for effective therapeutic applications. Nevertheless, various physical strategies have been introduced macromolecules into live cells.

1. Electroporation

Electroporation or electropermeabilization is a physical approach where electric field is applied to the cells to increase the permeability of the cell membrane by changing the transmembrane potential which disrupt the lipid bilayer integrity that allows drugs, proteins, nucleic acids inside the cells (**Figure 1.8**).[96] This approach has been shown an effective way to transport macromolecules across the cell membrane in very less time. Since,

electroporation is very popular method in gene therapy as it introduces recombinant DNA into eukaryotic cells efficiently by applying electric pulse to create temporary holes in plasma membrane.[97] In electroporation method, cells suspension are usually exposed to high voltage (100-200 V) to create transient pores outside the cell membrane, the pores allow macromolecules to internalize inside the cells. After internalization, the removal of electric field resulting in spontaneous sealing of pores. It shows highly effectiveness to other methods.[98] Electroporation has been shown effectiveness with nearly all cell types for transdermal drug delivery, gene therapy and for cancer tumor electro chemotherapy. [99,100]
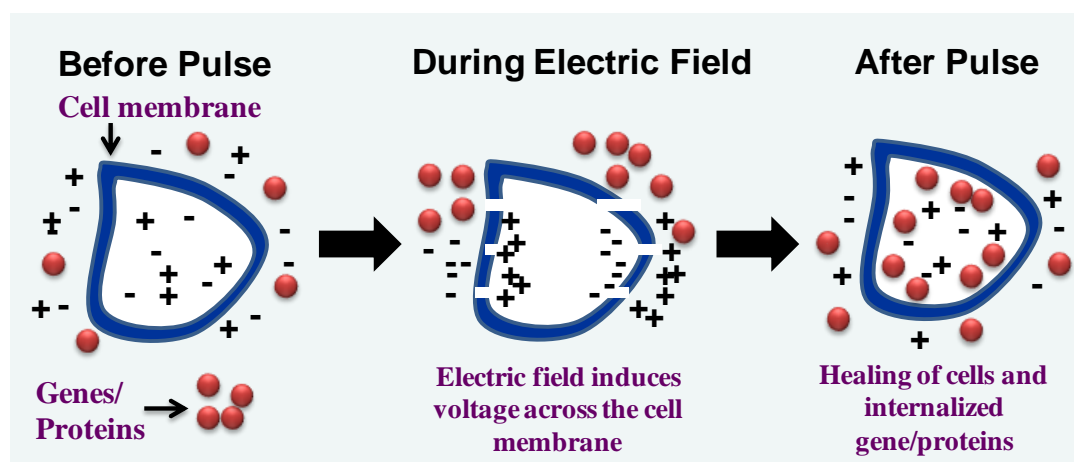
Figure 1.8 Illustration of using electroporation method. This method describes the use of electric field for delivery of macromolecules.[101]

2. Ultra-sonication

Ultrasound has been employed to enhance the delivery of macromolecules such as genetic materials and proteins for the last many years. A large number of studies have been employed the combination of utra-sonication enhanced the cell membrane permeability in cell culture. However, the main challenge in ultrasound-triggered therapy is the design of carriers that are both responsive to ultrasound and biologically active (**Figure 1.9**).[102] In ultrasound, the therapeutic ultrasound at a frequencies in the range of 1-3MHz with intensity up to 0.5-2.5 W/cm^2 have been used for enhanced delivery of macromolecules. The efficiency of ultrasonication is dependent on the frequency and intensity of ultrasound irradiation. This technique uses ultrasound waves to create plasma membrane defects by acoustic cavitation.[103] The major advantage of ultrasonication process is its safety, non-invasiveness for effective delivery of therapeutics directly to the cells.[104]
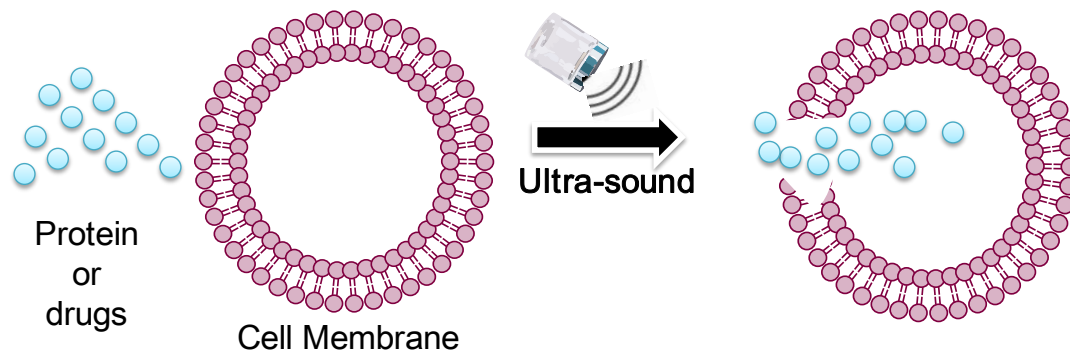
Figure 1.9 Ultrasonication induced permeabilization in the cell membrane.

3. Microinjection

Another popular method is microinjection. Microinjection is the most direct method for delivery of therapeutic macromolecules (**Figure 1.10**). In order to increase the permeability in the cell membranes, electroporation and ultrasonication have been employed in the form of electric fields and pressure waves have the same goal to disrupt the cell membrane and create a nanometre range holes to allow macromolecules inside the cells. In microinjection, glass pipette has been used to introduce macromolecules inside the cells. This technique has been widely used as physical penetration method for effective intracellular macromolecular delivery. In this technique, micro-capillary needle which usually ranging around 0.5 to 5 μm in diameter.[105] The stiffness of micro capillary is enough to penetrate the cell membrane.[106] Microneedles are relatively safer for delivery of drugs or nucleic as compared to elctroporation and utrasonication. This approach is commonly used in transdermal drug delivery as it means to deliver drugs into the skin in a minimally invasive manner.[107] However, the drawback of this method is difficult to apply large number of cells.
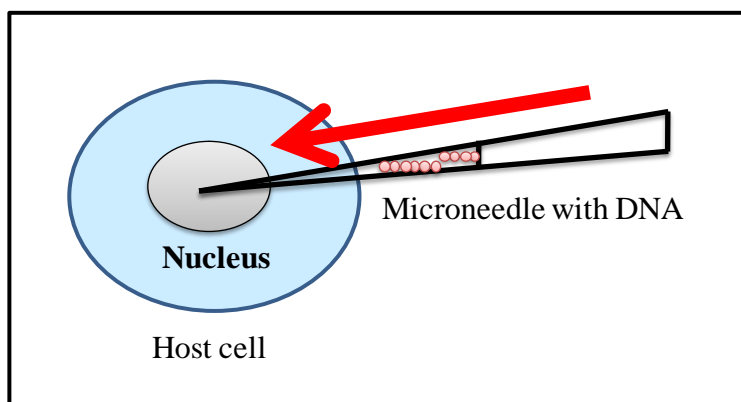
Figure 1.10 Microinjection method utilizes microneedles to deliver DNA directly to cell nuclei.

**Challenges that limits the existing physical strategy**

Many physical methods such as electroporation and ultrasonication have been used to facilitate the transfer of macromolecules from extracellular to inside the cells effectively. However, these methods could create transient membrane holes or defects using physical force such as electric field or laser irradiation. If parameters such as voltage shock, current pulse or ultrasound irradiation are given for prolonged exposure onto the cells, some pores outside the membrane might induces large or fail to close after membrane discharge which causes cell damage or rupture.[108, 109] Moreover, the transportation of macromolecules using physical method is non-specific. The improper ionic balance using physical method could result into in appropriate cell function and causes cell death.[110] In addition, simple method such as microinjection also has to ensure the stiffness of the needles. The variation in stiffness leads to break the needles or tear fail to distribute drugs or nucleic acids uniformly.[111] The methods like electroporation, ultrasonication are invasive in nature and could damage cellular membrane. Therefore, the development of new method is needed to overcome these limitations and major hurdles in delivery of macromolecules.

Attempt of using 'Freeze Concentration' approach for internalization

The use of freeze concentration concept in cytoplasmic delivery is relatively new comparing with other methods. Freeze Concentration is a physicochemical phenomenon wherein water molecules crystallizes to form ice, leading to increased in solute concentration in the remaining unfrozen solution forming a phase separation during freezing. Specifically, spontaneous ice nucleation occurs and ice grows in all directions when a solution is super-cooled at -5 to -45 ˚C. A high solute concentration remains in the unfrozen solution leading to a concentrated solute around the cells located in the residual solution. Before freezing actually occurs, the solution is in thermodynamic equilibrium, the concentration of any solute is uniform in unfrozen system. But when freezing starts in system, the growth of ice crystals separates the ions and salt and squeezed to the non-frozen region.[112]

On decreasing the temperature of aqueous solution, at certain point, two phases are generated. One is liquid phase and other is solid phase. The solute concentration is very concentrated in liquid phase. However, in solid phase, the pure ice was formed in ideal solution or some entrapment of solutes in practical state. This process is responsible for solute occlusion.

The idea of utilizing enhanced concentration after freezing can leads to increase association and internalized macromolecules inside the cells. **Figure 1.11** shows the schematic representation of cytoplasmic delivery mediated by freezing strategy.
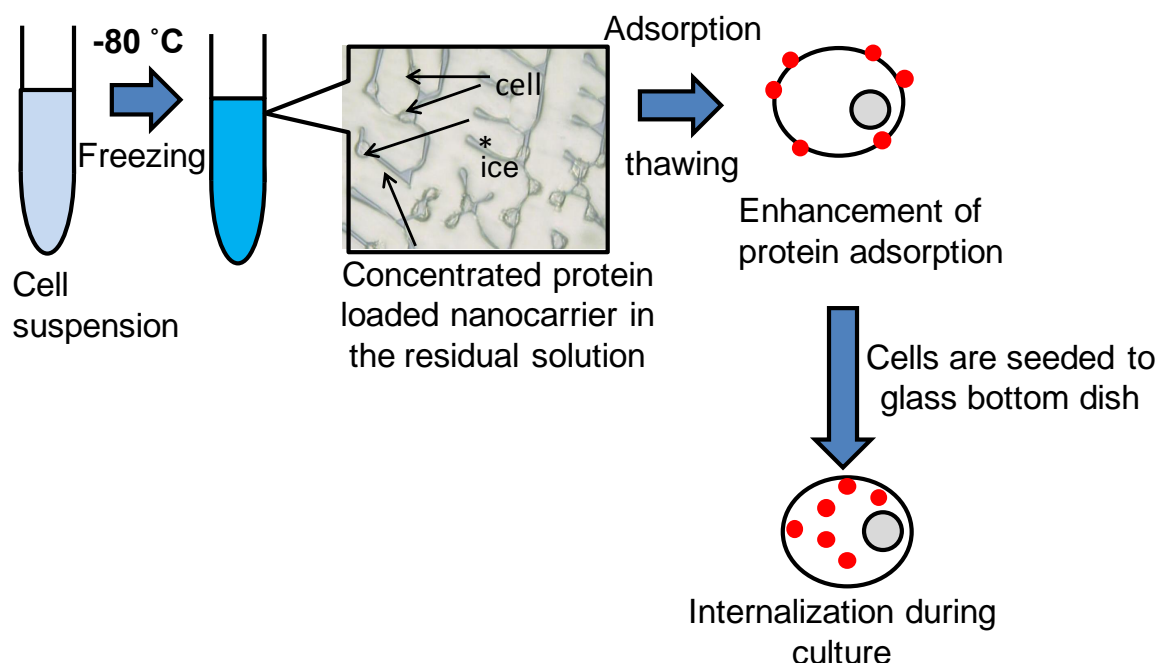
Figure 1.11 Schmatic illustration of use of freeze concentration method in cytoplasmic delivery of macromolecules

Phase diagram of sodium chloride as a general example of freeze concentration

The composition of a system after freeze concentration can be calculated from the phase diagram with the enthalpy and concentration. The study of freeze concentration of binary components or multicomponents are based on phase diagrams in which possible states of solid and liquid at thermodynamic equilibrium as a function of temperature and composition or concentration. The simplest type of phase diagram for binary systems; in literature, phase diagram of NaCl and H_2O can be found.[113] The phase diagram of sodium chloride depicts the exact relation between the concentration and freezing temperature (**Figure 1.12**). At the time of freezing, the increase in concentration in the unfrozen area after decreasing temperature can cause precipitation which eventually increased viscosity. At initial stage of freezing of solution, the unfrozen region changes into glassy state. Usually, the pure water freezes at 0 ˚C, the water molecules of hydrogen and oxygen have tightly bonded together and transformed into crystalline structure of ice. But presence of salt, makes it harder for water

molecules to bond into ice structure. Ice repels naturally for water molecules. The soluble salts are excluded from the ice and remain in the unfrozen solution on freezing the salt solution. Salt concentration considerably increases constantly when the temperature gets lowered. As the solution continues to cool, it transformed into salt crystal along with ice crystal. At low temperature, the mixture of salt and water which contain any solution known as eutectic temperature. The Eutectic composition can be described as particular mixture of salt and water (23.3% salt) which freezes at this temperature. This is just a general description of effect of freezing in binary components of solution. Such a diagram can be used to link the concentration and the freezing temperature. In human body, the isotonic salt concentration is about 0.9% NaCl. On the other hand, the eutectic freezing temperature of NaCl is almost 22 wt%. The water formed ice in the extracellular space which increases the concentration of salt solution. The rising extracellular salt concentration in the unfrozen region can cause more water osmotically leave the cells. This could cause damage the cells.[114] This equilibrium phase diagram helps to provide precise relation between the concentration and temperature. However, freezing of an aqueous solution cannot be predicted through equilibrium phase diagram.
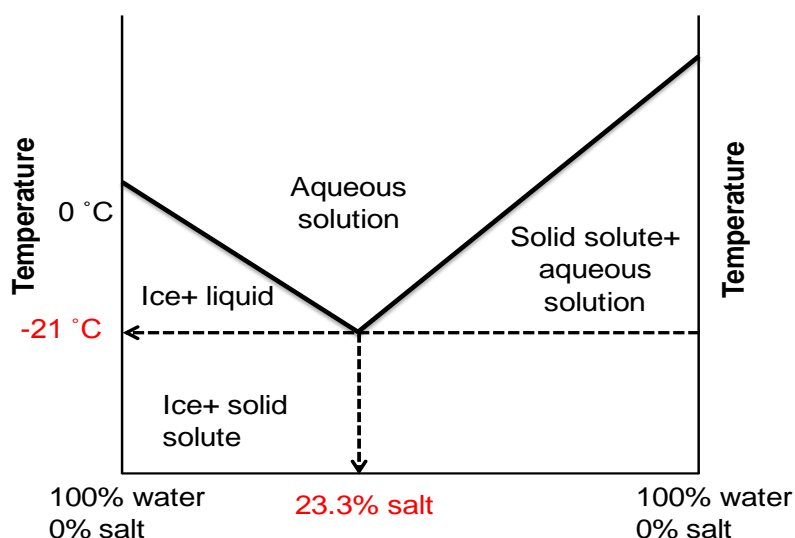
Figure 1.12 Phase diagram of water-NaCl system. When the temperature started to lowering down, ice crystals are started to form and separated into two areas.

Regardless, Bhatnagar et al. have determined the concentration associated with sucrose, glucose by using DSC endotherm. But this method is quite complicated and difficult to determine each freeze concentrated of multicomponent system.[115] However, there is almost no report and very hard to quantify the particular increased concentration in freezing system.

Parameters which influences by freeze concentration

Viscosity

The viscosity factor is generally influenced by the low temperature and concentration. The solutes eventually increase its viscosity because of freeze concentration. At extreme ultra old temperature, the concentration of solution are increases, viscosity also increases. This factor may determine the maximum limit of concentration during freezing.[116]

Osmotic Pressure

Osmotic pressure is an important factor that affects frozen cells. When cells are started to freeze, ice crystals are started to form slowly in outside matrix. Meanwhile, water is started to migrate out from the semi-permeable cells because of osmotic pressure difference. This results into cell shrinkage and damage across the membrane. After thawing, the water does not return to the cells and ultimately cell damage. [117]

The presence of ice and an increase in solute concentration have significantly effect on reaction rate. It is important to note that increase in concentration system marked many changed in physical properties such as pH, ionic strength, and viscosity in a system. It is worthwhile to point out that during freezing; that macromolecule such as native proteins could undergo a pH shift during freezing. Freezing process could affect the loss of functional properties and conformational changes of proteins. [118] Similarly; concentration effect could responsible to affect cells which ultimately cause damage to the cells.

Cryopreservation

In cellular process, the cells can be damage by low temperature because of the formation of ice during freezing because of dehydaration and intracellular ice formation.[119] Therefore, cryoprotectants are universally used to prevent them from freezing injury and enhanced their survival rate.[120] Common example of cryoprotectants is glycerol, DMSO, ethylene glycol. Cryoprotectants are sometimes called antifreeze proteins that prevent them from freezing completely. Cryoprotectant should be effective at depressing the melting point of water,[121] should be non-toxic towards the cells, do not precipitate or formed hydrates or formed eutectics. DMSO is commonly used as a cryoprotectant. This can easily penetrate the cell membrane and entered, remained inside the cells. It can prevent the excessive dehydration of cells by freezing process. However, DMSO shows extreme high cytotoxicity. Therefore, these issues stimulated to the development of new cryoprotective agents.

Polyampholytes as cryoprotective agents

Recently, Matsumura and co-workers found the use of polyampholytes as cryoprotective agents. They developed new, nontoxic polyampholytes which effective cryopreserved cells, showed high cell viability after freezing. They introduced negative charge using succinic anhydride in cationic polymer, ε-poly-L-lysine (PLL). Cryoprotective polyampholytes were synthesized on the converting the 65% α-amino group to carboxyl group. The cell viability was significantly higher than DMSO (**Figure 1.13**).[122] They also hypothesized the polyampholytes might formed soluble aggregates due to intermolecular interactions in ice which ultimately trapped in water and salts.[123] This factor could be responsible for osmotic dehydration and crystal formation during freezing.
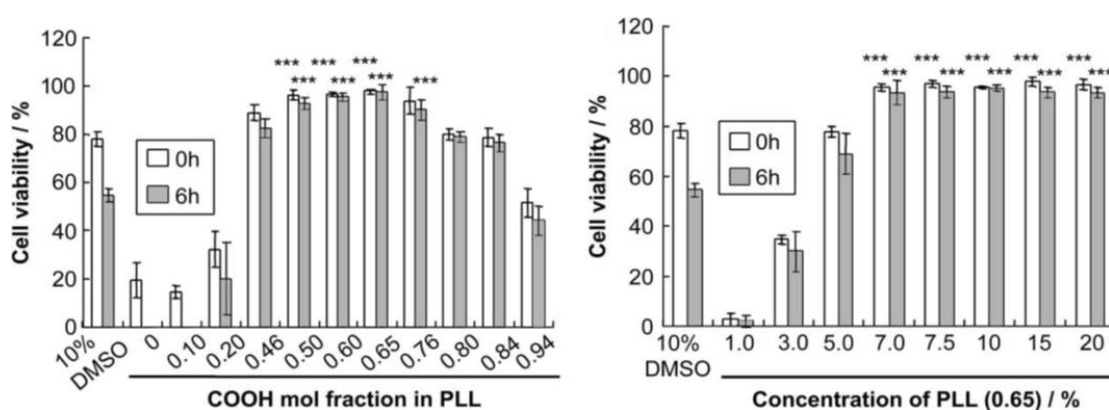
Figure 1.13 Cryoprotective properties of COOH-PLLs. (a) L929 cells were cryopreserved with 10% DMSO and 7.5% (w/w) PLL with different ratios of introduced COOH. Cell viability immediately (white bars), and 6h (gray bars) after thawing at 37 ˚C. **(b)** L929 cells were cryopreserved with various concentrations of PLL (0.65). Cell viability immediately (white bars), and 6 h (gray bars) after thawing at 37 C. Data are expressed as mean SD for 3 independent experiments (5 samples each). ***$P < 0.001$ vs 10% DMSO for the corresponding time period (0 or 6 h).[120]

Effect of slow and fast cooling rates in cells

Rapid and slow cooling rates have been shown to have different effects on the long-term viability of cells. A fast cooling rate is more likely to result in the formation of a large number of small-size intracellular ice crystals which unable to maintain equilibrium which causes intracellular ice formation. Intracellular ice formation is lethal for cells and is the most important cause for cell death during cryopreservation. Slow freezing favors the formation of larger size ice crystals, specifically in an extracellular location.[124] In addition, slow freezing results in a maximum displacement of water, which enhances the concentration of unfrozen fractions outside the

cells.[125] However, slow cooling results in the increase of the solution effect, which can be damaging to the cells.

Protein stability at low temperature

Similarly, there are many reports which indicated that freeze concentration may causes major shift in pH, induces aggregation, denaturation in bio-macromolecules especially in proteins. The freezing can cause several stress such as eutectic crystallization of solutes, pH changes etc.[126]However, there is various cryoprotectants have been used to prevent the structural stabilization of protein during freezing. Glycerol, trehalose, sucrose have been used for preventing destabilization of protein at low temperature.[127] Recently, our group found that newly developed polyampholyte as a cryoprotectant is able to prevent lactate dehydrogenase (LDH) enzymatic activity at extreme low temperature. Our group expected that polyampholyte might be able to prevent proteins from freezing damage. However, the investigation of activity of other proteins using polyampholyte as a cryoprotectant needs to be further investigated in the future.

Quantification of freeze concentration by determination of concentration factor

It has been known that in some chemical reaction, the rate acceleration in frozen system is fully dependent on the concentration effect of aqueous solution through ice crystal formation. Miyawaki et al. had proposed generalized model to explain the freeze concentration acceleration in the form of concentration factor (α) using frozen state.[128] The concentration factor is the freeze induced concentration by estimating freezable water and the fraction of frozen water. Theoretically, α which is concentration factor related to freezing point depression and estimated from the analysis on the fraction of frozen water.

The physicochemical meaning of α is to be as follows

α = [Freezable water]/ [Unfrozen water]………………………………… Equation 1

Determination of concentration factor for frozen solution

Miyawaki and co workers have proposed a generalized equation for determination of concentration factor of frozen solution.

The fraction of freezable water (F_{fw}) = (X_w - X_{uf})/X_w..................................Equation 2

X_w = water content/ total mass

X_{uf} = Unfreezable water content (water/ total mass)

Miyawaki et al, Pham et al., Pradipasena et al., have described the following equation which determined the fraction of frozen water in the freezable water.

$F_f/ F_{fw} = (1-t_F/t)$………………………………………………………….. Equation 3

Ff (fraction of frozen water in the total water) = frozen water/ total water

t_F = freezing

From this equation, unfrozen water fraction in the freezable water can be point of the system obtained as a function of solute concentration for samples determined

$(F_{fw}-F_f)/F_{fw} = t_F/t$………………………………………………………...…. Equation 4

From the equation 1, the concentration factor can be obtained as

$$\boxed{\alpha = F_{fw} / (F_{fw}-F_f) = t/t_F}$$ ……………………….. **Equation 5**

We can determine the concentration factor of unfrozen samples in the system from this equation.

Comparison of concentration factor of polyampholyte and DMSO cryoprotectant

The concentration factor of two types of cryoprotectant, polyampholyte and DMSO was determined by the measurement of freezing point as given in **equation 5**. Polyampholyte considerably showed high concentration factor than DMSO. This indicated that polyampholytes are more concentrated than DMSO. This might showed that extracellular concentration of certain materials is increases after ejection from ice crystals during freezing (**Figure1.14**)
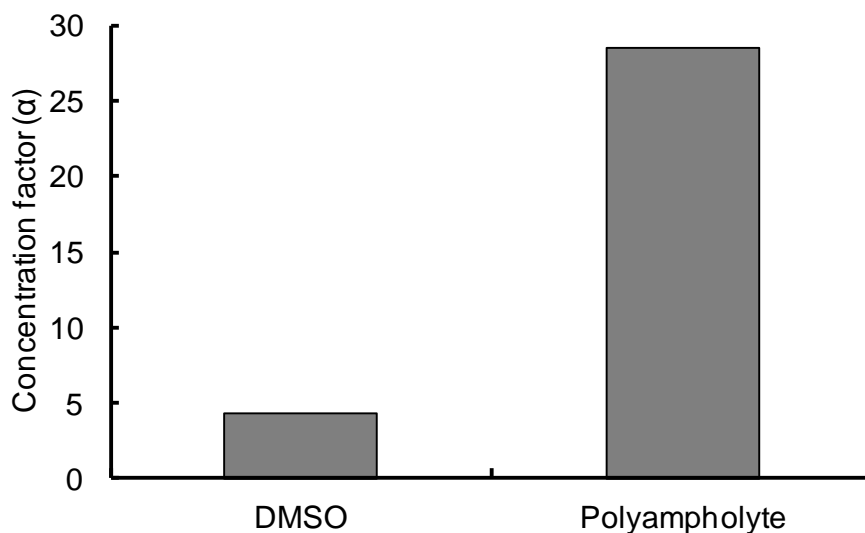
Figure 1.14 Freeze concentration factor was evaluated by determining the freezing point of wo cryoprotectant. The cryoprotectant was frozen completely at -20 °C in a cooling bath and then warmed again to melt at room temperature.

Previous applications of Freeze Concentration

1. Food industry

Previously, Freeze concentration has been successfully used in food industry. This method has been used in concentrating the fruit juices wherein water content of fruit juices is separated from the mixture in the form of ice-crystals. The concentrate can be used to make new products, or mixed with water to produce a juice with fresh taste.[129] The quality of food product is generally high at low temperature and no vapour-liquid interface occurs. Freeze concentration has been particularly successful in concentrating citrus juices, other beverages and high value extracts.[130] Freeze concentration also used in to produce pharmaceutical grade lactose and whey protein concentrate. This concentrate contains high protein that could be utilized as dietary supplement for humans and livestock.

2. Acceleration of chemical reaction using freeze concentration

Some chemical reaction also induced or accelerated in extreme low temperature. The first report for acceleration of chemical reaction induced by freeze concentration was reported by Pincock and co-workers.[131] The reaction proceeds due to freeze concentration of solutes which contained in the unfrozen solution of ice. In one study, Maeda et al., have reported the oxidation of nitrite by dissolved oxygen to form nitrate is known to be accelerated by 10^5 times by the freezing of the aqueous solution.[132]

1.6 Objective and content of this thesis

In the course of my doctoral research, I have developed efficient and versatile freeze concentration method for effective intracellular delivery of macromolecules. In addition, I also developed new polyampholyte based nanocarriers system which shows unique characteristics that make them ideal as delivery vehicles for transportation of macromolecules. Following listed **4 objectives** are comprised as the main focus in my doctoral research.

Protein-nanocarrier complex are present in the cells

Concentrated protein nanocarrier complex
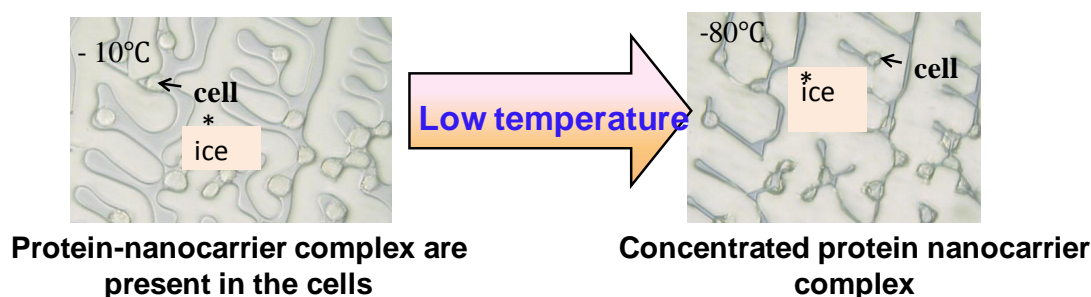
Figure 1.15 Cryomicroscopic image of cell suspension loaded with protein-nanocarrier complex. Cells were located in the remaining concentrated solution.

1. **Preliminary study of using freeze concentration methodology in protein delivery system**

Background Intracellular transports of macromolecules including proteins showed many desirable features that provide unique opportunities for therapeutic applications. However, macromolecules have very less tendency to cross the cell membrane. Electroporation, ultrasonications are the few strategies have been constantly used for introduction and penetration of macromolecules to the cells. But, few drawbacks such as high toxicity, loss of cell damage which causes toxicity have been associated with these methods. The efficient delivery of biomolecules into the cells is a major challenge in drug delivery. The advances in the design of strategy for efficient macromolecular delivery system is required facilitate increased opportunities for therapeutic applications. To find out alternative, I have developed an effective and versatile approach for efficient delivery system of macromolecules in **chapter-2.**

Outline At the initial stage, I investigated the freeze concentration approach to determine the utility of in delivery of proteins. The proteins were strongly adsorbed to the cell membrane

using this approach than non frozen conditions. However, the use of an efficient delivery agent is needed to access their site of action in the cytoplasm or nucleus. Therefore, new polyampholyte were also prepared to carry protein inside the cells. Polyampholyte were easily prepared by changing the succinylation ratio in poly-L-lysine. These polyampholytes were extremely small in sizes around 20 nm in diameter. Combining freezing and polyamopholyte nanoparticles approach, the proteins were greatly internalized inside the cells comparing with unfrozen system. New developed technology "freeze concentration" is described in chapter 2 is expected to overcome all the obstacles and used as aneffective strategy for cytoplasmic delivery.

2. Mechanistic overview of internalization and enhanced cytosolic delivery of proteins after freeze concentration

Background the initial study demonstrated the enhancement of protein cytoplasmic internalization using freeze concentration approach in chapter-2. The results from chapter-2 clearly indicated that freeze concentration was efficiently induces transportation of macromolecules. However the mechanism of internalization of protein delivery after freeze concentration technology could not be explained. It is important to understand the mode of entry and mechanistic pathway of particular protein-nanocarrier complexes for intracellular delivery. Particularly, intracellular localization and internalization are of great importance for designing the model system for effective macromolecular delivery. I tried to find out the mechanism of protein delivery after freezing method in **chapter-3**.

 Outline a new concept freeze concentration was employed for effective delivery of proteins in chapter-2. A new carrier system was developed by modifying biocompatible liposome with polyampholytes which shows more biocompatibility than polyampholyte nanoparticles which is prepared in chapter-2. In this chapter, the mechanistic studies were done to elucidate the pathway of protein internalization after freeze concentration. The unmodified liposomes and polyampholyte-modified liposomes were manifested different endocytic pathways. Moreover, Freeze concentration and polyampholyte-modified liposome were strongly enhances the protein transportation to the cytoplasm of the cells because of endosomal escape property by pH sensitive polyampholyte-modified liposomes. This system might be favorable for cancer immunotherapy.

3. The applicability of freeze concentration approach in Immunotherapy based applications

Background the non-toxic polyampholyte modified liposomes as a carrier and freeze concentration have been displayed the enhancement of cytosolic delivery of proteins in chapter-3. This system shows the enhancement of cytoplasmic protein delivery might be an effective approach in immunotherapy based application. Immunotherapy is the therapy for the treatment of diseases by inducing, enhancing or suppressing an immune response. Vaccines based on protein antigens have considerable interest because of their low toxicity and widespread applicability and constitute a new vaccination strategy for immunotherapy. Therefore, the precise delivery of antigens into the cytosol of antigen presenting cells, such as dendritic cells, macrophages are extremely important for enhancing the cellular immunity in cancer immunotherapy. Till date, various methods have been employed for increasing the immune response. However, a key limitation of currently systems is their inability to activate cytotoxic T lymphocytes (CTLs), a process that is critical for the development of immunity against viruses and tumors. Therefore, there is pressing need for development of new approach for immunotherapy applications. Hence, I intended to use freeze concentration method for immunotherapy.

Outline In this chapter, I investigated the utilization of freeze concentration approach in cancer immunotherapy applications. Ovalbumin as a protein antigen was encapsulated to liposomes with the size of 200-300 nm in diameter. The enhanced internalization of protein antigen in RAW 264.7 cells was found when freeze concentration approach was applied. Freeze concentration and polyampholyte-modified liposomes were strongly release protein antigens into the cytoplasm of antigen presenting cells for class I presentation. Additionally, freeze concentration accelerated the increased release of inflammatory cytokines such as IL-6 and TNF-α. This approach may find application as for adoptive-T cells immunotherapy for cancer.

4. Employing freeze concentration technique in gene delivery

Background Besides immunotherapy, gene therapy has become an attractive strategy for the treatment of various diseases associated with genetic malfunction. For effective gene transfer, vector is one of the key technologies which are needed for gene therapy because of its large

size; it is difficult to cross the cell membrane. Retroviruses, Adenoviruses are the few viruses that showed effective transportation of nucleic acids. But the clinical application of this approach is limited because of bearing the risk of mutational insertions, carcinogenesis and the induction of strong inflammatory response. Other alternative is the use of physical method such as electroporation and ultrasonication. However, numerous drawbacks have been associated with them. Ideally, system should be safe and perform the gene delivery in a rapid, efficient, and transient manner. In this study, I demonstrated the versatility of freeze concentration method in gene delivery method (Chapter-5).

Outline In previous objective, the freeze concentration method was intended to use in immunotherapy applications. The objective of this study was to use simple freeze concentration approach in gene delivery. Furthermore, constructing a gene vector with high transfection efficiency and low toxicity is a key prerequisite for efficient gene therapy. Therefore, I developed new low toxic polyampholyte nanoparticles for carrying genetic materials inside the cells. The polyampholyte nanoparticles were able to condensed DNA and protect DNA against enzymatic nuclease degradation. On combining with freezing method, polyampholytes nanoparticles were shown highly effective and efficient method for enhanced transfection efficiency after comparing with non-frozen system and commercial available transfecting agents such as lipofectamine and jet PEI. The low toxicity and higher transfection efficiency by freeze concentration strategy holds a great promise as an effective and unique approach for therapeutic applications. Finally, **Chapter 6** provides the concluding remarks of the overall obtained results and also suggested the new avenues for future research.

1.7 References

1. Riehemann, K.; Schneider, S.W.; Luger, T.A.; Godin, B.; Ferrari, M.; Fuchs, H. *Angew Chem Int Ed Engl*. **2009**, *48*, 872.

2. Desai, N. *AAPSJ*. **2012**, *14*, 2582.

3. Nikalje, A.P. *Med Chem* **2015**, *5*, 81.

4. Markman, J.L.; Rekechenetsky A.; Holler, E.; Liubimova, J.Y. *Adv. Drug Deliv. Rev.* **2013**, *65*, 1866.

5. Behnke, R.E.; Jonas, J.B. *Acta Opthamol.* **2011**, *89*, 108.

6. De Jong, W.H.; Borm, P.J.A. *Int. J Nanomedicine* **2008**, *3* (2), 133.

7. Bareford, L.M.; Swaan, P.W. *Adv. Drug Deliv. Rev.* **2007**, *59*(8), 748.

8. Liras, A. *Int Arch Med*. **2008**, *1*, 1.

9. Corey, D.R. *JAMA neurol*. **2016**, *73*, 1238.

10. Da, M.M.; Rede, T.; Naqvi, N.A.; Cook, P.D. *Biotechnol Annu Rev.* **2000**, *5*, 155.

11. Neidle, S.; Thurston, D.E. *Nature Rev. Cancer* **2005**, *5*, 285.

12. Walsh, G. *Nat. Biotechnol*. **2010**, *28*, 917.

13. Bruno, B.J.; Miller, G.D.; Lim, C.S. *Ther Deliv*. **2013**, *4*(11), 1443.

14. Leader, B.J.; Baca, D.E.; Golan. *Nat Drug Discov*. **2008**, *7*, 21.

15. Vasconcelos, L.; Parn, K.; Langel, U. *Ther. Delivery* **2013**, *4*, 573.

16. Kratz, F.; Elsadek, B. *J. Control. Release* **2012**, *161*, 429.

17. Dinca, A.; Chien, W.M.; Chin, M.T. *Int J Mol Sci* **2016**, *17* (2), 1.

18. Graham, S.; Hill, A.V.S. *Nat Rev Genetics* **2001**, *2*, 967.

19. Peterson, B.M.; Roberts, B.E.; Kuff, E.L. *Proc. Natl. Acad. Sci.* **1977**, *74*, 4370.

20. Saraswat, P.; Soni, R.R.; Bhandari, A.; Nagori, B.P. *Indian J Pharm Sci.* **2009**, *71* (5), 488.

21. Patil, S.D.; Rhodes, D.G.; Burgess, D.J. *AAPS J* **2005**, *7* (1), 61.

22. Burnett, J.C.; Rossi, J.J. *Chem Biol.* **2012**, *19*(1), 60.

23. Zhao, X.; Shi, H.; Sevilimedu, A.; Liachko, N.; Nelson, H.C.M.; Lis, J.T. *Nucleic Acids Res.* **2006**, *34*, 3755.

24. Park, W.; Na, K. *Wiley Interdiscip Rev Nanomed Nanobiotechnol* **2015**, *7*, 494.

25. Sercombe, L.; Veerati, T.; Moheimani, F.; Wu, S.Y.; Sood, A.K.; Hua, S. *Front Pharmacol.* **2015**, *6*, 1.

26. Bozzuto, G.; Molinari, A. *Int J Nanomedicine* **2015**, *10*, 975.

27. Jone, A. J. *Pharm. Sci. & Res.* **2013**, *5*, 181.

28. Xing, H.; Hwang, K.; Liu, Y. *Thernostics* **2016**, *6*(9), 1336.

29. Xu, Z.P.; Zeng, Q.H.; Lu, G. Q.; Yu, A.B. *Chem. Eng. Sci.* **2006**, *61*, 1027.

30. Arvizo, R.; Bhattacharya, R.; Mukherjee, P. *Expert Opin Drug Deliv*. **2010**, *7* (6), 753.

31. Jin, L.; Zeng, X.; Liu, M.; Deng, Y.; He, N. *Thernostics* **2014**, *4*(3), 240.

32. Ghosh, P.; Han, G.; De, M.; Kim, C.K.; Rotello, V.M. *Adv Drug Deliv.* **2008**, *60*, 1307.

33. Nune, S.K.; Gunda, P.; Thallapally, P.K.; Lin, Y.Y.; Forrest, M.L.; Berkland, C.J. *Expert Opin Drug Deliv.* **2009**, *6*, 1175.

34. Soenen, S.J.; Gil, P.R.; Montenegro, J.M.; Parak, W.J.; De Smedt, S.C. *Nano Today* **2011**, *6*, 446.

35. Zhang, J.; Lan, C.Q.; Post, M.; Simard, B.; Deslandes, Y.; Hsieh, T.H. ***Cancer Genomics Proteomics* 2006, *3*, 4147.**

36. Munyendo, W.L.L.; Lv, H.; Benza-Ingoula, H.; Baraza, L.D.; Zhou, J. *Biomolecules* **2012**, *2*(2), 187.

37. Su, Y.; Doherty, T.; Waring, A.J; Ruchala, P.; Hong, M. *Biochemistry* **2009**, *48*, 4587.

38. Chugh, A.; Eudes, F.O.; Shim, Y.S. *IUBMB Life* **2010**, *62*(3), 183.

39. Schmidt, N.; Mishra, A.; Lai, G.H.; Wong, G.C.L. *FEBS Letters* **2010**, *584*, 1806.

40. Madaan, K.; Kumar, S.; Poonia, N.; Lather, V.; Pandita, D. *J Pharm Bioallied Sci.* **2014**, *6*(3), 139.

41. Nanjwade, B.K.; Bechra, H.M.; Derkar G.K.; Manvi, F.V.; Nanjwade, V.K. *Eur J Pharm Sci* **2009**, *38*, 158.

42. Nanjwade, B.K.; Derkar, G.K.; Manvi, F.V.; Nanjwade, V.K *Eur J Pharm Sci.* **2009,** *38*(3), 185.

43. McNerny, D.Q.; Leroueil, P.R.; Baker, J.R. Wiley Interdiscip Rev. Nanomed Nanobiotechnol.**2010**, *2*(3), 249.

44. Trabulo, S.; Cardoso, A.L.; Mano, M.; Pedroso de Lima, M.C. *Pharmaceuticals (Basel)* **2010**, *3*(4), 961.

45. Alkilany, A.M.; Murphy, C.J. *J Nanopart Res*. **2010**, *12* (7), 2313.

46. Singh, N.; Jenkins, G.J.S.; Doak, S.H. *Nano Reviews* **2010**, *1*, 1.

47. Morachis, J.M.; Mahmoud, E.A.; Almutairi, A. *Pharmacol Rev.* **2012**, *64*, 505.

48. Liechty, W. B.; Kryscio, D. R.; Slaughter, B. V.; Peppas, N. A. *Annu Rev Chem Biomol Eng*. **2010**, *1*, 149.

49. Nguyen. K.T. *J Nanomed Nanotechnol* **2011**, *2*, 1.

50. Yokoyama, M.; Sugiyama, T.; Okano, T.; Sakurai, Y.; Naito, M.; Kataoka, K. *Pharm Res.* **1993**, *10* (6), 895.

51. Fetsch, C.; Gaitzsch, J.; Massager, L.; Battaglia, G.; Luxenhofer, R. *Sci Rep.* **2016**, *6*, 1.

52. Reddy, B.P.; Yadav, H.K.; Nagesha, D.K.; Raizaday, A.; Karim, A. *J Nanosci Nanotechnol.* **2015**, *15*(6), 4009.

53. Zhang Y.; Huang Y.; Li S. *AAPS PharmSciTech.* **2014**, *15*(4), 862.

54. Yokoyama M. *J Drug Target.* **2014**, *22*(7), 576.

55. Laschewsky, A. *Polymers* **2014**, *6*, 1544.

56. Janclauskaite, U.; Visnevskij, C.; Radzevicius, K.; Makuska, R. *Chemija* **2009**, *20*(2), 128.

57. Cao, S.; Barcellona, M.N.; Pfeiffer, F.; Bernards, M.T. *J. Appl. Polym. Sci.* **2016**, *133*, 1.

58. Barcellona, M.N.; Johnson, N.; Bernards, M.T. *Langmuir* **2015**, *31* (49), 13402.

59. Akiyama, E.; Morimoto, N.; Kujawa, P.; Ozawa, Y.; Winnik. F.M.; Akiyoshi, K. *Biomacromolecules* **2007**, *8* (8), 2366.

60. Shen, H.; Akagi, T.; Akashi, M. *Macromol. Biosci.* **2012**, *12*, 1100.

61. Panda, J.J.; Varshney, A.; Chaukahn, V.S. *J. Nanobiotechnology* **2013**, *11*, 1.

62. Rad-Malekshahi, M.; Lempsink, L.; Amidi, M.; Hennink, W.E.; Mastrobattista, E. *Bioconjugate Chem.* **2016**, *27* (1), 3.

63. Eckmann, D.M.; Composto, R.J.; Tsourkas, A.; Muzykantov, V.R. ***J. Mater. Chem. B***, **2014**, ***2,*** 8085.

64. Torchillin, V. *Drug Discov Today Technol* **2008**, *5*, 95.

65. Bareford, L.M.; Swaan, P.M. Endocytic mechanism for targeted drug delivery. *Adv. Drug Deliv Rev.* **2007**, *59* (8), 748.

66. Kou, L.; Sun, J.; Zhai, Y.; He, Z. *Asian J. Pharmacol.* **2013**, *8*, 1.

67. Oh, N.; Park, J.H. *Int J Nanomedicine* **2014**, *9*, 51.

68. Pacheco, P.; White, D.; Sulchek, T. *PLoS ONE* **2013**, *8*(4), 1.

69. Sahay, G.; Alakhova, D.Y.; Kabanov, A.V. *J Control Rel.* **2010**, *145* (3), 182.

70. Schäfer, V.; Von Briesen, H.; Andreesen, R.; Steffan, A.M.; Royer, C.; Tröster, S.; Kreuter, J.; Rübsamen-Waigmann, H. *Pharm Res* **1992**, *9*, 541.

71. Doherty, G.J.; McMahon, H.T. *Annu. Rev. Biochem* **2009**, *78*, 857.

72. Alberts, B.; Johnson, A.; Lewis, J. Transport into the cell from the plasma membrane: Endocytosis; Garland Science: New York, **2002**.

73. Panyam, J.; Labhasetwar, V. *Pharm Res.* **2003**, *20*(2), 212.

74. Prokop, A.; Davidson, J.M. *J Pharm Sci.* **2008**, *97* (9), 3518.

75. Nishikawa, T.; Iwakiri, N.; Kaneko, Y.; Taguchi, A.; Fukushima, K.; Mori, H.; Morone N.; Kadokawa, J. *Biomacromolecules* **2009**, *10*(8), 2074.

76. Lim, J.P.; Gleeson, P.A *Immunol Cell Biol.* **2011**, *89*, 836.

77. Parodi, A.; Corbo, C.; Cevenini, A.; Molinaro, R.; Palomba, R.; Pandolfi, L.; Agostini, M.; Salvatore, F.; Tasciotti, E. Nanomedicine (Lond) 2015, 10(2), 1923.

78. Mellman, I.; Fuchs, R.; Helenius, A.; *Ann. Rev. Biochem.* **1986**, *55*, 663.

79. Huatari, J.; Helenius, A. *EMBO J.* **2011**, *30* (17), 3481.

80. Ziello, J.E.; Huong, Y.; Jovin, I.S. *Mol, Med.* **2010**, *16*, 222.

81. Sakhrani, N.M., Padh, H. *Drug Des Delev Ther.* **2013**, *7*, 585.

82. Varkouhi, A.K.; Scholte, M.; Storm, G.; Haisma, H.J. *J Control Rel.* **2010**, *151*(3), 220.

83. Tian, W.D.; Ma, Y.Q. *Soft Matter* **2012**, *8*(8), 6378.

84. Oliveras, A.E.; Muthukrishnan, N.; Baker, R.; Wang, T.Y.; Pellois, *J.P. Pharmaceuticals (Basel)* **2012**, *5*(11), 1177.

85. Kessel, D.; Santiago, A.M.; Andrzejak, M. Photochem Photobiol. 2011, 87(3), 699.

86. Berg, K., Berstad, M., Prasmickaite, L.; Wevergang, A.; Selbo, P.K.; Hedfors, I.; Hoqset, A. *Top Curr Chem.* **2010**, *296*, 251.

87. Liang, W.; Lam, J.K.W. Endosomal Escape Pathways for Non-Viral Nucleic Acid Delivery Systems: Molecular Regulation of Endocytosis: InTech, **2012**.

88. Parodi, A.; Corbo, C.; Cevenini, A.; Molinaro, R.; Palomba, R.; Pandolfi, L.; Agostini, M.; Salvatore, F.; Tasciott, E. *Nanomedicine* **2015**, *10*, 1923.

89. Freeman, E.C.; Weiland, L.M.; Meng, W.S. *J Biomater. Sci Polym Ed.* **2013**, *24*(4), 398.

90. Agirre, M.; Zarate, J.; Ojeda, E.; Puras, G.; Desbrieres, J.; Pedraz, J.L.; *Polymers* **2014**, *6*(6), 1727.

91. Lau, W.L.; Ege, D.S.; Lear, J.D.; Hammer, D.A.; DeGrado, W.F. *Biophys J.* **2004**, *86*(1), 272.

92. Sayed, A.E.; Futaki, S.; Harashima, H. *AAPS J.* **2009**, *11*(1), 13.

93. Farhood, H.; Serbina, N.; Huang, L. *Biochimica et Biophysica Acta* **1995**, *1235*, 289.

94. Deshpande, P.P.; Biswaas, S.; Torchilin, V.P. *Nanomedicine (Lond)* **2013**, *8*(9), 1.

95.   Khalil, I.A.; Kogure, K.; Akita, H.; Harashima, H. *Pharmacol Rev.* **2006**, *58* (1), 32.

96.   Weaver, J.C.; *IEEE T Plasma Sci* **2000**, *28*, 24.

97.   Cadoret, F.; Soscia, C.; Voulhoux, R. *Methods Mol Biol.* **2014**, *1149*, 11.

98.   Zaharoff, D.A.; Henshaw, J.W.; Mossop, B.; Yuan, F. Exp Biol Med. (Maywood), **2008**, *233* (1), 94.

99.   Sersa, G.; Cemazar, M.; Rudolf, Z. *Cancer Therapy*, **2003**, *1*, 133.

100. 100 Gehl, J. *Acta Physiol Scand* **2003**, *177*, 437.

101. Xiong, W.; Wagner, T.; Yan, L.; Grillet, N.; Muller, U. *Nat Protocols* **2014**, *9*, 2438.

102. Pitt, W.G.; Husseini, G.A.; Staples, B.*J. Expert Opin Drug Deliv.* **2004**, *1*(1), 37.

103. Couture, O.; Foley, J.; Kassell, N.F.; Larrat, B.; Aubry, J.F. *Transl Cancer Res* **2014**, *3* (5), 494.

104. Miller, D.; Smith, N.; Bailey, M.; Czarnota, G.; Hynynen, K.; Makin, I. *J Ultrasound Med.* **2012**, *31*(4), 623.

105. Lee, K.; Lingampalli, N.; Pisano, A.P.; Murthy, N.; So, H. *ACS Appl. Mater. Interfaces* **2015**, *7*, 23387.

106. Prausnitz, M.R. *Adv. Drug. Deliv. Rev.* **2004**, *56*, 581.

107. Rrausnitz, M.R.; Langer, R. *Nat Biotechnol.* **2008**, *26*(11), 1261.

108. Fan, Z.; Kumon, R.; Deng, C. *Ther Deliv.* **2014**, *5*(4), 467.

109. Jiang, C.; Davalos, R.V. *IEEE T Bio-Med Eng.* **2015,** *62*, 4.

110. Mellott, A. J.; Forrest, M.L.; Detamore, M.S. *Ann Biomed Eng.* **2013**, *41* (3), 446.

111. Gonzalez-Perez, O.; Guerrero-Cazares, H.; Quiñones-Hinojosa, A. *J Vis Exp.* **2010**, *1* (46), 1.

112. Pham, Q.T. *Jpn J Food Eng.* **2008**, *9*, 21.

113. Cocks, F.H.; Browe, W.E. *Cryobiology* **1974**, *11* (4), 340.

114. Lodish, H.; Berk, A.; Zipursky, S.L.; *Molecular Cell Biology*; W.H Freeman: New York, **2000**.

115. Bhatnagar, B.S.; Cardon, S.; Pikal, M.J.; Bogner, R.H. *Thermochimica Acta* **2005**, *425*, 149.

116. Chen, Y.H.; Cao, E.; Cui, Z.F.; *Food Bioprod Proc* **2001**, *79*, 35.

117. Dumont, F.; Marechal, P.A.; Gervais, P. *Appl Environ Microbiol.* **2006**, *72* (2), 1330.

118. Mehta, N.K.; Elavarasan, K.; Manjunatha Reddy, A.; Shamasundar, B.A. *J Food Sci Technol.* **2014**, *51*(4), 655

119. Goa, D.; Critser, J.K. *ILAR J* **2000**, *41*(4), 187.

120. Fuller, B.J. *Cryo Letters* **2004**, *25*(6), 375.

121. Hopkins, J.B.; Baeau, R.; Warkentin, M.; Thorne, R. *Cryobiology* **2012**, *65*(3), 169.

122. Matsumura, K.; Hyon, S.H.; *Biomaterials* **2009**, *30* (27), 4842.

123. Matsumura, K.; Hayashi, F.; Nagashima. T.; Hyon, S.H. *Cryobiol Cryotechnol* **2013**, *59*, 23.

124. Bischof, J.C. *Annu. Rev. Biomed. Eng.* **2000**, *2*, 257

125. Mazur, P.; Cole, K.W.; *Cryobiology* **1989**, *26*, 1.

126. Kolhe, P.; Amend, E.; Singh, S.K. *Biotechnology Progress* **2009**, *26* (3), 727.

127. Olsson, C.; Jansson, H.; Swenson, J. *J. Phys. Chem. B* **2016**, *120*, 4723.

128. Miyawaki, O.; Nishino, H. *J. Food Eng*. **2016**, *190*, 109.

129. Sanchez, J.; Hernandez, E.; Auleda, J.M.; Raventos, M. *Food Sci. Technol Int* **2011**, *17*(1) 5.

130. Deshpande, S.S.; Cheryan, M.; Sathe, S.K. *Crit. Rev. Food Sci. Nutr.* **2009**, *20*, 173.

131. Pincock, R.E. *Acc. Chem. Res.* **1969**, *2*, 97.

132. Takenaka, N.; Ueda, A.; Daimon, T.; Bandow, H.; Dohmaru, T.; Maeda, Y. *J. Phys. Chem.* **1996**, *100* (32), 13874

Chapter 2

Protein Cytoplasmic Delivery Using Poyampholyte Nanoparticles and Freeze Concentration

2.1 Introduction

Over the past few decades, a significant amount of progress has been made regarding drug delivery technologies, which have engendered biomaterials for the intracellular and endocytic delivery of various therapeutic agents.[1] Examples of carriers include polymeric micelles,[2-4] liposomes,[5-7] microparticles,[8] nanoparticles,[9-11] nanogels,[12,13] drug polymer conjugates,[14] inorganic conjugations,[15] and other supramolecular assemblies.[16] However, challenges such as low specific targeting, insufficient cellular uptake, and low therapeutic efficiency still exist in regard to the delivery of clinically optimal levels of therapeutic molecules.[17] There is a great need for the development of approaches that can transport drugs precisely and safely to a target site with a controlled release to achieve the maximum therapeutic effect.[18] Currently, nanocarriers are promising vehicles with highly improved pharmacokinetics,[19] biodistributions, and toxicities, and they exhibit a number of other attractive features.[13] The intracellular delivery of proteins and peptides to living cells offers a powerful alternative to gene or siRNA transfections.[20] For such technology to be successful, the delivered protein needs to cross the plasma membrane to be efficiently released in the cytoplasm.[21] Methods such as electroporation, microinjection, or macromolecular systems have been adapted to introduce proteins into cells by penetrating cell membranes. Although the ability to introduce proteins into the cytoplasm of live cells was facilitated by the development of delivery reagents, the efficiency of the process remains low. Therefore, there is a pressing need to develop a novel method to enhance the intracellular uptake of drugs. Here, I propose a novel and effective method using the "freeze concentration" mechanism.[22-24]

Freezing is commonly believed to be the best method for long-term cell preservation. During freezing, ice can form in the extracellular space. The formation of ice can exclude solute molecules, leading to increased concentrations of electrolytes in the remaining extracellular solution via phase separation. The phenomenon is called freeze concentration.[22] Intracellular water can remain in a super-cooled unfrozen state, even at temperatures between -5 and -40 ^{o}C. The growing extracellular ice forms channels where the extracellular solution and the cells are displaced. In these channels, the target drug also can be concentrated around the cell membranes, and its adsorption might be enhanced if the drug molecules are encapsulated with cytocompatible carriers.

In order to improve the survival of cryopreseved cells, cryoprotective agents (CPAs) like dimethyl sulfoxide (DMSO), glycerol, and ethylene glycol are often utilized. The effects of

CPAs are determined by their ability to reduce the freezing and thawing points and to lower the cooling rate to avoid lethal intracellular freezing.

Previously, our group has developed a novel cryoprotectant as an alternative to DMSO. Cells were successfully cryopreserved using poly-L-lysine (PLL) reacted with succinic anhydride at an appropriate polyampholyte ratio.[24-27] The polyampholytes effected their cryoprotective properties by a different mechanism than DMSO, and the mechanism might be related to the control of freeze concentration. In this chapter, I attempted to use the freeze concentration method with polyampholytes by utilizing an enhanced concentration of peripheral solutes for the introduction of antigenic proteins into the cytosol of cells.[28]

Cytocompatible nanocarriers have been widely studied. Moreover, many researchers have shown that polymer-peptide conjugates form self-assembled nanostructures based on the interactions of well-defined amino acid residues.[29, 30] Polyampholytes have also gained great attention in various areas such as biotechnology, and have a promising future in the delivery of diagnostic agents. For example, Akashi and co-researchers reported amphoteric poly (amino acid) nanoparticles for protein delivery.[31]

Here, I describe the development of a novel protein delivery method to address the issues of inefficient cellular uptake and poor intracellular protein behaviors of protein-loaded nanoparticles using the freeze concentration mechanism and amphoteric nanocarriers. Specifically, nanoparticles formed by the self-assembly of amphiphilic charged polyampholytes containing extensive cross-linking points showed a high drug trapping efficiency. Nanoparticles were characterized by particle size, zeta potential, and morphological observation and interacted via hydrophobic and electrostatic interactions.

2.2 Materials and Methods

2.2.1 Preparation of polyampholytes and hydrophobically modified polyampholytes

Polyampholyte cryoprotectants were synthesized using a previously reported method.[24] Briefly, an aqueous solution of 25 % (w/w) PLL (10 mL, JNC Corp., Tokyo, Japan) and succinic anhydride (SA) (1.3 g; Wako Pure Chem. Ind. Ltd., Osaka Japan) were mixed at 50 $^{\circ}$C for 2 h to convert 65 % of the amino groups to carboxyl groups.

To develop novel polyampholyte nanoparticles, hydrophobic moieties were introduced on the polyampholyte. An aqueous solution of PLL (10 mL; 25 % w/w) was added to different concentrations of dodecylsuccinic anhydride (DDSA) (Wako Pure Chem. Ind. Ltd., Osaka,

Japan) at 100°C and allowed to mix for 2 h to obtain hydrophobically modified PLL (**Scheme 2.1a**). Subsequently, SA was added in 35-65 % molar ratios (COOH/NH$_2$) and was allowed to react for 2 h at 50 °C (**Scheme 2.1b**).

2.2.2 Characterization of polyampholytes

^{1}H NMR spectra were obtained at 25°C on a Bruker AVANCE III 400 spectrometer (Bruker BioSpin Inc., Switzerland) in D$_2$O.

2.2.3 Determination of Critical Aggregation Concentration (CAC)

The CACs of the self-assemblies were investigated by measuring the excitation spectra of pyrene in polyampholyte solutions. The polyampholyte was dissolved in phosphate buffered saline without calcium and magnesium (PBS (-)) at different concentrations (0.01, 0.02, 0.05, 0.1, 0.2, 0.5, 1, 2, 5, and 10 mg/mL). Next, 4 µL of pyrene (1.0 mM in acetone) was transferred to a 10 mL test tube and acetone was completely volatilized under a gentle steam of nitrogen. Different concentrations of polyampholyte were added (4 mL) to each tube. The resulting solutions were sonicated in an ultrasonic bath for 30 min and then heated for 3 h at 65 °C to equilibrate the pyrene and the polyampholytes. Subsequently, the samples were left to cool overnight at room temperature. The emission spectra of pyrene were recorded from 300 to 360 nm on a JASCO FP-6500. The excitation/emission slits widths were set as 3/3 mm. Spectra were accumulated with a scan speed of 100 nm/min. The intensity of pyrene at 338 nm (I_{338}) and 335 nm (I_{335}) was plotted against the concentration of polyampholyte.

2.2.4 Particle size and zeta potential measurements

The mean hydrodynamic diameters and zeta potentials of the aggregated polyampholyte nanoparticles were determined by dynamic light scattering (DLS) method on a Zetasizer 3000 (Malvern Instruments, Worcestershire, UK) with a scattering angle of 135°. Polyampholytes were diluted with PBS (-) at 10 mg/mL and were used for measurements.

2.2.5 Morphological analysis

The morphology of the polyampholyte nanoparticles was detected using a Hitachi H-600 transmission electron microscope (TEM) operated at an accelerating voltage of 100 kV. A drop of the polyampholyte nanoparticles was placed on a copper grid (200 mesh covered with carbon) and allowed to dry for 10 min prior to the measurement.

2.2.6 Preparation of protein-loaded polyampholyte nanoparticles and determination of protein adsorption on/into nanoparticles

   To prepare the protein-loaded polyampholyte nanoparticles, Bovine serum albumin (BSA) (Wako) and lysozyme (Wako) were chosen as model proteins. Polyampholyte nanoparticles (10 mg/mL) were mixed with the protein solutions (0.25, 0.5, 1.0, 2.0 mg/mL) of an equal volume, and were incubated for 2 h at room temperature and then centrifuged for 5 min at 10000 rpm using a centrifugal filter off (cut-off: 100 kDa for BSA and 50 kDa for lysozyme) in order to separate adsorbed and un-adsorbed proteins.[31] The amount of un-adsorbed protein was quantified by the Bradford assay using Bradford Ultra reagent (Expedeon Ltd., Harston, UK) at 595 nm. The adsorption efficacy was calculated using **Equation 2.1**.

Adsorption efficacy=(amount of protein adsorption/initial feeding amount of protein)*100 (**2.1**)

2.2.7 Cell culture

   L929 cells (American Type Culture Collection, Manassas, VA, USA) were cultured in Dulbecco's modified Eagle's medium (DMEM; Sigma-Aldrich, St. Louis, MO) supplemented with 10% fetal bovine serum (FBS) at 37 ^{o}C under 5 % CO_2 in a humidified atmosphere. When the cells reached 80 % confluence, they were removed by 0.25 % (w/v) trypsin containing 0.02 % (w/v) ethylenediamine tetraacetic acid (EDTA) in PBS(-) and were seeded on a new tissue culture plate for subculture.

2.2.8 Cytotoxicity assay

Cells suspended in 0.1 mL medium at a concentration of 1.0 x 10^4 mL were placed in 96-well culture plates. After 72 h incubation at 37 °C, 0.1 mL medium containing different concentrations polyampholytes was added to the cells, followed by 48 h incubation. To evaluate cell viability, 0.1 mL of 3-(4, 5-dimethyl thial-2-yl)-2, 5-diphenyltetrazalium bromide (MTT) solution (300 mg/mL in medium) was added to the cultured cells. The cells were then incubated for 4 h at 37°C. After incubating, the resulting color intensity was measured by a microplate reader (Versa max, Molecular Devices Co., CA, USA) at 540 nm, and was proportional to the number of viable cells. The cytotoxicity was represented as the concentration of the compound that caused a 50% reduction in MTT uptake by a treated cell culture compared with the untreated control culture (IC$_{50}$).[24]

2.2.9 Fluorescent labeling of polyampholytes and proteins

Hydrophobically modified polyampholytes and model proteins were labeled with a fluorescent dye for allow for observation with a confocal laser scanning microscope (CLSM). For polyampholytes labeling, a solution of PLL (25 w/w %) was treated with fluorescein isothiocynate (FITC-I, Dojindo, Kumamoto, Japan) at a 1/100 molar ratio for 24 h at room temperature. FITC-PLL was purified by dialysis (molecular weight cut off 3 KDa; Spectra/Por, Spectrum Laboratories, Inc., CA, USA) against water for 3 days. The same procedure was used to obtain hydrophobically modified polyampholytes. For BSA and lysozyme labeling, Texas Red (TR) conjugation was carried out as described in Section 2.10.

2.2.10 TR labeling of proteins (lysozyme/BSA)

Lysozyme or BSA (2 mg) was dissolved in chilled buffer (sodium bicarbonate, 0.1 M) and 50 μL of TR sulfonyl chloride solution (Dojindo, 1 mg in 50 μL in acetonitrile) was added with rapid mixing. After incubating for 1 h, the reaction mixture was desalted using a desalting column (for BSA; 30K, lysozyme; 3K) which was equilibrated by PBS buffer, and the resulting residue was lyophilized until usage.

2.2.11 Confirmation of freezing concentration

2.2.11.1 Solid state ^{1}H-NMR for determination of residual water

In order to measure the residual water during freezing, solid-state NMR experiments were performed on a 700-MHz JEOL ECA spectrometer, using a Doty Scientific Inc. (DSI) 4 mm HXY CP/MAS NMR probe. A DMSO saline solution (10 w/v %) and a saline solution of 7.5 % PLL-SA (65) were measured. The cryopreservation solution samples were sealed into DSI inner-sealing cells for an XC4 rotor and spun at 3.6-5.8 kHz at various temperatures ranging from 1 to -41 ^{o}C. The samples were cooled by replacing spinning and bearing gases with cooled N$_2$-gas passed through a liquid nitrogen cryostat with a DSI cold gas supply unit. All data were processed with the program NMRPipe.[48] NMRViewJ[49] was employed for spectral visualization and analysis. The intensities and line widths of the peaks were analyzed by IGOR (WaveMetrics). The contribution from frozen components was eliminated by baseline correction and line-shape analysis. The amount of residual water in ice was estimated by the peak intensities of the H$_2$O signal.

2.2.11.2. Cryomicroscopic observation of cells during freezing

The cryomicroscopy experimental procedures utilized here were similar to those described extensively in the literature.[50, 51] L929 cells were observed during freezing in the cryopreservation solution (10% DMSO and 10% PLL-SA (65)) using the cryomicroscope. A small drop (4 μL) of the cell suspension was pipetted in the center of a quartz crucible (15 mm in diameter), covered, loaded on a cooling stage (Linkam 10002L Cooling Stage, Linkam Scientific Instruments, UK), and cooled to -80 ^{o}C at 1°C/min. Ice was seeded at -2°C using a needle, pre-cooled in liquid nitrogen to avoid super-cooling. The morphology of the ice crystals was captured with a mounted photomicroscope (Digital Microscope, VHX-500, Keyence Corp., Tokyo, Japan).

2.2.12 Cell freezing with protein-loaded nanoparticles

To prepare protein-encapsulating polyampholyte nanoparticles, FITC-labeled polyampholyte nanoparticles (10mg/mL) and the same volume of TR-labeled protein (2mg/mL) were incubated for 2 h and centrifuged at 13200 g for 15 min. Un-adsorbed and adsorbed proteins were separated and washed by PBS(-) repeatedly.

L929 cells were counted and re-suspended in 1 mL of 10% PLL-SA(65) cryoprotective solution or 10% DMSO culture medium solution with protein-loaded polyampholyte nanoparticles (10 mg) without FBS at 4 ^{o}C at a density of 1x10^{6} cells/mL in 1.9 mL cryovials (Nalgene, Rochester, NY) and were stored in a -80 ^{o}C freezer overnight. These vials were thawed at 37°C, diluted with DMEM medium and cells were washed 3 times with DMEM. All cells were counted using a haemocytometer and the tryptan blue staining method. The reported viability values are the ratios of living cells to total cells. The adsorption of polyampholyte and encapsulated proteins onto L929 cells before and after freezing was observed using a CLSM (FV1000-D; Olympus, Tokyo, Japan).

2.2.13 Intracellular uptake of protein via endocytosis

After thawing, cells were again seeded in a glass bottom dish with DMEM and incubated for 3 days. Then they were washed with PBS (-) 3 times and were observed by a CLSM.

2.2.14 Statistical analysis

All data are expressed as the mean standard deviation (SD). Measurements for post-thaw viability were collected with n=5. All experiments were conducted in triplicate. Data among

the different groups were compared using a one-way analysis of variance (ANOVA) with a post-hoc Tukey–Kramer test.

2.3 Results and Discussion

2.3.1 Synthesis of hydrophobic polyampholytes

In order to develop novel nanocarriers to load proteins, hydrophobically modified polyampholytes were synthesized by the reaction of dodecyl succinic anhydride (DDSA) and succinic anhydride (SA) (**Scheme 2.1**) into PLL and were characterized by ^{1}H-NMR in D$_2$O. The degree of substitution of DDSA and SA was obtained by ^{1}H-NMR using **Equation (2.2)** and **(2.3)**:

Degree of substitution for DDSA (%) = (2*$A_{\delta0.74}$/3* $A_{\delta1.5-1.8}$)*100 (**2.2**)

Degree of substitution for SA (%) = (2*$A_{\delta2.4}$/4* $A_{\delta1.5-1.8}$)*100   (**2.3**)

$A_{\delta0.74}$ is the integral of the methyl peak from DDSA located at 0.74 ppm and $A_{\delta2.4}$ is the integral of the methylene peak of SA located at 2.4 ppm. $A_{\delta1.5-1.8}$ is the integral of the b-methylene peak of poly-lysine main chain located at from 1.5ppm (intact PLL) to 1.8ppm. The introduction rate of DDSA and SA was well controlled and is listed in **Table 2.1**. The ^{1}H-NMR spectra are shown in **Figure 2.1**. In this study, the modified PLL was denoted as PLL-DDSA (n)-SA (m), where *n* and *m* indicate the substitution value of DDSA and SA against the molar ratio of the amino groups, respectively. For example, PLL-DDSA(3)-SA(65) indicates that 3% of the amino groups have been substituted with DDSA and 65% of the amino groups have been substituted with SA, and PLL-SA(65) indicates that 65% of the amino groups have been substituted by SA without addition of DDSA. According to Huang et al.,[32] PLL hydrophobically modified with octenyl succinic anhydride self-assembled into micelles. The term 'micelles' in their report indicated self-assembled polycore particles. Generally, the term 'polymer micelles' is used to represent self-assembled aggregates of amphiphilic block copolymers with a hydrophobic core and hydrophilic shell.[33] However, when modifications were carried out using DDSA or octenyl succinic anhydride, the hydrophobic moieties must have been introduced randomly in PLL. Therefore, the self-assembled aggregates should have had a hydrophobic poly-core as the cross-linking point, similar to nanogels.[34] As such; the aggregation of hydrophobically modified PLL was described as nanoparticles in this study.
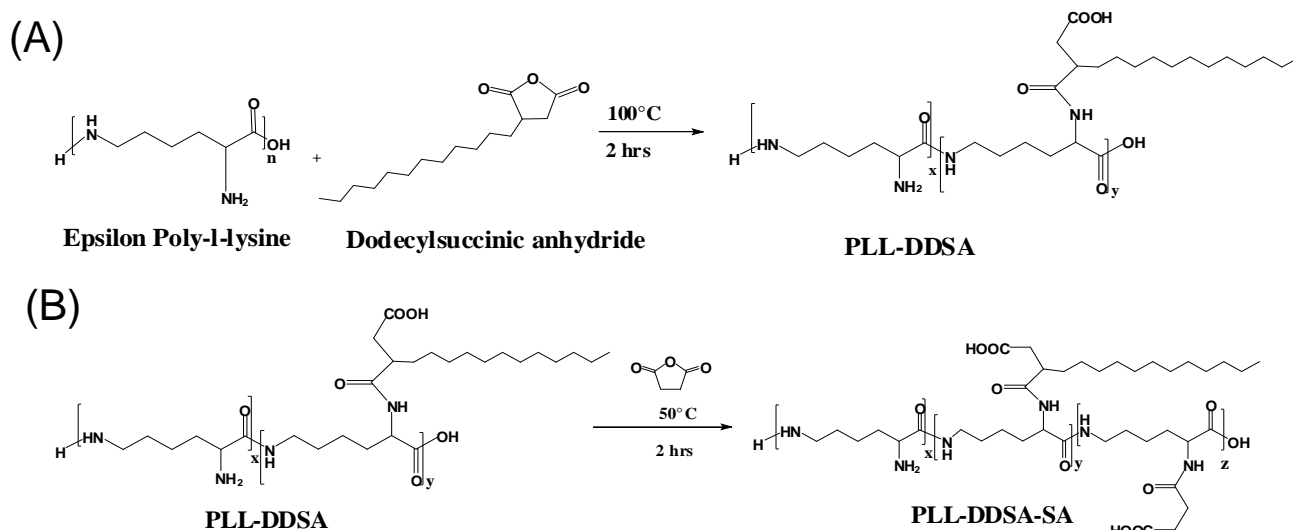
Scheme 2.1 Preparation of hydrophobically modified polyampholytes.
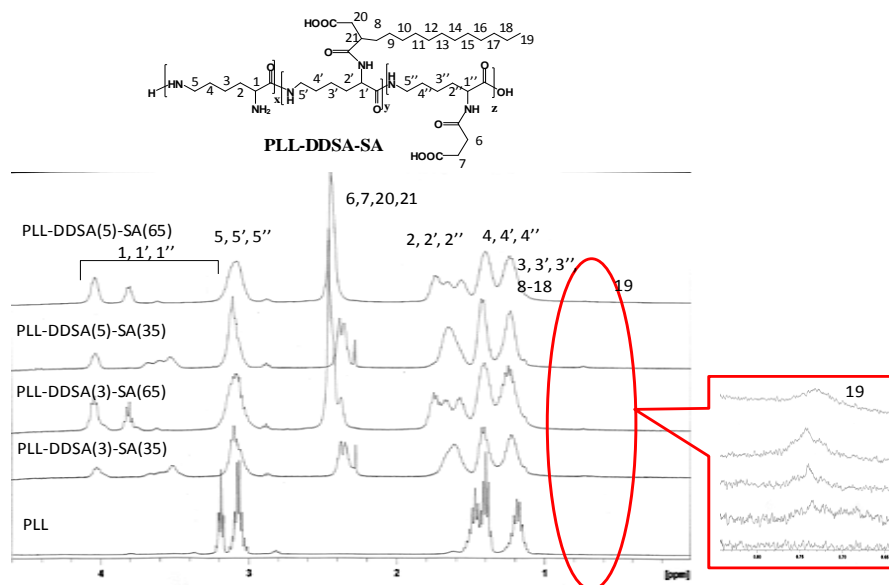
Figure 2.1. ^{1}H-NMR spectra of hydrophobically modified polyampholytes and intact PLL.

2.3.2 Characterization of polyampholyte nanoparticles

2.3.2.1 Nanoparticle size and morphology measurements

The size of nanoparticles has a strong influence in nanomedicines and can affect drug loading, drug release, and the stability of nanoparticles.[35] In terms of nanoparticle internalization into cells by endocytosis to achieve targeted delivery, an increase in particle size will decrease the uptake and affect the bioavailability and efficacy of drugs. Polyampholyte nanoparticles (10 mg/mL) were formulated by adding phosphate buffered saline without calcium and magnesium (PBS (-)). Dynamic light scattering (DLS)

measurements revealed that that PLL-DDSA(3)-SA(35), PLL-DDSA(5)-SA(35), PLL-DDSA(3)-SA(65), and PLL-DDSA(5)-SA(65) had average sizes of 16.2, 15.7, 18.4, and 13.5 nm, respectively, with narrow size distributions (PDI 0.1-0.2) (**Figure 2.2a, Table 2.1**). The DLS measurements correlated with transmission electron microscope (TEM) observations (**Figure 2.2b**), in that the hydrodynamic radius measured by DLS was almost equal to the size of the polyampholytes nanoparticles seen via TEM. Increased substitution of DDSA and SA led to smaller particles (around 13 nm) due to the compact packing of the hydrophobic groups. Characterization of the polyampholyte nanoparticles is summarized in **Table 2.1**.

Table 2.1. Summary of composition of polyampholyte nanoparticles including ^{1}H-NMR, diameter, polydispersity, zeta-potential, and CAC.

a) Determined by ^{1}H-NMR, ND: Not detected.

b) Determined by DLS.

c) Determined using excitation spectra of pyrene.

Samples	Composition in feed (molar %)		Composition in polymer (molar %)[a]		Diameter[b] (nm)	polydispersity[b]	Zeta potential[b] (mV)	CAC[c] (mg/mL)
	DDSA	SA	DDSA	SA				
PLL-SA(65)	0	65	0	63.5	ND	ND	ND	ND
PLL-DDSA(3)-SA(35)	3	35	2.7	34.8	16.15±0.23	0.165	+4.08	0.52
PLL-DDSA(5)-SA(35)	5	35	2.8	33.7	15.72±0.15	0.171	+2.61	0.14
PLL-DDSA(3)-SA(65)	3	65	4.8	64.2	18.56±0.44	0.167	-13.1	0.50
PLL-DDSA(5)-SA(65)	5	65	4.6	63.8	13.48±0.41	0.177	-14.0	0.11

TEM was used to visualize polyampholyte nanoparticles that were fabricated in PBS (-) at 1w/w %. The morphology of the nanoparticles was spherical as seen by TEM (**Figure 2.2b**), and the nanoparticles were smooth with nearly homogeneous structures. The size of the particles was smaller than those reported by Yu et al.,[32] in which PLL was treated with octenyl succinic anhydride (diameter c.a. 100 nm). This was likely due to the fact that the present nanoparticles exhibited intermolecular hydrophobic and electrostatic interactions which led to a more compact aggregation as compared to polycationic nanoparticles.
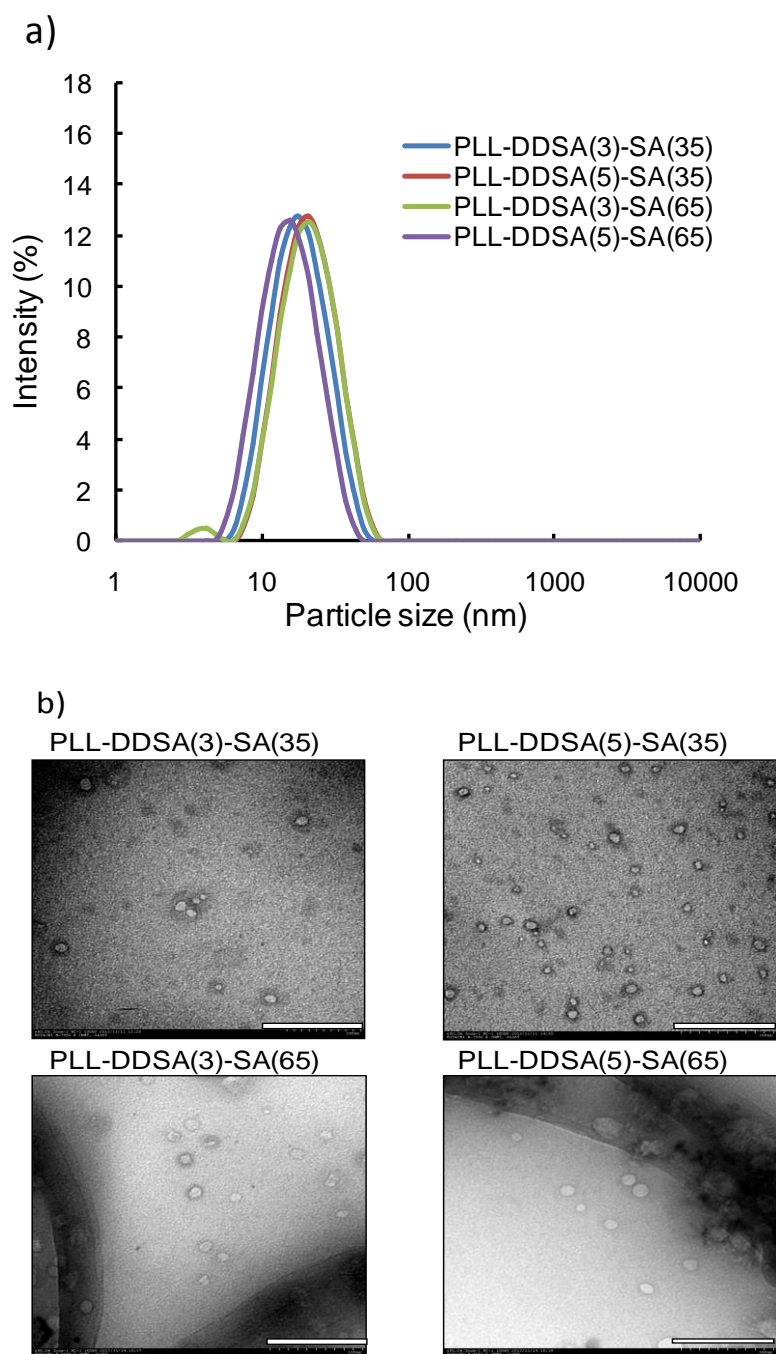
Figure 2.2 Size of polyampholyte nanoparticles prepared in PBS buffer (10 mg/mL). (a) Size distribution of different substituted polyampholyte nanoparticles as measured by DLS. (b) A typical TEM image of polyampholyte nanoparticles. The bars: 100 nm.

2.3.2.2 Aggregation of polyampholyte nanoparticles

The critical aggregation concentration (CAC) of the polyampholytes suggested the formation of self-assembled aggregates. The CACs of the hydrophobically modified PLLs were determined using the pyrene fluorescence excitation spectra method at 25°C.[36,37] Specifically, the excitation spectra of pyrene in PLL-DDSA(3)-SA(65) and PLL-DDSA(5)-SA(65) in water are shown in **Figure 2.3 a,c**. Based on the excitation spectra of pyrene and the red shift of the spectra, the ratio of the intensities of 338 nm to 335 nm (I_{338}/I_{335}) versus the concentration of PLL-DDSA(3)-SA(65) and PLL-DDSA(5)-SA(65) were plotted (**Figure 2.3 b,d**). The intensity and spectra of other polyampholytes are shown in **Figure 2.3 e-h**. The CAC value was estimated as the cross-point when extrapolating the ratio of I_{338}/I_{335} at low and high concentration regions and was found to be 0.5 mg/mL for PLL-DDSA(3)-SA(35) and PLL-DDSA(3)-SA(65). However, the value decreased for PLL-DDSA(5)-SA(35) and PLL-DDSA(5)-SA(65) to around 0.1 mg/mL (**Table 2.1**). These results can be explained by the fact that the more hydrophobic polyampholytes (PLL-DDSA(5)-SA(35), or -(65)) had increased intermolecular interactions, which led to aggregate formation at a lower concentration.
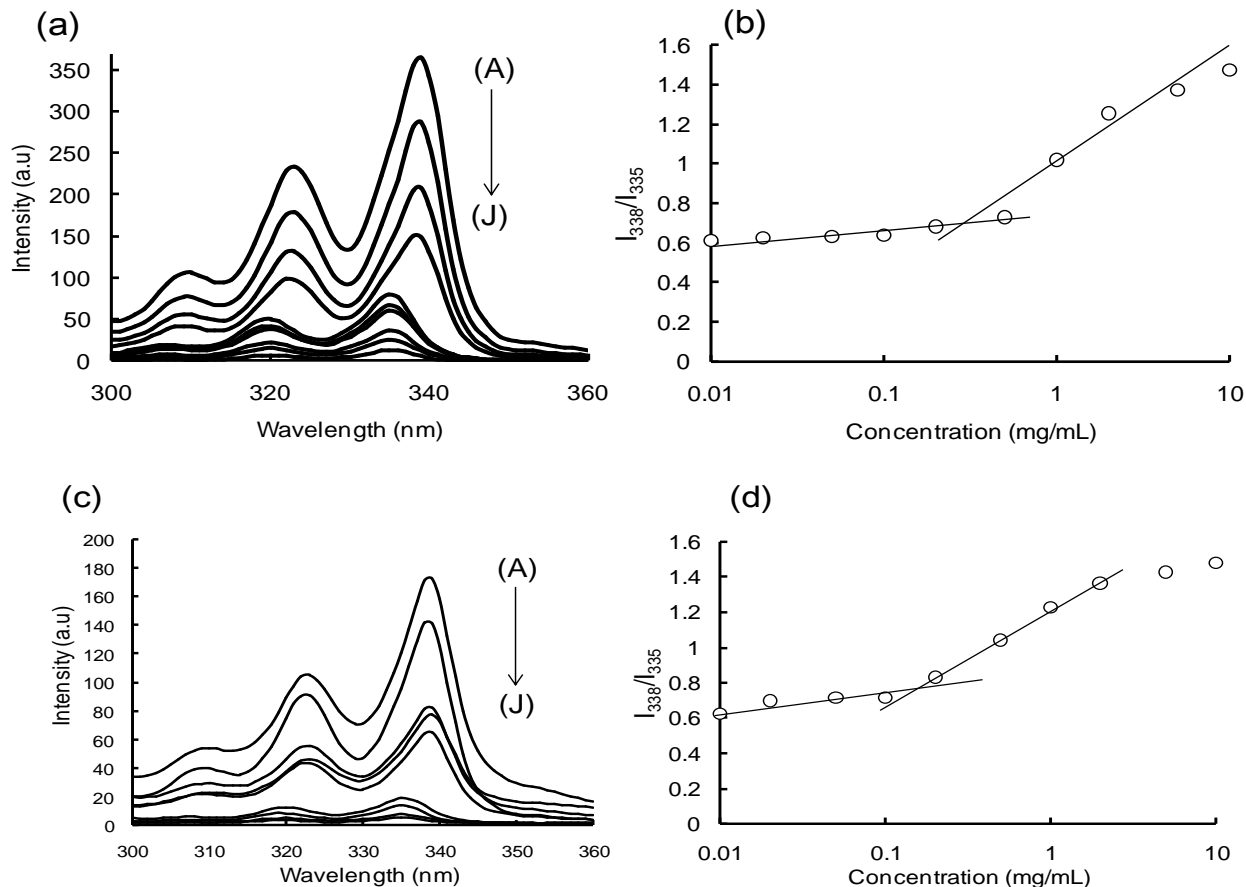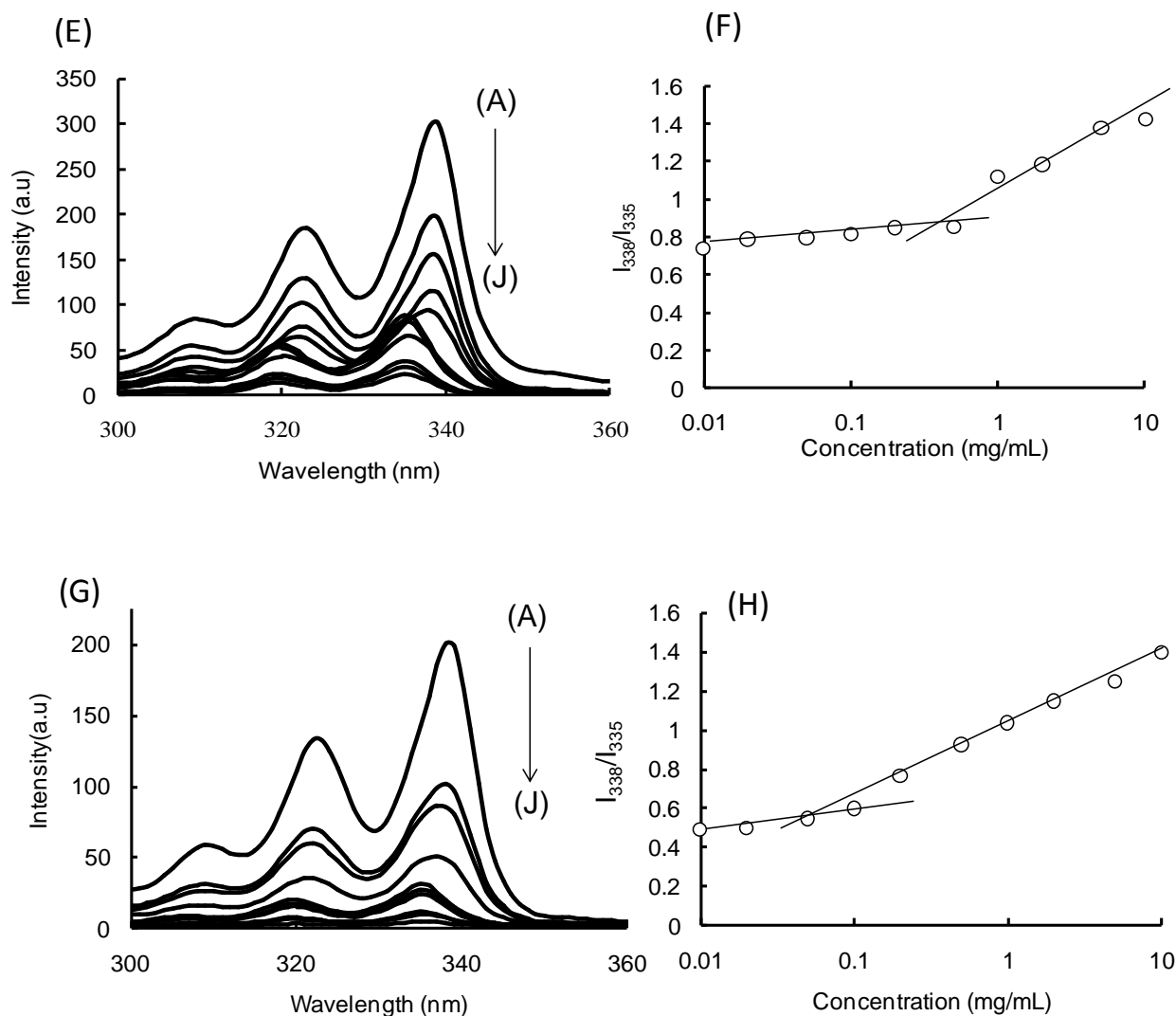
Figure 2.3 Determination of CACs of different nanoparticles. Pyrene excitation spectra of (a) PLL-DDSA(3)-SA(65) and (c) PLL-DDSA(5)-SA(65) (e) PLL-DDSA (3)-SA (35) (g) PLL-DDSA(5)-SA(35) solutions at different concentrations (A-J) 10, 5, 2, 1, 0.5, 0.2, 0.1, 0.05, 0.02, and 0.01 mg/mL, respectively. Plot of the ratio of I_{338}/I_{335} against the logarithm of the concentration of (b) PLL-DDSA(3)-SA(65), (d) PLL-DDSA(5)-SA(65), (f) PLL-DDSA (3)-SA(35) (h) PLL-DDSA(5)-SA (35).

2.3.2.3 Surface charges of nanoparticles

Zeta potential is an important characteristic for drug delivery. Surface charges can be governed by hydrophobicity and can influence particle stability.[38] To investigate the distribution of carboxyl groups on the surface, nanoparticles were suspended in PBS and the zeta potential was determined. The zeta potential of all polyampholytes was greatly affected by the balance between the amount of carboxyl groups and amino groups. Their surface charges were manipulated by the feed ratio of DDSA and SA. The zeta potentials of PLL-DDSA(3)-SA(35), PLL-DDSA(5)-SA(35), PLL-DDSA(3)-SA(65), and PLL-DDSA(5)-

SA(65) were +4.08, +2.61, −13.1, and -14.0 mV, respectively (**Table 2.1**). The zeta potential of hydrophobically modified PLL decreased with increased substitution of SA, and the change was due to the carboxyl groups of SA near the surface. Moreover, it was confirmed that PLL-DDSA(3 and 5)-SA(35) were cationic nanoparticles and PLL-DDSA(3 and 5)-SA(65) were anionic nanoparticles. On the other hand, PLL-SA(65) did not aggregate or have a zeta potential. As a comparison, it was previously reported that polyampholytes derived from poly(amino acids) without any hydrophobic modifications aggregated and showed negative and positive zeta potentials.[31] However, those polyampholytes had a molecular weight of more than 700000 and exhibited significant aggregation, whereas the current polyampholytes have a molecular weight of around 5000. The difference in molecular weight might explain why the nanoparticles required modification with hydrophobic moieties to induce aggregation.

2.3.3 Adsorption of proteins on/into polyampholyte nanoparticles

In order to evaluate protein adsorption on/into polyampholyte nanoparticles, bovine serum albumin (BSA, anionic protein) and lysozyme (cationic protein) as model proteins were selected. The adsorption efficiency of lysozyme was greater with anionic nanoparticles (PLL-DDSA(5)-SA(65)), whereas the adsorption efficiency of BSA was more effective with cationic nanoparticles (**Figure 2.4a,c**). This was ascribed to the strong electrostatic interactions between the hydrophobically modified nanoparticles and the proteins. The adsorption efficiency of BSA was almost 100% at 2 mg/mL, whereas lysozyme showed 90% efficiency (**Figure 2.4 b, d**). These results revealed the successful development of two types of protein-loaded nanoparticles by electrostatic interactions.
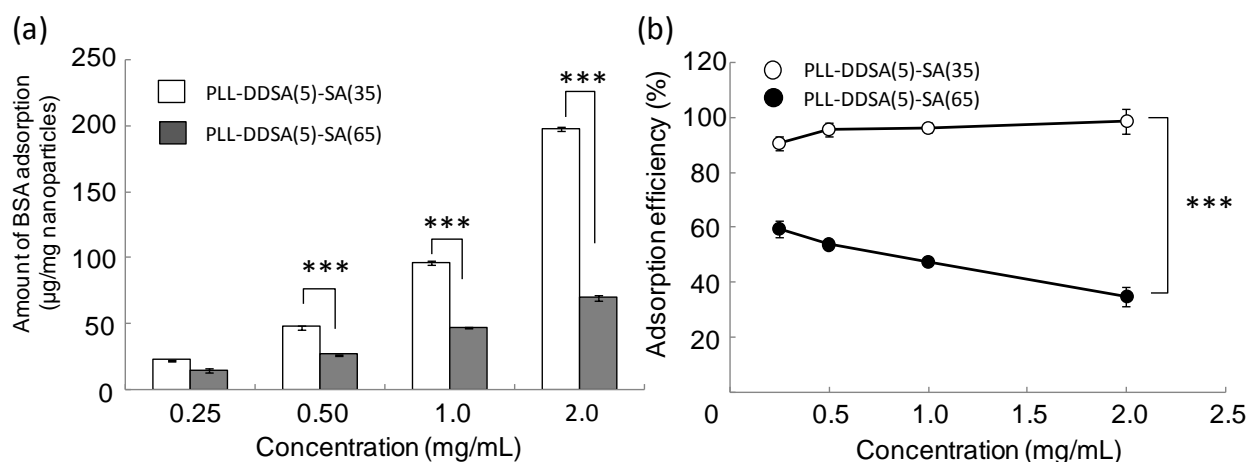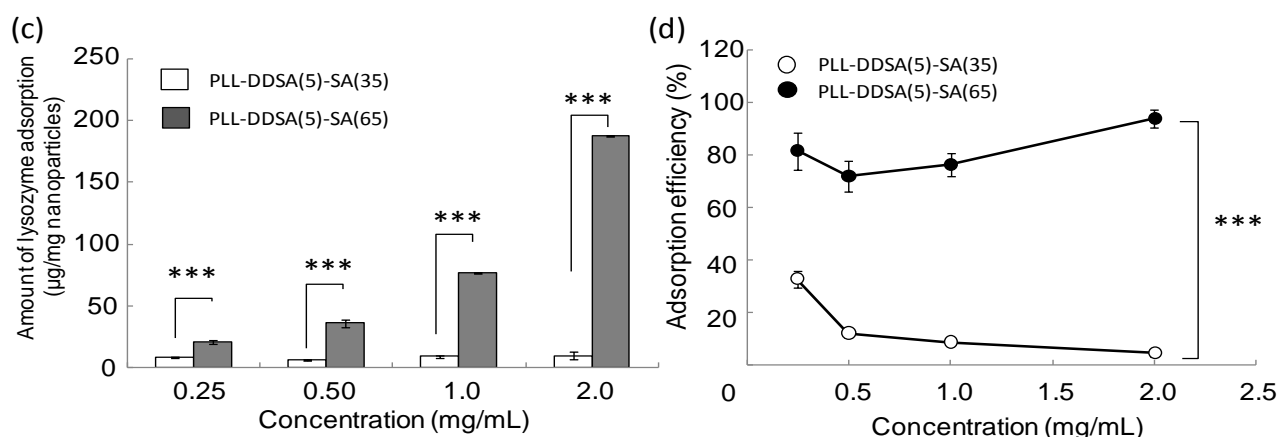
Figure 2.4 Protein adsorption on/into nanoparticles. Amount of (a) BSA and (c) lysozyme adsorption on/into polyampholyte nanoparticles and their adsorption efficiency with different concentrations of (b) BSA and (d) lysozyme. The change in slope corresponded to the CAC of each polyampholyte. Data are expressed as the mean ± SD. ***P < 0.001.
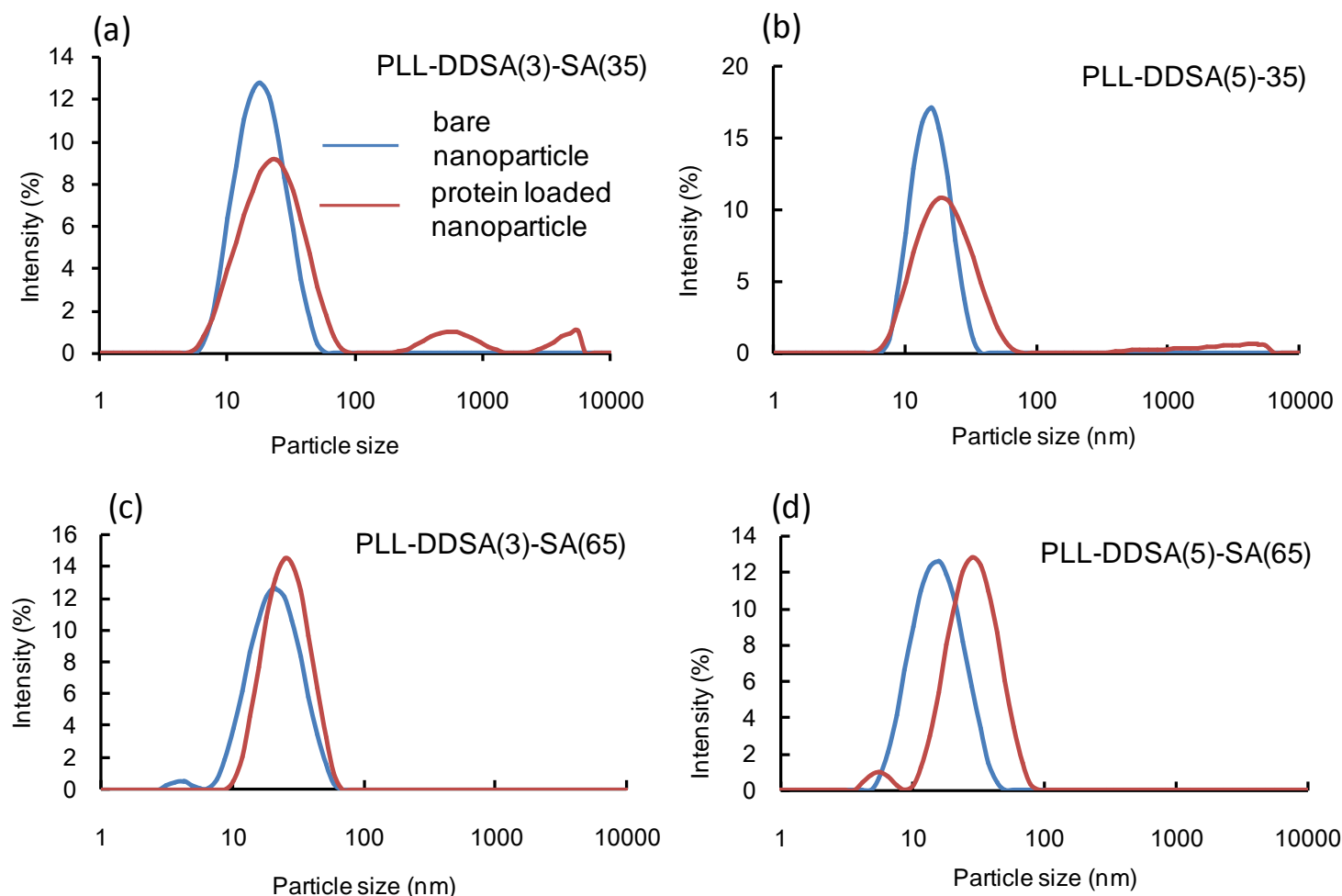
2.3.4 Characterization of protein-loaded polyampholyte nanoparticles

2.3.4.1 Particle size of protein-loaded polyampholyte nanoparticles

The particle size of the protein-loaded nanoparticles (20 nm) was slightly larger than the bare nanoparticles. The particles sizes increased due to the strong electrostatic interactions between the nanoparticles and proteins, as shown in **Figure 2.5** and **Table 2.2**.

Table 2.2 The size of hydrophobically modified polyampholyte nanoparticles before and after protein adsoprtion

Samples	Diameter before protein adsorption (nm)	Diameter after protein adsorption (nm)
PLL-DDSA(3)-SA(35)	16.15±0.23	22.61±0.16
PLL-DDSA(5)-SA(35)	15.72±0.15	19.57±0.28
PLL-DDSA(3)-SA(65)	18.56±0.44	22.40±0.17
PLL-DDSA(5)-SA(65)	13.48±0.41	24.65±0.38

Figure 2.5 Size distributions of polyampholyte nanoparticles before and after protein adsorption.

2.3.4.2 Stability of protein-loaded polyampholyte nanoparticles

The average size of bare and protein-loaded polyampholyte nanoparticles were measured and stored at 25˚C for 7 d. The stability of polyampholyte nanoparticles was mainly affected by the particle size and distribution. Specifically, the size of bare polyampholyte nanoparticles did not change after incubation for 7 d in PBS (-), highlighting the stability of the nanoparticles (**Figure 2.6 a**). However, the size of the BSA-loaded PLL-DDSA (3 or 5)-SA(35) increased up to 3-fold during storage(**Figure 2.6 b**). In contrast, lysozyme-loaded PLL-DDSA(3 or 5)-SA(65) did not change in size. Notably, the zeta potential of PLL-DDSA (3 or 5)-SA(35) was a smaller absolute value than that of PLL-DDSA(3 or 5)-SA(65), and PLL-DDSA(3 or 5)-SA(35) nanoparticles aggregated.
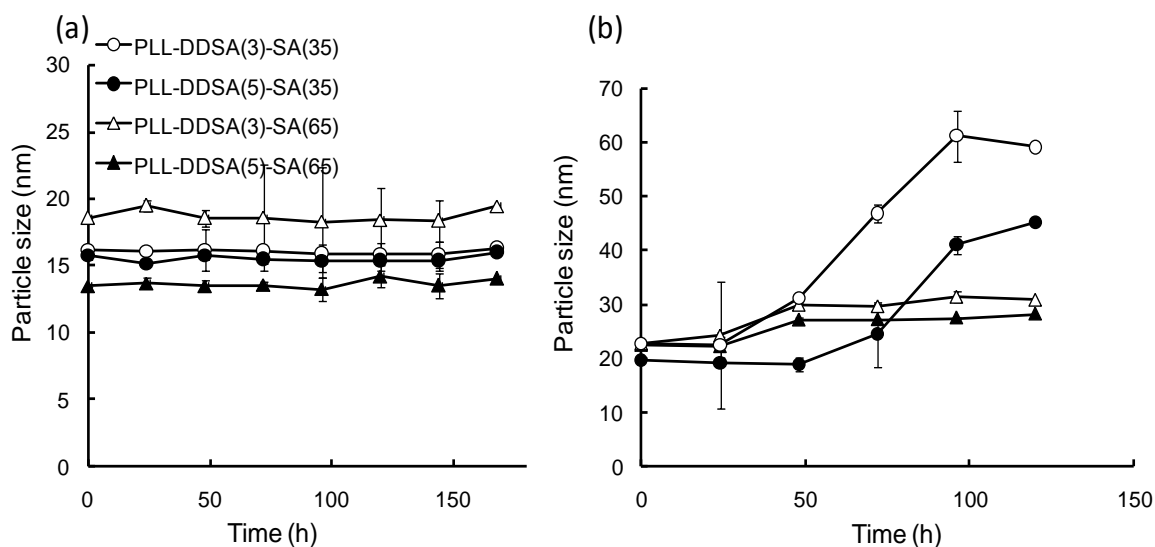
Figure 2.6 Size changes of (a) bare and (b) protein-loaded polyampholyte nanoparticles versus the incubation time at 25°C.

2.3.5 Freeze concentration

When cells are frozen with the appropriate concentration of cryoprotectant, ice crystal formation excludes solutes and the remaining solution can be concentrated. The cells located in the residual solution are exposed to a high osmotic pressure, leading to dehydration. By avoiding intracellular ice formation, cells can survive freezing.[39-41] Cryomicroscopic observations revealed that after ice crystal formation, residual water can exist in the cryoprotectant solutions and cells are located in the residual concentrated solution (**Figure 2.7 a**).

The residual water ratio during freezing in the presence of two types of cryoprotectants, 10% DMSO and 10% PLL-SA (65), was determined by solid-state ^{1}H-NMR and is given in **Figure 2.7 b**. The cells were in the highly concentrated residual water during freezing. Kataoka et al. reported that this freeze concentration mechanism was useful in a click chemistry reaction by the condensation of the reactants.[42] I also expected that the proteins in the medium were concentrated around the cell membranes, and could enhance the adsorption of the concentrated proteins.
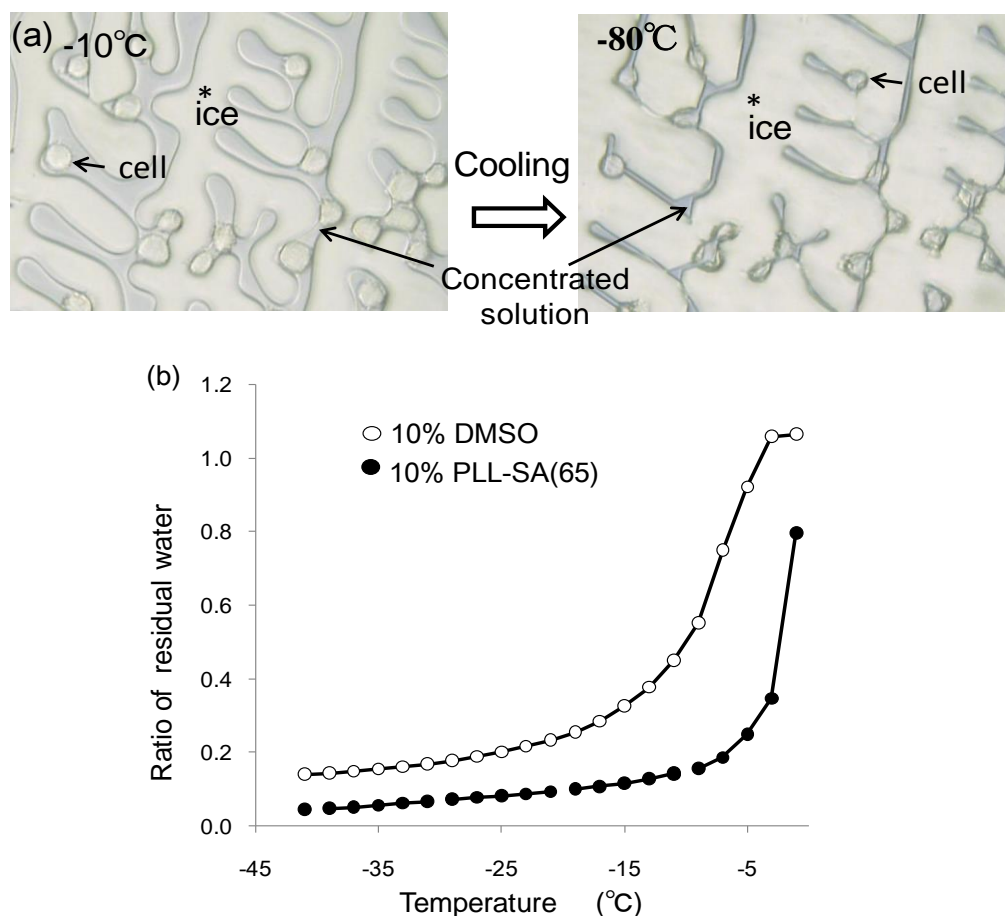
Figure 2.7 Freeze concentration during cell freezing with a cryoprotectant. (a) Cryomicrophotographs of cell suspension from −10 °C to −80 °C in the presence of 10% DMSO. Cells were located in the remaining concentrated solution. The bar: 10 μm. (b) Ratio of residual water during freezing with 10% DMSO and PLL-SA (65) measured by solid-state ^{1}H NMR.

2.3.6 Enhancement of protein adsorption by freeze concentration

### 2.3.6.1 Cell viability after freezing

L929 cells were frozen with protein-loaded polyampholyte nanoparticles (2 mg protein and 1 w/w% nanoparticles in the cell suspension) with 10 % PLL-SA (65) as a cryoprotectant. The cell viability after freeze-thawing is given in **Figure 2.8**. Over 80 % of cells survived freezing with 10 % DMSO and with 10 % PLL-SA (65). This result agreed with previous reports.[24,43,44] However, the cell viability after freezing with protein-loaded polyampholyte nanoparticles tended to decrease even with the addition of 10 % PLL-SA(65) as a cryoprotectant. Specifically, a significant decrease in the cell viability with PLL-

DDSA(3 or 5)-SA(35) was observed. PLL-DDSA(5)-SA(65) showed less of a decrease, regardless of the nature of the cryoprotectant (i.e., 10 % DMSO or PLL-SA(65)). These results might be explained by the cytotoxicity of the nanoparticles. The viability with various concentrations of nanoparticles was plotted (**Figure 2.9**) and the IC_{50} was 0.8 % (PLL-DDSA(3)-SA(35)), 1.0 % (PLL-DDSA(5)-SA(35)), 2.0 %(PLL-DDSA(3)-SA(65)), and 2.6 % (PLL-DDSA(5)-SA(65)). The high cytotoxicity of PLL-DDSA(3 or 5)-SA(35) may be due to the positive zeta-potential of the nanoparticles. The viability of cells with the positively charged nanoparticles was 60 %, whereas it was 80 % with the negatively charged nanoparticles. Therefore, I chose PLL-DDSA(3 or 5)-SA(65) for use in protein delivery by freeze concentration, as described in the following section.
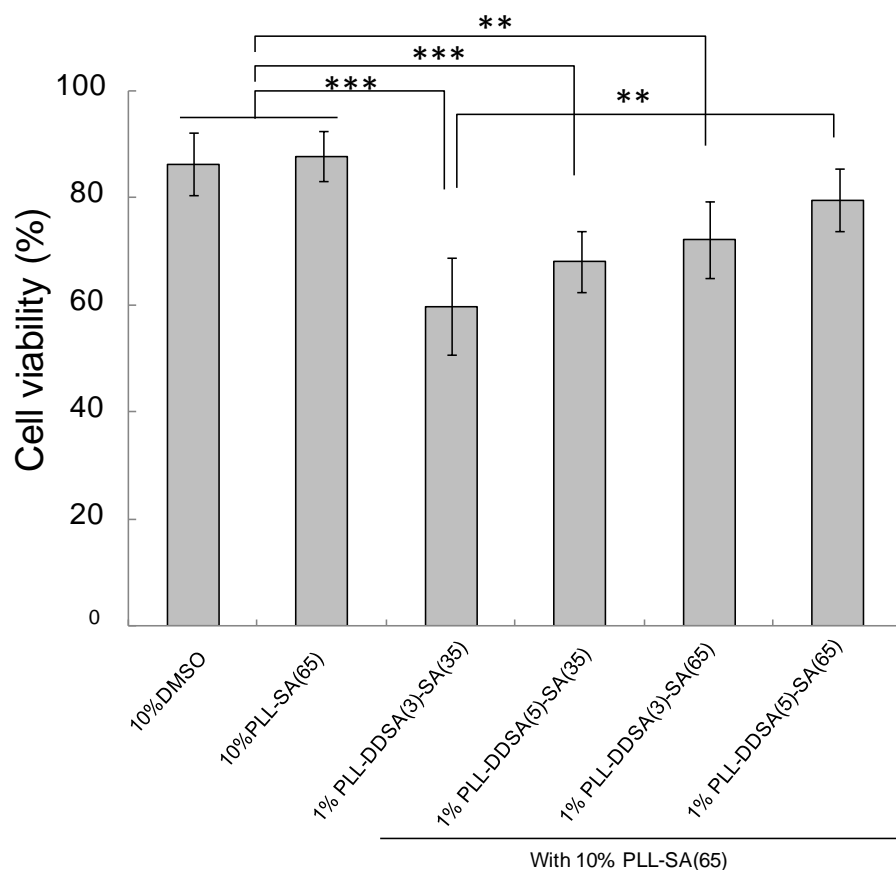
Figure 2.8 Cell viability after being frozen at $-80\,°C$ for 1 d with various protein-loaded nanoparticles in the presence of 10% PLL-SA(65) as a cryoprotectant. Cells were also frozen with cryoprotective solutions (10% DMSO and 10% PLL-SA(65); left two columns) alone. Data are expressed as the mean ± SD. ***$P < 0.001$, **$P < 0.01$.
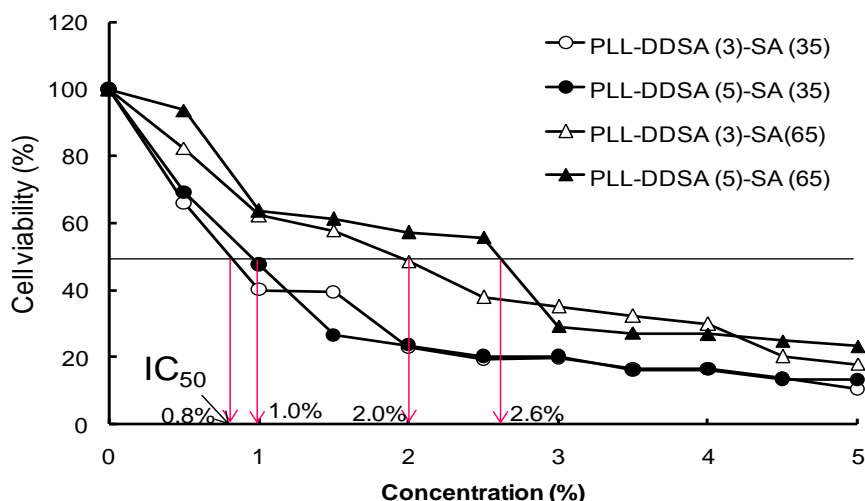
Figure 2.9. Cytotoxicity of nanoparticles. L929 cells were incubated with the indicated concentration of nanoparticles for 48 h, followed by the MTT assay. Data are described as the percentage of untreated cells. Meanvalues and standard deviations for independent triplicate experiments (8 samples each) are shown. IC_{50} represents the concentrationof nanoparticles thatcaused a 50% reduction in MTT uptake by atreated cell culture compared with the untreated controlculture.

2.3.6.2 Cellular delivery and uptake of BSA/Lysozyme delivered by the nanoparticles

Figure 2.10 a, b, c show the confocal microscope images of L929 cells before and after freezing in the presence of Texas red (TR)-conjugated, protein-loaded fluorescein isothiocynate (FITC)-conjugated polyampholyte nanoparticles with 10% PLL-SA(65) as a cryoprotectant. When cell were frozen in the presence of the FITC-conjugated PLL-SA(65) (TR-conjugated lysozyme), almost no fluorescence was observed around the cell membrane (**Figure 2.10 a**). Without DDSA, PLL-SA(65) did not form stable nanoparticles (**Table 2.1**) and showed no aggregation with lysozyme. Even if freeze concentration occurred, the concentrated polyampholyte and lysozyme might have had a weak affinity towards the cell membrane after thawing, and the protein would have diffused into the thawed solution. However, a high florescence (both FITC and TR) was observed on the cells after thawing (**Figure 2.10 b,c**), clearly indicating that the protein-loaded nanoparticles were condensed on the peripheral cell membrane by freeze concentration because of the high affinity between the cell membrane and the hydrophobic moieties of the nanoparticles. When poly(vinyl alcohol) and poly(ethylene glycol) modified with hydrophobic alkyl chains were added to cells, the micelle-like nanoparticles easily adsorbed on the cell membrane.[45] In the present study, the concentrations of the nanoparticles and the proteins were too low to identify the fluorescence

on the cells, but the hydrophobicity of the polyampholyte nanoparticles was strong enough to facilitate absorption onto the cell membrane, preventing diffusion into the medium after thawing. The enhanced protein adsorption to cells by freeze concentration occurred not only when PLL-SA(65) was used as a cryoprotectant, but also when DMSO was used (**Figure 2.11**). The fluorescence intensity with the two cryoprotectants was evaluated quantitatively using confocal microscopy. As shown in **Figure 2.10 d**, the fluorescence of TR, which was normalized by the intensity of each unfrozen control (white bar =100%), was significantly higher than that of the unfrozen cells with PLL-DDSA(3)-SA(65) and PLL-DDSA(5)-SA(65). The intensity was higher when PLL-SA (65) was used as compared to when DMSO was used, possibly because of a higher freeze concentration (**Figure 2.7b**). When the cells were frozen without cryoprotectants, cells did not survive and a very high fluorescence was observed because of cell membrane rupture (**Figure 2.12**). In addition, when PLL-DDSA (3 or 5)-SA(35) was used as a nanocarrier for BSA, enhanced TR-conjugated BSA adsorption was observed (**Figure 2.13**). However, the cytotoxicity of the cationic nanoparticles resulted in the low viability of the cells (viability 60%, **Figure 2.9**).
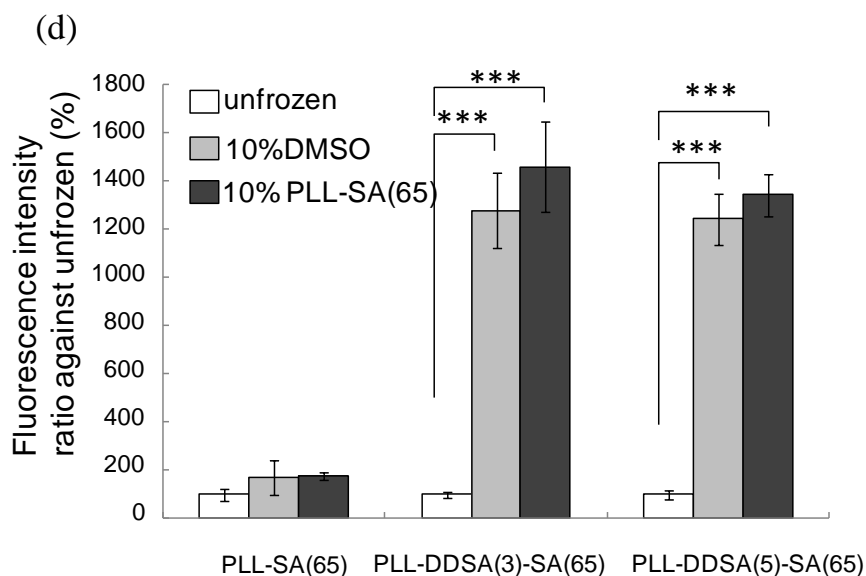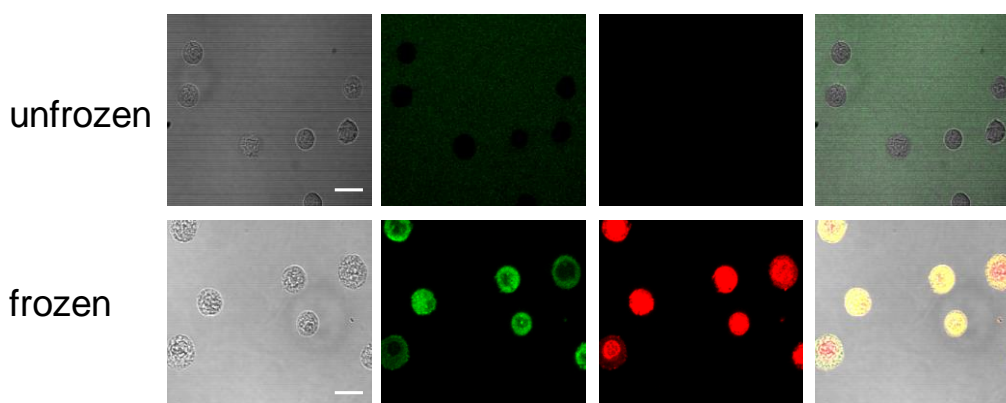
### (a) Cells frozen with mixture of protein and PLL-SA(65)
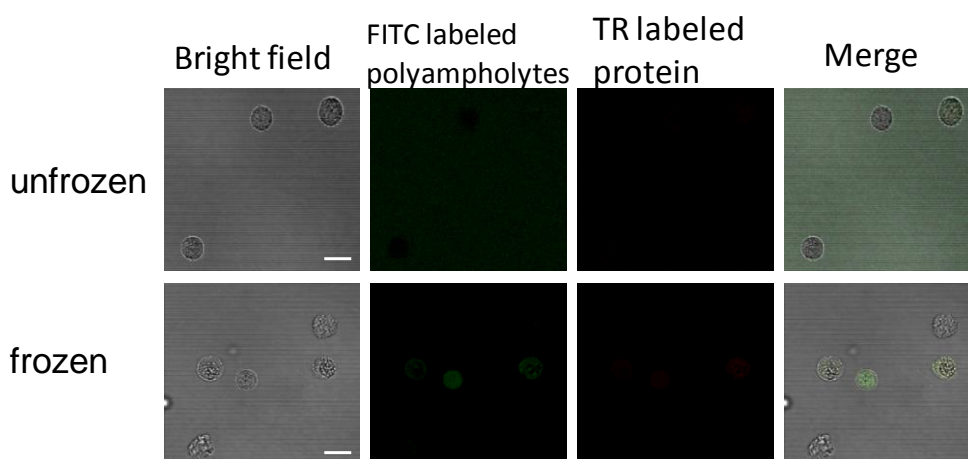
### (b) Cells frozen with protein-loaded PLL-DDSA(3)-SA(65)
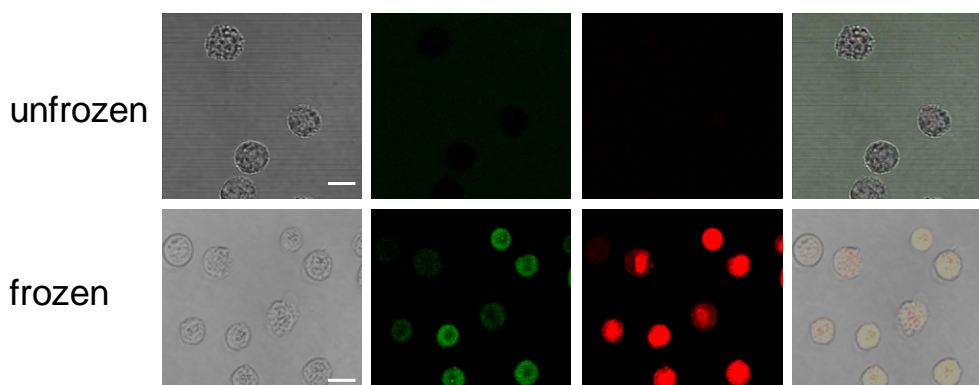
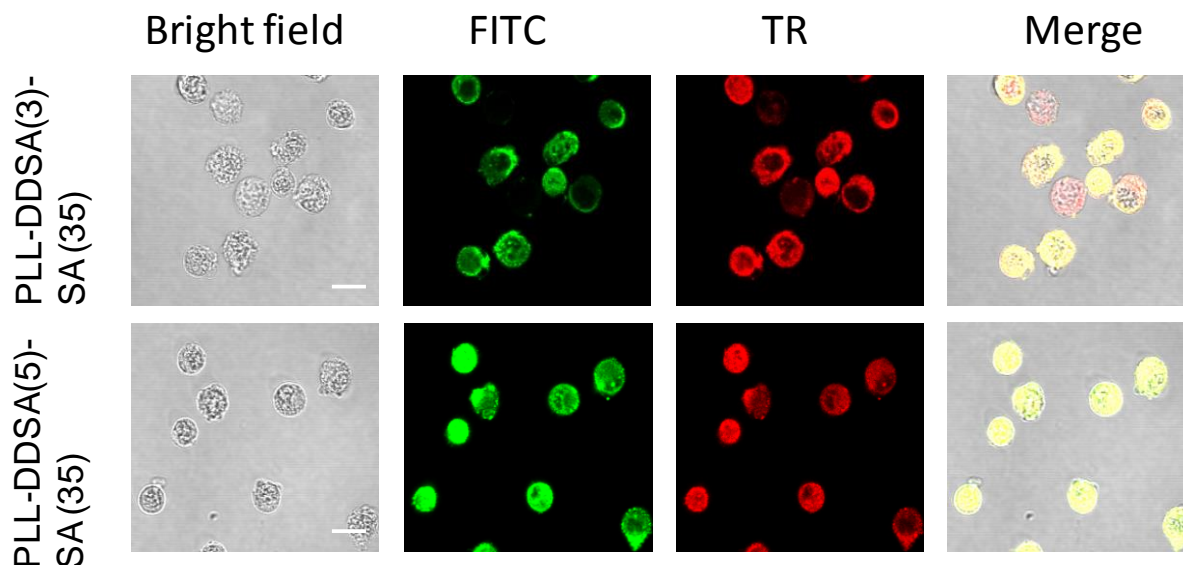## (c) Cells frozen with protein-loaded PLL-DDSA(5)-SA(65)

(d)

Figure 2.10 Confocal microphotographs of L929 cells before and after freezing with various protein-loaded polyampholyte nanoparticles with 10% PLL-SA(0.65) as a cryoprotectant. (a) Cells were frozen with lysozyme (2 mg) and PLL-SA(65). (b) Cell were frozen with protein-loaded PLL-DDSA(3)-SA(65) (lysozyme 2 mg, nanoparticles 10 mg in 1 mL DMEM). (c) Cells were frozen with protein-loaded PLL-DDSA(5)-SA(65) (lysozyme 2 mg, nanoparticles 10 mg in 1 mL). Nanoparticles were stained with FITC and lysozyme was stained with TR. The bars: 10 μm. (d) Quantitative analysis of fluorescence ratio of lysozyme adsorbed onto cells before and after being frozen with various protein-loaded nanoparticles. Data are expressed as the mean ± SD. ***$P < 0.001$
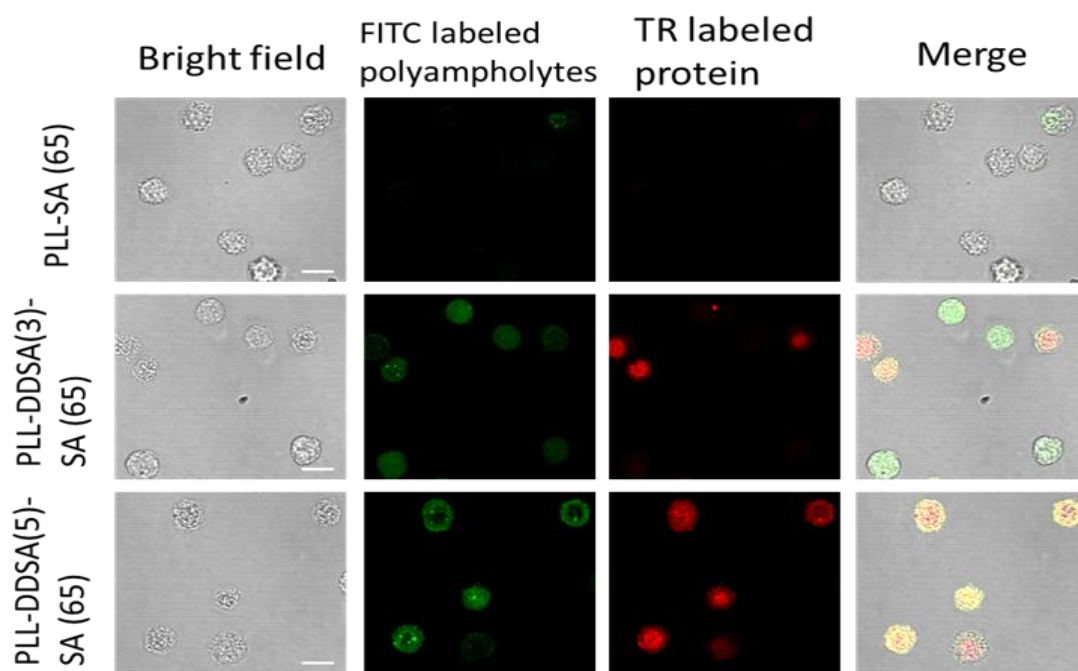
Figure 2.11 Confocal microphotographs of L929 cells after freezing with various protein-loaded polyampholyte nanoparticles with 10% DMSO as a cryoprotectant. The bars: 10μm.
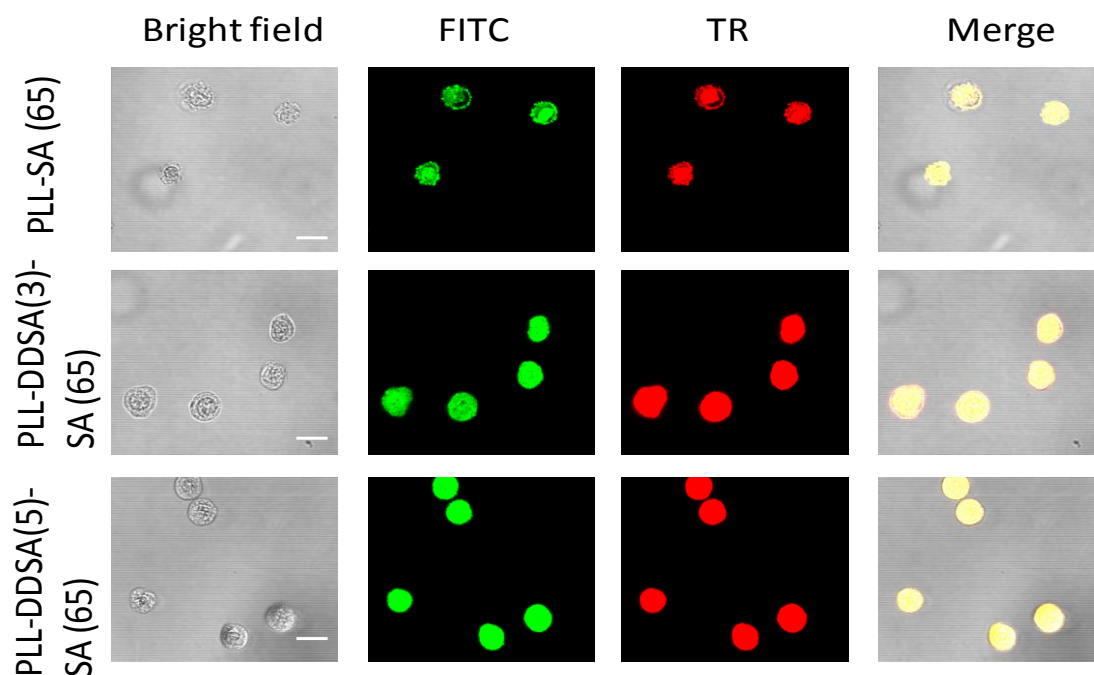

Figure 2.12 Confocal microphotographs of L929 cells after freezing with various protein-loaded polyampholyte nanoparticles without a cryoprotectant. No cells survived and a high fluorescence was observed because of cell membrane rupture. The bars: 10μm.

Figure 2.13 Confocal microphotographs of L929 cells after freezing with various BSA-loaded PLL-DDSA(3 or 5)-SA(65) nanoparticles with 10% PLL-SA(65) as a cryoprotectant. The bars: 10μm.

2.3.6.3 Internalization of protein-loaded nanoparticles by endocytosis

To evaluate the endocytotic uptake of BSA- and lysozyme-loaded polyampholyte nanoparticles by L929 cells, cells were seeded and incubated after thawing. Confocal microscopic images of cells frozen in the presence of lysozyme and PLL-SA(65) and lysozyme-loaded PLL-DDSA(3 and 5)-SA(65) nanoparticles are given in **Figure 2.14a**. From the four photos of the upper row, weak FITC and TR fluorescence was observed for the cells frozen without nanoparticles. In contrast, when cells were frozen with protein-loaded PLL-DDSA(3 and 5)-SA(65), a much higher fluorescence was obtained (middle and lower rows in **Figure 2.14a**). This clearly indicated that adsorbed protein and nanoparticles were internalized by endocytosis during culture. The mean intensity of the red fluorescence of cells is shown in **Figure 2.14b**. Each intensity was normalized by the intensity of the red fluorescence of the internalized TR-loaded lysozyme frozen without nanoparticles. This showed that a significantly higher internalization occurred when proteins were loaded with hydrophobically modified polyampholyte nanoparticles. The higher hydrophobicity enhanced the endocytosis of the protein-loaded nanoparticles. This result agreed the results of a previous study which showed that hydrophobic nanoparticles were easily internalized into cells by endocytosis.[46,47] When BSA-loaded PLL-DDSA(3 and 5)-SA(35) were used, similar results were obtained (**Figure 2.15**).
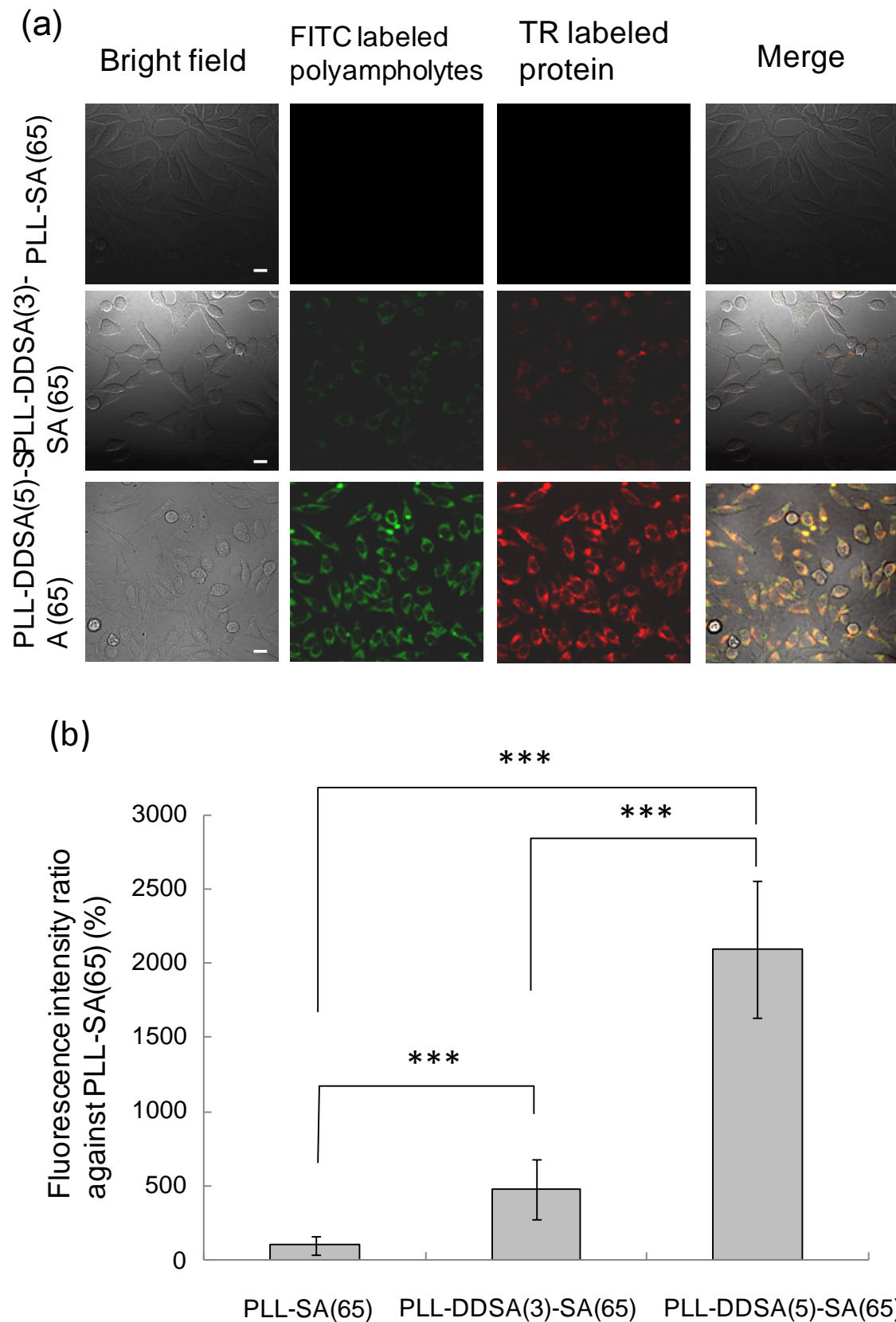
Figure 2.14 Protein internalization via endocytosis during culture after being frozen with lysozyme and PLL-(SA) and lysozyme-loaded PLL-DDSA(3 or 5)-SA(65) nanoparticles with 10% PLL-SA(65) as a cryoprotectant. The bars: 10 μm. Quantitative analysis of fluorescence ratio of lysozyme

internalized into cells after being frozen with various protein-loaded nanoparticles, against that with only PLL-SA(65). Data are expressed as the mean ± SD. ***$P < 0.001$
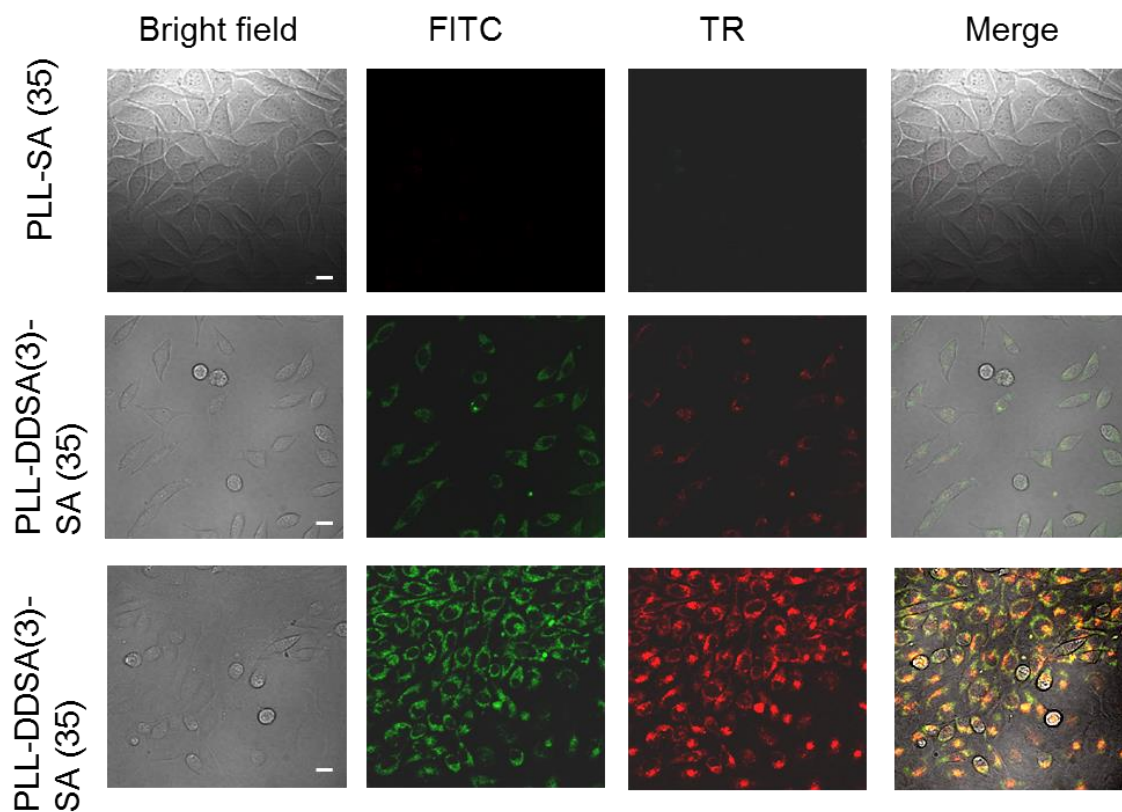
Figure 2.15 Protein internalization via endocytosis during culture after being frozen with BSA and PLL-(SA) and BSA-loaded PLL-DDSA(3 or 5)-SA(35) nanoparticles with 10% PLL-SA(65) as a cryoprotectant. The bars: 10μm.

2.4 Conclusion

In this study, the successful, efficacious, and safe delivery of proteins to cells was demonstrated using freeze concentration. First, I have developed self-assembled hydrophobic polyampholyte nanoparticles as delivery vehicles. These nanoparticles had narrow size distributions, exhibited positive and negative surface charges, and were used to adsorb and encapsulate model proteins lysozyme and BSA. Confocal fluorescence micrographs revealed that nanoparticles delivered their contents efficiently into the cytosol of cells after freezing. These results provided encouraging evidence for the development of an effective method for the cytoplasmic introduction of proteins. This technique might be useful for antigen cytoplasmic delivery to immune cells for immunotherapy or for gene delivery for gene therapy. In conclusion, freezing appeared to be a promising and versatile system for enhanced adsorption and internalization of drugs in vitro. Although further optimization of the cytotoxicity and protein adsorption onto the carriers should be conducted, I expect that this methodology can be globally applicable for the facile enhancement of protein delivery with nanocarriers.

2.5 References

1. Sengupta, D.; Eavarone, I.; Capila, G.; Zhao, N. Watson. *Nature* **2005**, *436*, 568.

2. Lundy, B.B.; Convertine, A.; Miteva, M.; Stayton, P.S. *Bioconjugate Chem.* **2013**, *24*, 398.

3. Deng , C.; Jiang , Y.; Cheng , R.; Meng, F.; Zhong, Z. *Nano Today* **2012**, *7*, 467.

4. Nishiyama, N.; Kataoka, K. *Pharmacology & Therapeutics* **2006**, *112*, 630.

5. Sakaguchi, N.; Kojima, C.; Harada, A.; Kono, K. *Bioconjugate Chem.* **2008,** *19*, 1040.

6. Han, S.; Mahato, R.I.; Kim, S.W. *Bioconjugate Chem.* **2001**, *12*, 337.

7. Takeuchi, Y.; Kurohane, K.; Ichikawa, K.; Yonezawa, S.; Ori, H.; Koishi, T.; Nango, M.; Oku, N. *Bioconjugate Chem.* **2003**, *14*, 790.

8. Sahoo, S.K.; Panda, A.K.; Labhasetwae, V. *Biomacromolecules* **2005**, *6*, 1132.

9. Kadir, M. A.; Kim, S. J.; Ha, E. J.; Cho, H. Y.; Kim, B. S.; Choi, D.; Lee, S. G.; Kim, B. G.; Kim, S. W.; Paik H. J. *Adv. Funct. Mater*. **2012**, *22*, 4032.

10. Xie, J.; Li, Y.; Xu, C.; Xia, M.; Qin, M.; Wei, J.; Wang, Q. *Biomater. Sci*. **2013**, *1*, 1216.

11. Li, Y.; Xiao, K.; J. Luo, J. Lee , S. Pan, K. S. Lam , *J. Controlled Rel.* **2010**, *144*, 314.

12. Takahashi, H.; Tahara, Y.; Sawada, S.; Akiyoshi, K. *Biomater. Sci.* **2013**, *1*, 842.

13. Maciel, D.; Figueira, P.; Xiao, S.; Hu, D.; Shi, X.; Rodrigues, J.; Tomas, H.; Li, Y. *Biomacromolecules* **2013**, *14*, 3140.

14. Larson, N.; Ghandehari, H. *Chem. Mater* **2012**, *24*, 840.

15. Wu, X.; Song, Y.; Han, J.; Yang, L.; Han, S. *Biomater. Sci.* **2013**, *1*, 918.

16. S. Salmaso, S. Bersani , F. Mastrotto , G. Tonon, R. Schrepfer , G.Stefano , P. Caliceti, *J. Controlled Rel.* **2012**, *162*, 176.

17. Serwer, L. P.; James, D. *Adv. Drug Deliv. Rev.* **2012**, *64*, 590.

18. Jaspreet, K.; Vasir, Labhasetwar, V. *Adv. Drug Deliv. Rev*. **2007**, *59*, 718.

19. Yamashita, F.; Hashida , M. *Adv. Drug Deliv. Rev.* **2013**, *65*, 139.

20. Benoit, D.; Boutin, M. *Biomacromolecules*, **2012**, *13*, 3841.

21. Cheng, R.; Feng, F.; Meng, F.; Deng, C.; Feijen, J.; Zhong, Z. *J. Controlled Rel.* **2011**, *152*, 2.

22. Englezos, P. *Dev. Chem. Eng. Mineral Process.* **1994**, *2*, 3.

23. Pham, Q. T. *Jpn J Food Eng*, **2008**, *9*, 21.

24. Matsumura, K.; Hyon, S. H. *Biomaterials* **2009**, *30*, 4842.

25. Matsumura, K.; Bae, J. Y.; Kim, H. H.; Hyon, S. H. *Cryobiology* **2011**, *63*,76.

26. Robin, R.; Minkle, J.; Matsumura, K. *J. Biomater. Sci. Polym. Ed.* **2013**, *24*, 1767.

27. Minkle, J.; Robin, R.; Hyon, S. H.; Matsumura, K. *Biomater. Sci.* **2014**, *2*, 308.

28. Yuba,E.; Harada, A.; Sakanishi, Y.; Watarai, S.; Kono, K. *Biomaterials* **2013**, *34*, 3042.

29. Annette, A. R.; Vandermeulen, G.W.M.; Klok, H. A. *Adv. Drug Deliv. Rev.* 2001, 53, 95.

30. Liu, R.; Lai, Y.; He, B.; Li, Y.; Wang, G.; Chang, S.; Gu, Z. *Int. J. Nanomedicine* **2012**, *7*, 5249.

31. Shen, H.; Akagi, T.; Akashi, M. Macromol.Biosci. 2012, 12, 1100.

32. Yu, H.; Huang, Y.; Huang, Q. *J. Agric. Food Chem.* **2010**, *58*, 1290.

33. Kataoka, K.; Matsumoto, T.; Yokoyama, M.; Okano, T.; Sakurai, Y.; Fukushima, S.; Okamoto, K.; Kwon, G. S. *J. Contolled Rel.* **2000**, *64*, 143.

34. Akiyoshi, K.; Deguchi, S.; Moriguchi, N.; Yamaguchi, S.; Sunamoto, J. *Macromolecules* **1993**, *26*, 3062.

35. Balasubramanian, S. K.; Poh, K. W.; Ong, C. N.; Kreyling, W. G.; Ong, W. Y.; Yu, L. E. *Biomaterials* **2013**, *34*, 5439.

36. Ananthapadmanabhan, K. P.; Goddard, E. D.; Turro, N. J.; Kuo, P. L. *Langmuir* **1985**, *1*, 352.

37. Astafieva, I.; Zhong, X. F.; Eisenberg, A. *Macromolecules* **1993**, *26*, 7339.

38. Mora-Huertas, C. E.; Fessi, H.; Elaissari, A. *Int. J. Pharm.* **2010**, *385*, 113.

39. Mazur, P.; Seki, S.; Pinn, I. L.; Kleinhans, F. W.; Edashige, K. *Cryobiology* **2005**, *51*, 29.

40. Matsumura, K.; Hayashi, F.; Nagashima, T.; Hyon, S. H. Cryobiology and *Cryotechnology* **2013**, *59*, 23.

41. Mandumpal, J. B.; Kreck, C. A.; Mancera, R. L. *Phys. Chem. Chem. Phys.* **2011**, *13*, 3839.

42. Takemoto, H.; Miyata, K.; Ishii, T.; Hattori, S.; Osawa, S.; Nishiyama,N.; Kataoka, K. *Bioconjugate Chem.* **2012**, *23*, 1503.

43. Matsumura, K.; Bae, J. Y.; Hyon, S. H. *Cell Transplant*. **2010**, *19*, 691.

44. Matsumura, K.; Hayashi, F.; Nagashima, T.; Hyon, S. H. *J. Biomater. Sci. Polym. Ed.* **2013**, *24*, 1484

45. Inui, O.; Teramura, Y.; Iwata, H. *ACS Appl. Mater. Interfaces* **2010**, *2*, 1514.

46. Wu, B.; Tang, S.; Chen, M.; Zheng, N. *Chem. Commun*. **2014**, *50*, 174.

47. Ding, H.; Ma, Y. *Nanoscale*, **2012,** *4*, 1116.

48. Delaglio, F.; Grzesiek, S.; Vuister, G. W.; Zhu, G.; Pfeifer, L.; Bax, A. *J. Biomol. NMR* **1995**, *6*, 277.

49. Johnson, B. A. *Methods Mol. Biol*. **2004**, *278*, 313.

50. Guha, A.; Devireddy, R. *Ann. Biomed. Eng.* **2010**, *38*, 1826.

51. Balasubramanian, S. K.; Bischof, J. C.; Hubel A. *Cryobiology* **2006**, *82*, 62.

Chapter 3

Enhanced Protein Internalization and Efficient Endosomal Escape using Polyampholyte-modified Liposomes and Freeze Concentration

3.1 Introduction

The targeted intracellular delivery of drugs has received considerable attention over the last few decades for improvement of biological activity.[1] Various biomaterials are available, and their use has already been shown to be a milestone in the treatment of deadly diseases.[2] Protein-based therapeutic materials play a prominent role in the medical field for the treatment of various disorders such as cancer,[3] diabetes,[4] and inflammatory diseases.[5] However, peptide-based drugs have several inherent problems as they show difficulty in entering the plasma membrane. Currently, several methodologies are being tested to improve their targeted delivery. Of these, controlled release has been reported for only a few methods, including electroporation,[6] microinjection,[7] and ultrasonication.[8] The most actively investigated approach, electroporation, induces cell death when the permeabilizing electric field is applied because of the associated loss of cell homeostasis.[9] Therefore, site-specific and efficient delivery systems still pose difficulties. Consequently, suitable nanocarriers have been studied for improving the safe and controlled release of peptides to ensure that they reach their targets to a greater extent.[10] To date, various nanocarriers including liposomes, polymeric micelles, and nanoparticles have been studied for the delivery of therapeutic materials;[11,12] however, many have shown limitations such as cytotoxicity, low stability, and low efficacy.[13,14] Among the nanocarriers, liposomes have attracted much attention as a desirable protein-based drug carrier system since they possess the advantages of being feasible under mild conditions, biocompatible with low toxicity, and exhibiting high affinity toward the cell membrane.[15] Furthermore, additional properties such as ease of size control and the ability to modify their surfaces enhances their suitability as a vehicle system

More recently, liposomes modified by polymers have been developed to improve their targeting ability. For example, many groups such as Kono et al. have successfully developed pH sensitive liposomes by modifying their surface using polyglycidol derivatives; these liposomes efficiently delivered antigenic molecules to the cytosol of dendritic cells in vitro. [18] There are applications for the transport and intracellular delivery of proteins using pH-sensitive liposomes in cancer therapy and also in gene therapy.

To address these issues, I developed an approach called freeze concentration, as previously described.[19] Freeze concentration is recognized as a physicochemical phenomenon wherein water molecules crystallize to form ice, leading to increased solute concentrations in the remaining unfrozen solution forming a phase separation during freezing.[20] Specifically, spontaneous ice nucleation occurs and ice grows in all directions when a solution is

supercooled at −5 to −45 °C. A high solute concentration remains in the unfrozen solution leading to a concentrated solute around the cells located in the residual solution.[21, 22] Previously, I have calculated the sodium ion concentration during freezing in the presence of a cryoprotectant by measuring the amount of residual water by using ^{1}H-NMR.19 When we used DMSO as a cryoprotectant, at −40 °C the sodium ion concentration was approximately 7 times higher than it was before freezing. When I used polyampholyte as a cryoprotectant, the sodium ion concentrated >10 times higher than that at room temperature. This finding indicates that the extracellular concentration of certain materials increases because they are ejected from ice crystals during freezing. This phenomenon might be one of the best strategies identified so far to enhance adsorption of the protein/carrier complex applied to cells, owing to the increase in the peripheral cell concentration. Within this strategy, the interaction between the cell membrane and protein/carrier complex is quite important because after thawing, the adsorbed complex should be internalized instead of diffusing back into the solution. This suggests that it can reduce the quantity of valuable materials that is internalized into cells. Additionally, freeze concentration strategies have several advantages in that they are simple, cost-effective, and highly reliable, and they are characterized by a lack of toxicity, high cell viability, and enhanced interaction between drugs and the cell membrane.

In my previous chapter I had designed novel polyampholyte nanoparticles as a carrier system by modification with dodecylsuccinic anhydride (DDSA) as a hydrophobic moiety that showed self-assembly, forming intermolecular hydrophobic and electrostatic interactions. However, these nanoparticles became cytotoxic at certain concentration levels.[19] These protein–nanocarrier complexes were highly internalized using the freeze concentration methodology, although the endosomal escape and uptake mechanism of the complexes that had obtained internalization by passing through the plasma membrane was not elucidated.

The endosomal escape process is crucial for the functionality of internalized proteins. Most particles enter cells through endocytosis and subsequently reach vesicles known as endosomes with pH 5.5 via the endosomal pathway.[23] However, numerous nanocarrier/protein complexes are entrapped within the endosome and are then destroyed after fusion with lysosomes, which are the primary sites of enzymatic degradation.[24, 25] Various pathways exist for the internalization of vesicles including caveolae-, clathrin-, or receptor-mediated endocytosis, phagocytosis, or macropinocytosis. The phagocytosis process is regulated by specialized cells such as macrophages and monocytes. In contrast, clathrin- and caveolae mediated endocytosis and macropinocytosis are important processes of

pinocytosis that include receptor ligand interactions based on particle size and surface chemistry.[26,27] Among the strategies utilised, membrane disruptive carriers have great potential to facilitate antigen escape from the endosomes.[28] This approach is beneficial for delivering anticancer drugs, genes, or vaccines into cancerous cells. In this chapter, I present the development of a new carrier system composed of liposomes modified by hydrophobic polyampholytes in which the liposomes themselves function as a low toxicity and biocompatible material. Lysozyme was used as a model protein in this study because it is positively charged under physiological conditions and has a high affinity for liposomes under aqueous conditions. The confirmation of efficient uptake of the protein/liposome complexes by endocytosis following freeze concentration was also investigated and furthermore, I describe the mechanism underlying the enhanced cellular uptake pathways for internalization. In addition, the endosomal escape ability of unmodified and polyampholyte-modified liposomes was also determined. These findings will provide a mechanistic understanding of the use of the novel freeze concentration approach for cell cargo delivery purposes. This methodology will likely be useful for in vitro gene delivery applications in future.

3.2 Materials and Methods

3.2.1 Reagents

DOPC, DOPE, Rh-PE, FITC-PE were purchased from Avanti Polar Lipids (Alabaster, AL, USA), and LysoTracker Green DND-26 and Hoechst 33342 were purchased from Molecular Probes Inc. (Eugene, OR, USA). Filipin, EIPA, and lysozyme were obtained from Sigma Aldrich (St Louis, MO, USA). Chloropromazine was obtained from Nacalai Tesque (Kyoto, Japan). Bradford Ultra was purchased from Expedeon Ltd (Cambridge, UK), and Sephadex G25 was obtained from GE Healthcare Bioscience Corp. (Piscataway, NJ, USA).

3.2.2 Preparation of FITC-labelled lysozyme

Lysozyme (10 mg) and FITC (1 mg mL^{-1}; Dojindo Laboratory, Kumamoto, Japan) solution was dissolved in sodium bicarbonate buffer solution (1 mL; 0.5 M, pH 9.0) with gentle stirring and incubated at 4 °C overnight with subsequent dialysis (molecular weight cut off: 3 kDa, Spectra/Por, Spectrum Laboratories, Inc., Rancho Dominguez, CA, USA) for 3 days against water and freeze dried.[18]

3.2.3 Preparation of polyampholyte cryoprotective agent and hydrophobic polyampholyte

A polyampholyte cryoprotectant was synthesized by succinylation of the polymer (PLL). To obtain the PLL-SA cryoprotective agent, an aqueous solution of 25% (w/w) PLL (10 mL, JNC Corp., Tokyo, Japan) and SA (1.3 g; Wako Pure Chem. Ind. Ltd, Osaka, Japan) were mixed at 50 °C for 2 h to convert 65% of the amino groups to the carboxyl groups (**Scheme 3.1**).[19,22] Polyampholyte nanoparticles were synthesized according to a previous report.[19] Briefly, an aqueous solution of ε-PLL (10 mL; 25% w/w, JNC Co. Ltd, Yokohama, Japan) was added to 5% molar ratio DDSA (Wako Pure Chem. Ind. Ltd, Osaka, Japan) at 100 °C and allowed to mix for 2 h to obtain hydrophobically modified PLL (**Scheme 3.1**). Subsequently, SA was added at 65% molar ratio (COOH/NH$_2$) and was allowed to react for 2 h at 50 °C (**Scheme 3.2**). The degrees of substitution of SA and DDSA were obtained by ^{1}H-NMR. The spectra were obtained at 25 °C on a Bruker AVANCE III 400 spectrometer (Bruker BioSpin Inc., Fällanden, Switzerland) in D$_2$O.

3.2.4 Preparation of liposomes

Liposomes were composed of a DOPC and DOPE mixture at a molar ratio of 1 : 1. We used DOPE because it tends to form a hexagonal inverted phase leading to the formation of a nonlamellar structure that can facilitate aggregation, which in turn favors destabilization.[51] Briefly, appropriate amounts of lipid DOPC (10 mg) and DOPE (9.46 mg) were dissolved in chloroform (1 mL). Chloroform was allowed to evaporate under a steady stream of nitrogen gas, following which the tubes were dried under vacuum to facilitate complete evaporation of the residual solvent. The dried lipids were dispersed in 1 mL of PBS (−) and extruded through a 100 nm polycarbonate membrane. When preparing lysozyme-encapsulating liposomes, lysozyme (10 mg) was dissolved in 1 mL PBS (−). Hydrophobic polyampholyte-modified liposomes were also prepared using the same method with the dry membrane of a lipid/polymer mixture (7: 3 w/w). Liposomes were then purified on a Sephadex G25 column to remove unreacted polyampholytes.[18]

3.2.5 Zeta potential and particle size measurements

The mean particle sizes, size distribution, and the surface charge measurements of the zeta potential of unmodified and polyampholyte modified liposomes were analysed by DLS analysis using a Zetasizer 3000 (Malvern Instruments, Worcestershire, UK) with a scattering angle of 135°. The colloidal suspension of liposomes was diluted with PBS and the particle

size analysis was carried out at a scattering angle of 135° and a temperature of 25 °C. The liposomes were dispersed in PBS (−) and the zeta potential values were measured at the default parameters of a dielectric constant at 78.5 and a refractive index at 1.6. Data were obtained as an average of more than 3 measurements on different samples.

3.2.6 Determination of encapsulation efficiency

After preparing lysozyme-modified liposomes or polyampholyte-modified liposomes, a working dispersion (1 mL) was made using a liposome suspension (20 µL) in PBS (−). Then the working dispersion (500 µL) was mixed with 6% (v/v) Triton X-100 (100 µL) and this solution was maintained at 65 °C for 5 min to disrupt all the vesicles. The solution (400 µL) was transferred into an ultra-0.5 centrifugal device for the removal of unencapsulated lysozyme (molecular weight cut off 50 kDa, Amicon® ultra (0.5 mL), Merck Millipore, Darmstadt, Germany) and centrifuged at 19 515g for 10 min.[52] PBS solution (400 µL) was again added, and the same procedure was repeated. The amount of un-encapsulated lysozyme was quantified by the Bradford assay using a Bradford Ultra reagent and the efficiency was determined by ultraviolet spectroscopy at 595 nm using lysozyme as a standard as follows:

% encapsulation efficiency= (Initial amount-unencapsulated protein)// (initial amount) x 100

3.2.7 Cell culture

Mouse fibroblast L929 cells (American Type Culture Collection, Manassas, VA, USA) were cultured in Dulbecco's modified Eagle's medium (DMEM; Sigma Aldrich) supplemented with 10% FBS at 37 °C under 5% CO_2 in a humidified atmosphere. When the cells reached 80% confluence, they were removed by 0.25% (w/v) trypsin containing 0.02% (w/v) ethylenediamine tetra-acetic acid in PBS (−) and were seeded on a new tissue culture plate for subculture.

3.2.8 Cytotoxicity assay of unmodified and polyampholyte-modified liposomes

Cytotoxicity was determined using an MTT assay. In a 96 well plate, L929 cells at a density of 1×10^3 cells per mL were cultured in each well and incubated under saturated humid conditions at 37 °C and 5% CO_2. After 24 h of incubation, unmodified liposomes and polyampholyte-modified liposomecontaining medium were added and incubated for 48 h. Then, 3-(4,5-dimethyl thial-2-yl)-2,5-diphenyltetrazalium bromide (MTT) solution (0.1 mL, 300 µg mL−1 in medium) was added to the cultured cells. The cells were incubated for 4 h at

37 °C. The solutions were removed and subsequently replaced by DMSO (100 μL) and allowed to stand for 15 min to allow a complete reaction. The resulting colour intensity measured using a microplate reader (Versa max, Molecular Devices Co., Sunnyvale, CA, USA) at 540 nm was proportional to the number of viable cells. The concentration of the liposomes leading to 50% cell killing (IC_{50}) was calculated from a concentration-dependent cell viability curve.[22]

3.2.9 Cell freezing with lysozyme-encapsulated liposomes

To prepare FITC-labelled lysozyme-encapsulating liposomes, Rh-PE-labelled liposomes (1.27×10^{-5} mol) and FITC-labelled lysozyme (10 mg mL^{-1}) were prepared as described previously.[18] The solution was applied to a Sepharose 4B column to remove unencapsulated proteins. L929 cells were counted and resuspended in 10% PLL-SA cryoprotectant (1 mL) to avoid freezing damage along with the unmodified or polyampholyte-modified liposome encapsulated lysozyme protein (5 mg mL^{-1}, 500 μL) without FBS at 4 °C at a density of 1×10^6 cells per mL in 1.9 mL cryovials (Nalgene, Rochester, NY, USA) and were stored in a −80 °C freezer overnight. These vials were thawed at 37 °C, diluted with DMEM, and the cells were washed 3 times with DMEM with 10% FBS.[19,22] The cell viability was analyzed by trypan blue dye exclusion using a hemocytometer. The total number of cells stained with trypan blue was recorded. Cell viability was determined as the number of viable cells divided by the total number of cells. Each condition was analyzed in triplicate. The adsorption of unfrozen and frozen protein-encapsulating liposomes was observed using a CLSM (FV-1000-D; Olympus, Tokyo, Japan).

3.2.10 Quantification of the adsorption of lysozyme protein onto cells by freeze concentration of unfrozen and frozen cells using flow cytometry

To determine the lysozyme protein uptake efficiency between unfrozen and frozen L929 cells, flow cytometric analysis was conducted. Cell freezing with the polyampholyte cryoprotectant solution incorporating lysozyme protein-encapsulating unmodified liposomes and polyampholyte-modified liposomes was discussed above. I used 1×10^6 cells for sample preparation and analysis by flow cytometry. The cells were then thawed, the old medium was removed, and the cells were washed 3 times with PBS (−).[53] Data acquisition and analysis were performed using a FACS Calibur instrument (BD Biosciences, Franklin Lakes, NJ, USA). The region of live cells was determined by FSC-SSC gating to exclude dead cells and debris noise. The flow cytometry analysis plot showed the gating strategy for identifying

stained and highly stained populations referring to non-stained cells (negative control) and cells cryopreserved in the absence of a cryoprotectant (positive control), respectively. A minimum of 20 000 cells were collected for each histogram.

3.2.11 Internalization

After thawing, the cells were washed with the medium and seeded in a glass bottom dish. The cells were incubated for 1 day. Then the attached cells were washed with PBS and the internalization of the protein/liposome complexes was observed using CLSM.

3.2.12 Determination of the internalization pathway via inhibition assay

Cells were pretreated with different concentrations of specific endocytotic inhibitors such as chloropromazine (for clathrin mediated endocytosis), EIPA (macropinocytosis), or filipin (caveolae-mediated endocytosis) to determine their optimal concentration using a trypan blue exclusion assay and then were cryopreserved with 10% polymeric cryoprotectant carrying unmodified or polyampholyte-modified liposomes in the cell culture medium at −80 °C. Solutions were thawed and the cells were counted to select the concentration producing the highest viability after inhibitor treatment. After addition of the optimized inhibitor concentration, cells at a density of 1×10^3 cells per mL were seeded into 96-well plates for at least 8 h to determine the uptake of particles from the extracellular solution. At the start of the experiment, the cell culture medium was aspirated and washed with PBS (−) 3 times to remove any traces of inhibitors. The mean fluorescence intensity was evaluated using a fluorescence microplate reader (Varioskan flash, Thermo Fisher Scientific, Inc., Waltham, MA, USA).[38] The endocytic uptake was also confirmed using CLSM.

3.2.13 Intracellular localization of lysozyme proteins in L929 cells

A thawed solution of L929 cells at a density of 1×10^3 cells per mL containing 10% cryoprotectant comprising lysozyme encapsulating unmodified or polyampholyte-modified liposomes was seeded onto a glass bottom dish. The cells were incubated for 12 h under a 37 °C humidified atmosphere with 5% CO_2. LysoTracker Green® DND-26 and Hoechst dye were added and incubated for 30 min prior to investigation. Samples were rinsed with PBS buffer and counterstained prior to imaging. The cells were analysed using CLSM.[54]

3.2.14 Internalization of the lysozyme protein using a currently available cationic amphiphile-based protein delivery reagent

A control experiment for protein delivery was performed using the PULSin™ protein delivery reagent (Polyplus transfection SA, Illkirch, France), according to the manufacturer's protocol for suspension cells. Briefly, 1×10^6 L929 cells were suspended in 1 mL serum-free medium in a sterile 15 mL centrifuge tube. In a separate tube, 7 μg of the lysozyme protein was mixed gently in 200 μL of HEPES buffer ((4-(2-hydroxyethyl)-1-piperazineethanesulfonic acid) (20 mM, pH-7.4)), after which 28 μL of the PULSin™ reagent was added immediately. Next, both solutions were incubated for 0.5 h or 4 h at 37 °C under a humidified atmosphere containing 5% CO_2. After incubation at 37 °C, the cells were centrifuged at 1000 rpm for 4 min and suspended in 1 mL cell growth medium. Cell viability was assessed by trypan blue exclusion. The cells were seeded in a glass-bottom dish to allow the internalization of proteins, as described previously.[35]

3.2.15 Statistical analysis

All data are expressed as means ± standard deviation (SD). All experiments were conducted in triplicate. To compare data among more than 3 groups, a 1-way analysis of variance with a post-hoc Fischer's protected least significant difference test was used. To compare data between 2 groups, the Student's t-test was used. The differences were considered statistically significant at a P value of <0.05.

3.3 Results and Discussions

3.3.1 Preparation of polyampholytes

A polyampholyte cryoprotectant was synthesized by succinylation with succinic anhydride (SA) to ε-poly-L-lysine (PLL) (PLL-SA, **Scheme 3.1**). From the [1] H-NMR chart, it was found that 65% of the amino groups were succinylated (**Figure 3.1**) and this compound was shown to have highly cryoprotective properties in 10% aqueous solution.[22] A hydrophobic-modified polyampholyte was synthesized by the reaction of PLL, DDSA, and SA (**Scheme 3.2**). The degree of substitution of SA obtained approximated 63.8% and of DDSA was 4.6% as determined by ^{1}H NMR (**Figure 3.1**). I denoted the polyampholyte cryoprotectant and hydrophobic polyampholyte as PLL-SA and PLL-DDSA-SA, respectively.
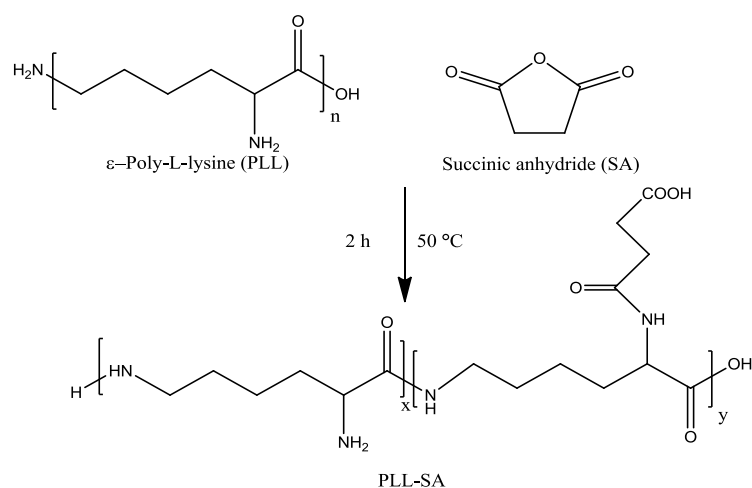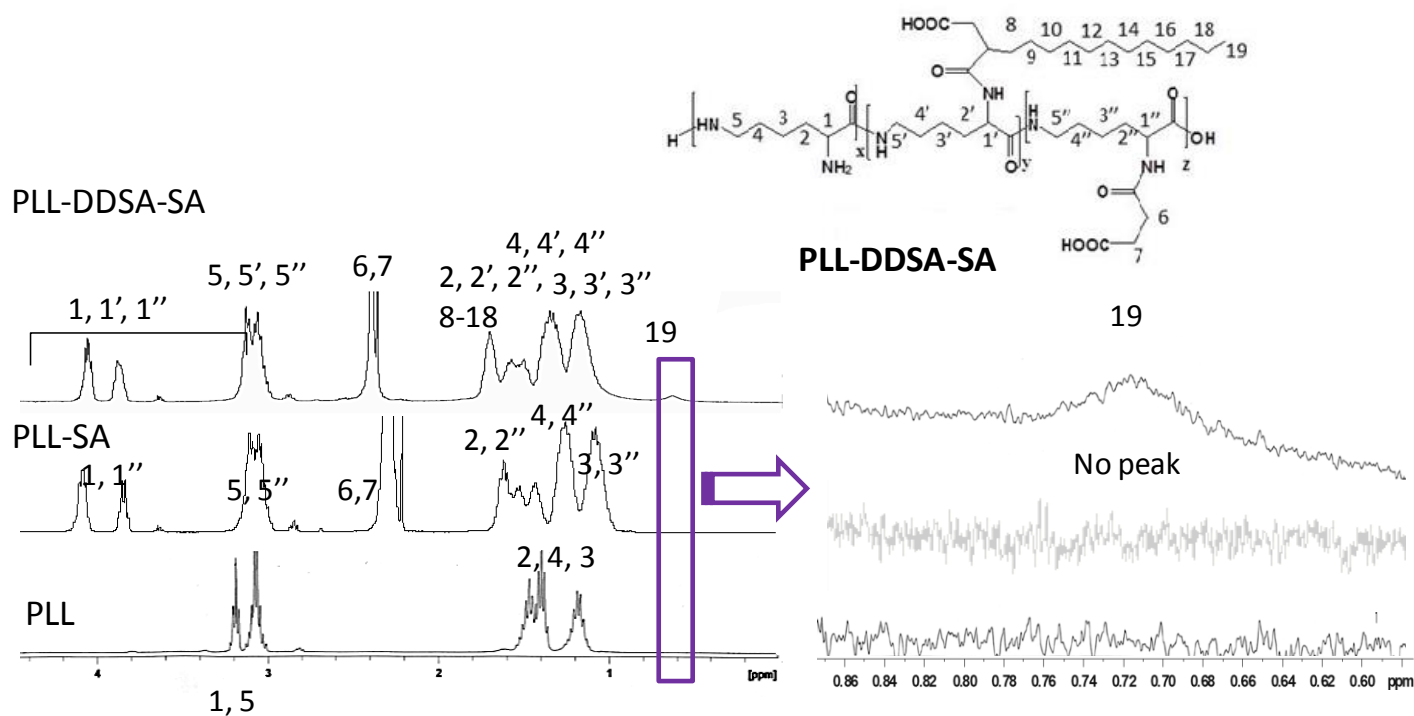
Scheme 3.1 Generation of polyampholyte cryoprotectant. PLL-SA was prepared using succinic anhydride
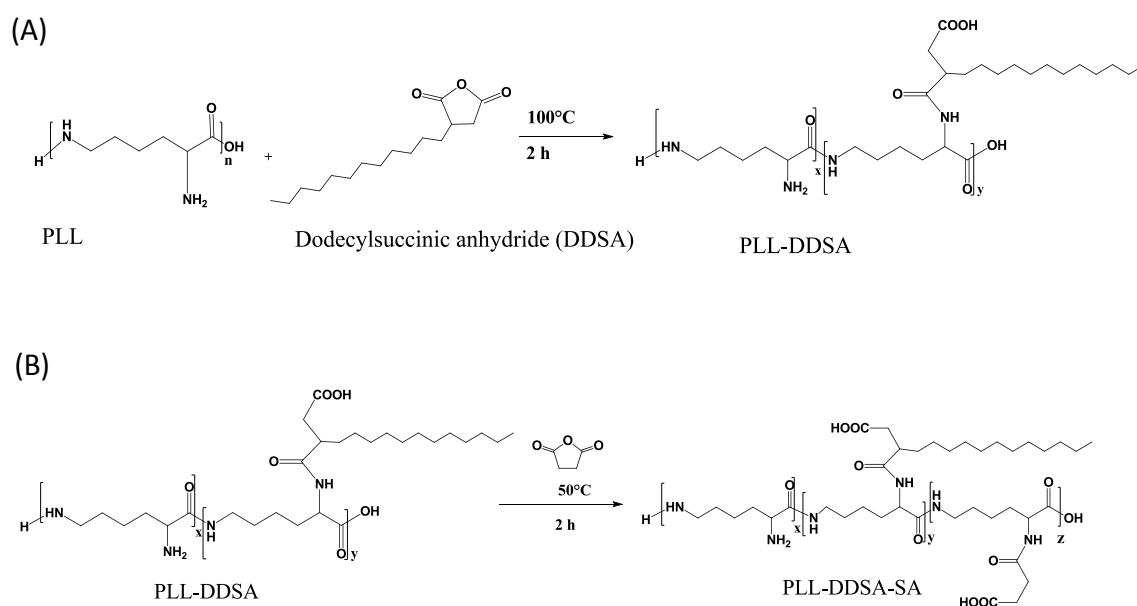
Scheme 3.2 Preparation of hydrophobically modified polyampholytes (PLL-DDSA-SA). (A) DDSA reaction with PLL. (B) SA reaction with DDSA-PLL

Figure 3.1 ^{1}H-NMR spectra of hydrophobically modified polyampholyte (PLL-DDSA-SA), polyampholyte (PLL-SA), and unmodified PLL.
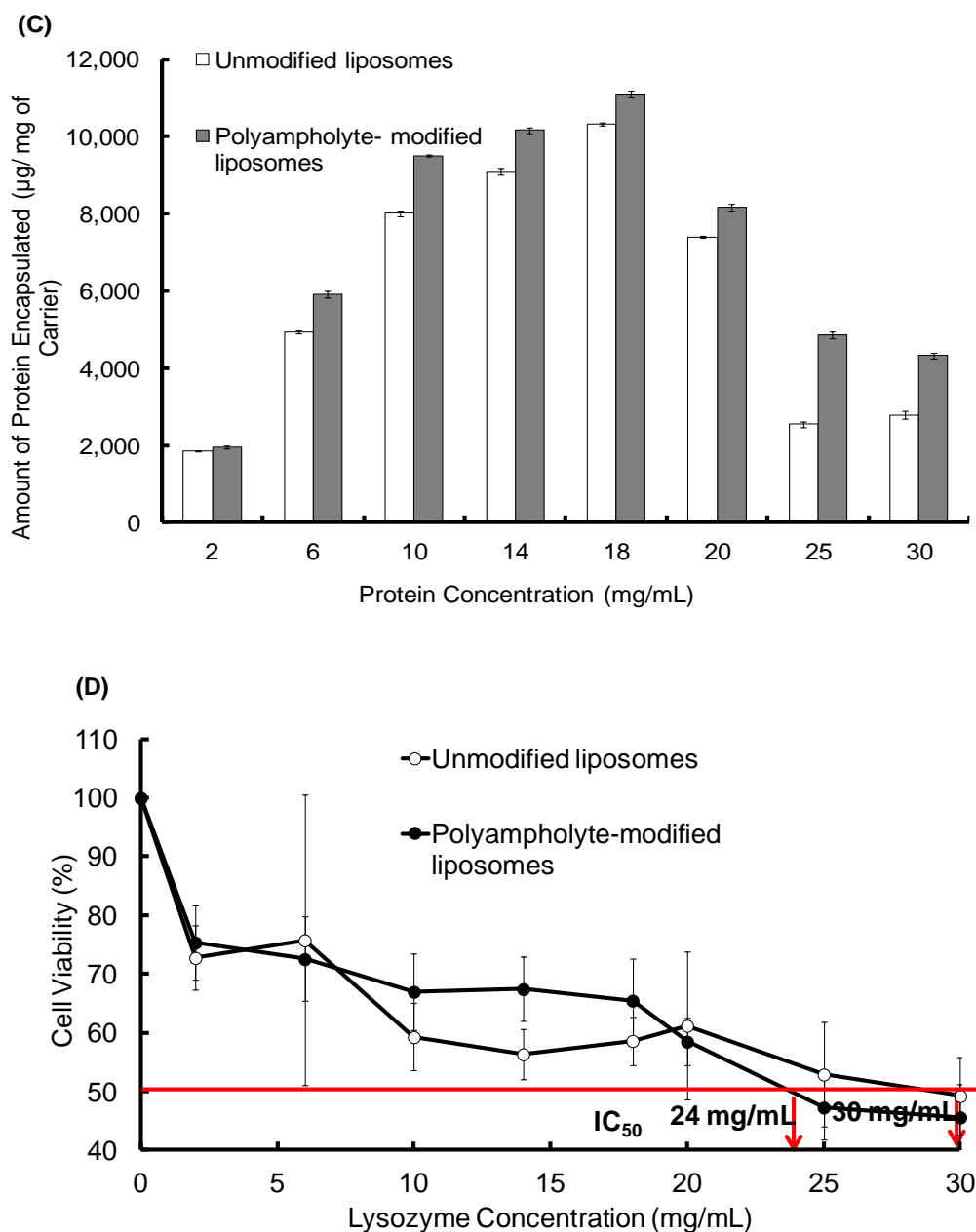
3.3.2 Preparation of protein-encapsulating liposomes

I prepared 2 types of liposomes, the first consisting of a 1 : 1 molar ratio of the zwitterionic lipids, 1,2 dioleoyl-snglycero-3-phosphocholine (DOPC) and 1,2, dioleoyl-sn-glycero-3-phosphoethanolamine (DOPE), and the other being a PLL-DDSA-SA-modified liposome. To encapsulate the lysozyme protein into the liposomes, I used the lipid film hydration method. Briefly, a DOPC/DOPE solution in chloroform was dried under vacuum to obtain a dry lipid layer including lipid film hydration with protein containing solutions with or without PLL-DDSA-SA that was subsequently extruded. The surfaces of lipid membranes composed of DOPC/DOPE with or without PLL-DDSA-SA were negatively charged. I investigated the amount of protein encapsulation into the liposomes and its efficiency using a Bradford assay. For protein encapsulation into liposomes, 1 mL phosphate buffer saline without calcium and magnesium (PBS (−)) containing various concentrations of lysozyme (2 to 30 mg mL^{-1}) was mixed with dried lipids and extruded to produce a liposome suspension, with or without PLL-DDSA-SA. A schematic illustration of unmodified and polyampholyte-modified liposomes is shown in **Figure 3.2 a**. The encapsulation efficiency was compared among various liposomes that constituted different concentrations of the lysozyme protein. **Figure 3.2 b** illustrates that the encapsulation efficiency of the lysozyme protein into unmodified liposomes decreases

with increasing amounts of loaded protein concentration. **Figure 3.2 c** shows the amount of the protein encapsulated at different loading concentrations under physiological conditions. **Figure 3.2 c** depicts the sharp increment that was observed upon increasing the amount of the encapsulated lysozyme protein but then decreases owing to the high concentration of the lysozyme protein and to a certain extent its hydrophilic nature. The same trend was observed for PLL-DDSA-SA-modified liposomes; however, the values of encapsulation efficiency were higher than those in unmodified liposomes at each lysozyme protein concentration. Introduction of polyampholyte molecules into the liposomes increased the minus value of the zeta-potential from −5.04 to −11.25 mV. This might explain the higher encapsulation efficiency of polyampholyte-modified liposomes due to the electrostatic interactions between the liposomes and lysozyme.

To optimize the conditions for the preparation of proteinloaded liposomes, cytotoxic behaviour was evaluated. Surface charge is an important factor that can be responsible for inducing cytotoxicity.[29] In this regard, cationic surface-charged liposomes showed a greater extent of cytotoxicity.[30] Therefore, I selected the negatively charged liposomes for use as a carrier in subsequent experiments.[31] **Figure 3.2 b** depicts that as the amount of lysozyme protein increases, the encapsulation efficiency considerably decreases, which results in the unencapsulated protein remaining in the solution. Therefore, the negative surface charges decrease their magnitude and ultimately show a positive charge that could potentially show toxic behaviour. **Figure 3.2 d** describes the high cell viability of L929 cells shifting downward as the loading amount of protein increases, which might be explained by the zeta potential. I therefore determined the zeta potential of unmodified and PLL-DDSA-SA-modified liposomes with different lysozyme protein loading amounts. The surface charges were shown to drastically change to a positive potential **(Figure 3.3).** We then investigated the cytotoxic effects after the addition of PLL-DDSA-SA to the liposomes. A small amount of PLL-DDSA-SA did not show any toxic activity. However after crossing the threshold ratio of 6: 4 (lipids: polyampholytes), the cell viability decreased drastically **(Figure 3.4).** This behaviour could possibly be due to the cytotoxicity of the polyampholyte at higher concentrations. Hence, I have chosen the liposome and polyampholyte composition (7: 3) and loading lysozyme protein concentration (10 mg mL^{-1}) accordingly for further investigations.

(A)

Protein loaded unmodified liposome

Polyampholyte
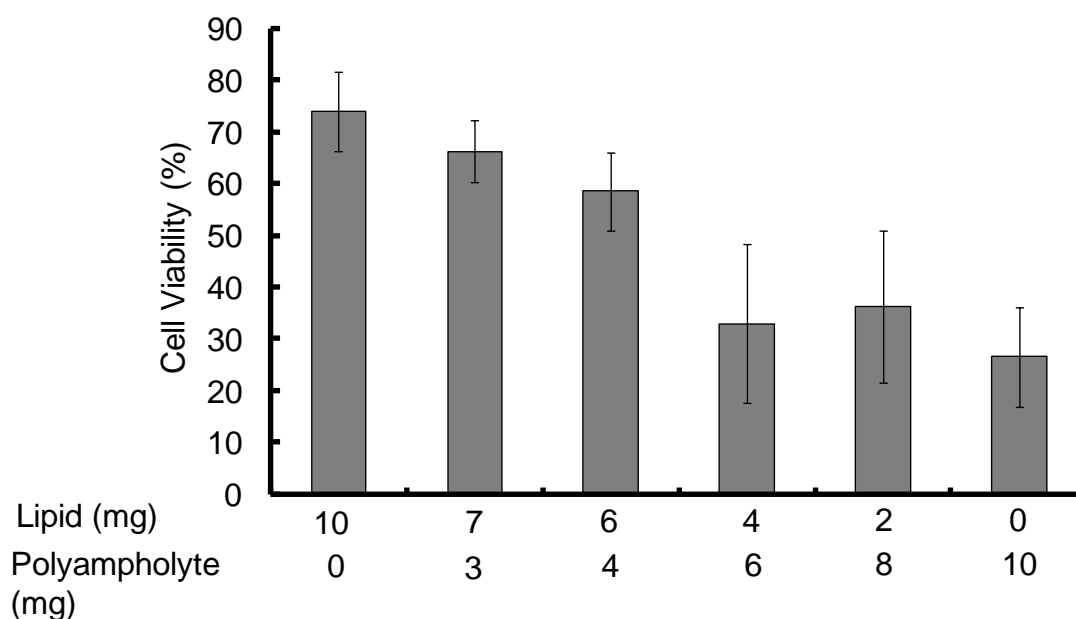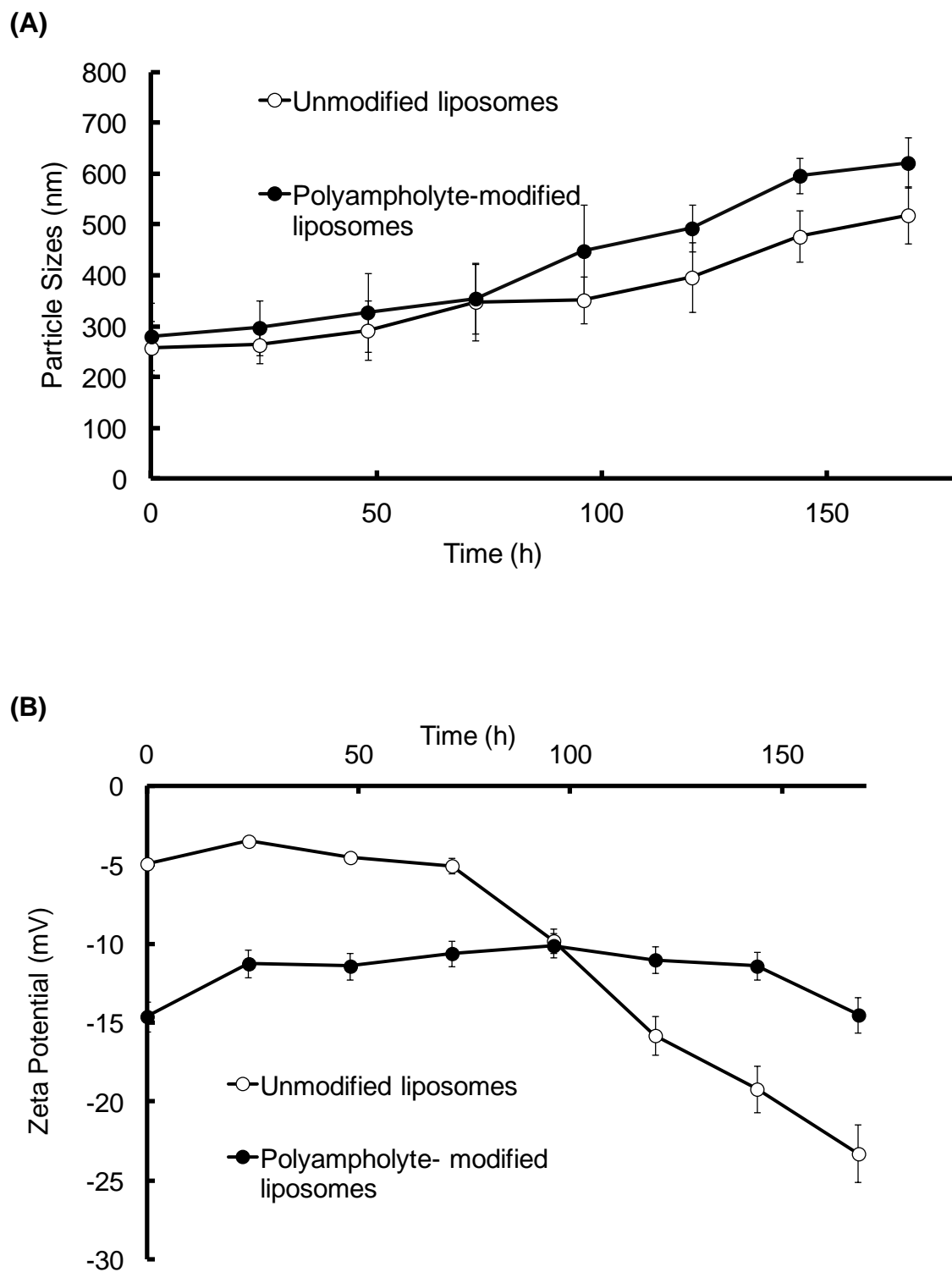
Protein loaded polyampholyte modified liposome

(B)
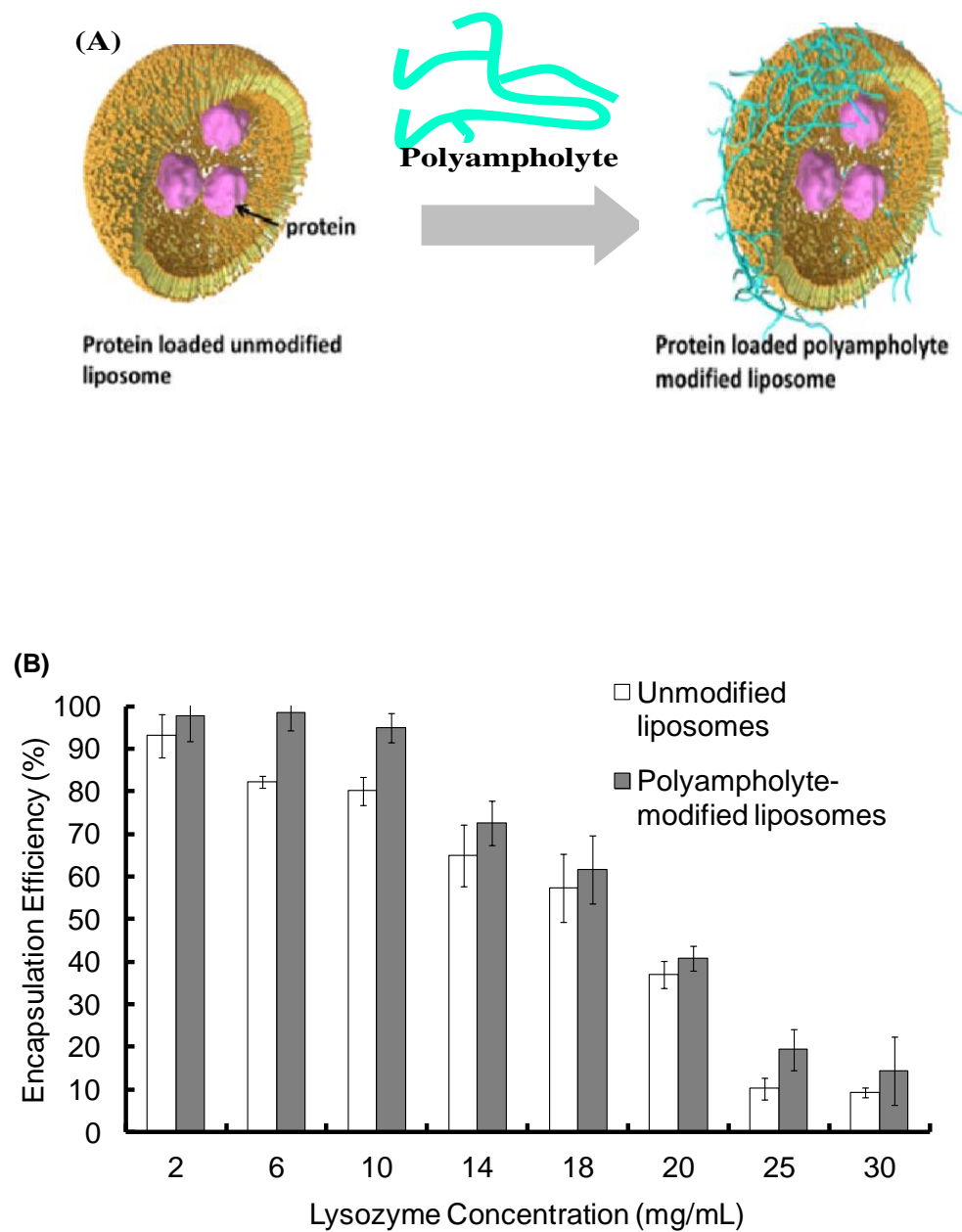
Figure 3.2 Protein encapsulation into unmodified and polyampholyte-modified liposomes with different protein concentrations (2 to 30 mg mL^{-1}). (a) Schematic illustrations of the preparation of protein loaded liposomes and polyampholyte-modified liposomes. (b) Encapsulation efficiency (c) amount of protein encapsulated, and (d) cytotoxicity of liposome-encapsulated proteins. L929 cells were incubated with liposomes loaded with different protein concentrations for 48 h, followed by MTT assay analysis. IC50 represents the concentration of proteins that caused a 50% reduction in MTT uptake by a treated cell culture compared with the untreated control culture; data are expressed as the mean ± standard deviation (SD).
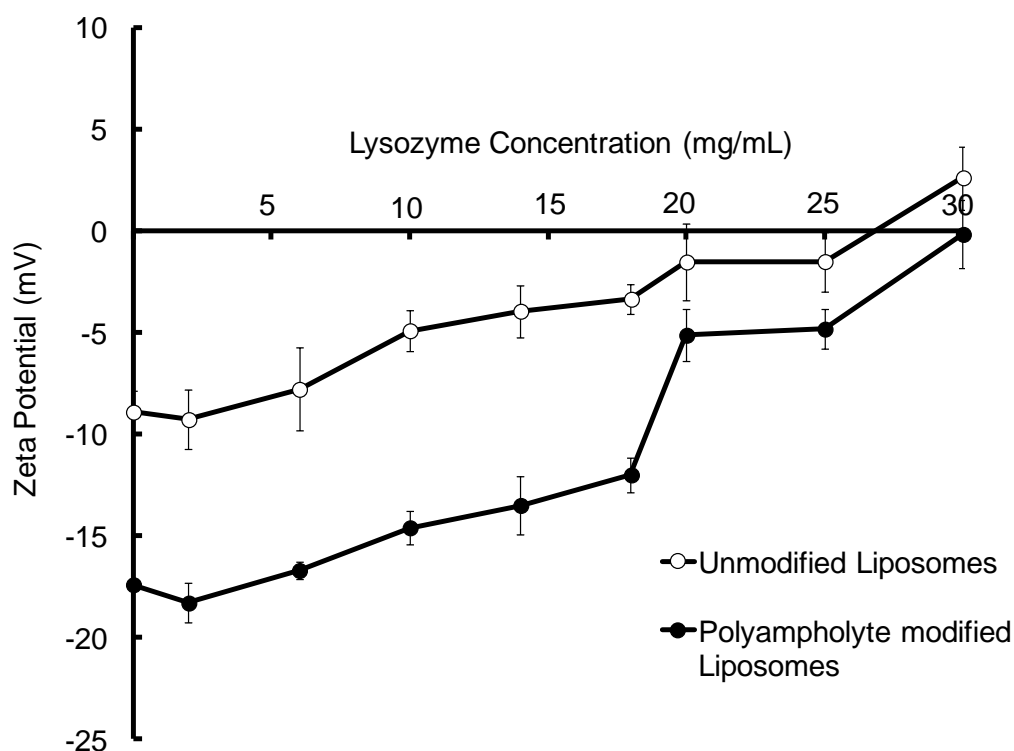
Figure 3.3 Zeta potentials of different concentrations of encapsulated proteins on unmodified liposomes and polyampholyte-modified liposomes.


Figure 3.4 Cytotoxicity of polyampholyte-modified liposomes with encapsulated lysozyme (10 mg/mL). L929 cells were incubated for 48 h with different ratios of liposomes and polyampholytes and a constant amount of lysozyme protein (10 mg/mL), followed by MTT assay analysis. Data are expressed as the mean ± standard deviation (SD).

(A)

(B)

Figure 3.5 Unmodified and polyampholyte-modified liposome-encapsulated proteins were incubated for 7 days at 25 °C. (a) Particle size; (b) Zeta potential.

Lysozyme-encapsulating liposomes showed increments in their particle size over 7 days as the potential significantly changed from −4.91 to −23.3 mV **(Figure 3.5 a and b).** On the other hand, the zeta potential of PLL-DDSA-SA-modified liposome complexes did not change even after 7 days **(Figure 3.5 b).** Furthermore, I investigated the particle size stability of unmodified or polyampholyte-modified liposomes under an ultra-cold temperature at −80 °C. Protein-encapsulated unmodified and polyampholyte-modified liposomes were frozen at −80 °C for 1 day with or without the use of any cryoprotectant. The solutions were thawed at 37 °C, and changes in particle sizes were investigated using dynamic light scattering (DLS). Without a cryoprotectant, the particle sizes were extremely large, showing the destabilization of protein molecules, which led to particle aggregation. However, the particle sizes of protein-encapsulated unmodified and polyampholyte-modified liposomes did not change when they were frozen in the presence of a polymeric cryoprotectant **(Figure 3.6).** These results clearly indicated that protein-encapsulated liposomes exhibit stability after treatment with a polymeric cryoprotectant. Based on these results, we successfully prepared stable liposomes loaded with a low-toxicity lysozyme and protein, both with and without PLL-DDSA-SA. The liposomes had a suitable size to serve as protein-delivery vesicles.
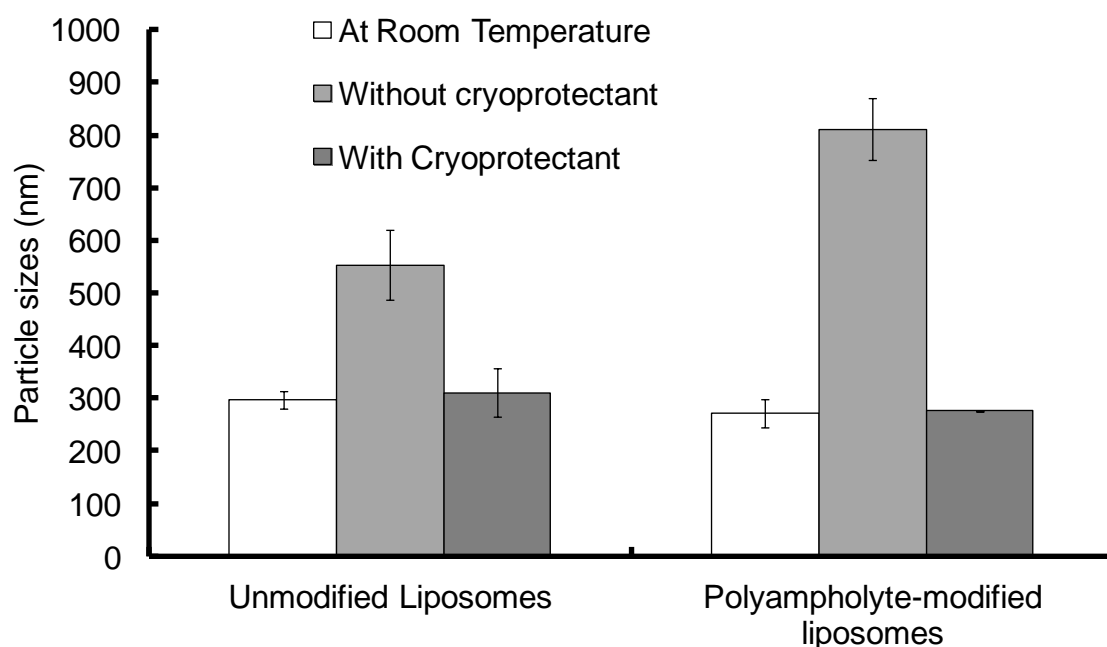

Figure 3.6 Particle sizes of unmodified liposomes and polyampholyte-modified liposomes were determined by DLS at 25ºC and at −80 ˚C, with and without 10% PLL-SA cryoprotectant. Data are expressed as the mean ± SD.

### 3.3.3 Adsorption of protein-encapsulating liposomes onto cells via freeze concentration

### 3.3.3.1 Confocal laser scanning microscopy (CLSM)

The adsorption of lysozyme protein loaded liposomes onto the cell membrane was investigated using previously frozen thawed solutions. At low temperature, the accelerated ice crystal formation excluding the remaining solution inevitably led to the formation of freezing-associated concentration. Therefore, I expected that the protein nanocarrier complex could enhance the interaction of the complex with the cells. L929 cells mixed with 1,2-dioleoyl-sn-glycero-3-phosphoethanolamine-N-(lissamine rhodamine B sulfonyl) (ammonium salt) (Rh-PE)-labelled liposomes and fluorescein isothiocyanate (FITC)-labelled lysozyme protein were cryopreserved with 10% PLL-SA cryoprotectant in culture medium without foetal bovine serum (FBS). Occasionally, low temperature leads to destabilization of the protein structure, which causes denaturation or aggregation. Therefore, cryoprotectants[32, 33] such as glycerol, ethylene glycol, and trehalose are used to stabilize the protein structure. A low toxicity polyampholyte cryoprotectant was utilised to stabilize the protein structure and also protect the cells from intracellular damage from ice crystals.[22] Cell viability was in the range of 85–90% for polyampholyte-modified liposomes whereas it was only 80% for unmodified liposomes (**Figure. 3.7**). The confocal microscopic images illustrated that freezing markedly enhanced the adsorption of lysozyme protein-loaded liposomes onto cell membranes and that polyampholyte modification tended to show higher fluorescence intensity compared to unmodified liposomes (**Figure 3.8 a** and **b**). In my previous study, I had already shown that freeze concentration and hydrophobicity play important roles to facilitate the adsorption onto the cell membrane.[19] Hydrophobic groups that markedly influence particle internalization also have been shown to profoundly influence their uptake by the cell membrane.[34] Thus, polyampholyte-modified liposomes showed enhanced adsorption onto the cell membrane after treatment with freeze concentration.
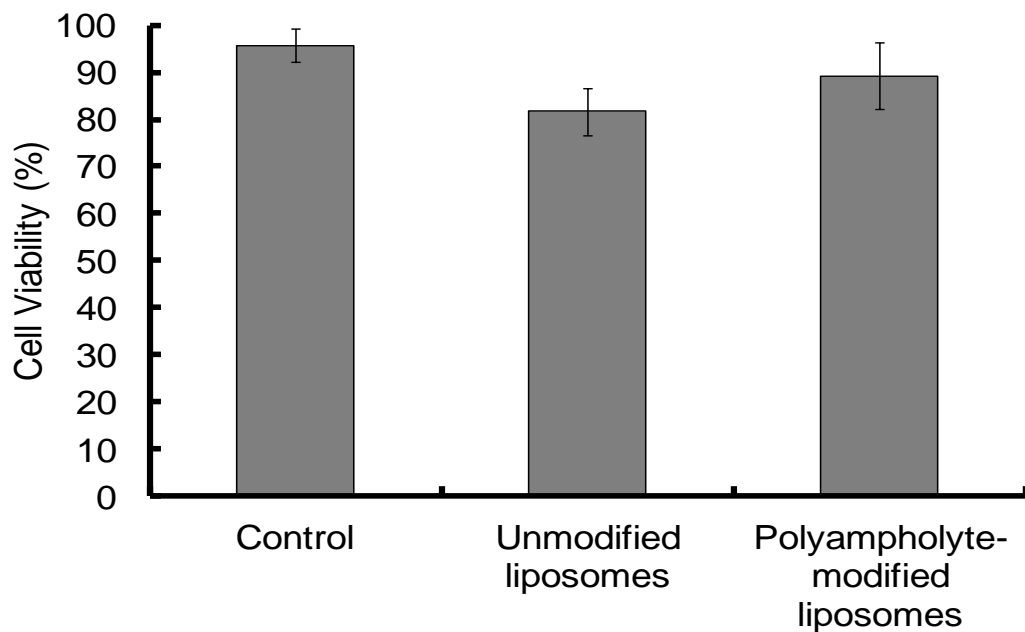
Figure 3.7 Cell viability after storage at −80 °C for 1 day along with unmodified or polyampholyte-modified liposomes in the presence of the polymeric cryoprotectant PLL-SA. Data are expressed as the mean ± SD.

(B)
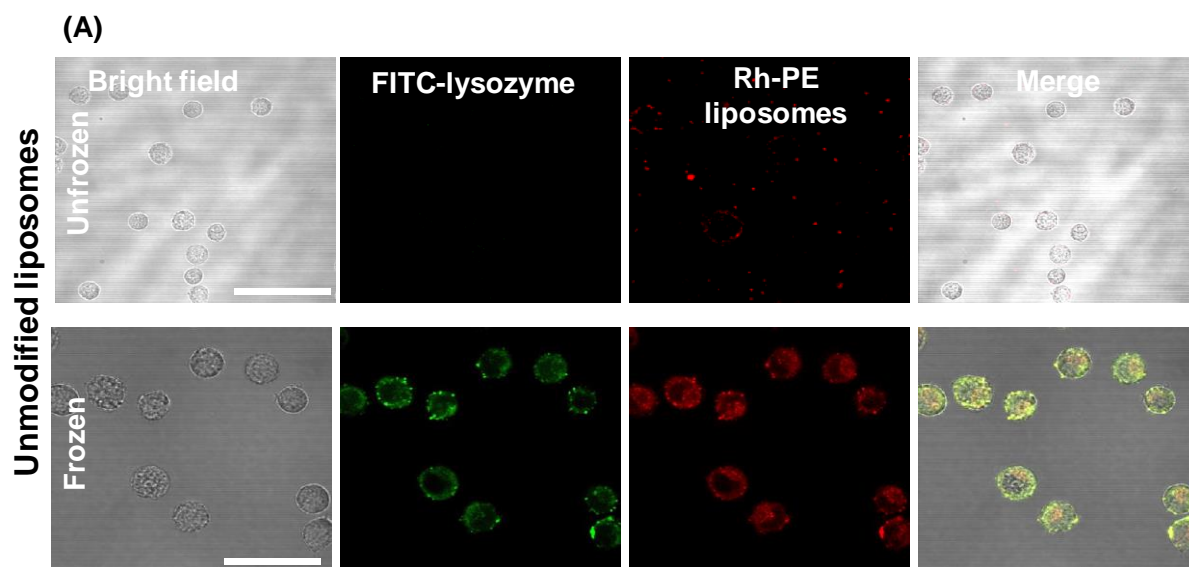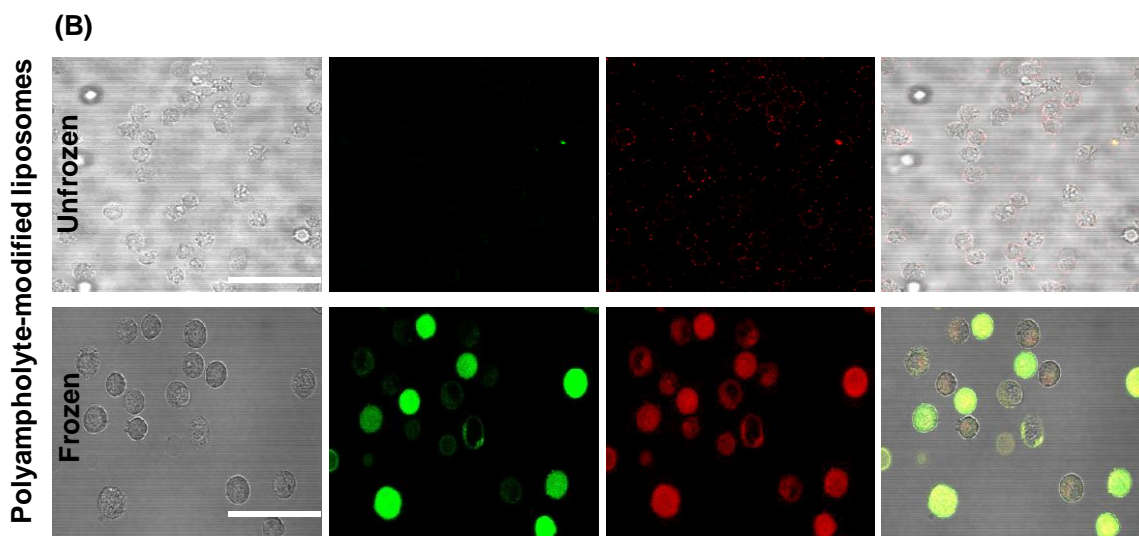
Figure 3.8 Confocal microphotographs of L929 cells before and after freezing along with protein-encapsulating carriers with 10% PLL-SA as a cryoprotectant. Liposomes were stained with FITC-PE and lysozymes were labelled by TR red. (a) Unmodified liposomes. (b) Polyampholyte-modified liposomes. Scale bars: 30 μm.
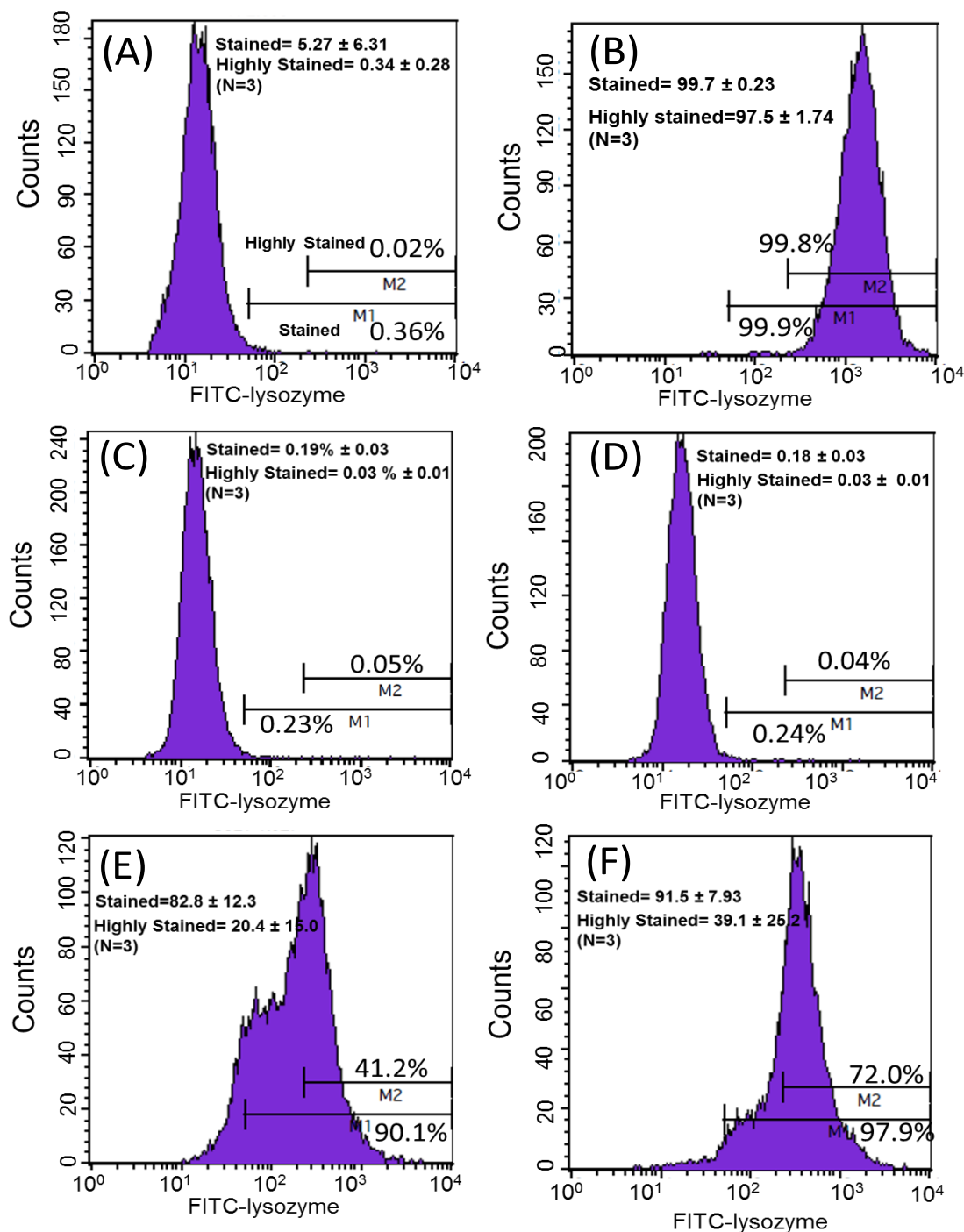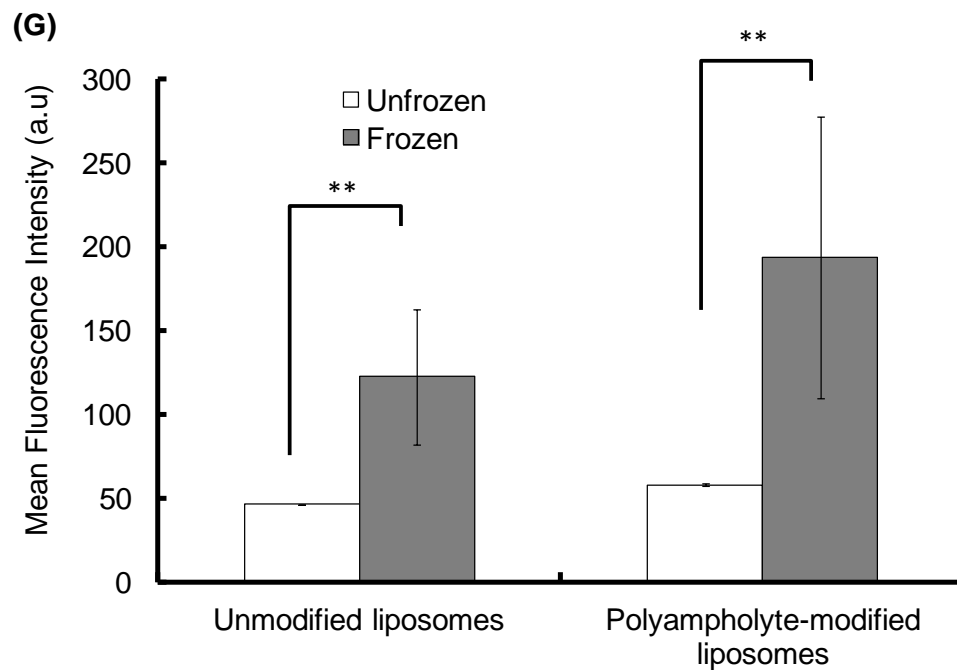
3.3.3.2 Flow cytometric analysis

To quantify the adsorption of lysozyme protein-loaded liposomes to cell membranes via freeze concentration, flow cytometric analysis of the frozen or unfrozen cells was performed. Cells were cryopreserved with an unmodified or polyampholyte-modified liposome-encapsulated lysozyme (5 mg mL^{-1}) in the presence of a polymeric cryoprotectant. The fluorescence of FITC-labelled lysozymes on the adsorbed cell membranes after thawing was investigated. Gates were established for distinguishing the stained and highly stained cells in the histogram plot (**Figure. 3.9 a–f**), which shows that the cells were highly stained when the freeze concentration method was applied. The negative control utilized only cells without any added labelled protein. For the positive control, I used a frozen, liposome-free bare lysozyme protein conjugated with FITC (10 mg mL^{-1}) without any cryoprotectant. In the absence of a cryoprotectant, the lysozyme protein exhibited the highest measured fluorescence because the cell membrane was ruptured by freezing damage and the liposomes were adsorbed onto the fragmented membrane structures and thus transferred directly into the cytoplasm (**Figure 3.9 b**). From the histogram of the frozen cells, the cells could be divided into 2 groups: stained and highly stained. These 2 types of stained cells might be attributed to the cells with different fluorescence intensities as shown in **Figure 3.9a** and **b**. In contrast, unfrozen cells

with both unmodified and polyampholyte-modified liposomes displayed a few positive cells (approximately 0.2% and and <0.1% for stained and highly stained groups, respectively; **Figure 3.9 c**, **d**). For frozen cells, the unmodified liposomes manifested the greater number of stained and highly stained cells ($82.8 \pm 12.3\%$ and $20.4 \pm 15.0\%$, respectively; **Figure 3.9 e**). In comparison to the unmodified liposomes, polyampholyte-modified liposomes showed a high trend of stained and highly stained cells (about $91.5 \pm 7.93\%$ and $39.1 \pm 25.2\%$, respectively; **Figure 3.9 f**). These data strongly suggest that the freeze concentration strategy can enhance the fluorescence intensity, compared with that observed in unfrozen cells. Based on flow cytometry data, the geometric mean of the fluorescence intensity revealed a 4-fold stronger binding after freezing for both unmodified and polyampholyte-modified liposomes as compared with that observed for unfrozen cells (**Figure 3.9 g**). These results indicate that in contrast to the unfrozen state, freeze concentration might enhance the lysozyme protein adsorption efficacy and thus the number of molecules bound to the surface of the cells. In addition, I conducted experiments to determine if only lysozyme (without freezing) adsorbs onto the cell membrane, given its positive charge. Confocal microscopy results showed that almost no lysozyme adsorption occurred due to its low concentration (**Figure 3.10**). This finding indicated that freeze concentration can be useful when low protein concentrations are involved.

As quantified **in Figure 3.9 g**, the cells treated with lysozyme protein loaded polyampholyte-modified liposomes showed enhanced fluorescence as compared to those treated with unmodified liposomes. This could be explained by the strong interaction of polyampholyte-modified liposomes with cells, which are likely to have more association owing to chargeinducing factors or hydrophobicity. The hydrophobicity of the liposomal membranes might be enhanced by the presence of polyampholyte nanoparticles that strongly favour the enhanced interactions between the liposomal membranes and cells. On the other hand, the effect was much more prominent upon increasing the dose of lysozyme protein-encapsulated in liposomes. The same observations for unmodified and polyampholyte-modified liposomes were noted even after low (1 mg mL^{-1}) and medium doses (3 mg mL^{-1}) were applied (Fig. S8†), wherein the gated numbers of stained and highly stained cells were higher than those obtained for unfrozen cells (5 mg mL^{-1}). For the low dose concentration (1 mg mL^{-1}) corresponding to unmodified to polyampholyte modified liposomes, the proportion of stained cells increased from $34.2 \pm 12.0\%$ to $48.7 \pm 9.50\%$ and the highly stained cells similarly increased from $5.61 \pm 2.93\%$ to $5.99 \pm 3.25\%$. From these results, it is suggested that the

efficiency is highly dependent on dose concentration, which resulted in a highly effective adsorption of the lysozyme protein (**Figure 3.11 a–d** and **Figure 3.9 e, f**). In addition, the geometric means, which were calculated from flow cytometric analyses, showed the enhancement of fluorescence intensity upon increasing the dose of the liposome-encapsulated lysozyme protein (**Figure 3.11 e**). Therefore, for my further investigations, I have chosen an optimum dose (final concentration 5 mg mL^{-1}, 500 µL) of the liposomeencapsulated lysozyme protein for efficacious delivery into cells. Based on the above findings, it is expected that this strategy would promote high internalization efficacy through an endocytic pathway. Thus, I evaluated protein internalization after its accumulation onto the membrane.

(G)

Figure 3.9 Flow cytometric analysis of frozen and unfrozen cells with various protein-loaded (5 mg mL^{-1}) liposomes. (a) Negative control (cells only); (b) positive control (cells cryopreserved without a cryoprotectant). Unfrozen cells with (c) unmodified liposomes or (d) polyampholyte-modified liposomes. Frozen cells with (e) unmodified liposomes or (f) polyampholyte-modified liposomes. (g) Mean fluorescence intensity of frozen and unfrozen unmodified liposomes and polyampholytemodified liposomes by flow cytometric analysis. Data are expressed as mean ± SD. **P < 0.01
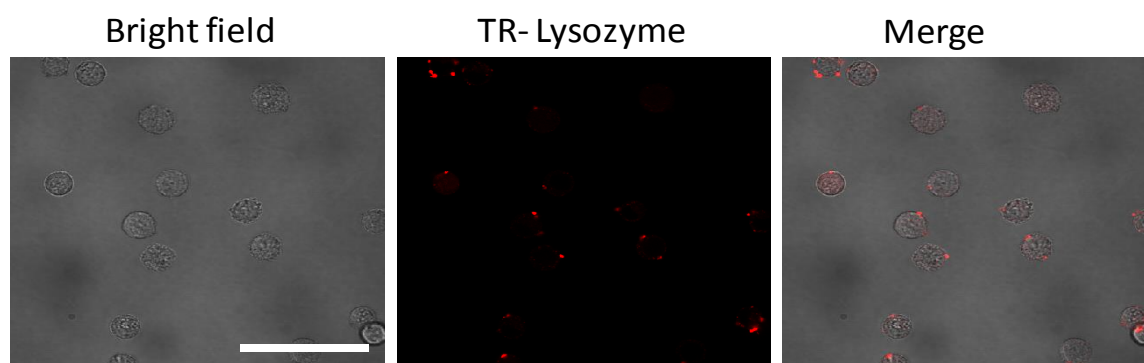
Figure 3.10 Confocal microphotograph of L929 cells (without freezing), using bare lysozyme proteins. Lysozyme proteins were stained with TR red. Scale bar: 10 μm
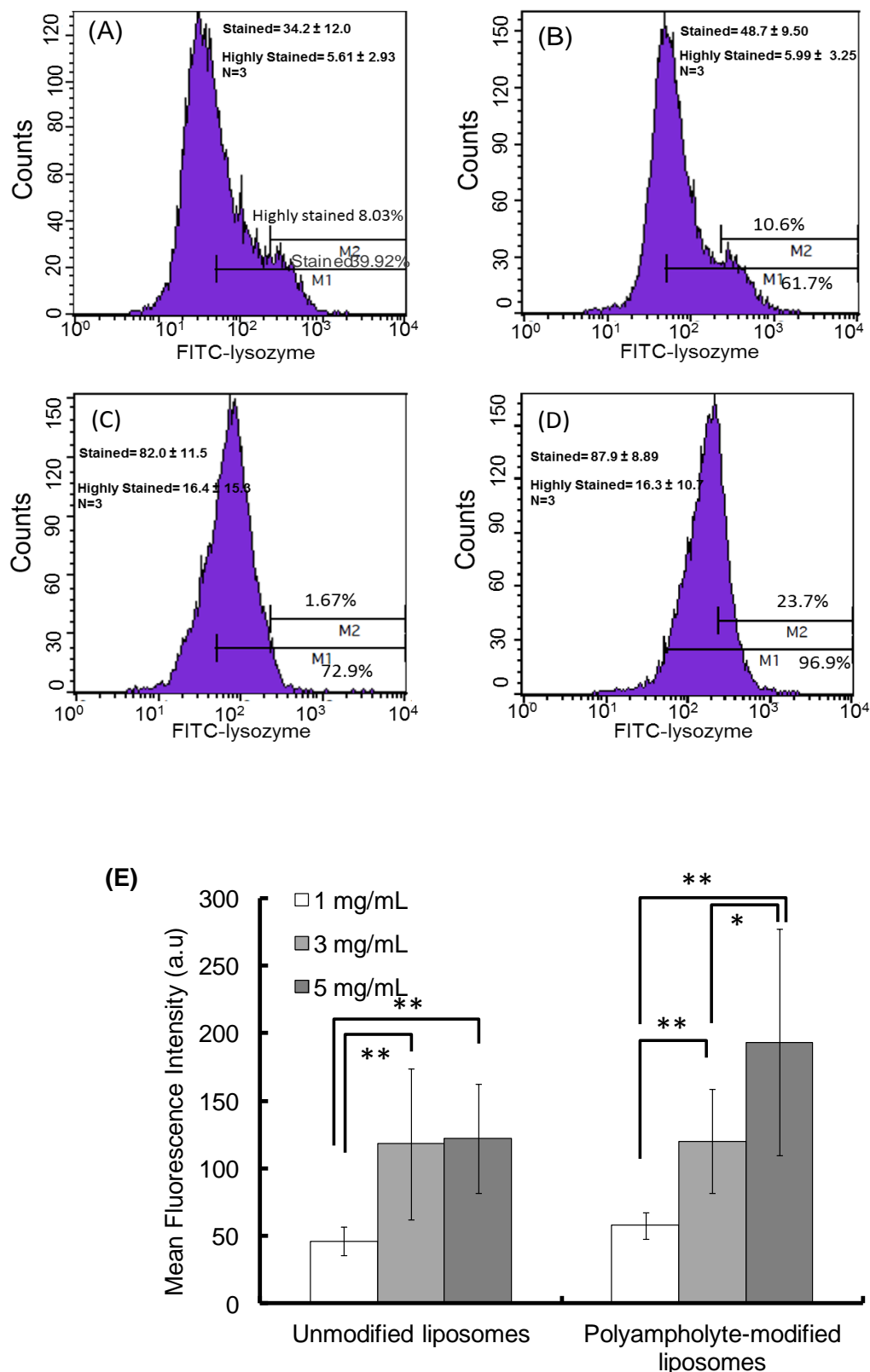
Figure 3.11 Flow cytometric quantification of the fluorescence intensity of cells before and after being frozen with various protein-loaded liposomes. I used 1×10^6 cells for sample preparation and analysis by flow cytometry, under the following conditions. (a) Low dose (1 mg/mL) of unmodified liposomes. (b) low dose (1 mg/mL) of polyampholyte-modified liposomes. (c) Medium dose (3

mg/mL) of unmodified liposomes. (d) high dose (5 mg/mL) of polyampholyte-modified liposomes. (e) Mean fluorescent intensity showing the dose dependency of FITC-conjugated lysozyme loading using unmodified and polyampholyte-modified liposomes. Data are expressed as the mean ± SD. **P < 0.01, *P < 0.05

3.3.3.3 Internalization of lysozyme protein-loaded liposomes after seeding

It is generally believed that membrane fusion is important for cytoplasmic delivery through endocytosis. Liposome uptake studies were performed on L929 fibroblast cells, wherein unmodified liposomes and polyampholyte-modified liposomes were labelled by FITC-phosphatidylethanolamine (FITC-PE) whereas the lysozyme protein was labelled by Texas Red (TR) dye. Cells mixed with lysozyme protein-loaded unmodified or polyampholyte-modified liposomes were cryopreserved at −80 °C in medium without FBS, replaced by fresh growth medium and seeded after thawing following incubation for 24 h at 37 °C to allow internalization. Cells were then washed with PBS and observed using CLSM. Both unmodified and polyampholyte-modified liposomes showed a tendency to be internalized using the freeze concentration methodology (**Figure 3.12 a** and **b**). Fluorescence was measured by confocal microscopy. The intensity of the red fluorescence of the internalized TR-labelled lysozyme protein showed that polyampholyte-modified liposomes exhibited a significantly greater capacity for protein intake in comparison with unmodified liposomes (**Figure 3.12c**). These results demonstrate that the freeze concentration technique can enhance the cytosolic delivery of proteins. Because it is important to compare this system with other current systems, control experiments were performed using a commercially available PULSin™ protein-delivery kit. This reagent contains cationic, amphiphilic molecules that enhance adsorption on the cell membrane, but the cationic charge causes cytotoxicity. I followed the delivery protocol for suspension cells to compare the results obtained with the freeze concentration methodology. Because a significant decrease in cell viability (<60% viability) was observed using the protein/PULSin™ complexes after a 4-h incubation (due to the cationic charge), I decreased the incubation time to 0.5 h at 37ºC, according to the protocol. The medium without FBS containing protein/PULSin™ complexes were replaced with fresh growth medium to allow protein internalization after seeding to the glass-bottom dish.[35] The fluorescence intensity of internalization of FITC-lysozyme/PULSin™ was lower compared with freeze concentration-mediated internalization (**Figure 3.13 a–f).** These results strongly suggested that the freeze concentration

methodology is more efficient and less toxic than the current method, based on cationic amphiphiles used to deliver proteins to the cytosolic compartment of cells.

Recent studies have shown that unmodified liposomal delivery efficiency is very low whereas liposomes modified with polymer are more capable to induce the selective release of materials from endosomes into the cytoplasm. Kono et al. reported that liposomes modified by polymer had a higher efficiency of entering the cells; ultimately resulting in internalization of the lysozyme protein.[36] Furthermore, they also indicated that the addition of polymer to liposomes effected the enhancement of intracellular delivery.[18] **Figure 3.12 a, b** show that the intensity of red-stained protein localized in the cytosol with polyampholyte-modified liposomes was greater than observed with unmodified liposomes. This finding suggested that polyampholyte-modified liposomes transferred more lysozyme protein to the cytosol of treated cells. This result is in good agreement with previous report.[19] This enhanced internalization might be due to the efficient release of the lysozyme protein to the cytoplasm via endosomal escape. Next, I investigated the internalization pathway to study endosomal escape using polyampholyte-modified liposomes.

(A) Unmodified liposomes

| Bright field | FITC-PE liposomes | TR-lysozyme | Merge |

(B) Polyampholyte-modified liposomes

(C)
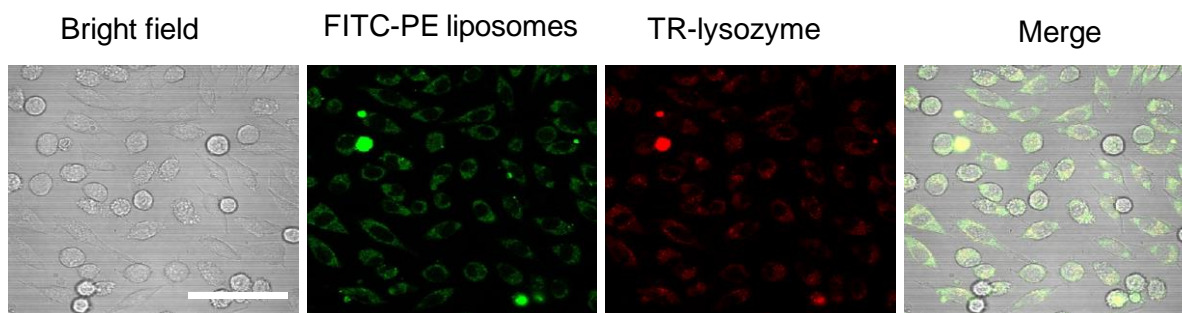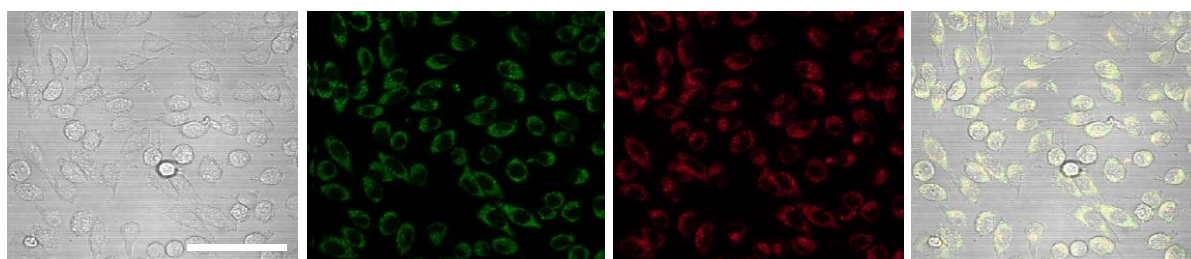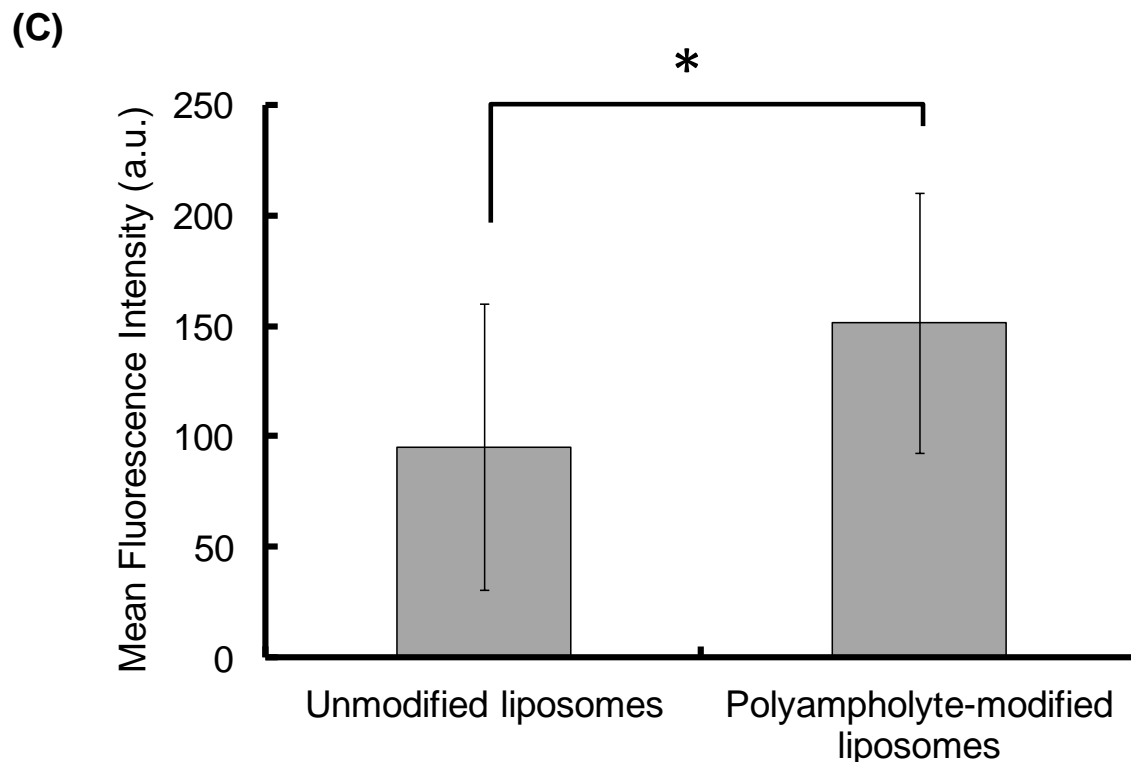
Figure 3.12 Confocal microphotographs of L929 cells. The images show that lysozyme protein internalization occurs via endocytosis during culture after being frozen with lysozyme-loaded modified liposomes using 10% PLL-SA as a cryoprotectant. (a) Unmodified liposomes; (b) polyampholytemodified liposomes. Scale bars: 50 μm. (c) Mean fluorescence intensity of unmodified and polyampholyte-modified liposomes after internalization as determined by confocal microscopy. Data are expressed as mean ± SD. *P < 0.05.
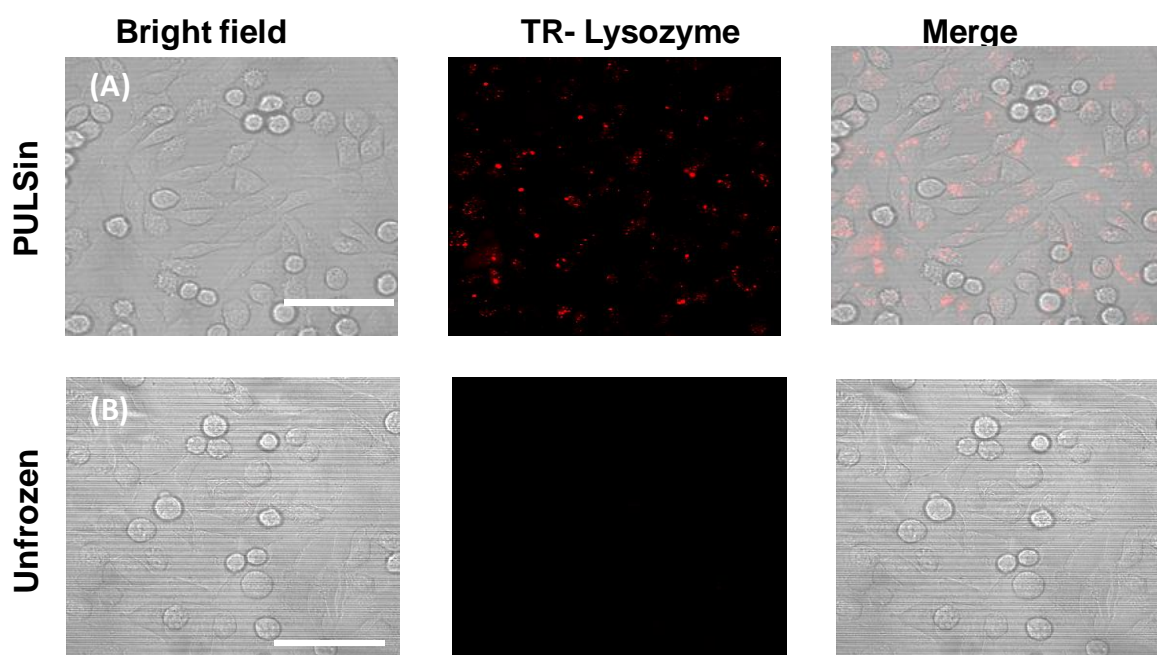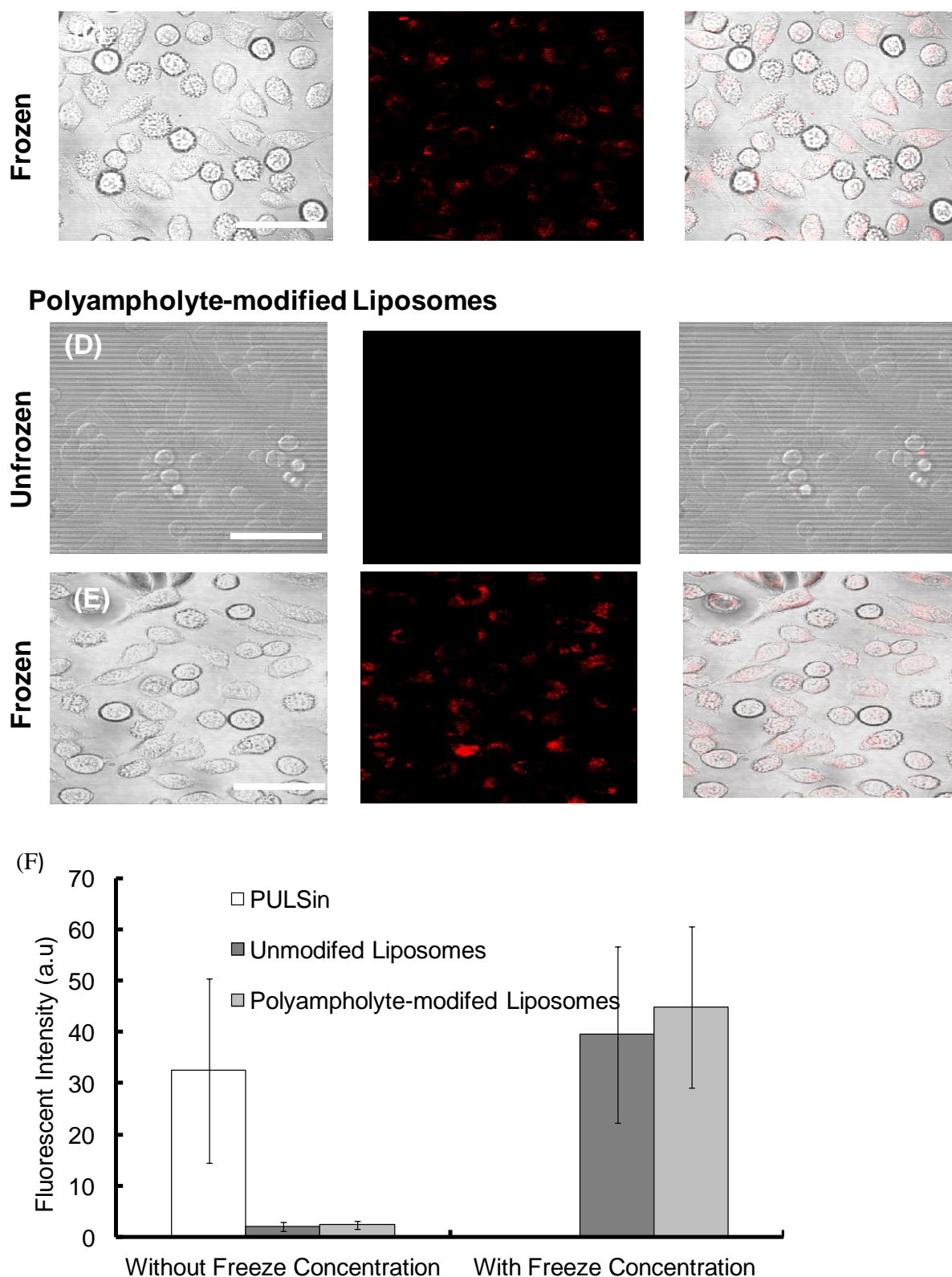
Figure 3.13 Confocal microphotograph showing internalization of TR-labelled lysozyme proteins in L929 cells. Cells were analyzed after a 6-h incubation, which was followed by adding lysozyme protein/carrier complexes. (a) PULSin/lysozyme protein complex (b, d) without freeze concentration of unmodified and polyampholyte-modified liposome/protein complexes. (c,e) Images taken after

freeze concentration of unmodified and polyampholytemodified liposomes. (f) Mean fluorescent intensity following internalization of the positive control (PULSin), or unmodified and polyampholyte modified liposomes, with or without freeze concentration. Data are expressed as the mean ± SD.

3.3.3.4 Internalization Mechanism of FITC-Lysozyme-Loaded Polyampholyte-modified Liposomes

Most particles cannot readily cross into cells because their large size and charge make it difficult to transfer through the plasma membrane; however, lipoparticles have the tendency to be transported by one of several modes. Therefore, it is important to elucidate the mechanism for the particles that actually obtain entrance into the plasma membrane of the cells. The endocytosis pathway is a specialized pathway that mediates the active transportation of nanomedicines and targets them to such regions as the mitochondria, endosome, nucleus, or other specific organelles.[37]

   To investigate the mechanism associated with unmodified or polyampholyte-modified liposomes entry into the plasma membrane after freezing, a variety of inhibitors were selected to block specific endocytic pathways. I chose 3 inhibitors of the endocytotic pathway: chlorpromazine (for clathrin-mediated endocytosis), 5(-N-Ethyl-N-isopropyl) amiloride (EIPA) (macropinocytosis), and filipin (caveolae-mediated endocytosis).[38] L929 cells were treated with different concentrations of each inhibitor followed by the addition of FITC-lysozyme-encapsulating liposomes in the presence of polymeric cryoprotectant, and measured using a fluorescence microplate reader and by CLSM. The cell viability was determined to optimize the inhibitor concentration to select concentrations not associated with cytotoxicity (**Figure 3.14**). For confirmation of the endocytosis mechanism, confocal microscope observation (**Figure 3.15**) and fluorescence microplate reader analysis (**Figure 3.16**) were conducted. These results showed agreement between the confocal images and the quantification of fluorescence for the determination of uptake. In these images, considerable fluorescence was observed in the L929 cells used as a positive control without any inhibitor for the unmodified and polyampholyte-modified liposomes; however, when specific inhibitors were used to block the pathway, a decrease in the fluorescence was observed that affected the uptake and did not allow the lysozyme protein to diffuse into the membrane. For unmodified liposomes, the fluorescence intensity after adding filipin declined considerably, whereas treatment with the other inhibitors had no such effect (**Figure 3.15a–d**). The

significant decrease in intensity following filipin treatment suggested that unmodified liposomes were internalized into fibroblast L929 cells by caveolae-mediated endocytosis (**Figure 3.16a**). Caveolae contain a hydrophobic domain that is rich in cholesterol and glycosphingolipids. When particles are internalized by caveolae, caveosomes are formed, which can directly transport the particles to specific organelles.[39] Many reports have indicated that charged particles were likely to adopt caveolae-dependent endocytosis.[40] However, in my investigation, using PLL-DDSA-SA-modified liposomes, the finding that both EIPA and filipin inhibitor significantly resulted in a decline of fluorescence intensity suggest that these, unlike unmodified liposomes, tend to adopt 1 of 2 pathways; caveolae-mediated endocytosis or macropinocytotic endocytosis (**Figure 3.15 e–h**, **Figure 3.16 b**). Consequently, it can be concluded that the hydrophobic polyampholyte in liposomes is responsible for promoting the macropinocytotic endocytic route. In macropinocytosis, the internalization of the particles occurs into large vacuoles called macropinosomes with a diameter of 0.5–1.0 μm.[41] Macropinocytosis has received much attention in gene delivery as well as in cancer therapy fields. The most advantageous feature of macropinocytosis is its allowance for endosomal escape, which can avoid the lysosomal degradation of antigens and genes. One report has demonstrated that an octaarginine peptide-mediated gene expression system that showed high transfection efficacy ultimately adopted the macropinocytotic pathway.[42] Thus, a notable finding in my study is that polyampholyte-modified liposomes adopted 2 methods of internalization. Various factors such as size[43] and surface charges[40] are associated with internalization, based on physicochemical characterization[44]. However, no common factor has been elucidated yet to explain the associated mechanism involving entry into endocytic pathways.

Taken together, these results suggested that both unmodified liposomes and polyampholyte-modified liposomes utilise caveolae-mediated endocytosis, but that polyampholyte triggers the adoption of an additional specific pathway, macropinocytosis, with a different uptake mechanism. Therefore, I suggest that polyampholyte-modified liposomes facilitate intracellular delivery through a different mechanism than occurs with unmodified liposomes.

(A) Unmodified liposomes

(B) Polyampholyte-modified liposomes
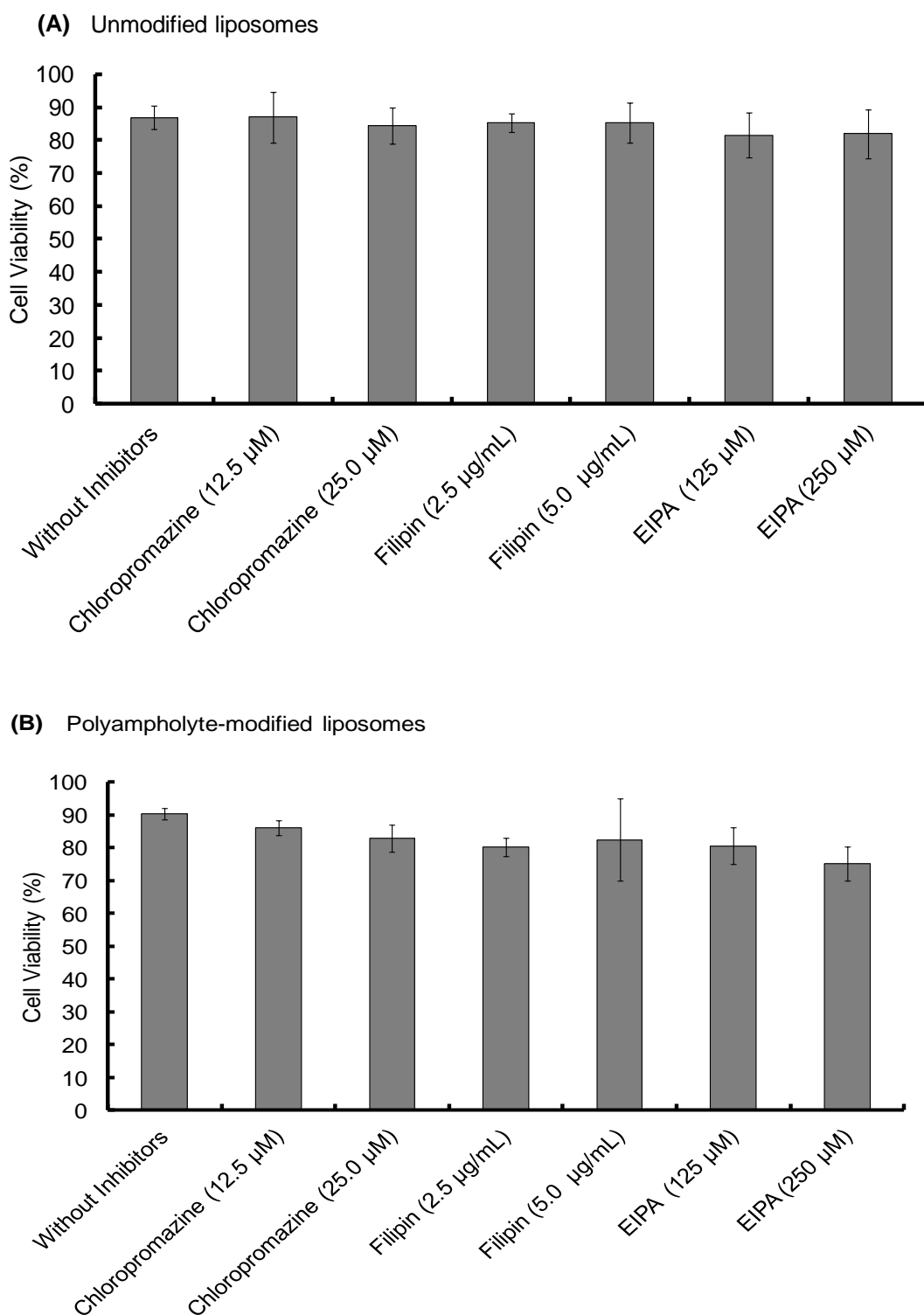
Figure 3.14 Quantification of cell viability determined by trypan blue-exclusion assays after the addition of different concentrations of endocytic inhibitors to protein-liposome complexes. (a) Unmodified liposomes. (b) Polyampholyte-modified liposomes. Data are expressed as the mean ± SD

Unmodified liposomes

Polyampholyte -modified liposomes
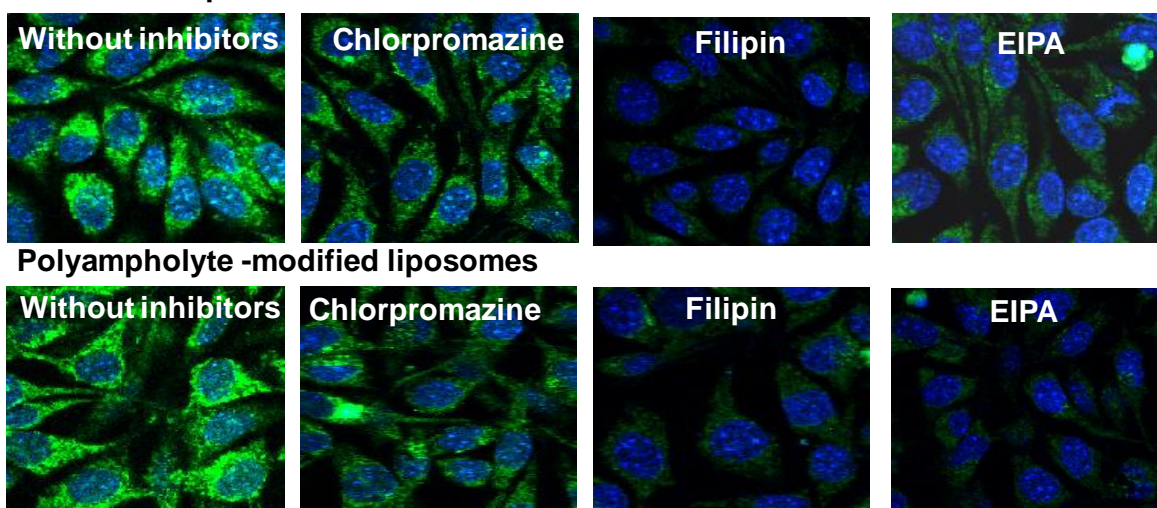
Figure 3.15 Effects of endocytic uptake of unmodified liposomes (a–d) or polyampholyte-modified liposomes (e–h). Encapsulated FITC-labelled lysozymes were pre-incubated with different inhibitors (chloropromazine, filipin, or EIPA) in the presence of a polymeric cryoprotectant at −80 °C. After thawing, the cells were seeded and incubated for at least 8 h. Confocal microscopy analysis without inhibitors (a, e), chloropromazine (B, F), filipin (c, g), or EIPA (d, h). Scale bars: 20 μm.
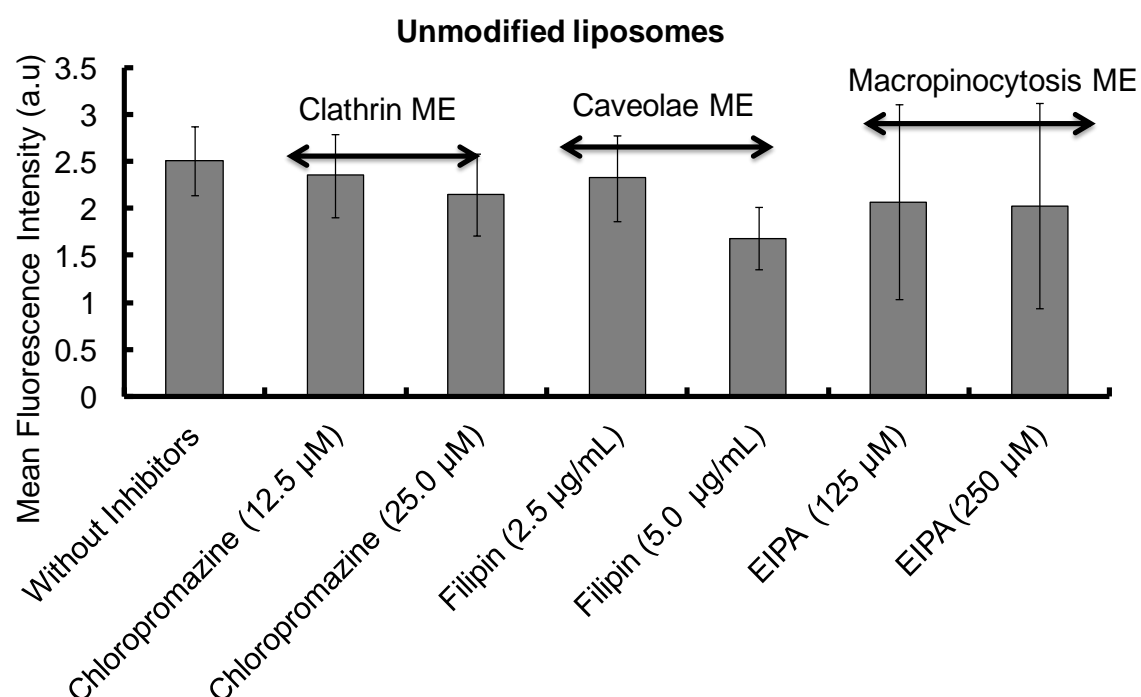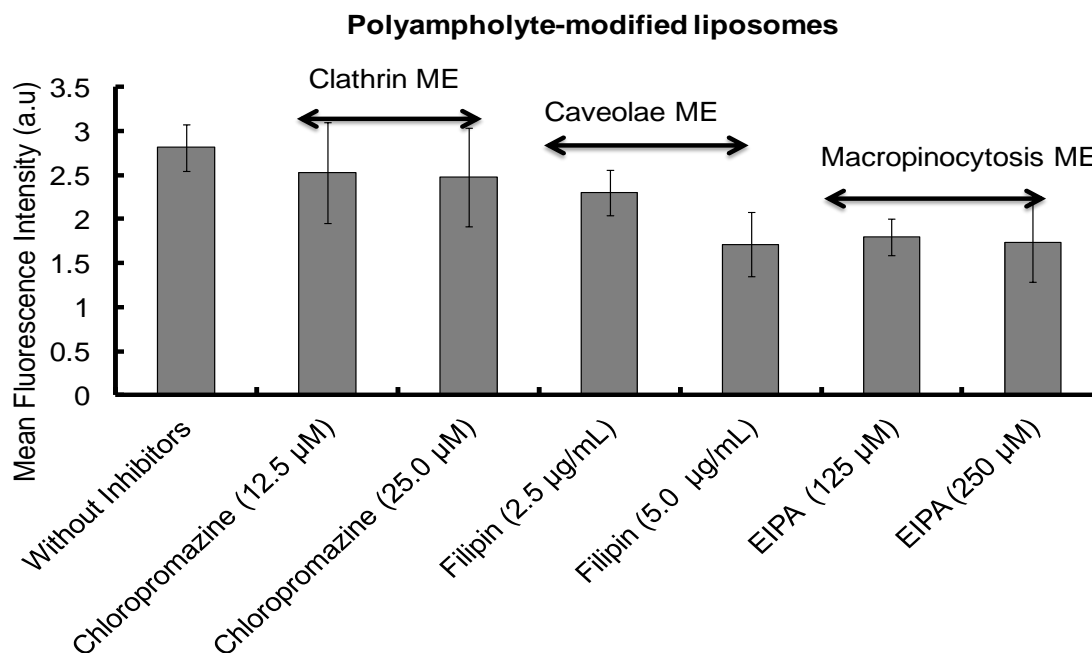
Figure 3.16 Quantitative analysis with a fluorescent microplate reader of the fluorescence intensity observed during endocytic uptake via clathrinmediated endocytosis (ME), caveolae ME, and macropinocytosis ME, following treatment with different inhibitors. (a) Unmodified liposomes. (b) Polyampholyte-modified liposomes. Data are expressed as mean ± SD. **P < 0.01, *P < 0.05 vs. without inhibition.

3.3.3.5 Intracellular Localization and Endosomal Escape of Lysozyme Proteins

To be effective for therapeutic purposes, it is required that delivered proteins must escape lysosomal degradation; in addition, they should be delivered into the cytosol of the cells for high efficiency. Thus, my investigation of the ability of materials to effect intracellular delivery also included an examination of the capability to release their contents into the cell cytoplasm.

To confirm the entry of lysozyme protein into endosomes and to determine whether or not the protein was subsequently trafficked to lysosomes wherein a large variety of macromolecules can be degraded, an investigation of intracellular trafficking is required for eventual successful design in protein delivery schemes. I examined the potential for endosomal protein escape using a combination of unmodified or polyampholyte-modified liposomes and freeze concentration-based internalization. To observe the intracellular distribution of cargo proteins in L929 cells, TR-labelled lysozyme-encapsulating liposomes

were prepared. The endosomes and lysosomes were stained with LysoTracker Green and nuclei were stained with Hoechst 33258 for 30 min respectively prior to observations. As shown in Fig. 7A, the colocalization of lysozyme proteins and lysosomes were represented by yellow fluorescent regions indicating the presence of the proteins in the endosomes, which is consistent with the internalization of unmodified liposomes. This shows that unmodified liposomes remain intact even after their release from the endosome, suggesting that the associated encapsulated lysozyme proteins might have difficulty being released from the vesicles. In contrast, the green fluorescence was partially separated from red fluorescence over time for polyampholyte-modified liposomes, indicating the successful release of their protein cargo (**Figure 3.17 b**). The images shown in **Figure 3.17** suggest a triggered release of lysozyme protein from endosomes for engineered liposomes incorporating hydrophobic polyampholytes. The possible mechanism behind endosomal release might be that polyampholytes could be adsorbed onto the endosome membrane thereby destabilizing it, which leads to the release of lysozyme protein; accordingly, I identified an enhanced *in vitro* endosomal escape efficacy with very low associated toxicity.

Therefore, I found that the fluorescence of TR-labelled lysozyme proteins did not increase and that they were effectively internalized with unmodified liposomes (**Figure 3.12 a**), whereas polyampholyte-modified liposomes led to efficient protein release and higher fluorescence due to the endosomal escape of proteins (**Figure 3.12 b, c**). I have also evaluated the size variation of liposomes with or without polyampholyte-modification caused by changing their pH using a DLS technique. Unmodified liposomes did not show any remarkable change even at different pH values. However, polyampholyte-modified liposomes showed a size increase, indicating aggregation at pH 5.5 (**Figure 3.17 c**). This factor might induce destabilization of the liposomal membrane because polyampholyte-containing carboxyl groups are protonate, [45] and these carboxylate ions can lose their negative charge causing destabilization of liposomal membranes.[46-50] Upon endocytosis, the low pH in the endosomes induces fusion of the liposomal membrane with the endosomal membrane, causing the release of the contents of the liposomes into the cytoplasm of the cells. One reason for this might be that pH- sensitive liposomes undergo an acidification responsible for disruption of the liposomal bilayer, with change of its configuration causing the release of encapsulated material through the endosomal pathway. Thus, the polyampholyte-modified liposomes were capable of enhancing the endosomal escape efficiency. In addition, after

escaping from endosomes, it is extremely important to investigate the lysozyme delivery to a disease site in future.
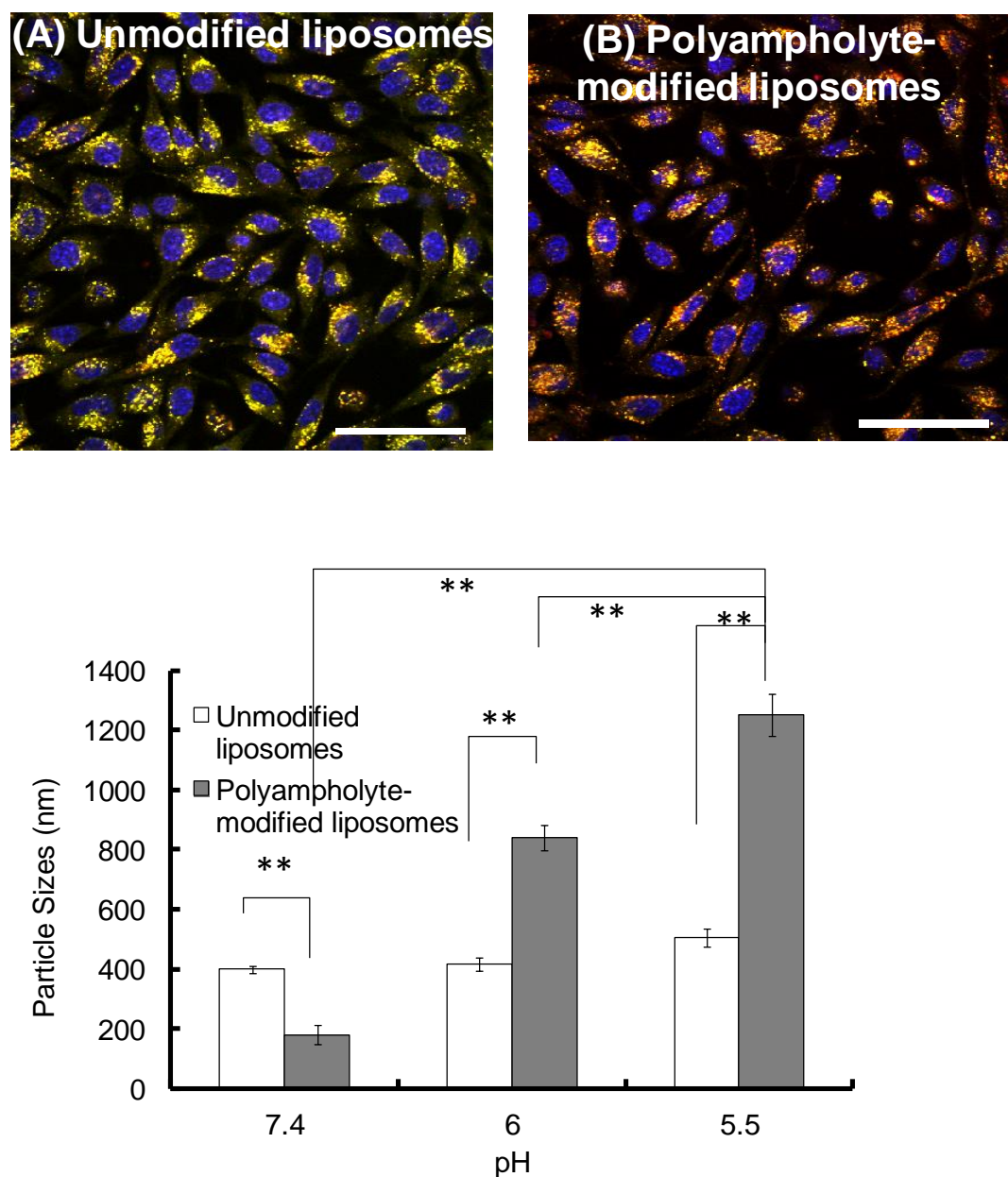
Figure 3.17 Intracellular delivery of TR-labelled lysozymes in L929 cells. I cryopreserved 1×10^6 cells with the polymeric cryoprotectant PLL-SA and protein containing liposomes. The cells were thawed and seeded for 12 h at 37 °C. After incubation, the endosomes/lysosomes and nuclei were stained by LysoTracker Green and Hoechst blue 33258, respectively. (A) Unmodified liposomes. (B) Polyampholyte-modified liposomes. Scale bar: 10 μm. (C) Mean diameter of unmodified or polyampholyte-modified liposomes after overnight incubation at various pH values. Data are expressed as mean ± SD. **$P < 0.01$.

3.4 Conclusion

In this study, I prepared a novel form of hydrophobic polyampholyte-modified liposomes using a combination of PLL-DDSA-SA. These polyampholyte-modified liposomes can successfully escape the endocytic pathway and can introduce lysozyme proteins into the cell cytosol through the use of a simplistic strategy involving freeze-thawing of cells with the encapsulated lysozyme protein complexes. The present study focused on providing a mechanistic overview of lysozyme protein delivery by using unmodified and polyampholytemodified liposomes in conjunction with the freeze concentration method. These hydrophobic polyampholyte-modified liposomes are stable at physiological pH 7.0, and exhibit low cytotoxicity and high protein encapsulation efficiency. The results of flow cytometry analysis show that by using the freeze concentration method, the uptake and adsorption of lysozyme proteins was enhanced by 4-fold in comparison with that obtained using unfrozen cells. In addition, I found that the unmodified and polyampholyte-modified liposomes adopted different pathways for the cytoplasmic delivery of proteins, with the latter preferentially bypassing lysosomal degradation. Therefore, although further investigation in vitro using immune cells and in vivo using model systems should be performed, these positive results including the protein endosomal escape property suggest that the intracellular delivery of lysozyme proteins by hydrophobic polyampholyte-modified liposomes and the freeze concentration methodology might be very beneficial for in vitro applications in cancer treatment or gene therapy in future.

3.5 References

1. De Jong, W. H.; Borm, P. J. A. *Int. J. Nanomed*. **2008**, *3*, 133.

2.   Lee, K. Y.; Mooney, D. *J. Prog. Polym. Sci.* **2012**, *37*, 106.

3. Weidle, U. H.; Schneider, B.; Georges, G.; Brinkmann, U. *Cancer Genomics Proteomics* **2012**, *9*, 357.

4.   Veiseh, O.; Tang, B. C.; Whitehead, K. A.; Anderson ,D. G.; Langer, R. *Nat. Rev. Drug Discov.* **2015**, *14*, 45.

5.   Patterson, H.; Nibbs, R.; McInnes, I.; Siebert, S. *Clin. Exp. Immunol*. **2014**, *176*, 1.

6. Charoo, N. A.; Rahman, Z.; Repka .M. A.; Murthy, S. N. *Curr. Drug Deliv.* **2010**, *7*(2), 125.

7. McAllister, D. V.; Allen M. G.; Prausnitz, M. R. *Annu. Rev. Biomed. Eng.* **2000**, *2*, 289.

8. Husseini, G. A.; Pitt, W. G. *J. Pharm. Sci.* **2009**, *98*(3), 795.

9.   Beebe, S. J.; Sain, N. M.; Ren, W. *Cells* **2013**, *2*, 136.

10. Kamaly, N.; Xiao, Z.; Valencia P. M.; Radovic- Moreno A. F.; Farokhzad, O. C. *Chem. Soc. Rev.* **2012**, *41*, 2971.

11. Gu, Z.; Biswas, A.; Zhao, M.; Tang, Y. *Chem. Soc. Rev.* **2011**, *40*, 3638.

12. Arayachukiat, S.; Seemork, J.; Pan-In, P.; Amornwachirabodee, K.; Sangphech, N. ; Sansureerungsikul, T.; Sathornsantikun, K.; Vilaivan, C.; Shigyou,K.; Pienpinijtham, P.; Vilaivan, T.; Palaga, T.; Banlunara, W.; Hamada ,T.; Wanichwecharungruang, S. *Nano Lett*. **2015**, *15*, 3370.

13. Pisal, D. S.; Kosloski, M. P.; Balu-Iyer, S. V. *J. Pharm. Sci.* **2010**, *99*(6), 2557.

14. Soenen, S. J.; Parak, W. J.; Rejman J.; Manshian, B. *Chem. Rev.* **2015**, *11*, 2109.

15. Torchillin, V. P. *Nat. Rev. Drug Discov.***2005**, *4*, 145.

16. Immordino, M. L.; Dosio, F.; Cattel, L. *Int. J. Nanomed.* **2006**, *1*(3), 297.

17. Martins, S.; Sarmento, B.; Ferreira, D. C.; Souto, E. B. *Int. J. Nanomed.* **2007**, *2*(4), 595.

18. Yuba, E.; Harada, A.; Sakanishi, Y.; Watarai, S.; Kono, K. *Biomaterials* **2013**, *34*, 3042.

19. Ahmed, S.; Hayashi, F.; Nagashima, T.; Matsumura, K. *Biomaterials* **2014**, *35*, 6508.

20. Bhatnagar, B. S.; Pikal M. J.; Bogner, R. H. *J. Pharm. Sci.* **2008**, *97*(2), 798.

21. Mazur P.; Rigopoulos, N. *Cryobiology* **1983**, *20*(3), 274.

22. Matsumura, K.; Hyon, S. H. *Biomaterials* **2009**, *30*, 4842.

23. Gruenberg, J.; Vandergoot, F. G. *Nat. Rev. Mol. Cell Biol.* **2006**, 7, 495.

24. Raagel, H.; Saalik .P; Pooga, M. *Biochim. Biophys. Acta* **2010**, *1798*, 2240.

25. Sahay, G.; Alakhova, D. Y.; Kabanov, A. V. *J. Controlled Rel.* **2010**, *145*(3), 182.

26. Sarker, S. R.; Hokama, R.; Takeoka, S. *Mol. Pharm.* **2014**, *11*, 164.

27. Varkouhi, A. K. ; Scholte, M. G.; Storm , Haisma, H. J. *J. Controlled Rel.* **2011**, *151*, 220.

28. Akagi, T.; Kim, H.; Akashi, M. *J. Biomater. Sci., Polym. Ed*. **2010**, *21*, 315.

29. Frohlich, E. *Int. J. Nanomed*. **2012**, *7*, 5577.

30. Takano, S.; Aramaki, Y.; Tsuchiya, S. *Pharm. Res*. **2003**, *20*(7), 962.

31. Mozafari, M. R.; Reed, C. J.; Rostron, C.; Kocum C.; Piskin, E. *Cell. Mol. Biol. Lett.* **2002**, *7*(2), 243.

32. Jain, N. K.; Roy, I. *Protein Sci.* **2009**, *18*(1), 24.

33. Fonte, P.; Sousa, S.; Costa, A.; Seabra, V.; Reis, S.; Sarmento, B. *Biomacromolecules* **2014**, *15*(10), 3753.

34. Liu, Y.; Yin, Y.; Wang, L.; Zhang, W.; Chen, X.; Yang, X.; Xu, J.; Ma, G. *J. Mater. Chem. B* **2013**, *1*, 3888.

35. Weill, C. O.; Biri, S.; Adib, A.; Erbacher, P. *Cytotechnology* **2008**, *56*, 41.

36. Yuba, E.; Harada, A.; Sakanishi, Y.; Kono, K. *J. Controlled Rel.* **2011**, *149*, 72.

37. Bareford, L. M.; Swaan, P. W. *Adv. Drug Deliv.* **2007**, *59*(8), 748.

38. Akagi, T.; Shima, F. Akashi, M. *Biomaterials* **2011**, *32*, 4959.

39. Kiss, A. L.; Botos, E. *J. Cell. Mol. Med.* **2009**, *13*, 1228.

40. Perumal, O. P.; Inapagolla, R.; Kannan, S.; Kannan, R. M. *Biomaterials* **2008**, *29*, 3469.

41. Cardarelli, F.; Pozzi, D.; Bifone, A.; Marchini C.; Caracciolo, G. *Mol. Pharm.* **2012**, *9*, 334.

42. Khalil, I. A.; Kogure, K.; Futaki ,S.; Harashima, H. *J. Biol. Chem.* **2006**, *281*, 3544.

43. Zhang, S.; Lykotrafitis, J. L. G.; Bao, G.; Suresh, S. *Adv. Mater.* **2009**, *21*, 419.

44. Kou, L.; Sun, J.; Zhai, Y.; He, Z. *Asian J. Pharm.* **2013**, *8*, 1.

45. Sakaguchi, N.; Kojima, C.; Harada, A.; Kono, K. *Bioconjugate Chem.* **2008**, *19*, 1040.

46. Felber, A. E.; Dufresne M. H.; Leroux, J. C. *Adv. Drug Delivery Rev.* **2012**, *64*, 979.

47. Meyer, O.; Papahadjopoulos, D.; Leroux, J. C. *FEBS Lett.* **1998**, *421*, 61.

48. Leroux, J. C.; Roux, E.; Garrec, D. L.; Hong, K.; Drummond, D. C.; *J. Controlled Rel.* **2001**, *72*, 71.

49. Drummond, D. C.; Zignani, M.; Leroux, J. C. *Prog. Lipid Res*. **2000**, *39*, 409.

50. Chen, T. ; McIntosh, D.; Yuehua, H.; Kim, J.; D. Tirrell, A.; Scherrer, P.; Fenske,D. B.; Sandhu A. P.; Cullis, P. R. *Mol. Membr. Biol*. **2004**, *21*, 385.

51. Balazs, D. A.; Godbey, W. T. *J. Drug Delivery* **2011**, *2011*, 1.

52. Xu, X.; Costa A.; Burgess, D. *J. Pharm. Res.* **2012**, *29*, 1919.

53. Huth, U. S.; Schubert, R.; Peschka-Su, R. *J. Controlled Rel*. **2006**, *110*, 490.

54. Fretza, M. M.; Koning, G. A.; Mastrobattista, E.; Jiskoot, W.; Storm, G. *Biochim. Biophys. Acta* **2004**, *1665*, 48.

Chapter4

A Freeze-Concentration and Polyampholyte-Modified Liposome–Based Antigen Delivery System for Effective Immunotherapy

4.1 Introduction

In recent years, enormous research efforts have been focused on the development of novel strategies for the treatment of serious diseases such as cancer.[1] Immunotherapy is one of these novel approaches that uses the body's own immune system to directly attack and destroy cancer cells.[2] Thus, the activation of the immune system in cancer therapy has become a very important topic amongst cancer researchers.[3] Antigen presenting cells (APCs) such as dendritic cells, macrophages, and B-cells, are essential in the activation of immune responses and therefore play an important role in immunotherapy. Antigen presentation can occur through both major histocompatibility complex (MHC) class I and MHC class II routes.[4] Generally, following internalization of an exogenous antigenic protein by APCs, the protein molecule is degraded to peptide fragments and these fragments are then presented at the cell surface by MHC class II molecules with the resulting induction of humoral immunity.[5] In contrast, endogenous protein molecules are degraded by cytosolic proteasomes present in the cytosol of APCs. Peptide fragments generated as a result of proteolysis are then presented by MHC class I molecules. An important function of the MHC class I molecule in cancer immunotherapy is to display antigenic proteins to cytotoxic T cells (CTLs).[6] After recognition of the antigen by CTLs, the target cell, which may be infected with a virus or be cancerous, is directly killed by the CTL. In some cases, exogenous antigen can be transferred to the cytosol resulting in the induction of MHC class I-presentation, a process known as cross-presentation (**Scheme 4.1**).[7] Previously, Hanlon et al. reported the cross-presentation through MHC class I instead of MHC class II using protein-loaded poly (lactic-co-glycolic acid) (or PLGA) nanoparticles that can escape from the endosomal compartment .[8] Similarly, Akagi et al. have described the use of γ-poly (glutamic acid)-based nanoparticles with entrapped ovalbumin (OVA) that allow for its delivery to the cytosol of cells and its subsequent cross-presentation.[9]
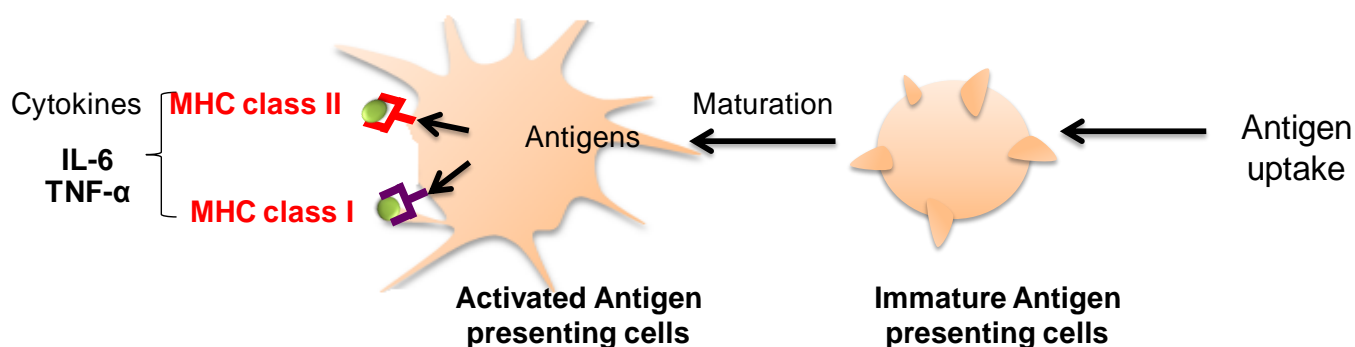
Scheme 4.1 Pictorial representation of activation of antigen presenting cells for immunotherapy

Many researchers in this area have recently focused on the development of carriers, which provide additional adjuvant activity for the induction of immune response. Nanocarriers such as nanoparticles[10], micelles[11], and nanogels[12] have been developed for the cytoplasmic delivery of antigens such as proteins, peptides, or genes. However, many of these are toxic[13] and are unstable.[14] Lipid-based delivery systems, such as liposomes, have been extensively used as carriers because of their biocompatibility, non-toxicity, and ability to undergo membrane fusion.[15] pH-sensitive liposomes modified by polymers have also recently been shown to be an effective approach for the efficient delivery of antigen molecules to APCs such as dendritic cells. Recently, Kono et al. have developed an efficient pH-sensitive liposome by modification with pH-sensitive polyglycidol derivatives.[16] They demonstrated pH sensitivity of the liposomes through their ability to deliver proteins to the cytosol without trafficking through the lysosome. Many polymers such as poly (N-isopropyl acrylamide) (PNIPAM), poly (alkyl acrylic acid), or poly (malic acid) have been used to modify the surface of liposomes in order to induce such pH-responsive behavior.[17] pH responsiveness in the liposomes is important because it promotes the fusion between liposomes and the endosomal membrane[18] causing the release of protein at acidic pH. Interestingly, these pH-sensitive liposomes have been shown to enhance the delivery of antigenic proteins into the cytosol of dendritic cells, thereby causing the induction of an efficient immune response.[16,17]

An important advancement in immunotherapy is therefore the development of physical strategies for the effective cytoplasmic delivery of antigens. Physical approaches such as

electroporation[19] and ultra-sonication[20] have already been developed for immunotherapy applications. However, the main drawbacks of these methods are low cell viability and phenotypic changes. Therefore, to improve on the physical method for effective cytoplasmic delivery of antigens, further research is required. To this end, I have previously developed a new freeze-concentration method that can deliver antigens to cells.[21,22] The gradual formation of ice crystals over a temperature range of -5 to -45°C excludes solute molecules, thereby enhancing the solute concentration in the extracellular solution by means of phase separation.[23] This phenomenon is referred to as "freeze-concentration". In the past, use of the freeze-concentration technology has been limited to the food industry and was used for the production of fruit juices, coffee, and tea-extracts.[24] In my earlier studies showed the effective use of freeze-concentration to enhance the concentration of proteins in the external media close to the cell membrane leading to membrane adsorption[21] and ultimately protein internalization[22] inside the cells. Freeze-concentration offers high cell viability, low cost, and an enhanced interaction between the protein-nanocarrier complex and the cell membrane.

In these previous studies, I also demonstrated the development of pH-sensitive liposomes, generated using a hydrophobic polyampholyte.[22] The hydrophobic polyampholyte nanoparticles were obtained by modification of ε-poly-L-lysine (PLL) with hydrophobic dodecylsuccinic anhydride (DDSA) and succinic anhydride (SA).[21] In the current study, using OVA as a model antigen for immunotherapy, I used both pH-sensitive liposomes and the freeze-concentration method for enhanced protein internalization to demonstrate efficient endosomal protein escape to the cytosol (**Figure 4.1**). Cytosolic delivery of OVA to a macrophage cell line resulted in the induction of an immune response involving MHC class I molecules as well as enhanced secretion of cytokines. My results suggest that through a combination of the use of non-toxic polyampholyte-modified liposomes and freeze-concentration, exogenous antigens may enter the classical class I pathway through the process referred to as 'endosomal escape'.
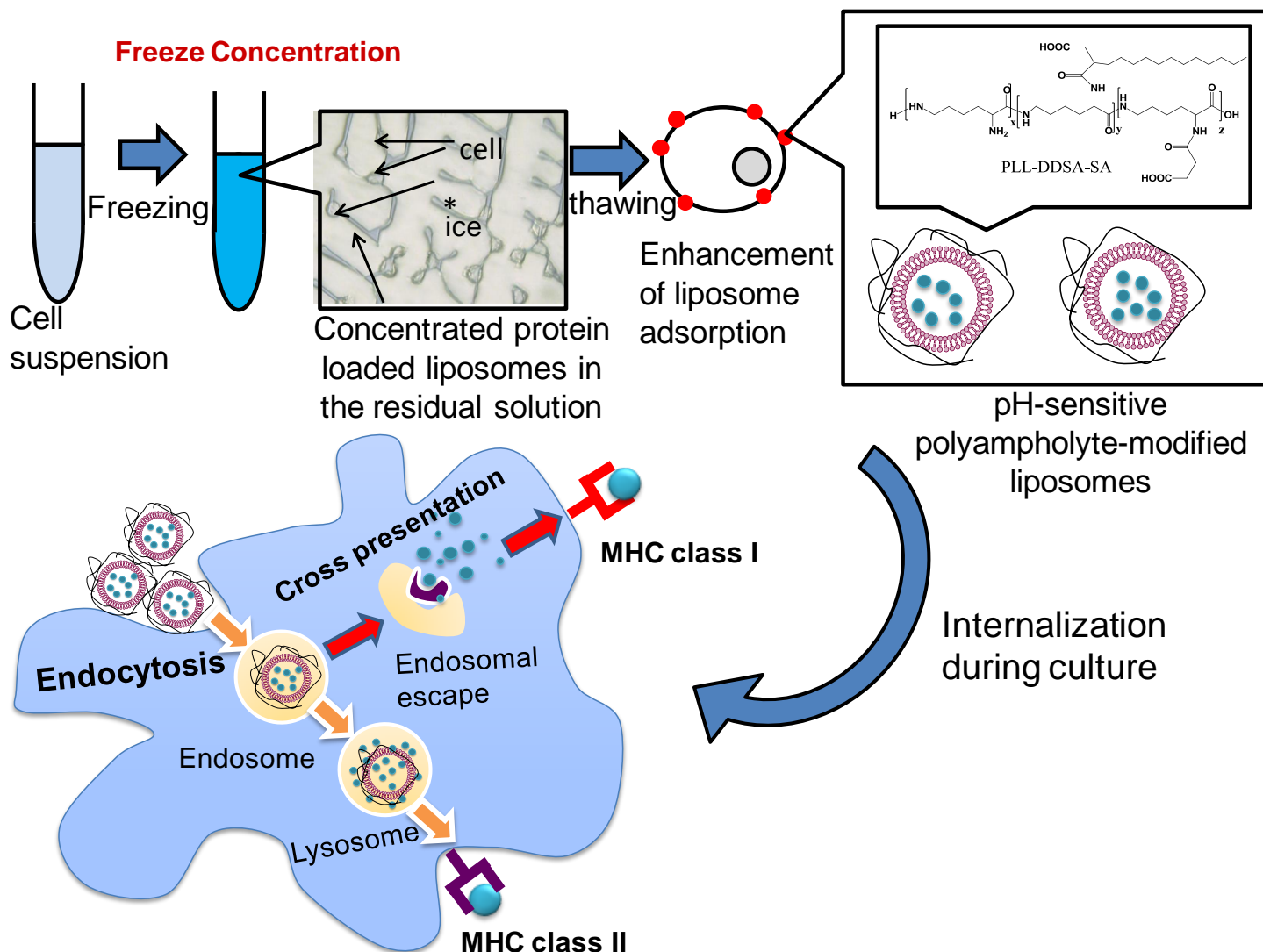
Figure 4.1. Schematic illustration of the expected mechanism of cross-presentation of pH sensitive polyampholyte-modified liposomes for immunotherapy. The polyampholyte-modified liposomes are efficiently internalized through the endocytic pathway after freeze-concentration and fuse with the endosomes. The pH sensitive liposomes can escape from the endosomes and release their antigenic protein cargo into the cytoplasm of the cells where they are processed by the proteasome. Cross presentation results in antigen presentation via MHC class I molecules. Any liposomes that do not escape from the endosome are trafficked through the lysosome and peptides derived from the protein cargo are presented via MHC class II molecules.

4.2 Materials and Methods

4.2.1 Chemicals and Reagents

Pyranine was purchased from TCI (Tokyo, Japan). Zwitterionic lipids such as 1, 2-dioleoyl-sn-glycero-3-phosphocholine (DOPC), 1, 2-dioleoyl-sn-glycero-3-phosphoethanolamine (DOPE) and fluorescently labeled 1,2-dioleoyl-sn-glycero-3-phosphoethanolamine-N-(lissamine rhodamine B sulfonyl) (ammonium salt) (Rh-PE) were obtained from Avanti Polar lipids (Alabaster, AL, US). Enzyme linked immunosorbent assay (ELISA) kits for measurement of interleukin (IL)-6 and tumor necrosis factor (TNF)-α were purchased from BD Biosciences (San Jose, CA, USA), and that for measurement of IL-1β was obtained from Life technologies (Carlsbad, CA, USA). Anti-MHC class-I PE, Anti-MHC class-II PE were purchased from BD Bioscience. *p*-Xylene-bis-pyridinium bromide (DPX) was obtained from Molecular Probes (Eugene, OR, USA). OVA protein (45 kDa) and monophosphoryl lipid A from *Salmonella minnesota R 595* (MPLA) were purchased from Sigma Aldrich (St. Louis, MO, USA). 2-(N-morpholino) ethanesulfonic acid (MES) was obtained from Dojindo (Kummoto, Japan)

4.2.2 Synthesis of polyampholyte cryoprotectant and polyampholyte nanoparticles

Polyampholyte cryoprotectant (PLL-SA) was prepared by succinylation of PLL based on previously published methods.[25] Briefly, an aqueous solution of PLL (25% w/w, 10 mL, JNC Corp., Tokyo, Japan) and SA (1.3 g, Wako Pure Chem. Ind. Ltd, Osaka, Japan) were combined at 50°C for 2 h to convert the amino group to a carboxyl group (**Scheme 3.1**). Hydrophobic polyampholytes were prepared according to previously published methods.[21, 22] Briefly, PLL was reacted with hydrophobic DDSA (5% molar ratio, Wako Pure Chem. Ind. Ltd.) at 100 °C for 2 h. Afterwards, SA was added at a 65% molar ratio (COOH/NH$_2$) and allowed to react for 2 h at 50°C (**Scheme 3.2**). The degrees of substitution of SA and DDSA were obtained using ^{1}H-NMR.

The polyampholytes were characterized by ^{1}H NMR spectra obtained at 25°C on a Bruker AVANCE III 400 spectrometer (Bruker BioSpin Inc., Switzerland) in D$_2$O.

The degrees of substitution of SA and DDSA were obtained by ^{1}H-NMR using equation.

$$\text{Degree of substitution for DDSA (\%)} = (2 * A_{\delta 0.74} / 3 * A_{\delta 1.5\text{-}1.8}) * 100$$

$$\text{Degree of substitution for SA (\%)} = (2 * A_{\delta 2.4} / 4 * A_{\delta 1.5\text{-}1.8}) * 100$$

$A_{\delta 0.74}$ is the integral of the methyl peak from DDSA located at 0.74 ppm and $A_{\delta 2.4}$ is the integral of the methylene peak of SA located at 2.4 ppm. $A_{\delta 1.5-1.8}$ is the integral of the b-methylene peak of poly-lysine at 1.5ppm to 1.8ppm.

4.2.3 Preparation of unmodified or polyampholyte modified liposomes encapsulating OVA

The preparation of unmodified or polyampholyte modified liposomes has been previously described by us.[22] The appropriate amount of lipid DOPC (5 mg) and DOPE (4.7 mg) were dissolved in chloroform (1 mL) and allowed to evaporate under steady stream of nitrogen gas to facilitate complete drying. A thin dry lipid membrane consisting of DOPC and DOPE was mixed with 1.0 mL of OVA (1 mg/mL, in milli-Q water) and the lipid suspension was extruded through a polycarbonate membrane (200 nm pore size) to obtain small unilamellar vesicles (SUVs). For the preparation of hydrophobic polyampholyte modified liposomes, a dry membrane of lipid mixtures with polymer (7:3 w/w) was also prepared by the same method. Ten micrograms of MPLA, which was extracted from lipopolysaccharides, was combined with 5 mg of DOPC and 4.7 mg of DOPE lipids, with or without polyampholytes, for the induction of the immune response.

4.2.4 Particle size measurement of unmodified or polyampholyte-modified liposomes encapsulated with OVA

Stability, surface charge and size distribution were measured by dynamic light scattering (DLS) using a Zeta sizer 3000 (Malvern Instruments, Worcestershire, UK) with a scattering angle of 135° at a temperature of 25°C. The liposomes were dispersed in phosphate buffer saline without calcium and magnesium (PBS (-)) and the zeta potential was measured at the default parameters (dielectric constant of 78.5, refractive index of 1.6).

4.2.5 Pyranine release from liposomes

Pyranine release from liposomes was measured as described in previous reports.[16,17,26] To prepare pyranine-loaded liposomes, unmodified and polyampholyte-modified liposomes were dispersed in aqueous solution containing 35 mM pyranine, 50 mM DPX, and 25 mM MES buffer solution and the pH adjusted to 7.4. The suspension of liposomes with encapsulated

pyranine (lipid concentration: 1 x 10^{-5} M) was added to PBS at varying pHs at 37°C and the fluorescence intensity of the mixed suspension was followed (excitation at 512 nm, emission from 450 to 600 nm) using a spectrofluorometer (JASCO FP-8600, Hachioji, Tokyo, Japan). The percentage release of pyranine from liposomes was defined as

Release (%) = (F_t/F_f) x 100

Where F_t is the fluorescence without addition of Triton-X-100 and F_f is the final fluorescent intensity after addition of Triton-X-100 (final concentration: 0.1%).

4.2.6 Preparation of FITC-labeled OVA protein

OVA (10 mg) and fluorescein isothiocyanate (FITC, 1 mg /mL; Dojindo\) was dissolved in sodium bicarbonate buffer solution (1 mL; 0.5 M, pH 9.0) with gentle stirring and incubated at 4°C overnight with subsequent dialysis (molecular weight cut off: 3 kDa, Spectra/Por, Spectrum Laboratories, Inc., Rancho Dominguez, CA, USA) for three days against water and freeze dried.[17, 22]

4.2.7 Cell Culture

Murine RAW 264.7 macrophages cells (American Type Culture Collection, Manassas, VA, USA) were used in this study and were cultured in Dulbecco's modified Eagle's medium (DMEM; Sigma-Aldrich) supplemented with 10% fetal bovine serum (FBS) at 37°C in a 5% CO_2 humidified atmosphere. When the cells reached 60% confluence they were sub-cultured by trypsinization with 0.25% (w/v) trypsin containing ethylenediamine tetraacetic acid (EDTA) in PBS (-) and were seeded onto new tissue culture plates.

4.2.8 Adsorption of OVA protein using unmodified or polyampholyte modified liposomes via freeze-concentration.

The FITC-OVA-loaded liposomes containing Rh-PE were prepared as follows. Briefly, lipid containing Rh-PE (0.5 mol %) was dispersed in PBS (-) containing FITC-OVA (1 mg/mL) and prepared by the same method described above. The protein-encapsulated solution was then purified using chromatography on a Sepharose 4B column to remove un-encapsulated proteins. RAW 264.7 murine macrophage cells, at a density of $1x10^6$ cells/mL, were re-suspended in 10% PLL-SA cryoprotective solution (1 mL) including unmodified or polyampholyte-modified liposome encapsulated OVA protein (0.5 mg/mL) in a 1.9 mL cryovial (Nalgene, Rochester, NY, USA) and were then placed in a -80°C freezer for 24 h.

After 24 h, the cells were thawed at 37°C and washed with DMEM medium containing 10% FBS. The purpose of using the polymeric cryoprotectant was to protect the cells from damage due to freezing and thereby maintain cell viability. Cell viability was determined by trypan blue staining solution and cell counting with a hemocytometer. The % viable cells were calculated as the number of viable cells divided by total number of cells. Similarly, for non frozen, unmodified and polyampholyte-modified liposomes encapsulated proteins were directly added to the cells without using freeze concentration. For analysis of the adsorption under non-frozen and frozen conditions, the cells were washed with PBS (-) and were observed using a confocal laser scanning microscope (CLSM, FV-1000-D; Olympus, Tokyo, Japan).

4.2.9 Intracellular delivery of OVA protein using freeze-concentration

After thawing, RAW 264.7 cells were washed three times using cell culture medium with 10% FBS. The cells were then seeded onto 35 mm glass bottom dishes and medium (1 mL) was added After incubation for 24 h, the attached cells were washed with PBS and internalization of protein/liposomes was observed using CLSM. In order to compare the effect of freezing on internalization with non-freezing, I gently added the appropriate protein-nanocarrier complex to RAW 264.7 cells and incubated them for 24 h to create a 'non-frozen' control. In all cases, liposomes were labeled with Rh-PE labeled lipid and the protein cargo was FITC-labeled OVA. All cells were washed with PBS (-) prior to observation of internalization CLSM.

4.2.10 Endosomal escape of OVA protein

A thawed suspension of RAW 264.7 cells (100 μL) at a density of 1×10^4 cells/mL containing 10% PLL-SA cryoprotectant with OVA-loaded unmodified or polyampholyte-modified liposomes was washed twice with cell culture medium containing 10% FBS and then seeded into a glass bottom dish. The cells were incubated for 24 h at 37°C in a humidified atmosphere containing 5% CO_2. LysoTracker Red®DND-26 (Molecular Probes) and Hoechst blue 33342 dye (ThermoFisher Scientifc, Waltham, MA, USA) were added and incubated for 30 min before observation. The localization of protein inside the cells was examined using CLSM.[24]

4.2.11 *In vitro* antigen presentation assay

The RAW 264.7 macrophage cell line at a density of 1×10^6 cells /well was used for the antigen presentation assay. Lipopolysaccharide (LPS, 10 µg, Sigma Aldrich), which is also known as endotoxin, was used as a positive control for the induction of a strong immune response acting through the toll like receptor-4 pathway. For the preparation of non-toxic immune-active liposomes, MPLA adjuvant was added to unmodified or polyampholyte-modified liposomes. MPLA is a non-toxic analog of LPS that is approved for clinical use as a vaccine adjuvant. It is considered as safe, well-tolerated, and it can enhance stimulation of the immune response. For the frozen system, 1×10^6 cells were frozen with polymeric cryoprotectant; 10% PLL-SA containing unmodified or polyampholyte-modified liposomes containing OVA at -80°C for 24 h, and the cells were then thawed at 37°C. Following this the cells were seeded (100 µL, 1×10^4 cells) into 12 well plates and fresh DMEM medium with FBS was added. The cells were then incubated for 48 h at 37°C, in a humidified atmosphere containing 5% CO_2. In contrast, for the non-frozen condition, 1×10^6 cells were seeded into 12 well plates and cultured under the same conditions. Afterwards, unmodified and polyampholyte- modified liposomes were added gently to the cells. To compare the use of non-frozen or frozen systems in immunotherapy, I used flow cytometry and ELISA assays to measure the levels of cells surface receptors and cytokines respectively.

4.2.12 Flow cytometry analysis

The cells from both the non-frozen and frozen conditions were scraped and washed with PBS buffer (containing 0.5 mM EDTA and 0.5% BSA/FBS). A mouse monoclonal antibody (mAb; anti MHC-I PE or anti MHC–II PE) in PBS-EDTA (50 µL) was added to the cell suspension, mixed and incubated at 4°C in the dark for 30 min on ice. The samples were divided into stained which is positive control and negative control that is unstained with mAb. The cells were then centrifuged at 120g for 4 min and re-suspended in PBS-EDTA. The cells were then transferred to a FACS tube and the positive control, non-frozen, and frozen samples were immunostained with fluorescently conjugated anti-mouse monoclonal antibodies. The negative control of each samples were carried out by replacing labeled anti-mouse monoclonal antibody to PBS buffer. Data acquisition and analysis were performed using FACS Calibur instrument (BD Bioscience, Franklin Lakes, NJ, USA). For each sample, 20,000 cells were counted and gated on the basis of 20,000 forward scattering and side scattering events. Stained cells were determined by reference to non-stained cells.

4.2.13 ELISA measurement of in vitro antigen response

The levels of TNF-α, IL-1β, and IL-6 in RAW 264.7 from cell culture supernatants were measured by ELISA assay in order to compare the non-frozen and frozen systems. Briefly, a monoclonal antibody specific for the particular assay from each kit was coated onto a 96-well plate. Samples and standard were added, allowed to incubate, washed, and detection antibodies were added. For the removal of excess antibody, Streptavidin-horseradish peroxidase (HRP) was added and incubated for 15 min in dark at room temperature. The solution was aspirated and thoroughly washed by washing buffer at least 4 times. After incubation and washing, 3, 3', 5, 5'-tetramethylbenzidine (TMB) was added followed by 30-min incubation. The reaction was terminated by the addition of 100 µL of stop solution (1 M phosphoric acid); the optical density of the sample was then read at 450 nm using a microplate reader (Versa max, Molecular Devices, Sunnyvale, CA, USA).

4.2.14 Statistical analysis

All data are expressed as means ± standard deviation (SD). All experiments were conducted in triplicate. To compare data among more than 3 groups, a one-way analysis of variance (ANOVA) followed by the Tukey–Kramer post-hoc test was used. To compare data between two groups, Student's t-tests were used. A P value of <0.05 was considered statistically significant.

4.3 Results and Discussions

4.3.1 Synthesis of polyampholytes

The polyampholyte cryoprotectant was prepared using PLL as described in my previous report.[25] A novel polyampholyte cryoprotectant, denoted as PLL-SA, was synthesized by changing the appropriate ratio of amino to carboxyl groups by succinylation with succinic anhydride (65 mol %) (**Scheme3.1**). This polyampholyte cryoprotectant showed extremely high cryoprotection ability in 10% aqueous solution in a variety of different cell lines.[25] The degrees of substitution of SA was found to be 62 % as determined by ^{1}H NMR (**Figure 4.2a**). Similarly, a hydrophobic-modified polyampholyte (PLL-DDSA), which had been synthesized previously by substitution of PLL with DDSA (5 mol %) (100°C for 2 h with constant stirring), was then substituted with SA (65 mol %) at 50°C for 2 h to synthesize the new hydrophobic polyampholyte PLL-DDSA-SA as described in chapter-2

and chapter -3 (**Scheme 3.2**).[21,22] Similarly, the degrees of substitution of DDSA was found to be 4.4 % determined by ^{1}H NMR. (**Figure 4.2**)
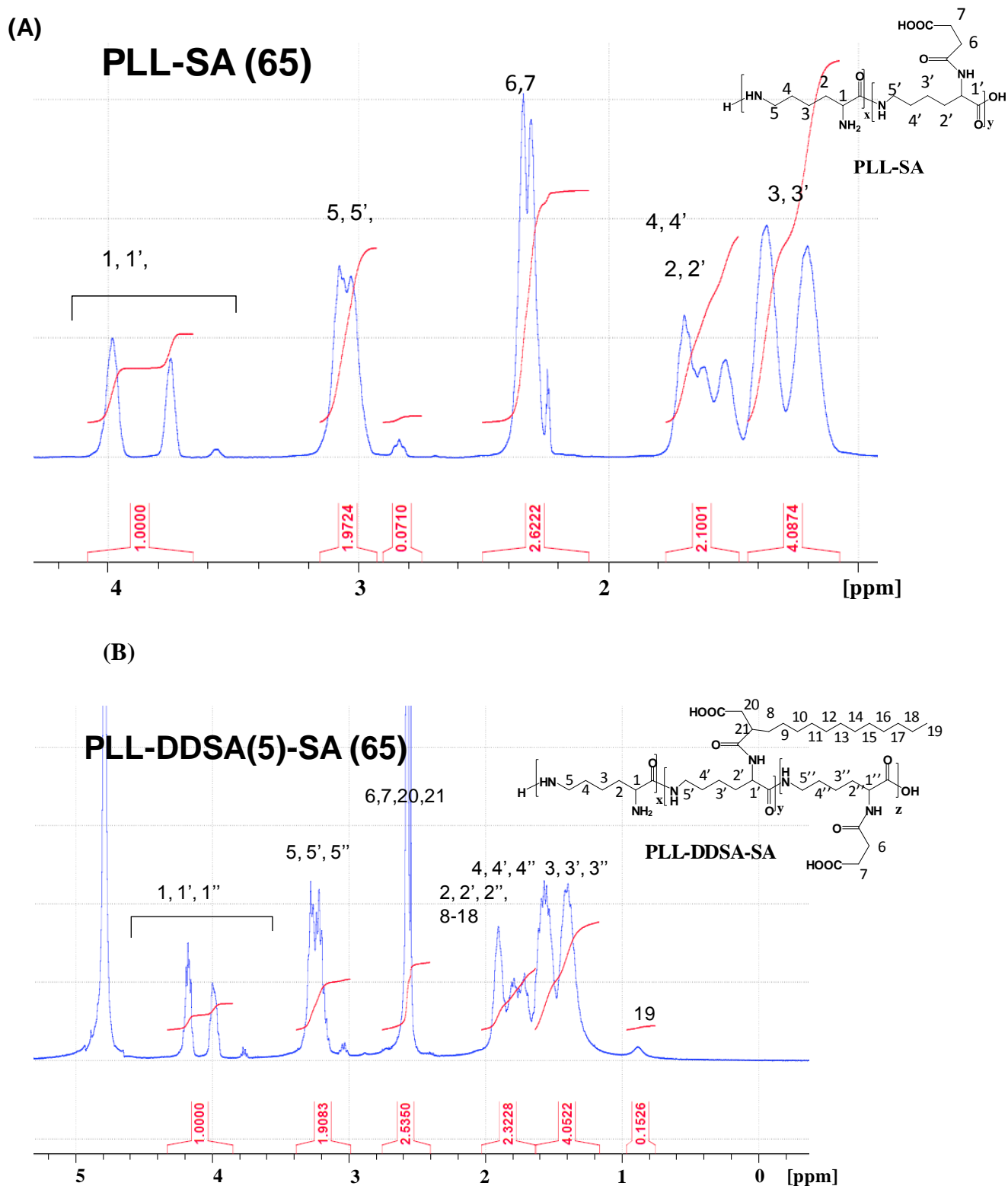

**Figure 4.2.** (a) ^{1}H NMR of PLL-SA (b) ^{1}H NMR of PLL-DDSA-SA

4.3.2 Preparation and characterization of unmodified or polyampholyte-modified liposomes encapsulating OVA

In my previous study I prepared two different type of liposomes.[22] One type was a zwitterionic liposome prepared by the combination of lipids such as DOPC and DOPE. The other type was a polyampholyte-modified liposome obtained after the addition of PLL-DDSA-SA to zwitterionic liposomes. I then investigated both the particle size and the zeta potential of unmodified and polyampholyte-modified liposomes. **Table 4.1** shows the zeta potential and the particle diameter, obtained using DLS method. The surface charge of polyampholyte-modified liposomes was around -18.43 mV whereas the unmodified liposomes were nearly -5.13 mV. The increased negative value for the surface charge of polyampholyte-modified liposomes compared to that for the unmodified liposomes indicated that the surface charge of the liposome was greatly enhanced when it was modified with hydrophobic polyampholytes. The reason for this is because the polyampholytes contain an excess number of carboxyl groups over amino group in their polymeric backbone. These results clearly indicate that the polyampholytes efficiently modified the surface of the liposome.

The particle size of the liposomes were similar for both unmodified and polyampholyte-modified liposomes with the unmodified liposome having a mean diameter of around 279 nm and the polyampholyte-modified liposomes being slightly larger in diameter at 305 nm. Next, I also evaluated the stability of both the unmodified and the polyampholyte-modified liposomes encapsulated OVA protein over time under physiological conditions. As shown in **Figure 4.3**, the polyampholyte-modified liposomes did not change their particle size whereas unmodified liposomes appeared to be unstable with evident changes in mean particle size being easily detected. These data suggest that hydrophobic polyampholytes might enhance the stability of liposomal membranes because of the presence of hydrophobic polymer chains.

Table 4.1 Zeta potential and particle size of unmodified and polyampholyte-modified liposomes. All data are expressed as means ± standard deviation (SD). All experiments were conducted in triplicate.

Samples	Zeta Potential (mV)	Particles Size (nm)
Unmodified Liposomes	-5.14 ± 3.1	279.4 ± 38.0
Polyampholyte-modified liposomes	-18.43 ± 1.3	305.0 ± 71.8
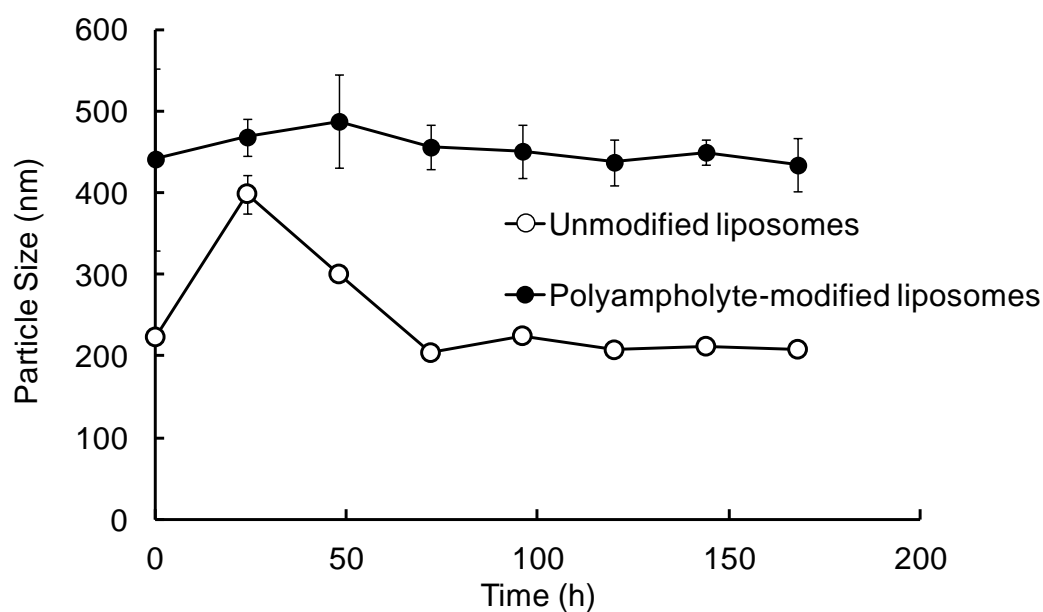
Figure 4.3 Particle size stability of unmodified and polyampholyte-modified liposomes encapsulated OVA over time at 25°C. Data are expressed as mean ± SD.

4.3.3 Adsorption of protein encapsulating liposomes onto cells under non-frozen and frozen conditions

To investigate the use of the freeze-concentration approach for cytosolic delivery of antigen proteins, I elected to use RAW 264.7 macrophage cells as representative APCs since these cells are readily cultured and display a robust immune response. I examined the adsorption of OVA-encapsulated liposomes onto RAW 264.7 macrophages with or without freezing.

As shown in **Figure 4.4 a, b**, confocal imaging of cells showed that the fluorescence signal from both unmodified and polyampholyte-modified liposomes loaded with OVA was significantly higher in the frozen condition compared to the non-frozen condition, indicating enhanced adsorption to the cell surface. These results indicate that freeze-concentration acts as a driving force that enhances the adsorption of liposomes to the cell membrane. Quantification of the fluorescence intensity also showed that under the frozen condition, both unmodified and polyampholyte-modified liposomes increased adherence around the cell membrane (**Figure 4.4 c**). As a control, I also examined the cell adsorption of free, un-encapsulated OVA protein, with and without the freeze-concentration approach. I found that free OVA protein does not adhere to the cell membrane under the non-frozen condition. OVA protein was found to adsorb to a low extent to the cell membrane after applying the freeze-concentration approach. These data indicate that free OVA has a low association with cells after thawing, thereby restricting its entry into cells (**Figure 4.5 a, b**).

In earlier reports, energy-based methods such as electroporation have been frequently used as a physical method for the delivery of protein antigens into cells, but the presence of a strong electrical field creates lethal nanopores in the membrane which disrupt cellular homeostasis and lead to cell damage and a decrease in overall cell viability.[26] Based on this, I examined cell viability following freeze-concentration in the presence of unmodified or polyampholyte-modified liposomes. Cell viability was 93% for polyampholyte-modified liposomes and 89% for unmodified liposomes; this difference was not significant (**Figure 4.6**). Taken together, these data indicate that the freeze-concentration method provides enhanced association of OVA-encapsulated liposomes onto cells while at the same time maintaining high cell viability.

Moreover, the stability of the protein-nanocarrier complex plays a crucial role in therapeutic applications at ultra-cold temperatures. I found that the particle size did not change significantly in either unmodified or polyampholyte-modified liposomes at -80°C[22],

indicating that the polymeric cryoprotectant stabilized and reduced liposome aggregation. Accordingly, I used a polymeric cryoprotectant and a protein-liposome complex for delivery of the protein antigen in conjunction with the freeze-concentration method.

Unmodified Liposomes
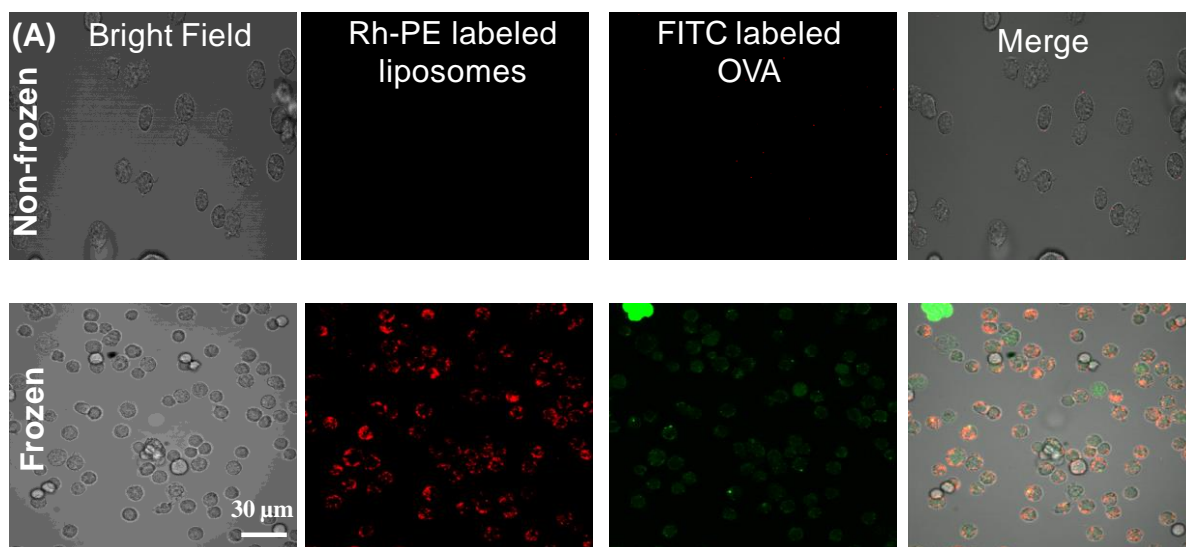
Polyampholyte modified liposomes
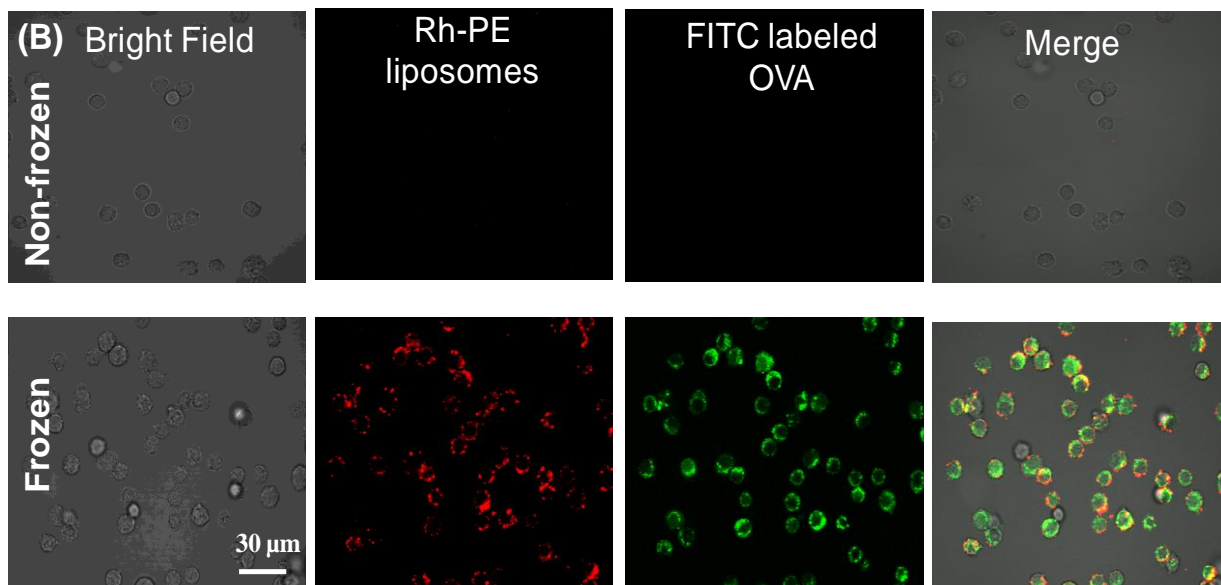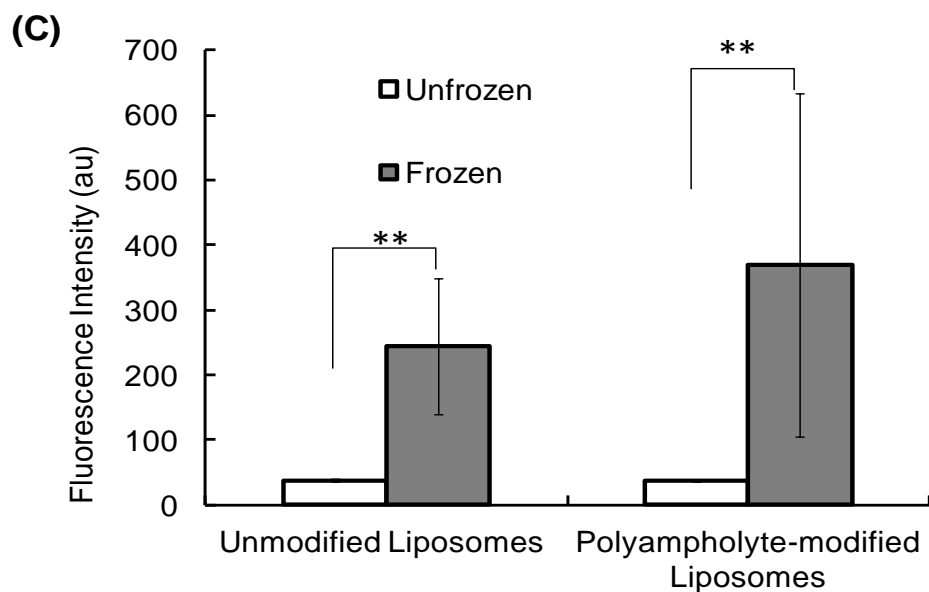
Figure 4.4 RAW 264.7 macrophage cells were cryopreserved using 10% PLL-SA in the presence of unmodified or polyampholyte-modified liposomes at -80°C for 24 h. Liposomes were stained with 0.5 mol% Rh-PE and the protein cargo (OVA) labeled with FITC. For non-frozen samples, unmodified and polyampholyte-modified liposomes were added to cells directly and incubated for 24 h. (A) Unmodified Liposomes (B) Polyampholyte-modified Liposomes. Scale bar: 10 µm (C) Quantification of mean fluorescence intensity obtained from confocal microscopy. Data are expressed as the mean ±SD. **P < 0.01.
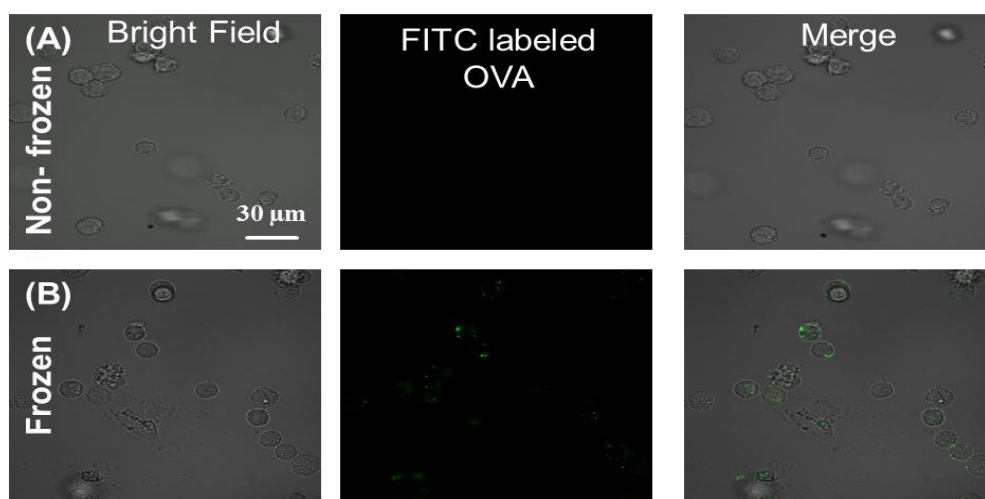
Figure 4.5 RAW 264.7 macrophage cells were cryopreserved using 10% PLL-SA in the presence of FITC-labeled OVA protein at -80°C for 24 h. (A) Non-frozen (B) Frozen. Scale bar: 30 µm
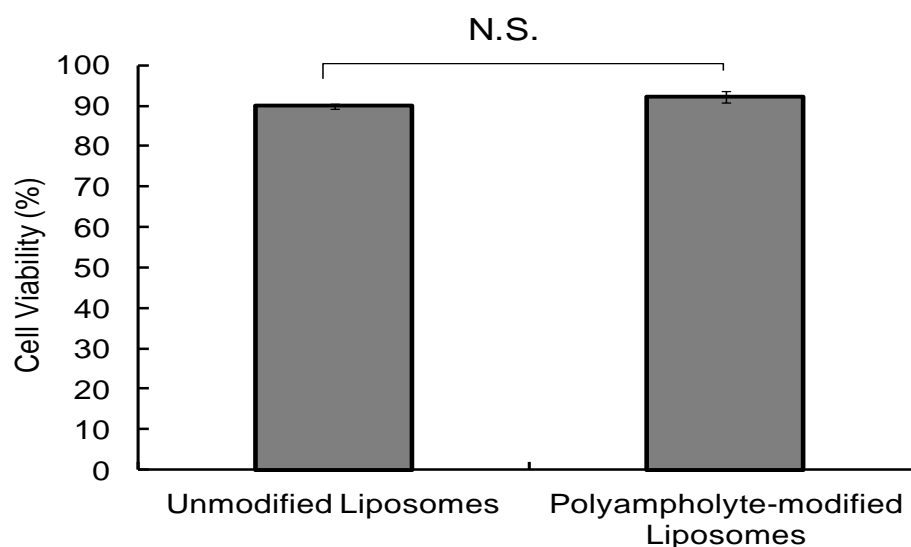
Figure 4.6 Cell viability of unmodified and polyampholyte-modified liposomes after storage at -80 °C for 24 h in the presence of cryoprotectant. Data are expressed as the mean ±SD NS: not significant.

4.3.4   Internalization of protein encapsulating liposomes onto cells via non-frozen and frozen

Following enhanced adsorption to the cell surface by freeze-concentration, the internalization of the protein nano-carrier complex inside the cells is an extremely important step in immunotherapy. In order to examine this, RAW 264.7 cells were frozen in the presence of OVA-encapsulated, unmodified or polyampholyte-modified liposomes and internalization of the liposome and OVA examined (**Figure 4.7a-d**). Both unmodified and polyampholyte-modified liposomes were efficiently internalized by RAW 264.7 cells following the freeze-concentration process (**Figure 4.7 b, d**). In contrast, in either of the non-frozen controls, there was very little internalization of the complex (**Figure 4.7 a, c**). This result demonstrated that freeze-concentration could accelerate internalization of the OVA encapsulated liposomes into cells. Additionally, as shown in **Figure 4.7 d** internalization was visibly greater when polyampholyte-modified liposomes were used rather than unmodified liposomes (**Figure 4.7 c**). Quantification of the fluorescein isothiocyanate (FITC) fluorescence intensity derived from the FITC-OVA cargo protein confirmed that freeze-concentration using polyampholyte-modified liposomes was more effective than unmodified liposomes (**Figure 4.7 e**). One possible explanation for this is that the hydrophobic nature of the polyampholyte might enhance the adsorption and interaction with the cell membrane.[27] Several studies have also

120

suggested that modification of liposomes with polymers enhances uptake and internalization of materials into the cytoplasm compared to unmodified liposomes.[28,29]These results are therefore in good agreement with previous reports.[21,22] In addition, as a control, I examined the internalization of un-encapsulated FITC-OVA protein under the non-frozen and frozen conditions. As for the similar study examining adsorption, I found that uptake of un-encapsulated FITC-OVA protein without liposomes was low under both non-frozen and frozen conditions (**Figure 4.8 a,b**). It has been shown from various studies that liposomes promote adhesion and increase the fusion and permeability of the cell membrane.[16,17] Therefore, in this study, I confirmed that liposomes are extremely crucial to enhance the interaction between the cell membrane and protein-carrier complexes.

Consistent with my previous studies, protein antigen adsorption and internalization increased after freezing.[21,22] As shown in **Figure 4.4a,b** the freeze-concentration method efficiently induces the adsorption of the FITC-labeled OVA-loaded protein-liposome complex to the cell membrane. This enhanced adsorption is likely due to a combination of the high affinity of the hydrophobic polyampholytes for the cell membrane as well as the freeze-concentration effect.[21,22] In OVA-encapsulated unmodified liposomes, the internalization was also enhanced (**Figure 4.7 b,d**), although the magnitude was lower than for polyampholyte-modified liposomes (**Figure 4.7 d**); presumably this reflects the freeze-concentration effect alone.
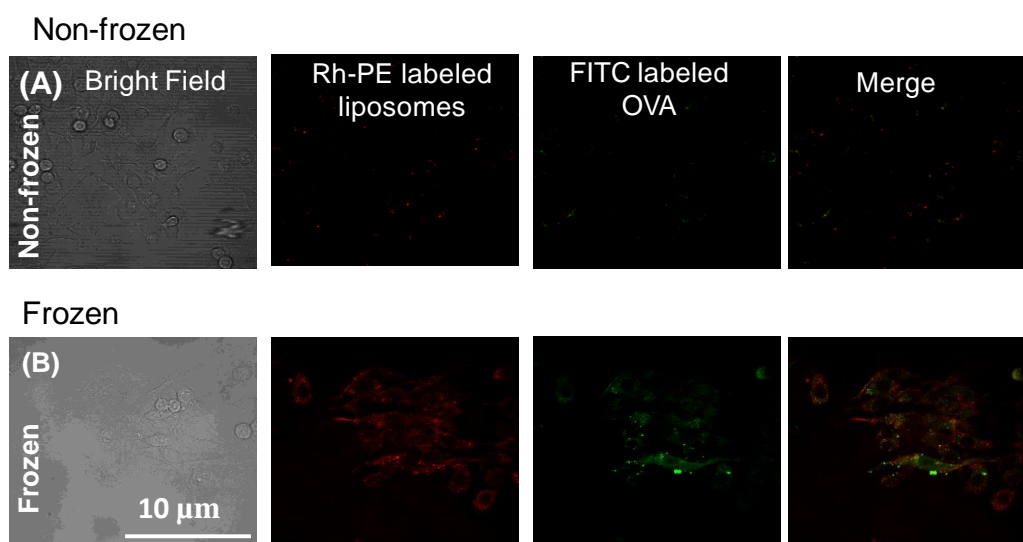
Polyampholyte-modified Liposomes

Non-frozen
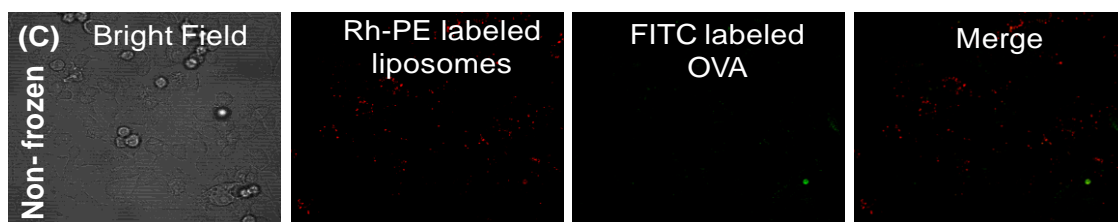
Frozen
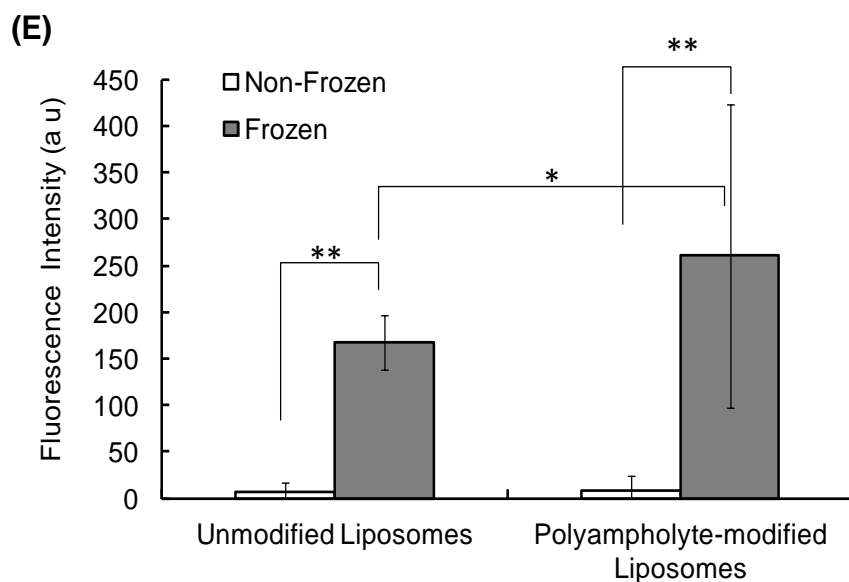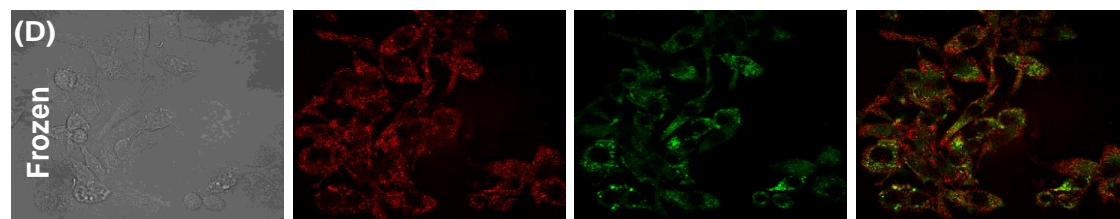
Figure 4.7 Confocal microphotograph showing Internalization of OVA in RAW 264.7 cells. (A, C) without freeze concentration of unmodified and polyampholyte-modified liposomes encapsulated OVA (B, D) With freeze concentration of unmodified and polyampholyte-modified liposomes encapsulated OVA. Scale bars: 10 μm. (E) Quantification of OVA internalization by fluorescence confocal microscopy in non-frozen and frozen liposomes. Data are expressed as mean ± SD. **P < 0.01, *P < 0.05
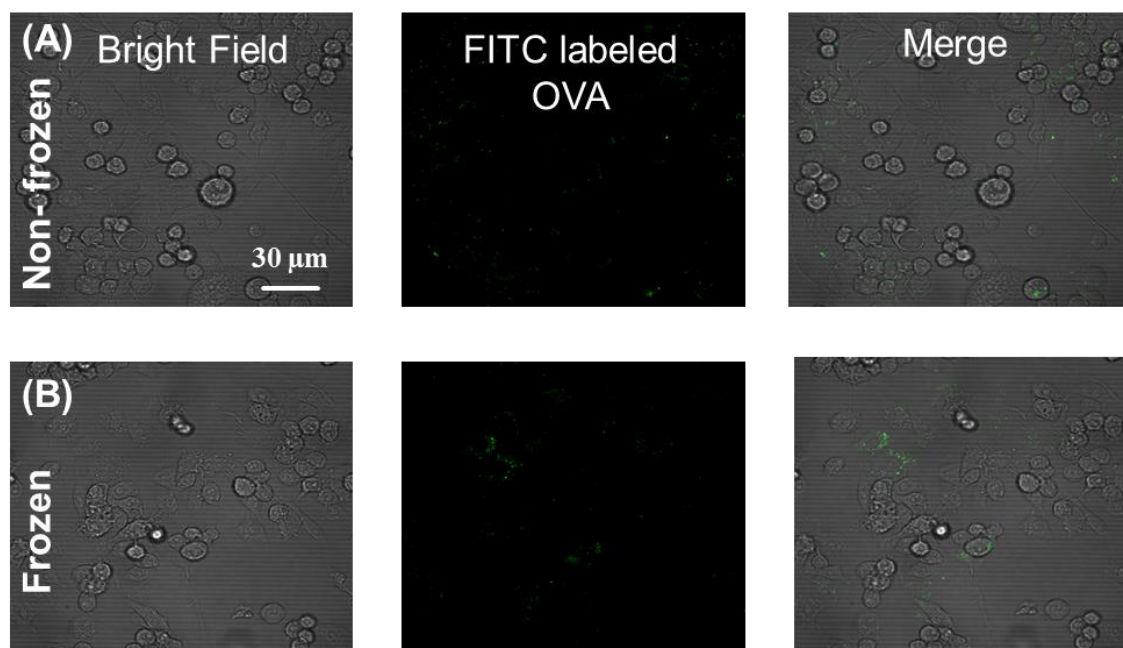
Figure 4.8 Confocal microscopy images showing internalization of OVA in RAW 264.7 cells after 24 h. (A) Non-frozen (B) Frozen. Scale bar: 30 μm

4.3.5   Endosomal escape of proteins from unmodified or polyampholyte-modified liposome

Escape of a liposomally encapsulated cargo protein from endosomes is an important event if this approach is to be considered as viable in immunotherapeutic applications. Normally, the majority of an internalized protein remains in the endosomes and is unable to reach the cytosol of cells, thus preventing MHC-class I expression. Therefore, I investigated the ability of OVA to escape from endosomes after freeze-concentration-based internalization. For unmodified liposomes, no green fluorescence was observed in the cytosol indicating that OVA remained in the endosomes (**Figure 4.9a**). Interestingly, in this study, I found that the freeze-concentration method increased FITC-OVA protein internalization with unmodified liposomes (**Figure 4.7b**). However, these unmodified liposomes did not show a significant release of FITC-OVA protein from the endosomes (**Figure 4.9a**). I cannot exclude the possibility that after using the freeze-concentration method, a small but undetectable amount of FITC-OVA could be released from the endosomes (**Figure 4.9 a**). In contrast, it is certain that a strong green fluorescent signal was observed using polyampholyte-modified liposomes, indicating efficient release of FITC-OVA from endosomes (**Figure 4.9 b**). These data

indicated that the pH-sensitive liposomes released the OVA protein more efficiently than unmodified liposomes.

To understand the pH sensitivity of the unmodified or polyampholyte-modified liposomes I compared release of pyranine, a fluorescent dye, from each type of liposome under different pH conditions. At physiological pH, both unmodified and polyampholyte-modified liposomes did not show any noticeable release of pyranine over time. In contrast, under mild acidic conditions (pH-5.5), polyampholyte-modified liposomes demonstrated a high release of pyranine, whereas unmodified liposomes showed only weak release of pyranine (**Figure 4.9 c**). I also investigated the effect of pH sensitivity of OVA-encapsulated liposomes using DLS analysis (**Figure 4.9 d**). The particle size of unmodified liposomes did not change on varying the pH from 7.4 to 5.5 whereas polyampholyte-modified liposomes tended to aggregate at acidic pH and exhibit a larger size.

I found that in polyampholyte-modified liposomes, but not in unmodified liposomes, destabilization of the liposome membrane and release of encapsulated OVA occurs readily at a mildly acidic pH of 5.5 (**Figure 4.9 a-d**). This is because at acidic pH, the carboxyl group present in the polyampholyte becomes protonated resulting in destabilization of the liposomal membrane and ultimately to release of the cargo protein. Therefore, after endocytosis, the low pH in the endosomes induces the fusion of the liposomal membrane with the endosomal membrane promoting the release of the resident cargo protein into the cytosol. My findings are in good agreement with previous reports.[16,17,22,30]; in particular, Yuba et al., showed that after modification with succinylated poly (glycidol) and 3-methylglutarylatedpoly (glycidol), liposomes obtained the ability to fuse at acidic pH and deliver their contents into the cytosol through fusion with endosomal membranes.[30] Based on these collective data, I conclude that polyampholyte-modified liposomes release OVA protein more efficiently than unmodified liposomes due to their pH sensitivity.

(D)
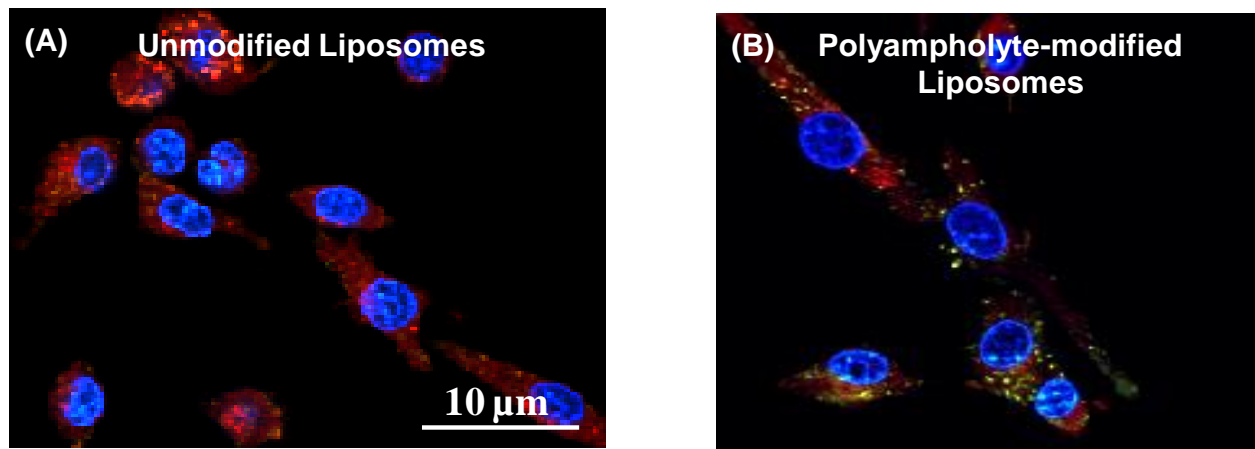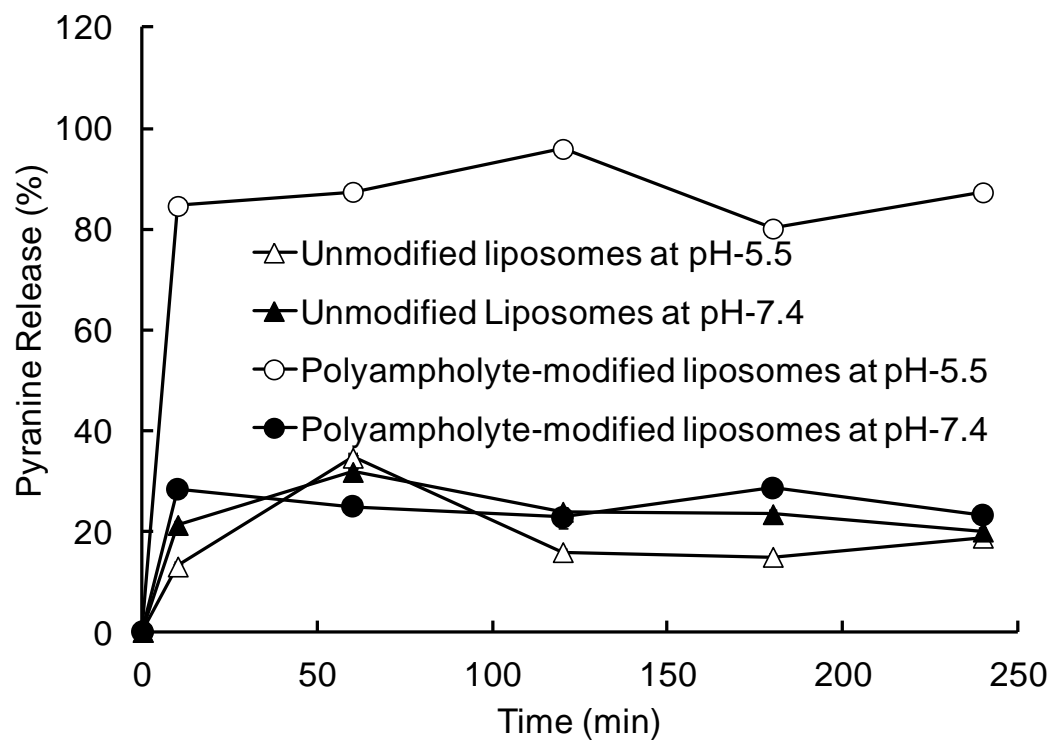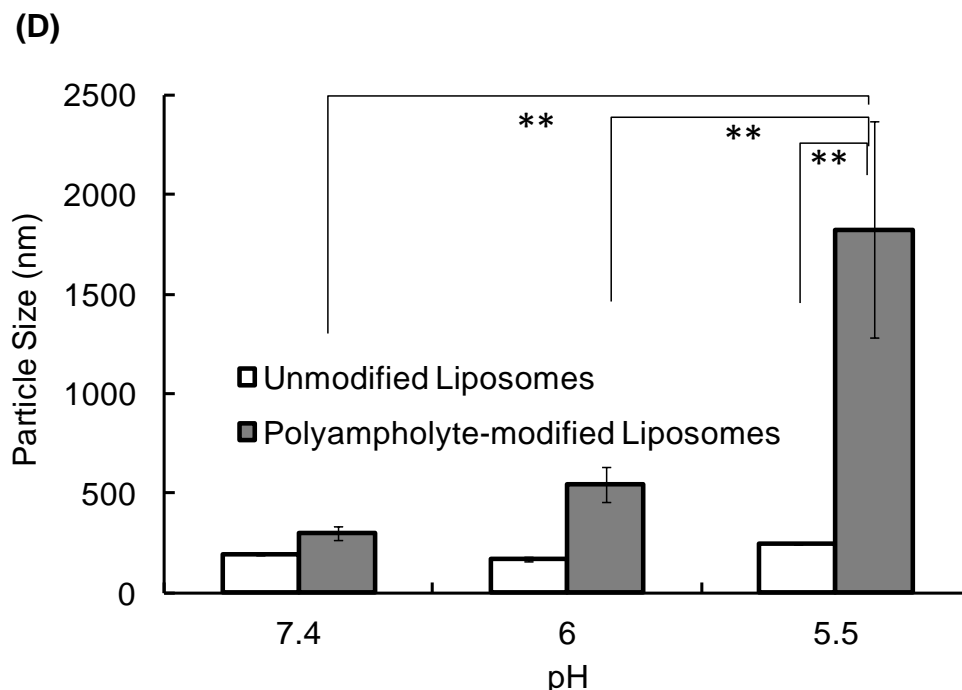
Figure 4.9 Endosomal escape of OVA protein in RAW264.7 cells. RAW264.7 cells (1×10^6 cells/mL) were cryopreserved with the polymeric cryoprotectant PLL-SA and OVA protein encapsulated liposomes at -80°C. The cells were thawed and then seeded for 24 h at 37°C. The late endosomes and nuclei were then stained using LysoTracker Red and Hoechst blue 33342 respectively. (A) Unmodified Liposomes (B) Polyampholyte-modified Liposomes. Scale bar: 10 μm. (C) pH- sensitive release of liposome contents. Time course of pyranine release from unmodified liposomes (triangle) and polyampholyte-modified liposomes (circle) at pH 5.5 (open) and pH-7.4 (closed). (D) Particle size of unmodified liposomes and polyampholyte modified liposomes at pH 5.5 and 7.4. Data are expressed as mean ±SD. **$P < 0.01$.

4.3.6 Macrophage activation using liposomes and the freeze-concentration method

In order to induce an immune response, APCs, such as dendritic cells or macrophages, must present antigenic peptides to MHC class I and MHC class II molecules which then respectively activate CD8 (+) cytotoxic T lymphocytes and CD4 (+) helper T cells.[16, 17] For this reason, I next analyzed the effect of activation of RAW 264.7 macrophages on the expression of MHC molecules in the presence of OVA-loaded liposomes containing monophosphoryl lipid A from *Salmonella minnesota R 595* (MPLA) as an adjuvant (immune

activator) in the membrane.[16] RAW 264.7 cells were incubated with unmodified or polyampholyte-modified liposomes under frozen or non-frozen conditions using lipopolysaccharide (LPS) as a positive control. Following this, I examined the cell surface expression of MHC class I and MHC class II molecules using flow cytometry with MHC molecule-specific antibodies (**Figure 4.10**). As negative controls, cells from the respective samples were included that lacked the appropriate MHC class molecule (**Figure 4.10 a-e**). Incubation of RAW 264.7 cells with polyampholyte-modified liposomes under freeze-concentration conditions caused a large increase (almost 3 fold) in MHC class I expression compared to non-frozen polyampholyte-modified liposomes (**Figure 4.10 i, j**). In contrast, there was virtually no effect on MHC class II expression observed under these or any other conditions (**Figure 4.10 k-o**). Interestingly, after addition of liposomes under non-frozen conditions, two peaks were observed indicating that some fraction of OVA remains intact inside endosomes (**Figure 4.10 g, i**). On the other hand, a single high intensity peak was obtained under freeze-concentration conditions, demonstrating that a large proportion of OVA was transferred to the cytosol of the cells. (**Figure 4.10 h, j**). OVA encapsulated unmodified liposomes also enhanced MHC class I surface expression with the freeze-concentration methodology as compared to the level of MHC class I induced by LPS (**Figure 4.10 f,h**).

MHC class I surface molecules increased significantly when freeze-concentration was used, particularly with polyampholyte-modified liposomes, but also to a lesser extent for unmodified liposomes. This suggests that the freeze-concentration method results in presentation of exogenous antigens to MHC class I molecules through enhanced delivery of the antigen into the cytosol of cells (**Figure 4.10 h, j**). In keeping with this, the levels of MHC class II molecules barely changed (**Figure 4.10 f-j** and **k-o**). Taken together, the data suggest that the liposomes are internalized through endocytosis and that the OVA protein cargo is released from the endosomes into the cytosol under mildly acidic conditions in the endosome by endosomal escape. My data clearly show that the polyampholyte-modified liposomes are pH sensitive, but the unmodified liposomes are pH-sensitive inside cells since they also increased MHC class I expression, albeit to a lower extent (**Figure 4.10 f-j**). In this study, zwitterionic liposomes composed of DOPC and DOPE were used. DOPE is unsaturated and has the ability to acquire a hexagonal phase at low pH and so it provides pH-sensitivity to zwitterionic liposomes.[31] The polyampholyte-modified liposomes have greatly enhanced endosomal escape because of the combination of a membrane-destabilizing

polymer and the presence of DOPE which significantly destabilize the endosomal membrane and allows for greater release of cargo into the cytoplasm (**Figure 4.9 a-d**). Numerous studies have shown that exogenous protein antigens can be presented on MHC class I molecules via a process known as cross-presentation[30,32] The physiological mechanism of cross-presentation remains unclear.[33] In my study, the exogenous liposome-encapsulated antigen (OVA) is internalized through endocytic pathways and, after escaping from endosomes into the cytoplasm through a pH-dependent mechanism, is degraded by proteasomes. While I have not directly proven that OVA-derived peptides are presented in the context of MHC class I molecules present on APCs in this study, I aim to focus on this question in future studies.

A few studies have also reported the phenomenon of greater increases in expression of MHC class I surface molecules compared to MHC class II molecules in immune cells.[34] One study compared the expression of cell surface molecules using the RAW 264.7 cells following LPS stimulation, and showed enhanced expression of MHC class I compared to MHC class II molecules.[35]

The function of MHC class I molecules is to activate cellular immunity. So, from the viewpoint of cancer immunotherapy, the MHC class I molecules are extremely beneficial in inducing activation of CD8 (+) cytotoxic T lymphocytes (CTLs).[6] CTLs recognize the complex between tumor antigens and MHC class I molecules that are expressed on cancer cells and directly kill tumor cells. The data presented here clearly show that the freeze-concentration method introduces antigens into the cytosol of RAW macrophage cells effectively resulting in increased MHC class I expression.

In order to confirm that the effects on MHC class I expression were specific, I examined the effect of the freeze-concentration method in cells in the absence of liposomes and OVA. There was a slight increase in fluorescence demonstrating that stress caused by freezing induces MHC class I expression compared with that in non-frozen condition (**Figure 4.11 a-b**). From these results, it has been suggested that freezing could affect in expression efficiently.

In conclusion, the freeze-concentration method strongly enhanced cell surface expression of MHC class I as compared to the non-frozen method. In contrast, the cell surface expression of MHC class II was not up-regulated to any significant extent under any of the conditions used in this study (**Figure 4.10 f-j** and **k-o).** These results demonstrated that freeze-concentration increased levels of the OVA-loaded liposomes around the cell membrane and triggered their internalization, thereby enhancing the immune response.
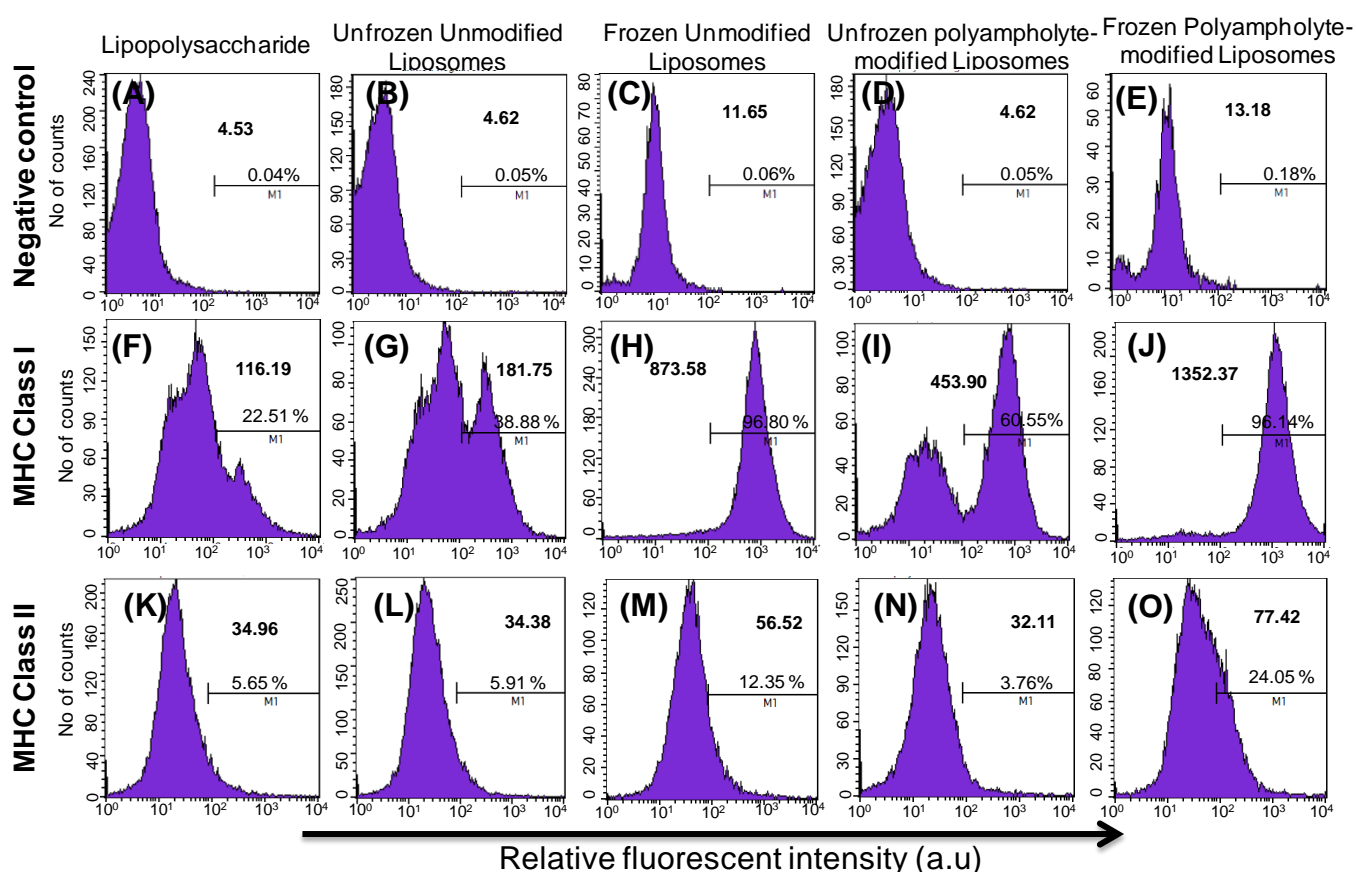
Figure 4.10 Expression of MHC class I and MHC class II analysis using RAW 264.7 macrophage cells treated with unmodified and polyampholyte-modified liposomes. As a positive control, LPS (10 µg) was to stimulate the RAW macrophage cell line. (a-e) Negative control for each sample is shown. Cells were stained with either a mAb, anti MHC class-I (f-j), or anti MHC class-II (k-o). The mean fluorescence intensity is shown as a value on the right hand side of each panel M1 represents the percentage of stained cells from the histogram. The mean fluorescence intensity for untreated RAW 264.7 cells was 4.43.
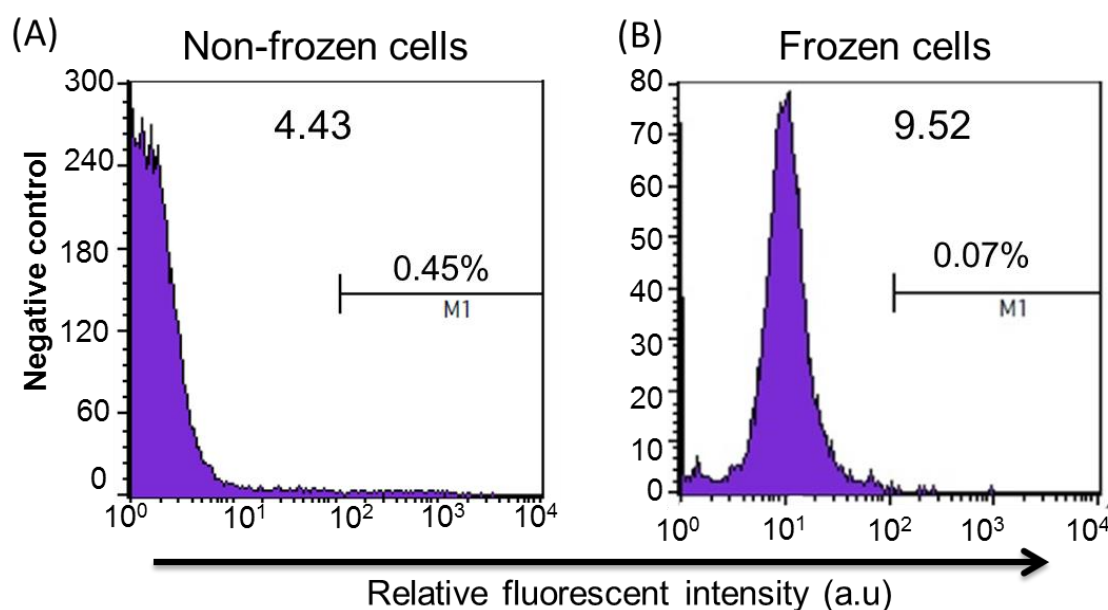
Figure 4.11 Flow cytometry analysis of unfrozen and frozen RAW 264.7 macrophage cells. The cells were unstained with antibody marker (mab). The mean fluorescence intensity is shown as a value on the right hand side of each panel. M1 represents the percentage of stained cells from the histogram. (A) Non-frozen (B) Frozen

4.3.6   ELISA studies to examine cytokine secretion

Cytokines are signaling molecules that are secreted by macrophages, B lymphocytes, and T lymphocytes, and play an important role in the regulation of the immune system. These pro-inflammatory cytokines are usually induced by LPS, play key roles in the inflammatory response, and are well known to be secreted by macrophages and monocytes as part of the innate immune system.[36,37] IL-1β is a potent pro-inflammatory cytokine that is important in host-defense responses to infection and injury. IL-6 supports the growth of B cells as well as regulatory T cells. TNF-α regulates the function of immune cells and is essential in the control of intracellular pathogens and for stimulating the recruitment of inflammatory cells to an area of infection.

Hence, I next examined the production of immune-stimulatory cytokines such as IL-1β, IL-6, and tumor necrosis factor (TNF)-α following RAW 264.7 macrophage stimulation using OVA-encapsulated liposomes, with or without freezing, with LPS as a positive control.

As shown in **Figure 4.12 a, b** secretion of TNF-α and IL-1β from RAW 264.7 cells incubated with unmodified liposomes or polyampholyte-modified liposomes under the non-frozen state was very low compared to that observed in the presence of LPS. In contrast, RAW 264.7 cells, incubated with either unmodified- or polyampholyte-modified liposomes under freeze-concentration conditions, secreted large amounts of both TNF-α and IL-1β to levels that were similar to those seen for the positive control LPS. However, as shown **Figure 4.12 c**, a different trend was seen for IL-6. A large amount of IL-6 was secreted from RAW 264.7 cells incubated with polyampholyte-modified liposomes, almost doubling under the freeze-concentration compared to the non-frozen condition. Interestingly, a large amount of IL-6 was also secreted from RAW 264.7 cells incubated with unmodified liposomes, and freeze-concentration increased IL-6 secretion only marginally.

Both TNF-α and IL-1β secretion were drastically enhanced to similar extents when either unmodified- or polyampholyte-modified liposomes were used under freeze-concentration conditions compared to non-frozen conditions (**Figure 4.12 a,b**). In contrast, IL-6 secretion was increased only slightly by freeze-concentration in unmodified liposomes but was noticeably increased under freeze-concentration conditions in polyampholyte-modified liposomes. Compared to TNF-α and IL-1β secretion, these differences in IL-6 secretion might be attributed to the pH-sensitivity property of polyampholyte-modified liposomes, which could allow for antigens to be delivered more efficiently to the cytosol of cells and therefore allow for more cytokine secretion compared to that in unmodified liposomes (**Figure 4.12 c**). As a control, I also investigated the effect of the freeze-concentration method on RAW264.7 macrophages in the absence of both adjuvant and liposomes. There was no significant effect on secretion of cytokines in only cells with or without freezing. This result indicated that freeze-concentration alone does not activate the cells but requires the presence of adjuvants (**Figure 4.12 a-c**).

In my study, both unmodified- and polyampholyte-modified liposomes, despite the presence of MPLA as an adjuvant, produced a low secretion of cytokines under non-frozen conditions when compared to LPS (**Figure 4.12 c**). This is perhaps not surprising considering that LPS has been reported to induce inflammatory cytokines to a much greater extent than MPLA.[36,38,39] In contrast, a large amount of cytokine secretion was observed when freeze-concentration was employed (**Figure 4.12 a-c**).

This enhanced secretion of cytokines might be due to freeze-concentration allowing for an increase in the adjuvant activity of MPLA therefore resulting in more efficient release of the antigen, leading to increased secretion of pro-inflammatory cytokines in the frozen situation compared to the non-frozen situation. However, the data obtained for TNF-α and IL-1β demonstrated that freeze-concentration enhances the secretion in both the unmodified and polyampholyte-modified systems, which suggests the presence of a different mechanism of action which still needs to be explored in future studies.

Regardless, I have developed a new and facile freeze-concentration method that enhances the immune response of macrophages to liposomes encapsulated with the antigen OVA. The freeze-concentration method enhances the adsorption between cells and proteins without any toxicity and cell damage. In my earlier studies, I demonstrated enhanced cellular adsorption and internalization of proteins using this freeze-concentration approach. This study focused on the effective use of this freezing method in enhancing the immune response in RAW 264.7 macrophage cells. Moreover, endosomal antigen escape, which is of particular use in immunotherapy, can be achieved using delivery of the protein cargo through pH-sensitive liposomes created by modification with hydrophobic polyampholytes.

(A)

(B)

(C)
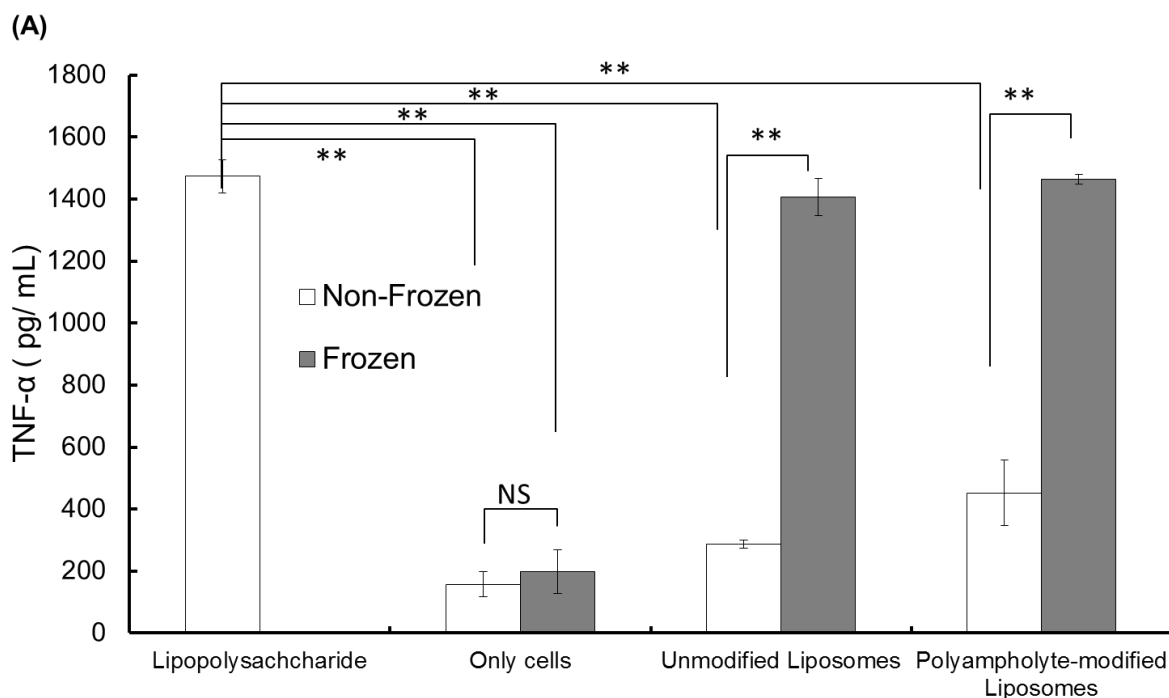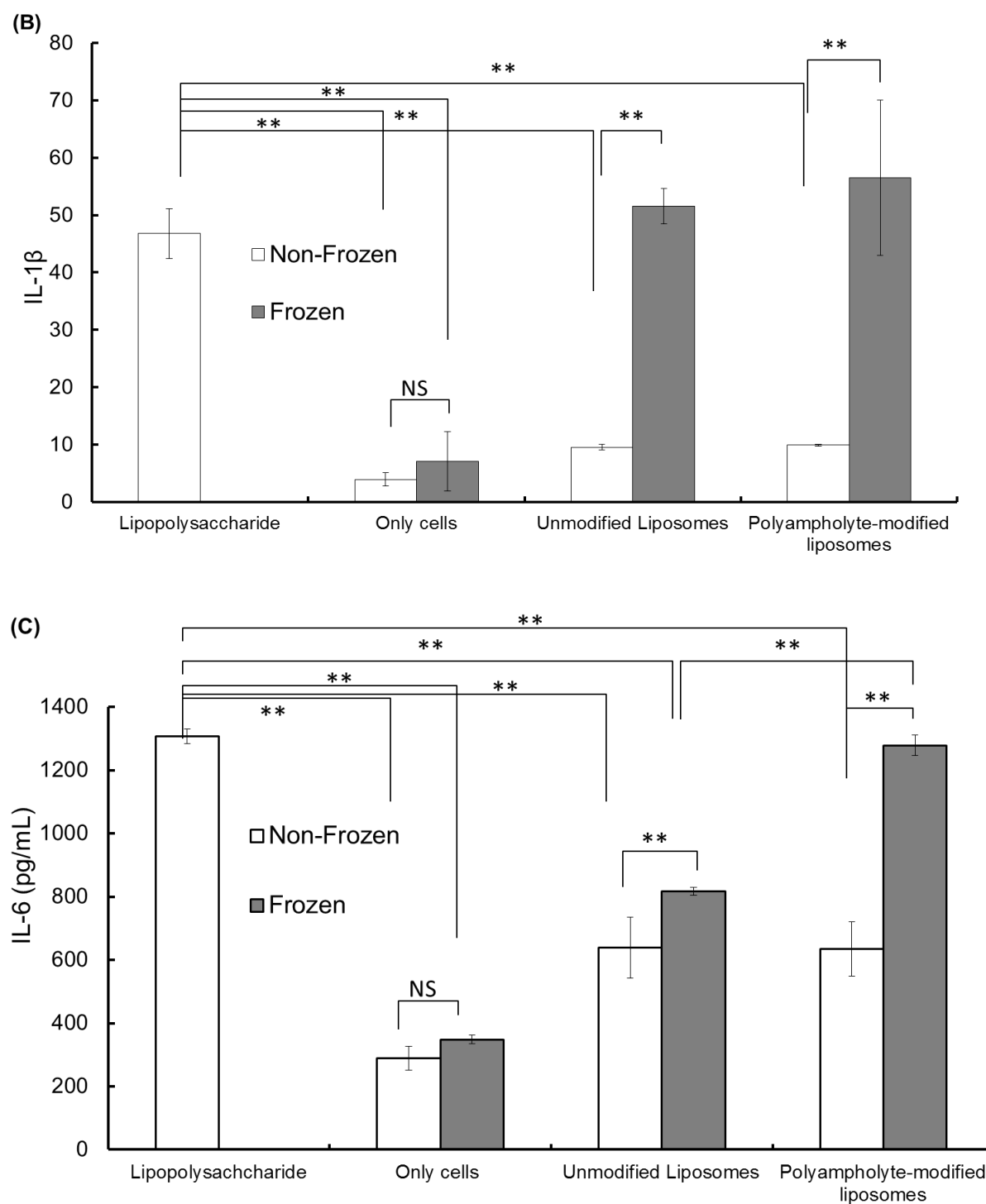
Figure 4.12 Cytokine secretion in RAW 264.7 macrophage cells after 48 h. Cells were treated with unmodified or polyampholyte-modified liposomes encapsulated OVA. For positive control, RAW 264.7 macrophage cells were stimulated by LPS. The cell culture supernatant of non-frozen or frozen was collected, and the concentration of individual cytokines was measured by ELISA. (a) TNF-α (b) IL-1β (c) IL-6. The experiments were performed in triplicate. Data are expressed as mean ±SD. **P < 0.01.

4.4 Conclusion

In conclusion, I found that freeze-concentration enhances antigen expression, processing, and presentation in APCs. I have also found that liposomes with an encapsulated antigen elicit significantly higher MHC class I presentation activity and cytokine release using the freeze-concentration method compared to the non-frozen system. Moreover, polyampholyte-modified liposomes have a destabilizing property at acidic pH that can lead to efficient endosomal escape, which allows for cross presentation through MHC class I molecules. These results suggest that a combination of freeze-concentration and polyampholyte-modified liposomes are a promising strategy for the safe delivery of antigens that contribute to the establishment of immunotherapy. Further, clinical studies will be required to assess if the freeze-concentration method is an effective strategy for immunotherapy applications. To the best of my knowledge, this is the first report which uses freeze-concentration as a physical method for effective immunotherapy. Although this technique might be applicable only in an *in vitro* antigenic delivery system it may be suitable for establishing adoptive immunotherapy, this pioneer study therefore offers a new possibility for immunotherapy application that avoids cell damage, is simple and does not require expensive equipment.

4.5 References

1. Yang, F.; Jin, C.; Subedi, S.; Lee, C.L.; Wanq, Q.; Jiang, Y. *Cancer Treat Rev.* **2012**, *38*, 566.

2. Jessy, T. *J Nat. Sci. Biol. Med.* **2011**, *2*, 43.

3. Liu, Y.; Zeng, G. *J Immunother.* **2012**, *35*, 299.

4. Palucka .K; Bancherea. J. *Nat. Rev. Cancer* **2012**, *12*,265.

5. Robinson, J.H.; Delvig, A.A. *Immunology* **2002**, *105*,252.

6. Moron, G.; Dadaglio, G.; Leclerc, C. *Trends Immunol.* **2004**, *25*, 92.

7. Vyas, J.M.; Vanderveen, A.G.; Ploegh, H.L.; *Nat. Rev. Immunol.* **2008**, *8*, 607.

8. Shen, H.; Ackerman, A.L.; Cody, V.; Giodini, A.; Hinson, E.R.; Cresswell, P. *Immunology* **2006**, *117*, 78.

9. Akagi, T.; Wang, X.; Uto, T.; Baba, M.; Akashi, M. *Biomaterials* **2007**, *28*, 3427.

10. Kelly, C.; Jefferies, C.; Cryan, S.A. *J Drug Deliv.* **2011**, *2011*, 1.

11. Purwada, A.; Tian, Y.F.; Huang, W.; Rohrbach, K.M.; Deol, S.; August, A. *Adv. Heathc. Mater.* **2016**, *5*, 1413.

12. Lee, Y.; Ishii, T.; Kim, H.J.; Nishiyama, N.; Hayakawa, Y.; Itaka, K.; Kataoka, K. *Angew. Chem. Int. Ed.* **2010**, *49*, 2552.

13. Yildirimer, L.; Thanh, N.T.K.; Loizidou, M.; Seifalian, A.M. *Nano Today* **2011**, *6*, 585.

14. Narvekar, M.; Xue, H.Y.; Eoh, J.Y.;Wong, H.L. *AAPS Pharm Sci. Tech.* **2014**, *15*, 822.

15. Puri, A.; Loomis, K.; Smith, B.; Lee, J.H.; Yavlovich, A.; Heldman, E. *Crit. Rev. Ther. Drug Carrier Syst.* **2009**, *26*,523.

16. Yuba, E.; Harada, A.; Sakanishi, Y.; Watarai, S.; Kono, K. *Biomaterials* **2013**, *34*,3042.

17. Yuba, E. *Polym. J.* **2016**, *48*,761.

18. Yessine, M.A.; Lafleur, M.; Meier, C.; Petereit, H.U.; Leroux, J.C. *Biochim. Biophys. Acta* **2003**, *1613*, 28.

19. Ponsaerts, P.; Tendeloo, V.F.I.V.; Berneman, Z.N. *Clin. Exp. Immunol.* **2003**, *134*,378.

20. Unga, J.; Hashida, M. *Adv, Drug. Deliv. Rev.* **2014**, *72*,144.

21. Ahmed, S.; Hayashi, F.; Nagashima, T.; Matsumura, K. *Biomaterials* **2014**, *35*, 6508.

22. Ahmed, S.; Fujita, S.; Matsumura, K. *Nanoscale* **2016**, *8*, 15888.

23. Bhatnagar, B.S.; Pikal, M.J.; Bogner, R.H. *J. Pharm Sci.* **2008**, *97*, 798.

24. Machado, J.A.S.; Ruiz, Y.; Auleda, J.M.; Hernandez, E.; Reventos, M. *Food Sci. Technol. Int.* **2009**, *15*,303.

25. Matsumura, K.; Hyon, S.H. *Biomaterials* **2009**, *30*, 4842.

26. Majid, S.; Yusko, E.C.; Billeh, Y.N.; Macrae, M.X.; Yang, J.; Mayer, M. *Curr. Opin. Biotechnol.* **2010**, *21*,439.

27. Daleke, D.L.; Hong, K.; Papahadjopoulos, D. *Biochim. Biophys. Acta* 1990, 1024,352.

28. Ding, H.M.; Ma, Y.Q. *Sci. Rep.* **2013**, *3*, 1.

29. Simoes, S.; Moreiraa, J.N.; Fonsecab, C.; Duzgunes, N.; Pedrodo de Lima, M.C. *Adv. Drug Deliv. Rev.* **2004**, *56*,947.

30. Yuba, E.; Kojima, C.; Harada, A.; Tana, Watarai, S.; Kono, K. *Biomaterials* **2010**, *31*, 943.

31. Shalaev, E.Y.; Steponkus, P.L. *Biochim. Biophys. Acta* **1999**, *1419*, 229.

32. Fahres, C.M.; Unger, W.W.J.; Garcia-Vallejo, J.J.; Kooyk, Y.V.; *Front Immunol.* **2014**, *5*, 1.

33. Ackerman, A.L.; Creswell, P. *Nat. Immunol.* **2014**, *5*, 678.

34. Murthy, N.; Xu, M.; Schuck, S.; Kunisawa, J.; Shastri, N.; Frechef, J.M.J. *Proc. Natl. Acad. Sci. U.S.A.* **2003**,*100*,4995.

35. Berghaus, L.J.; Moore, J.N.; Hurley, D.J.; Vandenplas, M.L. Fortes, B.P. Wolfert, M.A. *Comp. Immunol. Microbiol. Infect. Dis.* **2010**, *33*, 443.

36. Soromou, L.W.; Zhang, Z.; Li, R.; Chen, N.; Guo, W.; Huo, M. *Molecules* **2012**, *17*, 3574.

37. Fournier, B.; Philpott, D.J. *Clin Microbiol Rev*. **2005**, *18*, 521.

38. Gaekwad. J.; Zhang, Y.; Zhang, W.; Reeves, J.; Wolfert, M.A.; Boons, G.J. *J Biol Chem.* **2010**, *285*, 29375.

39. Romero, C.D.; Varma, T.K.; Hobbs, J.B.; Reyes, A.; Driver, B.; Sherwood, E.R. *Infect Immun.* **2011**, *79*, 3576.

Chapter 5

Effective gene delivery using polyampholyte nanoparticles and freeze concentration

5.1 Introduction

Recently, gene therapy has drawn significant attention as a promising strategy for the treatment of various genetic disorders such as cancer, neurodegenerative diseases, or autoimmune diseases[1]. Gene therapy requires the insertion of a gene(s) into cells in order to replace a defective gene. Usually, gene-based delivery involves encapsulation of the gene of interest in order for it to be delivered successfully to the target cells[2]. However, nucleic acids such as DNA and RNA cannot cross the cell membrane because of both their large size and their hydrophilic nature caused by the presence of the negatively charged phosphate groups[3]. Generally, gene transfection is performed by one of three methods, viral (transduction), physical, or non-viral (chemical). Traditionally, gene therapy has most often been performed using recombinant viruses such as retroviruses, adenoviruses, and herpes simplex virus[4]. While these vectors have been shown to be an effective method for delivering genes into cells, issues around their long-term safety, including their inherent toxicity and immunogenicity[5], remain to be solved.

Crossing the plasma membrane is considered to be the most important and critical step in DNA transfection. In this regard, different physical methods have been designed to internalize genetic material across the cell membrane.Electroporation[6], ultra-sonication[7], and the use of a gene-gun[8], are a few of the physical methods that have been reported to produce effective transfection of cells. These methods facilitate the transfer of genetic material from outside of the cell to the nucleus by creating transient membrane defects, or holes, through the use of physical force. However, these energy-based methods have severe drawbacks; for example, the high voltage required for electroporation can irreversibly damage cells and tissues and affect overall cell viability[9]. Therefore, the most challenging task in physical gene delivery methods is to design an effective method that significantly reduces the risk of cell toxicity and is easy to use.

In previous studies, I have reported the development of a freeze concentration method that can enhance delivery of proteins to cells while maintaining high cell viability[10, 11]. Freeze concentration is a physical phenomenon that occurs during freezing at extremely low temperatures. As water crystallizes into ice crystals, the ice-crystals exclude solute molecules, thereby enhancing the concentration of the solutes around the ice crystals[12]. As the temperature is lowered more and more (i.e. super-cooling), the remaining solution becomes more and more concentrated[13]. Previously, this freeze concentration technology has been

effectively used in the production of fruit juices[14] and for food preservation[15]. The freeze concentration method is also recognized as the best method for long-term preservation of the quality of the original material. I hypothesized that freeze-concentration could also be used to assist in the delivery of DNA or DNA-complexes to cells.

Although physical methods allow for effective penetration of DNA molecules into cells, the action of nucleases on the internalized naked DNA severely reduces transfection efficiency. Therefore, the use of non-viral carriers, prepared using chemical methods, has become an important method to provide efficient gene delivery. The utilization of such carriers is crucial in order to protect the gene from nuclease enzymatic degradation and thereby improve its stability[16]. Hence, a tremendous amount of effort has been invested in the development of new non-viral carriers that have low toxicity, but high transfection efficiency, for use in gene therapy. Improving, the transfection efficiency of non-viral carriers is a particularly difficult challenge since they generally fall far below the efficiencies of viral carriers[4]. The use of non-viral carriers that are lipid-based[17], polymer-based[18], or are functional inorganic nanoparticles[19], has recently expanded; in fact, some of these approaches have been used in clinical trials[18]. Among these, polymer-based gene delivery systems have attracted a significant amount of attention for use in gene transduction. To date, various cationic polymers including polyethyleneimine (PEI)[20], poly-L-lysine (PLL)[21], chitosan[22] and polyamidoamine (PAMAM)[23] have been described as being useful as carriers for gene transfection. PLL, in particular, has been widely used as a gene delivery carrier because it protects DNA from nuclease digestion. However, despite this, PLL has the drawback that it has low transfection efficiency compared to PEI and PAMAM because of inefficient endosomal escape[24]. Over the past few years, PEI has emerged as being the most effective gene delivery carrier and is frequently used both *in vitro* and *in vivo* with high transfection efficiency. This high transfection efficiency of PEI appears to be related to its buffering capacity. Once inside the endosome it can bind protons brought into the endosome via the endosomal ATPase. This movement of protons promotes a corresponding influx of chloride anions from ATPase pump. Together, these ion transport events trigger endosome swelling and disruption causing release of DNA into the cytoplasm[25]. PEI can exist in both linear and branched forms. The linear PEI polymer lacks a primary amino group but instead contains secondary amines that link the polymer units together. On the other hand, branched PEIs contain primary, secondary, and tertiary amino groups in their polymeric backbone. The

strong positive charge on PEI leads to a strong interaction with the cell surface and this can cause cell damage[26].

A significant amount of effort has been made to overcome this shortcoming of PEI, primarily through modification of the primary amine in the polymeric backbone. Recently, Wagner et al. reported the modification of branched PEI through succinylation. This modification resulted in a modified PEI with low toxicity and efficient gene transfection capability[27]. In another study, Yu et al. developed a non-toxic, biocompatible, modified PEI with high transfection capability after modification of PEI with amino acids[28]. Other reports have focused on modification of PEI using PEG[29] and sugars[30].

Among other formulations, nanoparticle-based gene delivery has also gradually gained attention and they are now being extensively used as carriers. Nanoparticles have excellent physical properties including controllable adsorption and release, good particle size, and desirable surface characteristics[31].

In this study, I prepared a new self-assembled polyampholyte by modification of branched PEI (25 kDa) with butylsuccinic anhydride (BSA). Importantly, I combined the freeze concentration methodology with this modified polyampholyte as the gene carrier and examined gene transfection efficiency. The polyampholyte I prepared was physically characterized in terms of particle size, zeta potential, and ability to bind and complex plasmid DNA (pDNA). A high transfection efficiency using the combination of freeze concentration and this modified polyampholyte was obtained, especially when compared with commercially available transfection carriers. This is the first report to explore a freeze concentration-based strategy for enhancing *in vitro* gene delivery and I expect this approach to widely improve the transfection efficiency of plasmid DNA.

5.2 Materials and Methods

5.2.1 Materials

Branched PEI (molecular weight 25kDa), Tris-ethylenediaminetetraacetic acid (EDTA) buffer and Dulbecco's modified Eagle's medium (DMEM) were purchased from Sigma Aldrich (St. Louis, MO, USA), deoxyribonuclease I (DNase I, RT grade), butylsuccinic anhydride (BSA) and succinic anhydride (SA) were obtained from Wako Pure Chem. Ind. Ltd., (Osaka, Japan). 3-(4,5-dimethylthiazol-2yl)-2,5-diphenyltetrazoliumbromide (MTT) was purchased from Dojindo (Kumamoto, Japan), pAcGFP1-N2 plasmid was from

Clontech, (Palo Alto, CA, USA), pGL4.51[luc2/CMV/Neo] was from Promega (Madison, WI, USA) and *Escherichia coli* DH-5α competent cells was from TAKARA Bio (Otsu, Japan). Plusglow liquid medium was obtained from Nacalai-tesque, (Kyoto, Japan), Genopure plasmid maxi kit was purchased from Roche, (Mannheim, Germany) and e-poly-L-lysine (PLL) was from JNC Corp., (Tokyo, Japan).

5.2.2 Transformation and purification of plasmid DNA

pAcGFP1-N2 plasmid containing the green fluorescent protein (GFP) gene and pGL4.51[luc2/CMV/Neo] containing the luciferase gene were transformed into *Escherichia coli* DH-5α competent cells, and the transformants were streaked onto LB agar plates with the appropriate antibiotic. After incubating the plates at 37°C overnight, a colony was inoculated into Plusgrow liquid medium containing the appropriate antibiotic and cultured at 37°C, at 200 rpm overnight. The plasmids were isolated and purified from the bacterial cell culture using a Genopure plasmid maxi kit according to the manufacturer's protocol. The purified plasmids were re-suspended in Tris- EDTA buffer. The concentrations of the purified plasmids were determined using a Nanodrop 1000. The plasmids were stored at -20°C until use.

5.2.3 Preparation of a polyampholytecryoprotectant

To protect the components of my system from damage caused by freezing, a polyampholyte cryoprotectant was synthesized by succinylation of PLL as described in my previous reports.[32-34] Briefly, an aqueous solution of 25% (w/w) PLL (10 mL) and succinic anhydride (SA) (1.3 g) were mixed at 50°C for 2 h to convert 65% of the amino groups to carboxyl groups (**Scheme 3.1**).The polyampholyte cryoprotectant is referred to as PLL-SA.

5.2.4 Preparation of self-assembled hydrophobically modified polyampholytes

In order to prepare the non-toxic gene carrier, I modified branched PEI by succinylation using a previously reported procedure[27]. Briefly, PEI (0.5 g) was dissolved in 8.5 mL of water and mixed with1.5 mL of a NaCl solution (3M). The solution was then adjusted to pH 5 using 1M hydrochloric acid. The desired amount of BSA (0.266 g, 20 mol %) was first dissolved in DMSO and was then added drop-wise to PEI to obtain BSA modified PEI (PEI-BSA). The reaction was carried out at 100°C for 2 h with constant stirring. For the preparation of succinylated PEI (PEI-SA), SA (0.171 g, 15 mol %) was dissolved in DMSO and added drop-wise to the PEI solution and reacted for 2 h at 50°C.

Finally, the resultant solutions were dialyzed against water (3000 molecular weight cut off, Spectra/Por membrane) for three days. After purification, the resultant products were freeze dried. The synthesized polyampholytes were characterized by ^{1}H NMR. Spectra were measured in D_2O at 25°C on a Bruker AVANCE II 400 spectrometer (Bruker BioSpinInc., Fällanden, Switzerland).

5.2.5 Analysis of polyampholyte composition using X-Ray Photoelectron Spectroscopy (XPS)

XPS was used to analyze the composition of modified PEI derivatives. XPS excites a surface by X-ray irradiation allowing determination of the binding energy of ejected electrons. These binding energies are related to the atomic species present on the surface. To perform this, samples of the PEI derivatives (1% w/v) were prepared in PBS (-) and a small drop placed on the glass substrate. The samples were left to air dry for 4 h and then further dried under a vacuum for one day. Measurements were recorded using a VG scientific ESCALAB 250Xispectrometer (ThermoFisher Scientific, Waltham, MA, USA) with aluminum (15 kV) as a radiation source. Photoelectrons were analyzed at a take-off angle normal to the interface. High-resolution C1s, N1s, and O1s spectra were collected with an analyzer pass energy of 20eV. The binding energy scales were referenced by setting the C1s binding energy to 285.0 eV.

5.2.5 Determination of the critical aggregation concentration (CAC) of the polyampholyte

The critical aggregation concentration (CAC) of the self-assembled polyampholyte was investigated using the pyrene excitation spectra method as described in my previous study[10]. First, 10 μL of a pyrene solution (1.0 mM in acetone) was transferred to a 10 mL glass tube. The pyrene solution was completely evaporated under a gentle steam of nitrogen. Next, the polyampholyte solution at different concentrations (10, 5, 2.5, 1.25, 0.625, 0.312, 0.125, 0.075, 0.032 and 0.01 mg/mL) was dissolved in phosphate-buffered saline without calcium and magnesium (PBS (-)) and transferred to the glass tube. The resulting solutions were sonicated in an ultrasonic bath for 30 min and heated for 3 h at 65°C to equilibrate pyrene with the polyampholyte. After equilibration, the samples were left to cool overnight at room temperature. The critical aggregation concentration of PEI-BSA was estimated by examining the emission spectra of pyrene from 300 to 360 nm using a spectrofluorometer

(JASCO FP-8600, Tokyo, Japan).The intensity of pyrene at 338 nm (I_{338}) and 335 nm (I_{335}) was then plotted against the concentration of polyampholyte.

5.2.6 Dynamic light scattering (DLS) and zeta potential

The hydrodynamic diameters of PEI-BSA and PEI-BSA/pDNA complexes were analyzed by DLS analysis using a Zetasizer 3000 (Malvern Instruments, Worcestershire, UK) with a scattering angle of 135°. The polyampholytes were dispersed in PBS (-) and the zeta potential values were measured at the following default parameters: a dielectric constant of 78.5, a refractive index of 1.6, and a concentration of 0.5 mg/mL. Data were expressed as an average of three measurements.

5.2.7 Agarose gel electrophoresis

5.2.7.1 Complex formation between polyampholytes and pDNA

A gel retardation assay was performed to confirm the pDNA condensation ability of the polymer. The gels were prepared with 1% (w/v) agarose in TAE buffer (40 mM Tris, 40 mM acetic acid, 1mM EDTA, pH 8.5). A fixed amount of plasmid DNA (1 μg) was then combined with different amounts of polyampholyte in 50 μL of PBS (-). The solution was mixed gently by vortex and was incubated for 30 min at room temperature before loading onto the agarose gel. The PEI-BSA-pDNA complex and control pDNA were electrophoresed at a constant 100 V for 25 min in TAE buffer. After electrophoresis, the gel was stained with ethidium bromide and visualized using a UV trans-illuminator.

5.2.7.2 Nuclease stability test of the polyampholyte-pDNA complex

Protection of plasmid DNA from nucleases is one of the most important properties for effective and safe gene delivery both *in vitro* and *in vivo*. To examine whether the modified polyampholyte can protect the loaded plasmid DNA from nuclease digestion, I evaluated DNase I-mediated digestion of polyampholyte: DNA complexes using agarose gel electrophoresis. Briefly, 50 μL of PEI-BSA-DNA complexes (2:1, w/w) were incubated with different amounts of DNase I (0.1, 0.2, and 0.4 U/μg of DNA) in DNase I/Mg^{2+} digestion buffer (50 mM Tris-HCl, pH 7.6, and 10 mM MgCl$_2$). pDNA (1 μg) was treated with DNase I at 0.1 U/μg as a reference. The samples were incubated in a shaking water bath (100 rpm) for 30 minutes at 37°C. Afterwards, the enzymatic digestion reaction was terminated by the addition of 5 μL EDTA solution (0.5 M, pH 8.0) for 10 min at room temperature. To

determine the release of DNA from inside the polyampholyte-DNA complex, complexes were dissociated by the addition of heparin solution, an anionic glycosaminoglycan, at a final concentration of 1% (w/v) to release the DNA. The samples were further incubated in a water bath for 3 h at 37°C. The extracted DNA samples were centrifuged and analyzed by electrophoresis on a 1 % (w/v) agarose gel in TAE buffer as described above. Undigested pDNA was used as a control.

5.2.8 Preparation of polyampholyte-pDNA and commercially available carrier-pDNA complexes

Briefly, the reporter genes pAcGFP1-N2 (for the GFP study) or pGL4.51 (for the luciferase study) were added to polyampholyte NPs at a fixed ratio (PEI-BSA:pDNA; w/w). The amount of polyampholyte NPs were 2, 5, 7, and 10 μg and the concentration of pDNA was fixed at 1 μg in 50 μL PBS (-). The mixture was then incubated at room temperature for 30 min. The resultant polyampholyte–pDNA complex was directly used for further study. For the control experiment, jetPEI® (Polyplus-transfection SA, Illkirch, France) and Lipofectamine 3000 (ThermoFisher Scientific) were used as commercially available transfection carriers. These commercially available carriers have both been used extensively for gene transfection studies with great success.[19, 35] To prepare the jetPEI® and pDNA complex, I followed the manufacturer's protocol. Briefly, 1 μg of pDNA and 2 μL of jetPEI® were dissolved in 50 μL of NaCl solution separately. Both solutions were mixed together, vortexed immediately and incubated at room temperature for at least 30 min. Similarly, to prepare Lipofectamine 3000-pDNA complexes, Lipofectamine 3000 (7.5 μL) was dissolved in opti-MEM (125 μL). Plasmid DNA (1 μg) and P 3000 reagent (5 μL) were also dissolved in opti-MEM (125 μL). The Lipofectamine 3000 and plasmid DNA solutions were gently mixed together followed by incubation at room temperature for 15 minutes to form the Lipofectamine 3000-pDNA complex.

5.2.9 Cell Culture

Human embryonic kidney cells (HEK-293T, American Type Culture Collection, Manassas, VA, USA) were cultured in DMEM supplemented with 10 % fetal bovine serum (FBS) at 37°C in a 5% CO_2 humidified atmosphere. When the cells reached 80% confluence, they were removed by 0.25% (w/v) trypsin containing 0.02% (w/v) EDTA in PBS (-) and were seeded onto a new tissue culture plate for subculture.

5.2.10 *In vitro* cytotoxicity assay

The cytotoxicity of branched PEI, PEI-SA, and PEI-BSA was evaluated by MTT assay using HEK-293T cells. Briefly, cells (1×10^3 cells/mL) were seeded into a 96 well plate with 0.1 mL of growth medium containing 10% FBS. Cells were incubated at 37°C for 72 h before the addition of test materials. Then, 0.1 mL medium containing different concentrations of polyampholytes was added to the cells, followed by incubation for 48 h. To determine the cell viability, 0.1 mL of MTT solution (300 μg/mL in medium) was added to the cultured cells and the cells were further incubated for 4 h. Next, the medium was removed and 0.1 mL of DMSO was added to each well to dissolve the MTT formazan crystals and allowed to stand for 15 min to allow complete color development. The resulting color intensity was measured using a microplate reader (Versamax, Molecular Devices, Sunnyvale, CA, USA) at 540 nm, and was proportional to the number of viable cells. The concentration of polyampholyte leading to 50% cell killing (IC_{50}) was calculated from a concentration-dependent cell viability curve.

5.2.11 Cell freezing with polyplexes and lipoplexes

HEK-293T cells were counted and re-suspended at a density of 1×10^6 cells/mL in 10% PLL-SA cryoprotective solution at 4°C. One mL of re-suspended cells in cryoprotectant was added to a 1.9 mL cryo-vial (Nalgene. Rochester, NY) and polymer-pDNA complexes (50 μL, without FBS) were added and the cryo-vial was stored at -80°C overnight. After freezing overnight, the vials containing cells and polymer-pDNA complexes were thawed at 37°C and washed three times with DMEM medium. Cells were counted with a hemocytometer using the trypan blue staining method. Cell viability was determined as the number of viable cells divided by the total number of cells. The adsorption of non-frozen and frozen polymer-pDNA complex to the HEK293 T cells was observed using a confocal laser scanning microscope (CLSM, FV-1000-D; Olympus, Tokyo, Japan).

5.2.12 *In vitro* gene transfection using the freeze concentration method

After thawing, and washing with DMEM medium three times, the cells were seeded onto a glass-bottomed dish and incubated for 10 h to allow cell attachment and gene expression to occur. To create the non-frozen system for comparison, the same amount of polymer-pDNA complex was gently added to the cells and also incubated for 10 h. At the

time of observation, the attached cells were washed three times with PBS (-) and GFP expression observed using CLSM.

5.2.13 Comparison of luciferase activity in the frozen and non-frozen systems

The transfection efficiency was evaluated by measuring luciferase activity in transfections performed using the frozen method and compared transfections performed using the non-frozen method. In the case of the frozen method, the cell suspension was prepared as described above, except cells were seeded into 12 well plates. For the non-frozen method, the polymer-pDNA complex was added gently and directly to HEK-293T cells in 12 well plates. Both sets of plates were incubated for 48 h. At the time of observation, cells were washed three times with PBS (-). Cells extracts were prepared by scraping cells into lysis reagent (200µL/well; 25mM Tris phosphate, 2mM DTT, 2mM 1,2 diaminocyclohexane N,N,N',N' tetraacetic acid, 10% glycerol,1% Triton X-100, pH-7.4) followed by transfer to a micro-centrifuge tube and storage on ice for 5 min prior to centrifugation at 19515 *g* for 2 min. The supernatant was withdrawn and transferred to a new centrifuge tube. To measure luciferase expression, luciferase assay kit reagent (100 µL, Promega) was added to a luminometer tube, the cell supernatant was added, the mixture vortexed, and luciferase activity was recorded using a luminometer (Berthold Technology, Lumat 3 LB 9508). The luminometer program was adjusted to perform a 2 s measurement delay followed by a 10 s measurement for luciferase activity. The luciferase activity was expressed as relative light unit (RLU) and results were normalized to total cell protein measured by using bicinchoninic acid (BCA) protein assay kit (ThermoFisher Scientific). All experiments were performed in triplicate.

5.2.14 Intracellular localization of DNA in HEK-293T cells

Thawed HEK293T cells containing 10% cryoprotectant and either branched PEI: pDNA (2:1, w/w) or PEI-BSA:DNA (2:1,w/w) were seeded onto a glass bottomed dish at a density of 1×10^3 cells/mL. The plasmid used was pAcGFP-N2 labeled with Cy3 dye. The cells were incubated for a further 24 h in a 5% CO_2 humidified atmosphere at 37°C. LysoTracker Green® DND-26 and Hoechst dye were then added and the cells incubated for 30 min further prior to analysis. Samples were rinsed with PBS buffer and the cells were counterstained with lysotracker green for endosomes and cell nuclei were stained with Hoechst 33342 prior to imaging using CLSM.

5.2.15 Statistical analysis

All data are expressed as means ± standard deviation (SD). All experiments were conducted in triplicate. To compare data among more than three groups, a one-way analysis of variance (ANOVA) followed by the Bonferroni post-hoc test was used. A P value of <0.05 was considered statistically significant.

5.3 Results and Discussions

5.3.1 Preparation of polyampholyte as acryoprotectant

In a previous study, I developed a new, non-toxic, polyampholyte cryoprotectantthat protected cells from freezing-induced damage.[32] This polyampholyte cryoprotectant was synthesized by succinylation of PLL with succinic anhydride (SA). Succinylation of PLL with 65 mol% of SA introduced carboxyl groups as a result of the reaction of SA with amino groups. The polyampholyte cryoprotectant is referred to as PLL-SA (**Scheme 3.1**). The synthesis of polyampholytecryoprotectant was confirmed by ^{1}H-NMR in D_2O (**Figure 4.2**). From the ^{1}H-NMR spectra it was found that 63% of the amino groups in PLL were succinylated. This cryoprotectant has been used previously for the cryopreservation of various cell lines with low toxicity.

5.3.2 Preparation of self-assembling hydrophobic polyampholytes

For the preparation of the nanocarrier, I developed a new amphiphilic self-assembled hydrophobic polyampholyte by modifying branched PEI with hydrophobic BSA(20 mol %) to yield PEI-BSA. The reaction is shown in **Scheme 5.1a**. I also prepared a second polyampholyte, where branched PEI was modified with SA to yield PEI-SA, as shown in **Scheme 5.1b**. The modified PEIs were compared with PEI using^{1}H NMR in D_2O (**Figure 5.1**).I observed that unmodified PEI displayed a proton signal around 2.5-3.0 ppm (**Figure 5.1a**). After succinylation with succinic anhydride, the peak separated into three different peaks at 2.5, 3.2, 3.5 ppm respectively. Peaks above 2 ppm and below 4 ppm are associated with CH_2 proton signals and so the three new peaks might be associated with the primary, secondary, and tertiary amines of branched PEI, respectively (**Figure 5.1b**). Moreover, on further substitution of branched PEI with hydrophobic BSA, I observed a new peak at 1.1 ppm, which represents the methyl group from BSA (**Figure 5.1c**). The two CH_2 proton signals at 1.6 and 1.8 ppm belong to the CH_2 signals of the butyl group (**Figure 5.1c**). Furthermore, the degree of substitution of succinic anhydride and butylsuccinic anhydride on

branched PEI was measured using XPS analysis and is shown in **Table 5.1**. The substitution was calculated as a function of % atomic oxygen content present in the polymers. From this, I calculated the degree of substitution (DS) of SA in PEI-SA to be 9.38 % and the DS of BSA in PEI-BSA to be 9.35 % (**Table 5.1**). These DS values were smaller than the feeding ratio (for PEI-SA: 15%, for PEI-BSA: 20%), suggesting steric hindrance of the substituted chain.
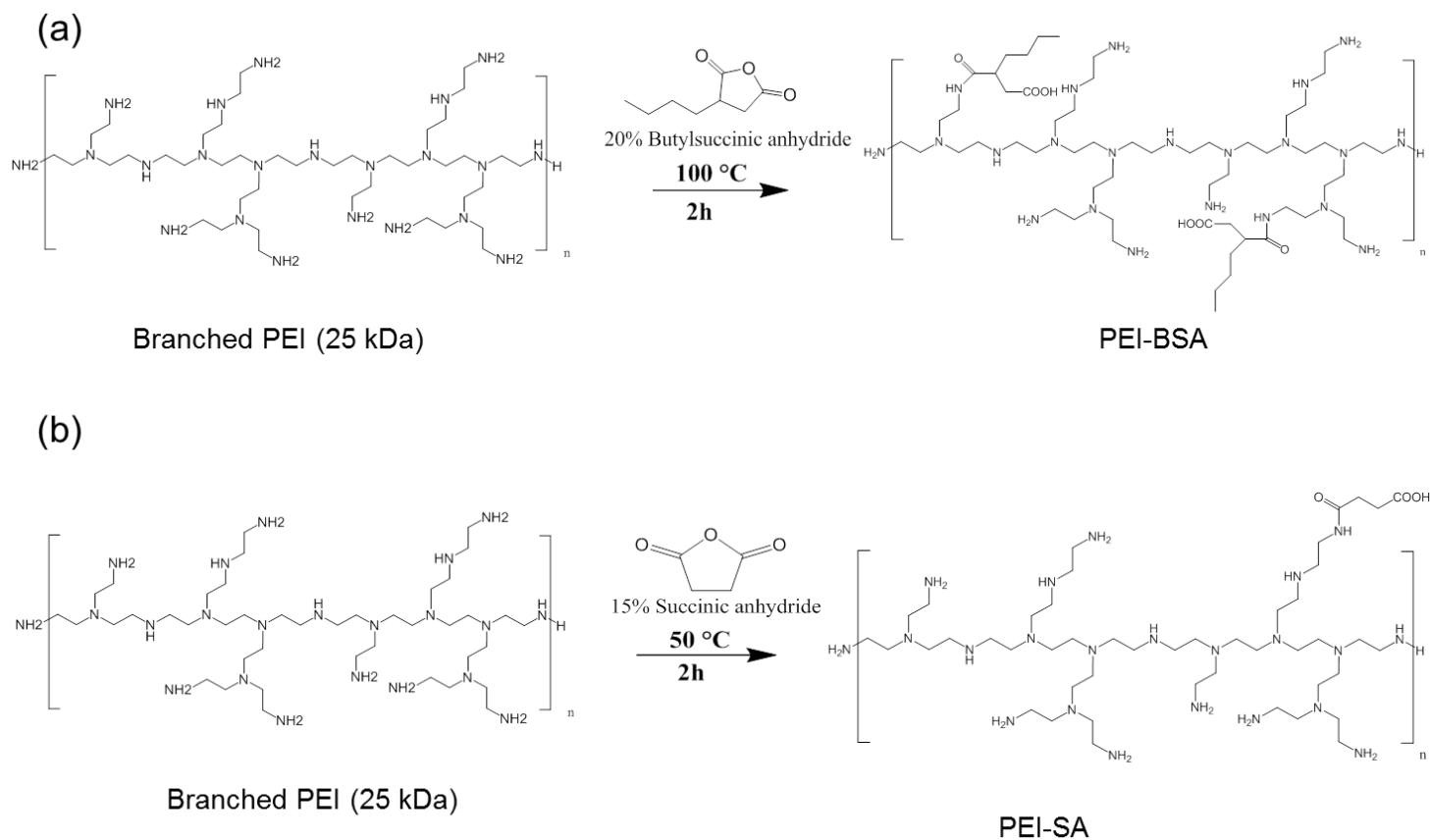
Scheme 5.1 (a) Preparation of a hydrophobically modified polyampholyte by modification of branched PEI using BSA (b) Preparation of a polyampholyte by modification of branched PEI using SA.
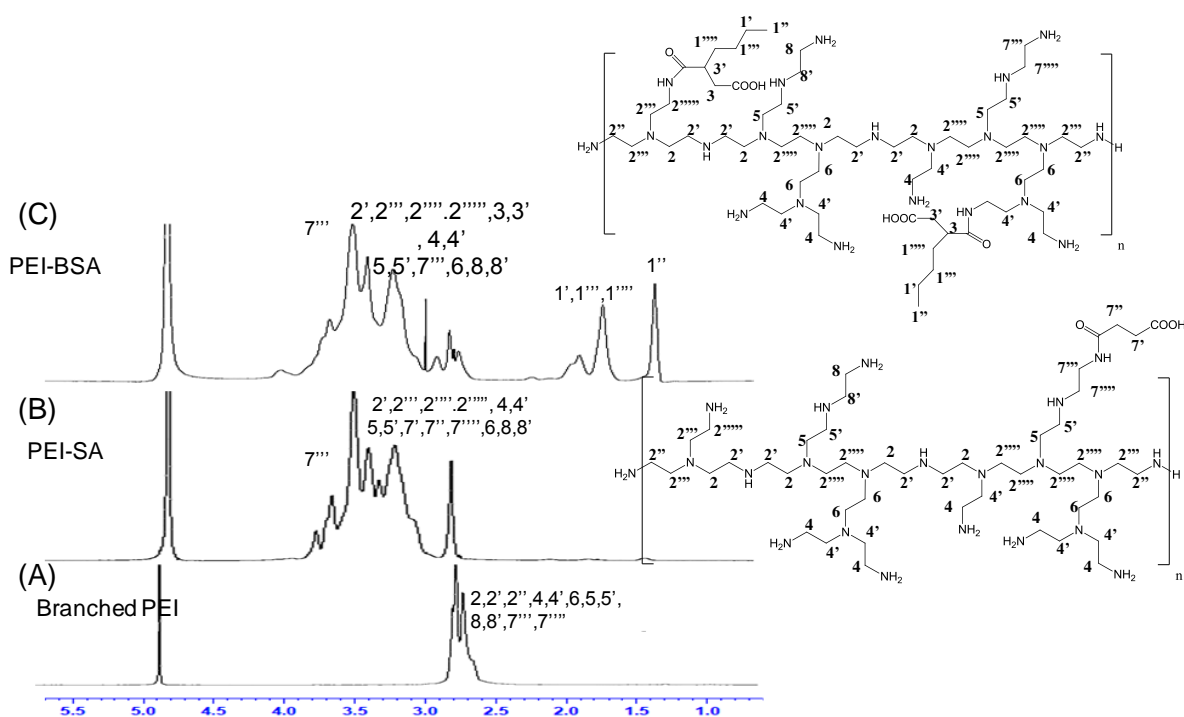
Figure 5.1. ^{1}H-NMR of Pristine PEI, PEI-SA and PEI-BSA

Table 5.1 Determination of the degree of substitution by elemental analysis (atomic (At) %) using XPS

| Samples	C (At%)	N (At%)	O (At%)	Degree of substitution (%)
PEI-SA	70.552	21.780	7.692	9.38
PEI-BSA	73.228	19.861	6.909	9.35

5.3.2 Characterization of the polyampholytes

5.3.2.1 Critical aggregation concentration (CAC)

I characterized the critical aggregation of PEI-BSA by measuring the pyrene fluorescence excitation spectra at 25°C. Pyrene is highly hydrophobic and therefore its solubility in water is very low but it can easily solubilize into the hydrophobic region of macromolecules. The pyrene excitation spectra of PEI-BSA, at different concentrations of the polyampholyte, are shown in **Figure 5.2a**. **Figure 5.2b** shows the variation in the pyrene fluorescence intensity ratio (I_{338}/I_{335}) in relation to polymer concentration. The intensity ratio significantly increased with increasing polymer concentration; the CAC value was estimated from the cross-point on the graph and was around 0.625 mg/mL, suggesting that the association between polymer side chains via inter- or intra-molecular association leads to the formation of aggregates at concentrations above this
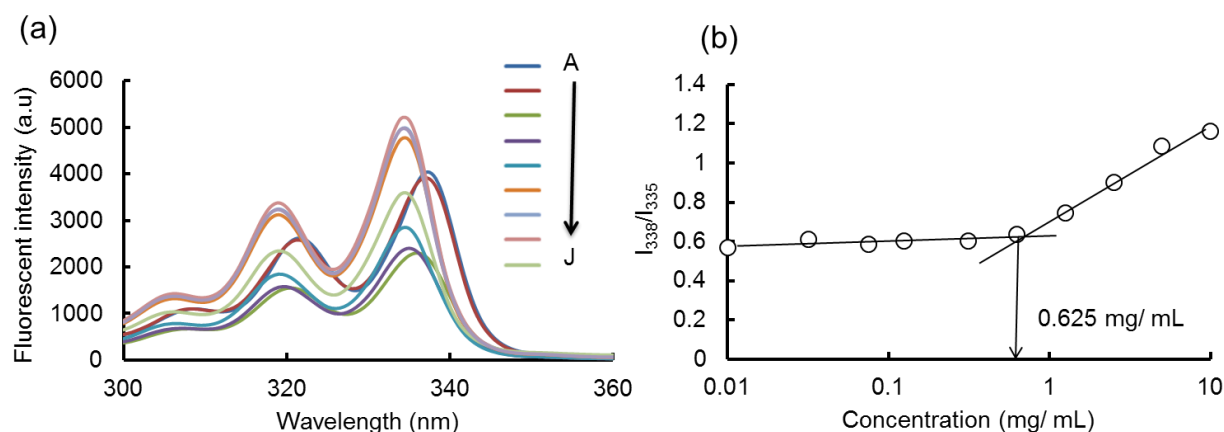
Figure 5.2 .CACs of PEI-BSA. (a) Pyrene excitation spectra (A-J) of PEI-BSA solutions at different polyampholyte concentrations, 10, 5, 2.5, 1.25, 0.625, 0.312, 0.125, 0.075, 0.032 and 0.01 mg/mL, respectively. (b) The ratio of I_{338}/I_{335} against polyampholyte concentration.

5.3.2.2 Particle Size

Particle size is an important factor that can influence the internalization of particles across the plasma membrane. Therefore, I investigated the particle size of PEI-BSA using DLS analysis. I found that the particle size of PEI-BSA was extremely small, being around 20.7±0.6 nm in diameter with a narrow size distribution (polydispersity index (PDI) 0.3) (**Table 5.2**). On the other hand, PEI-SA was much larger, having a particle size around 147.9±44.0 nm in diameter (**Table 5.2**). The reason for this might be related to the presence

of self-aggregates in PEI-BSA, which would lead to a reorganization into compact particles. These self-aggregates are likely to be formed via non-covalent attractive forces such as intermolecular hydrophobic and electrostatic interactions. Many studies have reported that nanoparticles smaller than 200 nm enter cells more efficiently and more rapidly than larger particles.[36]

Table 5.2 Characterization of polyampholytes including diameter, zeta potential, polydispersity and CAC.

Samples	Diameter[a] (nm)± SD	Zeta potential (mV) ± SD	CAC[b] (mg/mL)	PDI
Branched PEI	ND	51.9± 0.8	ND	ND
PEI-SA	147.9± 44.0	41.8± 1.2	ND	0.62
PEI-BSA	20.7± 0.6	34.4± 3.5	0.625	0.33

[a]Determined by DLS.
[b]Determined by using excitation spectra of pyrene.

5.3.2.3 Surface charge

Nano-particle properties such as positive surface charge are extremely important for an efficient interaction with the cell membrane. In my study, I found that branched PEI had a highly positive surface potential, being around 51.9±0.8mV. Following succinylation of PEI with succinic anhydride, the positive charge density of the polymer was reduced, with PEI-SA having a zeta potential of 41.8±1.2mV. Further, modification with hydrophobic butylsuccinic anhydride led to a larger decrease in surface potential to34.4±3.5mV. The reduction in positive surface charge is likely reflective of the reduced number of amine groups in the polymeric chains after modification by BSA or SA, as shown in **Table 5.2**.

5.3.3 Characterization of pDNA loaded polyampholytes

5.3.3.1 Particle Size

I next evaluated the particle size of PEI-BSA and pDNA-loaded PEI-BSA. As expected, the particle size of the latter was drastically increased due to the strong electrostatic interactions between PEI-BSA and the pDNA, compared with PEI-BSA, as shown in **Figure 5.3a**. The particle size of PEI-BSA was 18 nm but increased to 255 nm after pDNA adsorption. For efficient gene transfer, the carrier-pDNA complex should be small and compact. The formation of a complex between PEI-BSA and pDNA with both a suitable size and surface charge is an important criterion for polycations, when used as gene carriers for internalization into cells. For this reason, I evaluated particle size of the PEI-BSA-pDNA complex, as a function of the PEI-BSA: pDNA (w/w) ratio over a range from 0.25 to 10. The particle sizes of PEI-BSA: pDNA complexes plotted against the PEI-BSA: pDNA (w/w) ratios are shown in **Figure 5.3b**. I found that the size of the PEI-BSA-pDNA complex decreased with increasing PEI-BSA concentrations. The size of pDNA without PEI-BSA was around 1979± 181.5nm as 0:1 w/w ratio of PEI-BSA:pDNA However, when the PEI-BSA:pDNA (w/w) ratio reached 2:1 and 5:1, the particle sizes were around 280.33±207.2 nm and 117.26±12.4nm respectively, as shown in **Figure 5.3b**. This reduction in size likely arises as a result of the formation of an optimized PEI-BSA-pDNA complex, which maximizes ionic interactions. From these data, it is clear that PEI-BSA can condense pDNA into a nano-sized complex that is suitable for endocytic cellular uptake.

5.3.3.2 Surface charge

Similarly, I also characterized the zeta potential of PEI-BSA and pDNA complex at different polyampholyte: DNA w/w ratios. As shown in **Figure 5.3c**, the surface potential of the different polyampholyte-pDNA complexes tends to become more positive as the concentration of polyampholyte increased. The zeta potential of bare DNA without PEI-BSAwas found to be at -10.48 mV when the polyampholyte: pDNA (w/w) ratio was 0:1, whereas the surface potential rapidly increased to a positive value as thepolyampholyte:pDNA (w/w) ratio was increased to 1:1. Overall, I observed that the zeta potential of the PEI-BSA-pDNA complex escalated from -8.31±1.0 to 21.02±1.6 mV as the PEI-BSA:pDNA (w/w) ratio increased from 0.25:1 to 10:1. This change in positive charge of the PEI-BSA-pDNA suggests that the efficient complexation of pDNA with PEI-BSA that

can be observed by measuring the surface charge potential. Based on this, it was apparent that PEI-BSA was able to condense pDNA at PEI-BSA/ pDNA ratios ranging from 1:1 to 10:1.

5.3.3.3 Stability

A long half-life is considered to be an essential property for nanoparticles to effectively deliver a target gene into the target cell or tissue of interest. Therefore, the inherent stability of polymer-pDNA complexes is very important in successful delivery of genetic-based materials. Consequently, in this study, I characterized the physical stability of PEI-BSA-pDNA complexes over a period of seven days under physiological conditions, both in the presence and absence of pDNA. I found that the size of uncomplexed PEI-BSA did not change over this time interval, as shown in **Figure 5.3d**. This result suggests that the introduction of a hydrophobic modification such as butylsuccinic anhydride on branched PEI can improve the nanoparticle stability presumably due to the compact self-assembled nanostructure. Similarly, the PEI-BSA-pDNA complex also maintained a stable size over this one-week period (**Figure 5.3d**). These data strongly suggest that the stability of PEI-BSA-pDNA complexes arises because of electrostatic interaction leading to efficient compaction of the pDNA.
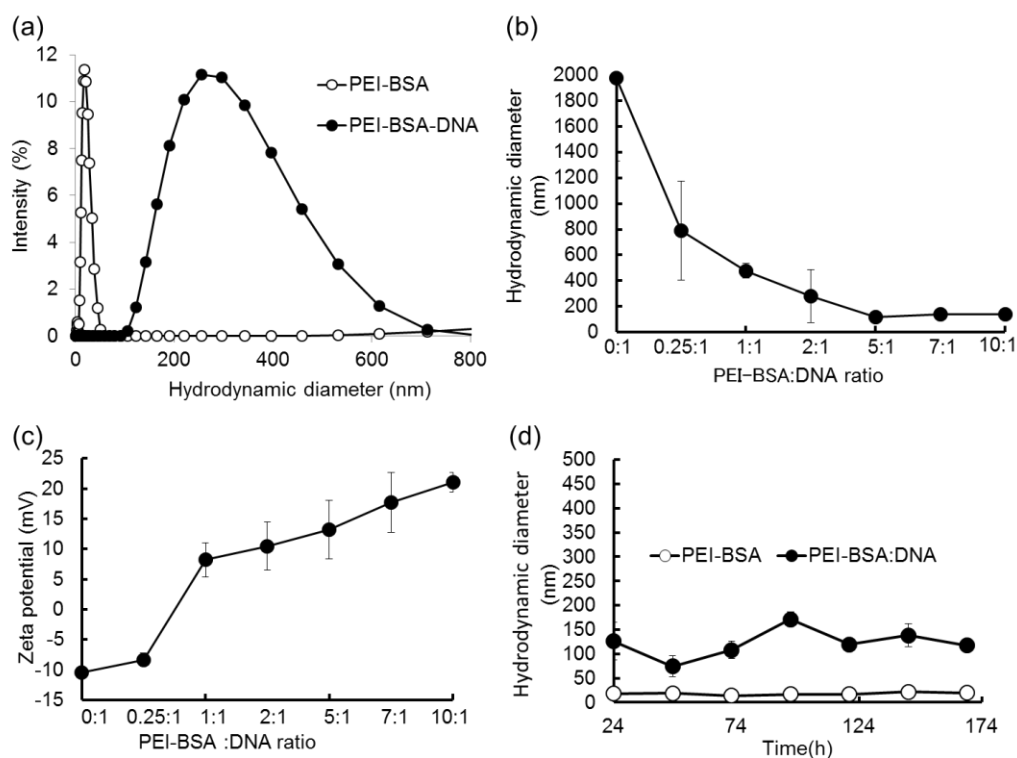
Figure 5.3 Physical characteristics of polyampholytes (a) Comparison of polyampholyte particle sizes, with or without pDNA, measured by DLS analysis. Open circle, PEI-BSA alone, closed circle,

PEI-BSA-pDNA. (b) Hydrodynamic diameter and (c) Zeta potential and of PEI-BSA-pDNA complexes at different PEI-BSA/pDNA ratios ranging from 0:1 to 10:1 (d) Particle size stabilities of PEI-BSA and a PEI-BSA:pDNA(2:1)complex over time at 25°C.
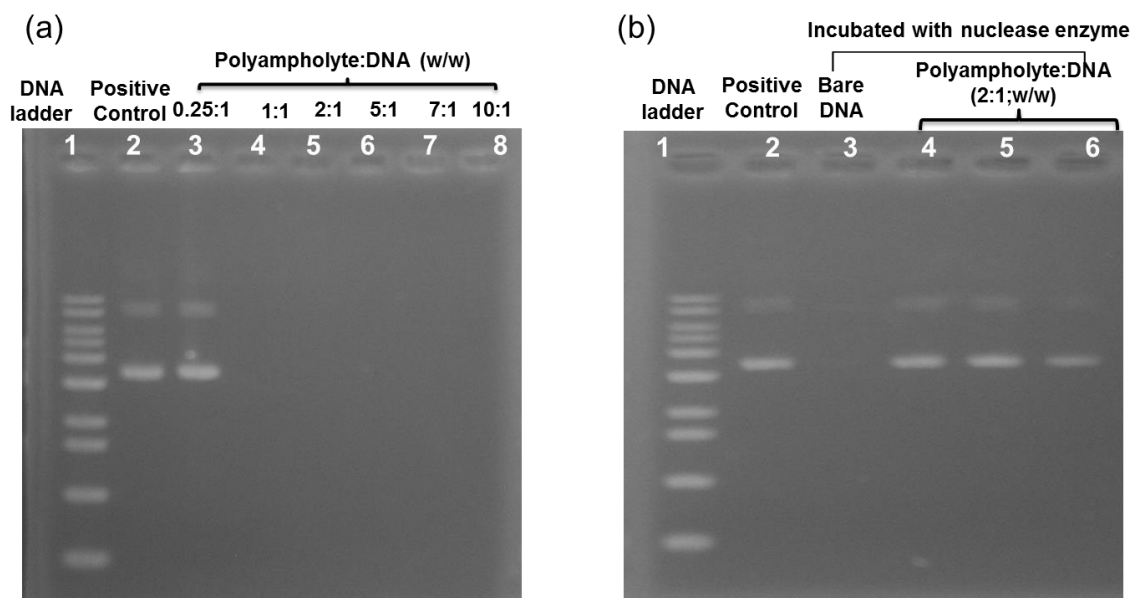
5.3.3.4 Agarose gel electrophoresis studies

5.3.3.4.1 Complex formation between pDNA and polyampholytes

DNA condensation is required in order for a PEI-BSA-pDNA complex to be formed. The complexation and binding ability of PEI-BSA with pDNA was measured by agarose gel electrophoresis. The PEI-BSA-pDNA complexes were prepared by varying the concentration of PEI-BSA from 0.25 to 10 μg while the concentration of pDNA was fixed at 1 μg in 50 μL PBS (-) (**Figure 5.4a**). As shown in **Figure 5.4a**, un-complexed pDNA was clearly visible. After the introduction of PEI-BSA at a ratio of 0.25:1 (w/w) a band corresponding to un-complexed pDNA was still clearly visible. However, as the PEI-BSA:pDNA ratio increased above 0.25:1 (i.e. 1:1 to 10:1) it was apparent that the band corresponding to the un-complexed pDNA disappeared. This could be explained by the fact that once pDNA was associated with the PEI-BSA, it was too large to diffuse through the agarose gel matrix and therefore could not undergo electrophoresis. The results of agarose gel electrophoresis indicated that PEI-BSA may bind with pDNA at different mass ratios of polymer to pDNA to form complexes (**Figure 5.4a**). In addition, these results were clearly in good agreement with the data showing zeta size and zeta potential of the PEI-BSA-pDNA complex (**Figure 5.3b, c**).

5.3.3.4.2 Stability against nucleases

It is important for carriers to protect pDNA from enzymatic degradation in order to be able to efficiently release the DNA for gene expression, both *in vitro* as well as *in vivo*. To investigate the stability of DNA loaded PEI-BSA against enzymatic degradation, I examined the ability of PEI-BSA to protect pDNA from DNase I-induced digestion at 37°C. Following incubation with DNase I, I used heparin to disrupt the PEI-BSA-pDNA complex to release pDNA. In this case, heparin serves to competitively displace polycations (such as the amine groups in PEI-BSA) from the pDNA. As shown in **Figure 5.4b**, incubation of un-complexed pDNA with DNase I at 0.1 U/μg for 30 min resulted in complete digestion of the pDNA. In contrast, following incubation of the PEI-BSA-pDNA complex (2:1 w/w ratio) with

increasing concentrations of DNase I (0.1, 0.2 or 0.4 U/μg) pDNA could still be readily released from the PEI-BSA-pDNA complex demonstrating that PEI-BSA protects the pDNA cargo from enzymatic degradation.


Figure 5.4. Agarose gel electrophoresis studies. (a) Complex formation between polyampholyte and pDNA. The amount of plasmid DNA was fixed at 1 μg, and the complexes were prepared using different amount of PEI-BSA in PBS (-). Lane-1; 1 kbDNA ladder, Lane 2; pDNA control Lane 3- 8; PEI-BSA/pDNA complexes at different mass ratios 0.25:1, 1:1; 2:1, 5:1,7:1 and 10:1 (b) Protection of pDNA within the PEI-BSA/pDNA complex against nuclease activity. Lane 1: 1 kb DNA ladder, Lane 2: pDNA control Lane 3: pDNA alone incubated with DNase I at 0.1 U/μg DNA for 30 min; Lane 4- 6: PEI-BSA:pDNA (2:1 w/w) was incubated with different amounts of DNase I at 0.1, 0.2, or 0.4 U/μg DNA for 30 min. After treatment with DNase I the enzyme was deactivated by adding EDTA and subsequently heparin was added to each sample before agarose gel electrophoresis.

5.3.4 Cytotoxicity assay

The *in vitro* toxicities of different polymers were measured as a function of polymer concentration using an MTT assay. **Figure 5.5** demonstrates the cell viability of different polymer samples at different concentrations after 48 h treatment. Branched PEI (25 kDa) had the highest toxicity whereas PEI-SA and PEI-BSA were less toxic. The cell viabilities in cells treated with PEI-SA and PEI-BSA were greater than 70% at a concentration of 10 μg/mL, while the cell viability in cells treated with PEI was just 54%. Branched PEI (25 kDa) has been previously reported to have high cell toxicity[37]. PEI toxicity appears to be mainly

associated with a high net-positive charge on the polymer due to the numerous amino groups present in the polymeric backbone (**Figure 5.5**).The reduced toxicity of PEI-SA or PEI-BSA compared to PEI likely arises as a result of the modifications that reduce the number of amine groups in the polymer backbone. These data fit in with previous reports where modification of branched PEI has been shown to decrease polymer toxicity[27-30]. In addition, these data further support the use of PEI-BSA as a low-toxicity gene delivery vehicle.
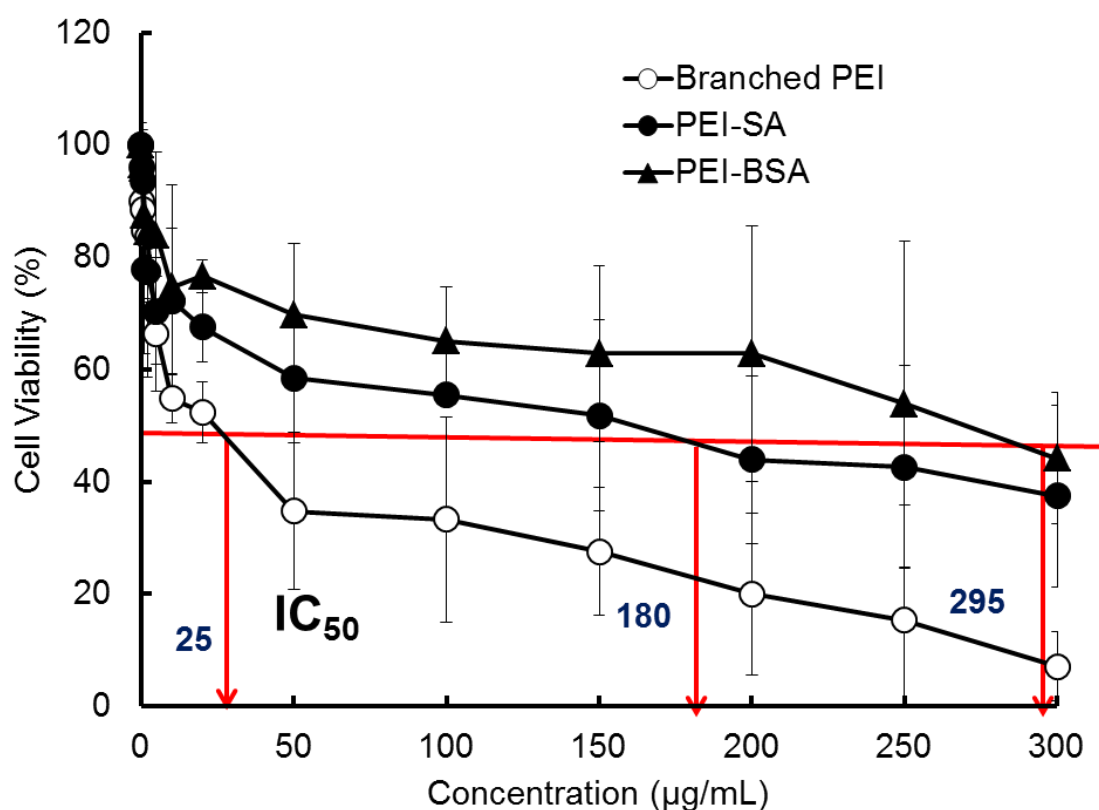
Figure 5.5 HEK293T cells were incubated with different concentrations of branched PEI, PEI-SA, or PEI-BSA for 48 h, followed by MTT assay analysis. IC$_{50}$ represents the concentration of polyampholyte that caused a 50% reduction in MTT uptake in a treated cell culture compared with an untreated control culture; data are expressed as the mean ± standard deviation (SD)

5.3.5 Enhancement of gene delivery using freeze concentration

5.3.5.1 Cell freezing with polyampholyte-DNA complexes

In this study, I elected to use HEK-293T cells for transfection studies because they contain the SV40 large T antigen, which allows for substantial replication of transfected plasmids[38]. To demonstrate the effect of freezing on transfection, HEK293T cells were frozen in the presence of increasing amounts of PEI-BSA along with a fixed quantity of pDNA (1 µg) to give PEI-BSA:pDNA (w/w) ratios of 2:1, 5:1, 7:1, and 10:1 in the presence of 10%

PLL-SA as a cryoprotectant. The final freezing volume was 50 μL in PBS(-). The commercially available transfection reagents jetPEI® and Lipofectamine 3000 were also used as a comparison. As illustrated in **Figure 5.6**, cell survival was greater than 90% in the presence of the polymeric cryoprotectant 10% PLL-SA. Next, I investigated the adsorption of cyanine3 (Cy3)-labeled pDNA complexes to the cell membrane to compare the freeze concentration method versus the non-freezing method, along with a comparison between the commercially available transfection reagent jetPEI® and PEI-BSA. As shown in **Figure 5.7a**, enhanced adsorption of Cy3 labeled-pDNA was found when the freeze concentration approach was used for jetPEI® compared to the non-frozen method. Similarly, enhanced adsorption of Cy3-labeled pDNA was evident when the freeze concentration approach was used for PEI-BSA (**Figure 5.7b**) compared to the non-frozen method. The Cy 3 fluorescence intensity was quantitated using confocal microscopy. In addition to confirming that the freeze concentration method increases Cy3 pDNA adsorption to HEK-293T cells compared to the non-frozen method, I also showed that PEI-BSA allowed for better Cy3 pDNA adsorption to cells than jetPEI® (**Figure 5.7c**). Taken together, these data indicate that freezing enhances the level of polymer:pDNA complexes around the cell membrane and that PEI-BSA was more effective as a carrier than jetPEI®. One possible explanation for this difference is the fact that PEI-BSA, which contains a hydrophobic alkyl group, could more effectively interact with the cell membrane via hydrophobic interactions. These data are consistent with prior studies that demonstrated effective adsorption of materials using this freeze concentration approach[10, 11].
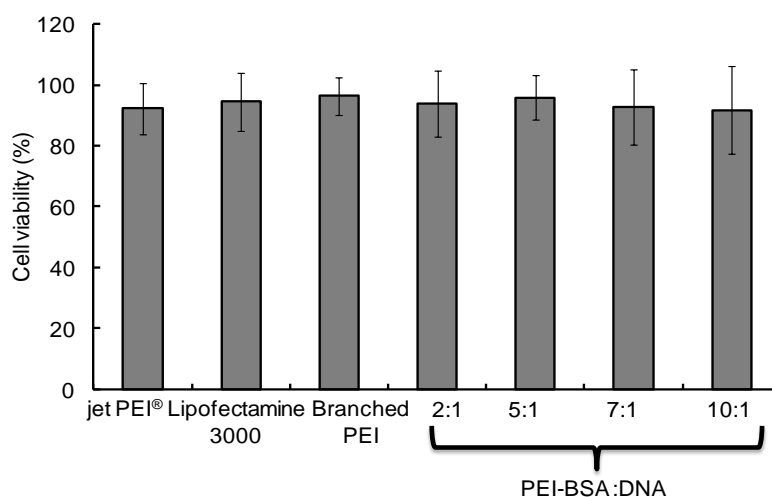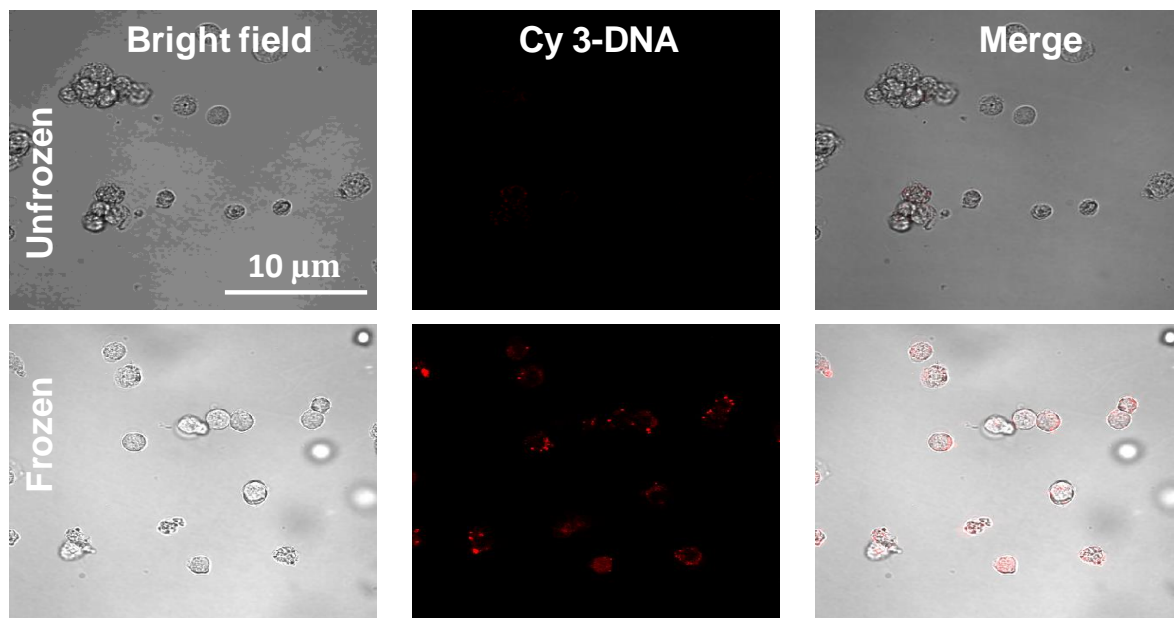

Figure 5.6 Cell viability after being frozen at -80 ˚C for 1d with commercial available transfecting carriers such as jetPEI®, Lipofectamine3000, branched PEI and PEI-BSA of different amount loaded
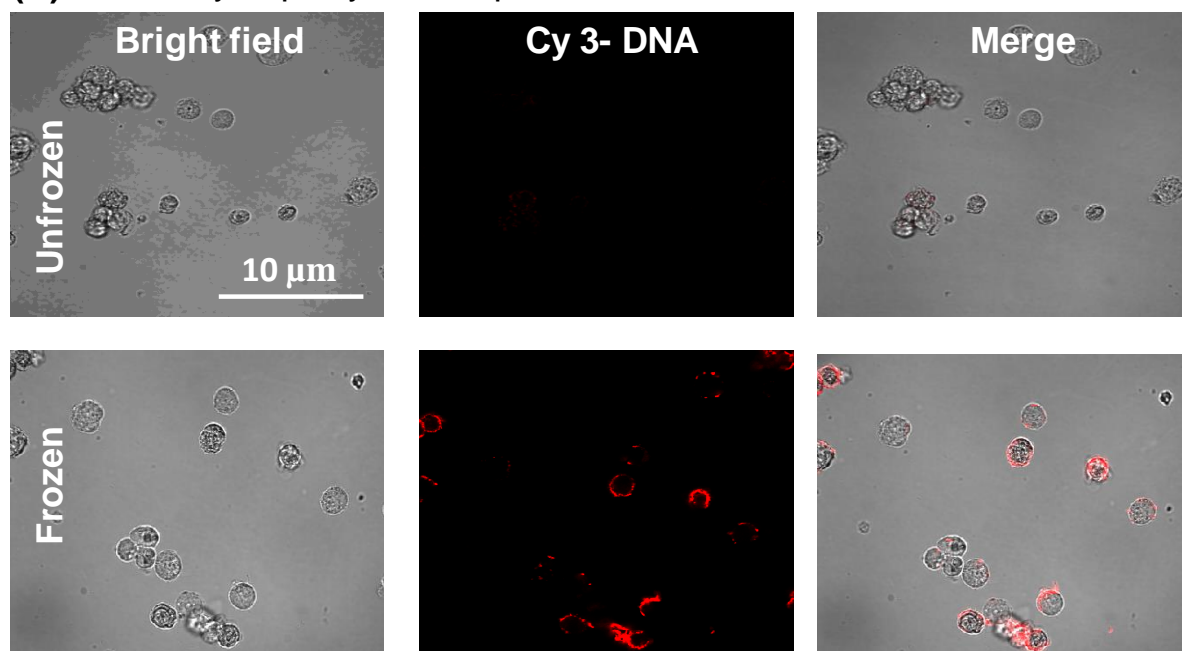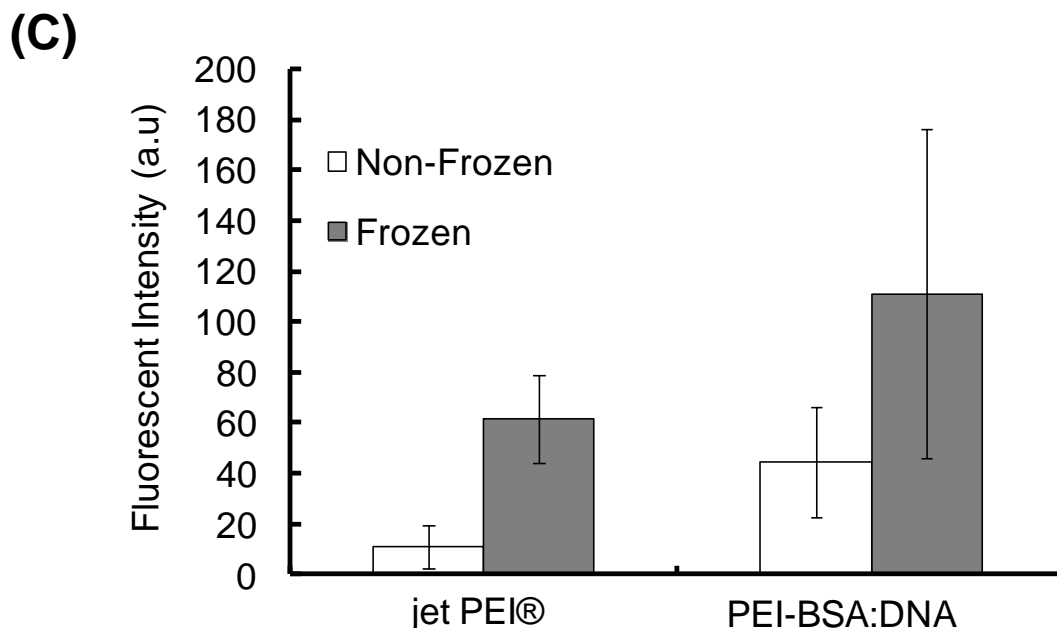
pDNA. The cells were frozen with cryprotective solution 10% PLL-SA. Data are expressed as mean ± SD.

(A) With jetPEI®

(B) With Polyampholyte Nanoparticles PEI-BSA

(C)

Figure 5.7 Confocal images of HEK 293 T cells before and after freezing with Cy3 labeled pDNA frozen with using 10% PLL-SA as a cryoprotectant (A) jetPEI®(B) PEI-BSA. Scale bars: 10 μm. (C) Mean fluorescent intensity of comparison of Cy3-labeled pDNA adsorbed onto before and after being frozen with jetPEI®and PEI-BSA as determined by confocal microscope. Data are expressed as mean ± SD

5.3.5.2 Transfection studies using confocal microscopy

The *in vitro* transfection process was then evaluated using pDNA encoding GFP as a reporter gene. To perform this, I cryopreserved HEK-293T cells with nanocarrier-pDNA complexes in the presence of the polymeric cryoprotectant 10% PLL-SA for 24 h. After thawing, the cell suspension was seeded onto the bottom of a glass dish and then incubated for a further 10 h. In order to compare with the non-frozen method, nanocarrier-pDNA complexes were gently added directly to HEK-293T cells seeded on the bottom of a glass dish and these were also incubated for a further 10 h. GFP expression was examined using CLSM. Transfection studies were first performed using the commercially available carriers jetPEI® and Lipofectamine 3000. JetPEI® is a linear PEI derivative that is well suited for plasmid DNA delivery whereas Lipofectamine 3000 is a lipid-based transfection agent generally regarded as being highly efficient for gene transfection. As shown in **Figure 5.8 a,b** HEK-293T cells transfected with GFP using the freeze concentration method gave

significantly better GFP expression that cells transfected using the non-frozen method, which showed barely any GFP expression, regardless of which of the commercial carriers was used. One possible explanation for this is that the freezing process likely increases the concentration of carrier-pDNA system in the environment around the around the cell membrane, after which the carrier-pDNA can enter the cell rather than diffusing away from the cells. Previous work from my group also indicates that freeze concentration may have a beneficial effect on protein internalization[10,11]. I also used the same experimental approach to examine the effect of both branched PEI and PEI-BSA as carriers during transfection of HEK-293T cells with a pDNA encoding GFP to allow a comparison with the commercially available carriers. A branched PEI:pDNA complex (5:1 w/w ratio) and several different PEI-BSA:pDNA complexes (2:1, 5:1, 7:1, and 10:1 w/w ratios) were used under freeze concentration and non-frozen conditions. **Figure 5.8c-g** shows the confocal images for GFP expression. The use of branched PEI as a carrier resulted in barely any GFP expression regardless of whether freezing was used (**Figure 5.8c**). In contrast, the transfection efficiency was significantly higher when PEI-BSA was used as carrier and was even more pronounced under freeze concentration conditions (**Figure 5.8d**). Interestingly, as the ratio of PEI-BSA:pDNA increased from 2:1 to 5:1, the gene transfection efficiency increased but further increases in the PEI-BSA:pDNA ratio (7:1 to 10:1) appeared to cause a decrease in expression (**Figure 5.8f,g**). The reason for this is not known. It has been known from the literature that branched PEI is considered to be a good transfection carrier[39]. However, in my study, modified PEI was found to be a better transfection carrier than branched PEI. As these data were largely qualitative, I next sought to quantify the gene transfection efficiency in my system more precisely using luciferase as a reporter rather than GFP.
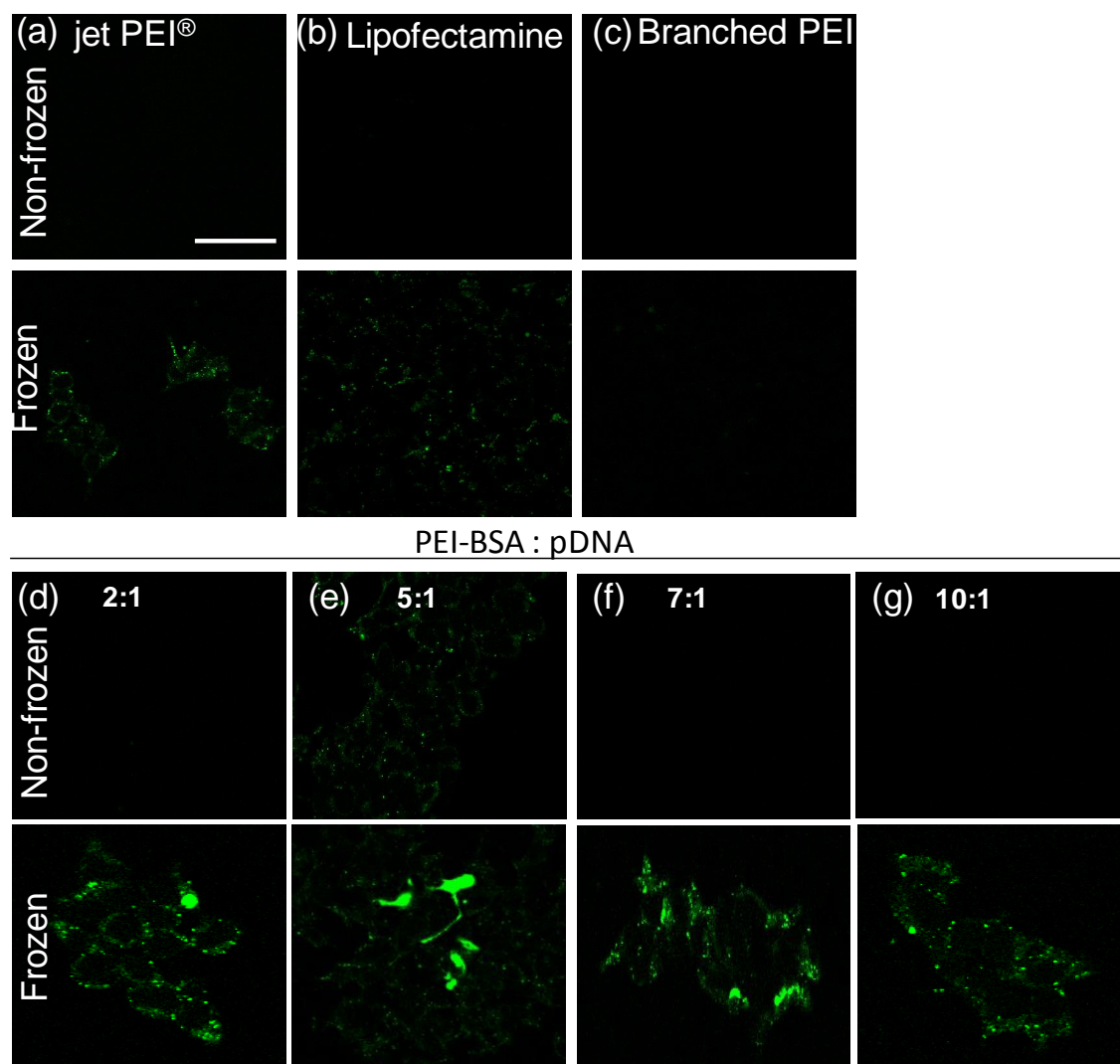
Figure 5.8 Comparison of the in vitro transfection efficiency of different pDNA complexes in HEK-293T cells using a pDNA encoding GFP. HEK-293T cells were either frozen in the presence of the different pDNA complexes along with 10% PLL-SA as a cryoprotectant (Frozen) or the pDNA complexes were added directly to the cells without freezing (Non-frozen) and were incubated for 10 h. Each commercially available transfection reagents was incubated with plasmid DNA (1μg)(a) jetPEI® (b) Lipofectamine 3000 (c) Branched PEI, and PEI-BSA:pDNA ((d) 2:1, (e)5:1, (f) 7:1, (g) 10:1, w/w). Confocal microscopy images showing GFP expression are shown. Scale bars: 50 μm.

5.3.5.3 Luciferase expression of unfrozen and frozen system

The experimental conditions used to analyze gene transfection efficiency using luciferase were modified slightly compared to the GFP study. For GFP expression, cells were cultured for 10 h post-plating (and post-transfection) to allow for expression of GFP to evaluate transfection efficiency. However, for luciferase expression, cells were transfected with the pGL4.51 plasmid (which contains the luciferase gene) and were cultured for at least 48 h to

allow for sufficient enzyme expression to occur. As for the GFP experiment, complexes of jetPEI® and Lipofectamine 3000, a complex of branched PEI (5:1 ratio w/w), and several different PEI-BSA complexes (2:1, 5:1, 7:1, and 10:1 w/w ratios) were evaluated under freeze concentration and non-frozen conditions. As shown in **Figure 5.9**, luciferase reporter gene expression was significantly higher using the freeze concentration method, compared to the non-frozen method for all transfection carriers. Freeze concentration resulted in an almost 10-fold enhancement in luciferase expression for both jetPEI® and Lipofectamine 3000. This result confirmed my previous finding for GFP, namely that freeze concentration increased the transfection efficiency of both carriers. Surprisingly, jetPEI® luciferase expression was found to be higher than Lipofectamine 3000 in both the non-frozen and freeze concentration conditions. Other studies have reported that jetPEI® can provide a higher transfection efficiency compared to Lipofectamine[40,41]. One possible reason for the reduced transfection efficiency of Lipofectamine 3000 compared to jetPEI® is that it can adsorb onto large anionic serum protein aggregates. These large aggregates most likely will not be able to cross the cell membrane and deliver pDNA to the cells[42]; it is possible that pDNA-jetPEI® could prevent this aggregation. Another possible reason for this difference is that, depending on the carrier, there might be differences in how efficiently different intracellular processes such as nuclear translocation or integration of a vector into chromosomal DNA occur. In this study, I did not examine these factors but my future studies will focus on understanding these different transfection efficiencies.
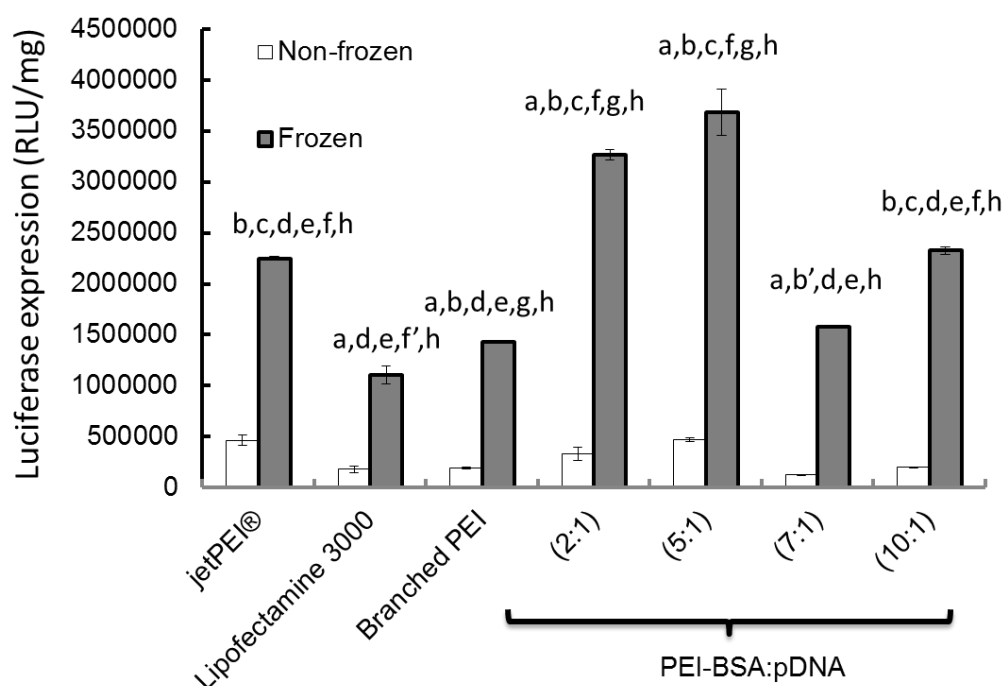
Figure 5.9 Comparison of the *in vitro* transfection efficiency of different pDNA complexes in HEK-293T cells using a pDNA encoding luciferase. HEK-293T cells were either frozen in the presence of the different pDNA complexes along with 10% PLL-SA as a cryoprotectant (Frozen) or the pDNA complexes were added directly to the cells without freezing (Non-frozen). Luciferase expression was measured using a luminometer 48 hours later. The pDNA(1µg) was complexed with either jetPEI[®], Lipofectamine 3000, Branched PEI, or PEI-BSA:pDNA (at various ratios of 2:1, 5:1, 7:1, or 10:1, w/w). Scale bars: 10 µm. White bar: Non-frozen; grey bar: Frozen. Data are expressed as the mean ± standard deviation (SD). a: $p < 0.01$ vs. Jet PEI[®], b: $p < 0.01$ vs. Lipofectamine 3000, b': $p < 0.05$ vs. Lipofectamine 3000, c: $p < 0.01$ vs. branched PEI, d: $p < 0.01$ vs. PEI-BSA:DNA (2:1), e: $p < 0.01$ vs. (5:1), f: $p < 0.01$ vs. (7:1), f': $p < 0.05$ vs. (7:1), g: $p < 0.01$ vs. (10:1), and h: $p < 0.01$ vs. corresponding non-frozen condition.

Figure 5.9 also shows that HEK-293T cells treated with PEI-BSA had significantly enhanced luciferase expression (approximately 10-fold) using the freeze concentration method compared to cells treated using the non-frozen method. In particular, the transfection efficiencies of PEI-BSA:pDNA at ratios of 2:1 and 5:1 (w/w) were significantly higher than at ratios of 7:1 and 10:1, consistent with the GFP experiment (compare **Figure 5.9** with **Figure 5.8 d-g**). This difference in transfection efficiency might arise as a result of less binding of PEI-BSA to pDNA. When the PEI-BSA:pDNA (w/w) ratio was greater than 5:1, the increased positive charge on the polymer will likely result in a stable complex with the

pDNA, making it more difficult to dissociate the PEI-BSA-pDNA complex. As a result, this may cause a reduction in transfection efficiency. These results therefore demonstrate that effective gene delivery is dependent on the ratio of PEI-BSA to pDNA using both the frozen and non-frozen methods. One other point of interest is that at 10:1 (PEI-BSA:pDNA, w/w), luciferase expression increased compared with that at 7:1 (PEI-BSA:pDNA, w/w) (**Figure 5.9**). In addition, as was seen in the GFP experiment, the efficiencies of the luciferase transfections using branched PEI were lower than for PEI-BSA using both the non-frozen and the frozen methods (**Figure 5.9**). Overall, as expected, freeze concentration increased luciferase expression in a similar manner to that which was observed in the GFP transfection studies (**Figure 5.8a-g**).

Gabrielson and co-workers demonstrated enhanced transfection efficiency after using of acetylated PEI, which they attributed to weak binding between the acetylated PEI and pDNA. They also demonstrated that acetylated PEI releases more pDNA than branched PEI using a heparin displacement assay[43]. Wagner et al. have also shown that modification of branched PEI with succinic anhydride displayed a high efficiency in siRNA-mediated knockdown of a target gene compared with branched PEI 25kDa[27].

Forrest et al. have also shown that partial acetylation of PEI also enhances gene transfection efficiently[44]. These reports are complementary to my data. Nevertheless, in my present study, PEI-BSA produced significantly much better transfection efficiency than the commercially available carriers jetPEI® and Lipofectamine 3000. My data also suggests that there is an optimal ratio of PEI-BSA to DNA that should be determined in order to enhance transfection efficiency. Finally, my results also demonstrated the considerable enhancement in transfection efficiency is obtained when the freeze concentration method is combined with PEI-BSA and suggests that this approach has the potential to be used as an efficient gene delivery system *in vitro*.

5.3.5.4 Intracellular distribution of polyampholytes -pDNA complex

For an effective transfection method to be useful in therapeutic applications, it is important that the transfection system facilitates the escape of pDNA from the endosome and allow for its efficient transfer to the nucleus. Therefore, I next sought to understand the endosomal escape capability of my transfection system. To study this, I used confocal microscopy to observe the intracellular localization of the polyampholytes. To achieve this, plasmid pAcGFP1-N2 was labeled with Cy3 dye and the endosomes were stained with

Lysotracker green while cell nuclei were stained with Hoechst 33342. In order to observe the intracellular distribution of pDNA after freeze concentration, the thawed HEK-293T cell suspensions were seeded into plates and cultured for 24 h. As shown in **Figure 5.10a**, Cy3-pDNA was still present in endosomes in the case of the branched PEI-DNA complex as evidenced by the yellow color. In fact, the majority of Cy3-pDNA was present in endosomes and only a very small amount of pDNA was released. In contrast, in the case of PEI-BSA-pDNA complexes, more pDNA was clearly visible in the cytoplasm, with much lower levels being evident in the endosome (**Figure 5.10b**).This data indicated that pDNA was efficiently released from endosomes when PEI-BSA was used. The most probable reason for this enhanced release of pDNA from polyampholytes is due to weaker binding between pDNA and the polyampholyte resulting in more efficient release of pDNA. Therefore, one of the other reasons for there being enhanced transfection efficiency with PEI-BSA might be because of this reduced binding between the polyampholyte and pDNA leading to facile un-packaging of the pDNA. In contrast, branched PEI might be expected to exhibit a strong interaction with pDNA and this will tend to reduce the transfection efficiency.
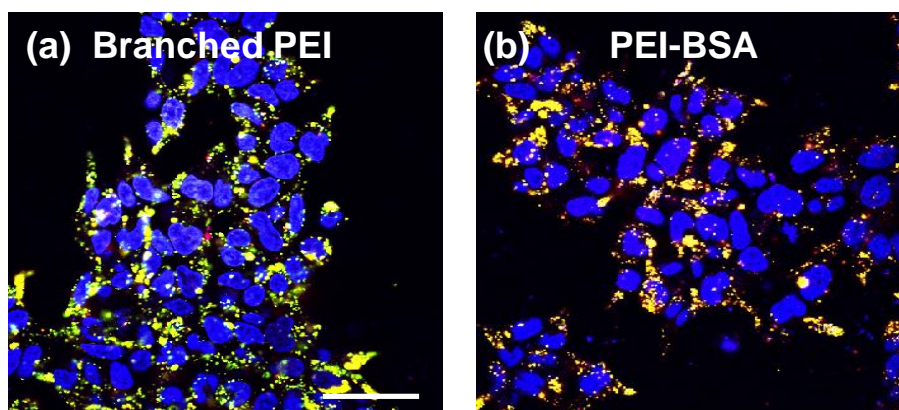
Figure 5.10 Intracellular localization of Cy-3 labeled pDNA in HEK293T cells. HEK293T cells (1 x 10^6 cells) were cryopreserved in the presence of polymeric cryoprotectant10% PLL-SA and the Cy3-labeled pDNA (1μg). The cells were thawed and seeded for 24 h at 37°C. Following this, the endosomes/lysosomes and nuclei were stained using Lysotracker green and Hoechst blue 33342, respectively. (a) Branched PEI (b) PEI-BSA. Scale bar: 50 μm.

Various hypotheses explaining endosomal escape has been proposed over the past few years. Branched PEI 25kDa is thought to be an effective transfection agent due to the 'proton sponge' hypothesis, which is thought to facilitate the escape of complexes from endosomes.

According to this hypothesis, polymers with pKa values between neutral and endosomal pH, such as PEI, have the ability to buffer the ATPase-mediated acidification of endocytic vesicles. In PEI, every third atom of PEI is nitrogen that could be potentially protonated, thereby providing a strong buffering capacity. A relatively large number of protons may therefore accumulate in the endocytic vesicles. The influx of positive charge (hydrogen ions) would have to be balanced by an influx of counter-ions (primarily chloride) leading to endosome swelling, rupture of the endosome membrane, and eventual release of the DNA into the cytosol. However, this proposed mechanism is controversial, since a recent study did not observe any change in endosomal pH after exposure to PEI over a 24 h period[45].

Recently, numerous studies have shown that efficient transfer of DNA inside the cell might arise as a result of a weak interaction between the carrier and DNA in the endosome allowing for subsequent release of DNA into the cytoplasm and a resultant increase in transfection efficiency[43,44,46]. Similar work has been performed by Uludag et al., in which they showed that branched PEI modified by either oleic acid or stearic acid gave enhanced transfection efficiency compared with commercially available transfection reagents[46]. Other reports, also similar to my results, have shown that the presence of long alkyl chains in the carrier would be expected to strengthen the interaction with the cell membrane, increasing endocytosis and thereby also enhancing the transfection efficiency[47-50]. With regard to endosome escape, I have shown that that PEI-BSA:pDNA complex could efficiently escape from endosomes also resulting in increased transfection efficiency with low toxicity. However, the mechanism for efficient endosome escape to the cytoplasm is not yet fully understood, but I believe that it is due to weak binding between the polymer carrier and pDNA. In addition, the use of freeze concentration to further enhance transfection efficiency may prove to be extremely useful for gene delivery *in vitro*. My data clearly indicate that, after freeze concentration, polyampholytes were capable of enhancing DNA escape from endosomes, which will also enhance transfection efficiency. I think it will be extremely important to elucidate the exact mechanism of endosomal escape that occurs after using the freeze concentration method and I plan to investigate this in the near future.

5.4 Conclusion

In this study, I demonstrated the effective use of a freeze concentration method as part of a cell transfection system. I found that freeze concentration accelerates and enhances gene expression and is an additional facile procedure even when used with currently available transfection reagents, such as jetPEI® or Lipofectamine 3000. Furthermore, I also developed new self-assembling polyampholytes as non-viral carriers. These polyampholytes were extremely small in size, were able to condense DNA efficiently, and were found to be much less toxic compared to branched PEI. In HEK-293T cells, confocal microscopy analysis of transfected GFP expression and direct luciferase activity measurements revealed that maximum transfection efficiency depends on the appropriate polyampholyte:DNA ratio and is enhanced using the freeze concentration method. These findings provide an effective, simple, and non-toxic approach for enhancing gene delivery. The present studies suggest that the unique combination of a polyampholyte non-viral carrier and a physical method such as freeze concentration might be a safe and efficient system for *in vitro* gene delivery. Further work should focus on evaluating the use of this system in clinically relevant studies to assess its potential as a system for the treatment of genetic diseases.

5.5 References

1. Chen, J.; Guo, Z.; Tian, H.; Chen, X., *Mol.Ther. Methods Clin. Dev* **2016**, *3*, 1.

2. Manjila, S.B.; Baby, J.N.; Bijin, E.N.; Constantine, I.; Pramod, K.; Valsalakumari, J.. *Int. J. Pharm. Investig.* **2013**, *3*, 1.

3. Dizaj, S.M.; Jafari, S.; Khosroushahi, A.Y., *Nanoscale Res. Lett.* **2014**, *9*, 1.

4. Nayerossadat, N.; Maedeh, T.; Ali, P.A., *Adv. Biomed. Res.* **2012**, *1*, 1-11.

5. Thomas, C.E.; Ehrhardt, A.; Kay, M.A., *Nat. Rev. Genet.* **2003**, *4*, 346.

6. Zhou, R.; Norton, J.E.; Dean, D.A., *Methods Mol. Biol.* **2008**,*423*, 233.

7. Zhang, Y.; Tachibana, R.; Okamoto, A.; Azuma, T.; Sasaki, A.; Yoshinaka, K.; Tei, Y.; Takagi, S.; Matsumoto, Y. *Int. J. Hyperthermia* **2012**, *28*, 290.

8. Aravindaram, K.; Yang, N.S., *Methods Mol. Biol.* **2009**,*542*, 167.

9. Beebe, S.J.; Sain, N.M.; Ren, W. *Cells* **2013**, *2*, 136.

10. Ahmed, S.; Hayashi, F.; Nagashima, T.; Matsumura, K., *Biomaterials* **2014**, *35*, 6508.

11. Ahmed, S.; Fujita, S.; Matsumura, K., *Nanoscale* **2016**, *8*, 15888.

12. Bhatnagar, B.S.; Pikal, M.J.; Bogner, R.H., *J. Pharm. Sci.* **2008**, *97*, 798.

13. Pham, Q.T., *Jpn J Food Eng*. **2008**, *9*, 21.

14. Machado, J.A.S.; Ruiz, Y.; Auleda, J.M.; Hernandez, E.; Reventos, M., *Food Sci. Technol. Int.* **2009**, *15*, 303.

15. Kiani, H.; Sun, D.W., *Trends Food Sci. Technol.* **2011**, *22*, 407.

16. Luo, D.; Saltzman, W.M., *Nature Biotechnol* **2000**, *18*, 33.

17. Pezzoli, D.; Kajaste-Rudnitski, A.; Chiesa, R.; Candiani, G., *Methods Mol. Biol.* **2013**, *1025*, 269.

18. Midoux, P.; Breuzard, G.; Gomez, J.P.; Pichon, C., *Curr. Gene Ther.* **2008**, *8*, 335.

19. Liu, G.; Swierczewskaa, M.; Leea, S.; Chena, X., *Nano Today* **2010**, *5*, 524.

20. Lungwitz, U.; Breunig, M.; Blunk, T.; Gopferich, A., *Eur. J. Pharm. Biopharm.* **2005**, *60*, 247.

21. Zhou, D.; Li, C.; Hu, Y.; Zhou,H.; Chen, J.; Zhang, Z.; Guo, T., *J. Mater.Chem.* **2012**, *22*, 10743.

22. Oliveira, H.; Pires, L.R.; Fernandez, R.; Martins, M.C.; Simoes, S.; Pego, A.P. *J Biomed. Mater. Res. A*. **2010**, *95*, 801.

23. Huang, R.; Ke, W.; Liu, Y.; Jiang, C.; Pie, Y., *Biomaterials* **2008**, *29*, 238.

24. Tamboli, V.; Mishra, G.P.; Mitra, A.K., *Ther. Deliv.* **2011**, *2*, 523.

25. Varkouhi, A.K.; Scholte, M.; Storm, G.; Haisma, H.J., *J. Control. Release* **2010**, *151*, 220.

26. Moghimi, S.M.; Symonds, P.; Murray, J.C.; Hunter, A.C.; Debska, G.; Szewczyk, A. *Mol. Ther.* **2005**, *11*, 990.

27. Zintchenko, A.; Philipi, A.; Dehshahri, A.; Wagner, E., *Bioconjugate Chem.* **2008**, *19*, 1448.

28. Zhang, Q.F.; Lua, C.R.; Yin, D.X.; Zhang, J.; Liu, Y.H.; Peng, Q.; Xu, Y.; Yu, X.Q., y. *Polymers* **2015**, *7*, 2316.

29. Hu, Y.L.; Zhou, D.Z.; Li, C.X.; Zhou, H.; Chen, J.T.; Zhang, Z.P.; Guo, T.Y., *Acta Biomater.* **2013**, *9*, 5003.

30 Englert, C.; Fevre, M.; Wojtecki, R.J.; Cheng, W.; Xu, Q.; Yang, C.; Ke, X.; Hartlieb, M.; Kempe, K.; Garcia, J.M.; Ono, R. J.; Schubert, U.S.; Yang, Y.Y.; Hedrick. J.L. *Polym. Chem.* **2016**, *7*, 5862.

31. De Jong, W.H.; Borm, P.J. *Int. J. Nanomedicine* **2008**, *3*, 133.

32. Matsumura, K.; Hyon, S.H., *Biomaterials* **2009**, *30*, 4842.

33. Matsumura, K.; Kawamoto, K.; Takeuchi, M.; Yoshimura, S.; Tanaka, D.; Hyon, S.H., *ACS Biomater Sci Eng.* **2016**, *2*, 1023.

34. Matsumura, K.; Hayashi, F.; Nagashima, T.; Hyon, S.H., *J. Biomater. Sci. Polym. E*d. **2013**, *24*, 1484.

35. Read, M.L.; Singh, S.; Ahmed, Z.; Stevenson, M.; Briggs, S.S.; Oupicky, D.; Barrett, L.B.; Spice, R.; Kendall, M.; Berry, M.; Preece, J.A.; Logan, A.; Seymour, L.W. *Nucl Acids Res* **2005**, *9*, 1.

36. Shang, L.; Nienhaus, K.; Nienhaus, G.U., *J Nanobiotechnology* **2014**, *12*, 1.

37. Kafil, V.; Omidi, Y., *Bioimpacts: BI* **2011**, *1*, 23.

38. Mahon, M.J., *BioTechniques* **2011**, *51*, 119.

39. Dong, W.; Li, S.; Jin, G.; Sun, Q.; Ma,D.; Hua, Z., *Int. J. Mol. Sci.* **2007**, *8*, 81.

40. Yamano, S.; Dai, J.; Moursi, A.M., *Mol. Biotechnol.* **2010**, *46*, 287.

41. Lehnera, R.; Wanga, X.; Hunziker, P., *Eur. J. Nanomed.* **2013**, *5*, 205.

42. Zou, W.; Liu, C.; Chen, Z.; Zhang, N.,. *Nanoscale Res. Lett.* **2009**, *4*, 982.

43. Gabrielson, N.P.; Pack, D.W., *Biomacromolecules* **2006**, *7*, 2427.

44. Forrest, M.L.; Meister, G.E.; Koerber, J.T.; Pack, D.W., *Pharm Res.* **2004**, *21*, 365.

45. Benjaminsen, R.V.; Mattebjerg, M.A.; Henriksen, J.R.; Moghimi, S.M.; Andresen, T.L., *Mol. Ther.* **2013**, *21*, 149.

46. Alshamsan, A.; Haddadi, A.; Incani, V.; Samuel,J.; Lavasanifer, A.; Uludag, H., *Mol. Pharm.* **2009**, *6*, 121.

47. Hu, F.Q.; Chen, W.W.; Zhao, M.D.; Yuan, H.; Du, Y.Z., *Gene Ther.* **2013**, *20*, 597.

48. Kim, W.J.; Cheng, C.W.; Lee, M.; Kim, S.W., *J. Control. Release* **2007**,*118*, 357.

49. Guo, S.; Huong, Y.; Wei, T.; Zhang, W.; Wang, W.; Lin, D.; Zhang, X.; Kumar, A.; Du, Q.; Xing, J.; Deng, L.; Liang, Z.; Wang, P.C.; Dong, A.; Liang, X.J., *Biomaterials* **2011**, *32*, 879.

50. Liu, Z.; Zhang, Z.; Zhou, C.; Jiao, Y., *Prog. Polym. Sci*. **2010**, *35*, 1144.

Chapter 6

Conclusions

6.1 Summary

This thesis describes the development of novel and effective freeze concentration method for enhanced cytoplasmic delivery of macromolecules and addresses the feasibility of this method to be employed in gene therapy and immunotherapy applications.

In **Chapter 2,** a novel freeze concentration method was presented. At extreme ultra low temperature, the proteins were successfully adsorbed and transported to the cytoplasm of the cells comparing with non-frozen system. Moreover, I also developed safe and effective hydrophobic polyampholyte nanoparticles as a novel vehicle to carry proteins inside the cells. The surface charges of polyampholyte nanoparticles were easily manipulated and controlled by changing the introduction ratio of anionic functional group in polymeric backbone. In addition, polyampholyte nanoparticles have proven to be less loxic than cationic polymers. CLSM images demonstrated the effective delivery of proteins to the cytosol of the L929 cells by the combination of novel freeze concentration approach and hydrophobic polyampholyte nanoparticles. From the best of my knowledge, this was the first study of using novel, simple freeze concentration approach that can effective delivered proteins. In conclusion, freezing method was found to be effective and versatile for enhanced adsorption and internalization of protein *in vitro*.

Chapter 3 describes the development of new polyampholyte-modified liposomes as a carrier by incorporating the polyampholytes therein. These polyampholyte-modified liposomes were relatively more biocompatible and non-toxic comparing with polyampholytes. Furthermore, I utilized freeze concentration method as to deliver encapsulated protein complexes. Flow cytometry results were manifested the adsorption of protein towards the cells was enhanced by 4 fold comparing with non-frozen system. Moreover, I intended to elucidate the mechanism of endocytic pathway using unmodified and polyampholyte-modified liposomes for delivery of proteins. Inhibition studies demonstrated that the internalization mechanism differs between unmodified and polyampholyte-modified liposomes. In this study, I found the freeze concentration method successfully induces the efficient internalization of proteins simply by freezing cells with protein and nanocarrier complexes. Furthermore, polyampholyte-modified liposomes exhibited high efficacy in facilitating endosomal escape to enhance protein delivery to the cytoplasm with low toxicity. These results strongly suggested that the freeze concentration-based strategy could be widely utilized for efficient cargo delivery into the cytoplasm in vitro in cancer treatment.

In Chapter 4, towards extending the applicability of freeze concentration and pH sensitive polyampholyte-modified liposomes, I demonstrated the efficacy of using this system in immunotherapy based applications. Immunotherapy is the treatment of disease by inducing, enhancing, or suppressing an immune response. Freezing method treated immune RAW 264.7 cells showed high protein uptake efficiency compared to non-frozen condition. Also, freeze concentration of polyampholyte-modified liposomes encapsulating OVA antigen resulted in efficient OVA uptake and also allowed for its delivery to the cytosol. Efficient delivery of OVA to the cytosol was shown to be partly due to the pH-dependence of the polyampholyte-modified liposomes. Cytosolic OVA delivery also resulted in significant up-regulation of the Major histocompatibility complex class I pathway through a process known as cross-stimulation, and well as an increase in the release of cytokines such as IL-1β, IL-6, and TNF-α. Administration of freeze concentration method treated cells is extremely effective for the induction of immunity. The combination of freeze concentration method and polyampholyte-modified liposomes can efficiently introduce antigen protein to MHC class I molecules for cancer immunotherapy applications.

Chapter 5 demonstrated the effective *in vitro* gene delivery. Generally, the delivery of macromolecules is restricted by countless barriers such as toxicity, poor cellular uptake and poorly defined biodistributive characteristics. To address these issues, a unique and novel freeze concentration method was presented for effective cytoplasmic delivery of genes. Freeze concentration method was successfully internalized biomacromolecules inside the cells which indicated that freeze concentration approach might be effective approach for therapeutic applications. Additionally, new low toxic polyampholyte nanoparticles were also prepared using branched polyethyleneimine. The polyampholyte was self assembled to formed nanoparticles through hydrophobic and electrostatic interactions in aqueous solution and showed extremely small in size around 20 nm. Further, agarose gel electrophoresis analysis indicated that polyampholytes were able to complex with pDNA and provided stability against nuclease degradation. CLSM images and luciferase expression showed that freeze concentration method and polyampholyte nanoparticles were successfully enhancing the transfection efficiency. Moreover, the enhanced escaping of pDNA from endosomes using polyampholyte nanoparticles was found than branched PEI. The efficient combination of freeze concentration and polyampholyte nanoparticles showed a great potential for *in vitro* gene therapy.

The schematic representation of overall summary of thesis are indicated below
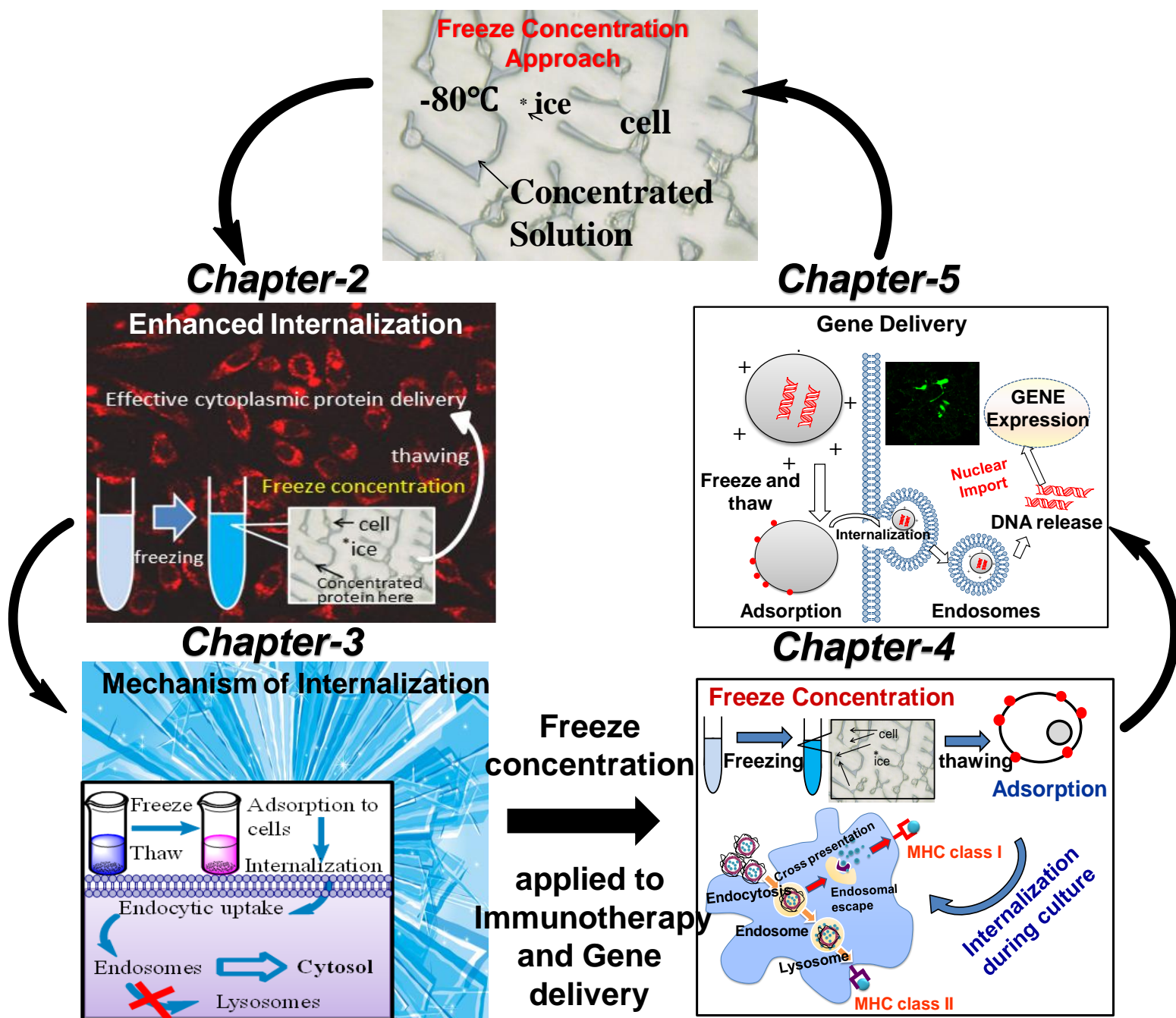
Figure 6.1 Schematic representation of thesis summary

6.2 Outlook

Freeze Concentration method: A contribution to Nanomedicines

A novel and unique freeze concentration method have been developed for effective delivery of macromolecule to address number of challenges exist that most molecules face in their ability to be delivered effectively at target site. Freeze concentration was found to be a versatile method which has been shown to be effective for delivery of model proteins and genes. I believe I have been successfully able to develop new strategy which can have broad applications in nanomedicines.

In **chapter 2**, the feasibility of freeze concentration strategy in protein delivery system was effectively demonstrated. The increased adsorption and internalization of macromolecules inside the cells indicated that freeze concentration method might be able to overcome the barriers of penetrating molecules inside the cells. However, it was a fundamental study which describes the suitability of freeze concentration approach. In future, freezing method can be employed by the use of therapeutic proteins such insulin to control diabetes.

Chapter 3 describes the development of more biocompatible and non-toxic pH sensitive polyampholyte modified liposomes. The mechanistic studies give more understanding the internalization and enhanced cytosolic delivery after freezing. In order to use them for clinical applications, *in vivo* using model system can be carried out.

In **Chapter 4**, the suitability of freeze concentration approach was effectively demonstrated in immunotherapy applications. The increased expression of cytokines and cell surface proteins are indicated that freeze concentration might be a promising method that contributes to the establishment of immunotherapy. Further, clinical studies will be required the effectiveness of freezing approach.

Chapter 5 describes the further applicability of freeze concentration method in gene delivery applications. It is well understood that internalization of genetic based materials indie the cells is very challenging due to its large size. Freeze concentration strategy has shown the potential in gene delivery applications. The association of freeze concentration and polyampholyte nanoparticles might be a great prospective for *in vitro* gene therapy.

6.3 Future perspectives and Scope from thesis

From this thesis, I believe that freeze concentration has a great potential to develop as next generation physical method for effective delivery of therapeutic macromolecules. This strategy has been shown the excellent quality for delivery of macromolecules. This method is simple, safe, avoids cell damage and does not require expensive equipments. Although, the freeze concentration system has broad range of applications that covers the area of macromolecule delivery but these are model system only. In order to use this methodology for therapeutic applications, further work is required to use therapeutic proteins such as insulin or therapeutic genes for treatment of various diseases.

Nonetheless, this technique was found to be favorable for *in vitro* delivery applications only. Freeze concentration method is restricted to use for *in vivo* applications. However, this strategy might be suitable for adoptive T cell immunotherapy for cancer. Due to unique enhancement in transporting macromolecule to cells property, freeze concentration method could be used to enhance the immune functionality of T cells and transferred to the cancer patient with the goal of recognizing, targeting and destroying tumor cells.

Moreover, freeze concentration method can also be applied in cell based gene therapy applications. Generally cell based gene therapy application has been applied to boost antitumor immunity and also enhances the immunity against other diseases. I expect that freeze concentration approach could show a great potential for effective cell therapy.

This has covered some pit-holes in the research field. I expect my study will assist in the development of better systems in the future.

Achievements

Original Papers

1. **Sana Ahmed**, Fumiaki Hayashi, Toshio Nagashima and Kazuaki Matsumura, Protein Cytoplasmic Delivery using Polyampholyte Nanoparticles and Freeze Concentration. *Biomaterials,* 2014, 35, 6508-18.

2. **Sana Ahmed**, Satoshi Fujita and Kazuaki Matsumura , Enhanced Protein Internalization and Efficient Endosomal Escape using Polyampholyte-modified Liposomes and Freeze Concentration. *Nanoscale*, 2016, 8, 15888-901 (**Selected as Journal back cover**)

3. **Sana Ahmed** and Kazuaki Matsumura, Novel Concentration-based freezing method for efficient protein delivery**. *Cryobiol Cryotechnol*., 2016, 62,143-147.

4. **Sana Ahmed**, Satoshi Fujita and Kazuaki Matsumura, A Freeze Concentration and Polyampholyte-Modified Liposome based Antigen Delivery System for Immunotherapy. *Adv. Healthcare Mater*. **2017, DOI: 10.1002/adhm.201700207**

5. **Sana Ahmed,** Tadashi Nakaji-Hirabayashi, Takayoshi Watanabe, Takahiro Hohsaka and Kazuaki Matsumura. Freezing Assisted Gene Delivery Combined with Polyampholyte Nano-carriers. **Submitted**

Book Chapter

1. Medical Application of Polyampholytes in Biopolymers for Medical Applications, Kazuaki Matsumura, Robin Rajan, **Sana Ahmed** and Minkle Jain., *CRC Press*, pp 164-181.

Proceeding

1. **Sana Ahmed**, Kazuaki Matsumura, Freezing assisted Protein Delivery by using Polymeric Cryoprotectant. *MRS Proceeding* 2014, Volume *1622*, DOI http://dx.doi.org/10.1557/opl.2014.39

Awards

1. Got a chance to record <u>5 min talk as a reward</u> on the website of Materials Research Society after <u>Nomination for Best Poster in MRS Fall meeting 2013,</u> Boston, USA, December 4th, 2013.

   http://www.prolibraries.com/mrs/?select=session&sessionID=2892

2. **Best Poster Award** in 9th International conference on Fiber and Polymer Biotechnology held in Osaka, Japan on 8th September 2016.

   https://www.jaist.ac.jp/english/whatsnew/awards/2016/09/21-1.html

Acknowledgement

I wish to express by sincere thanks to those who have contributed, supported and made it possible to complete my doctoral thesis dissertation.

Firstly, I would like to express my sincerest gratitude to my supervisor **Assoc. Prof. Kazuaki Matsumura** for his help, guidance and support during my PhD course. I would like to thank him for the kind of freedom he has given me to work and allowing me the opportunity to explore the work in my own way. His patience and constant guidance have made everything smoother and overcome many hurdles during my PhD research. All of achievements during my study would not be possible without his advice and constant support. I am extremely fortunate to have such a great advisor for my PhD. I hope that I have his believe in every aspect of my work; I expect I did respect them all to the best of my ability.

Besides my supervisor, I would like to thank Prof. Kohki Ebitani for his support during my doctoral study. Special thanks to Assoc. Prof. Satoshi Fujita, University of Fukui for his kind help in FACS related experiments. Also, sincere thanks go to my minor research supervisor Assoc. Prof. Tsutomu Hamada, School of Materials Science, JAIST for providing me the opportunity to work in his lab. He was always available whenever I needed to discuss. I would like to extend my thanks to Assist. Prof. Takayoshi Watanabe for his guidance and assistance during gene transformation and electrophoresis experiments. Thanks are also due to Assist. Prof. Takashi Sakamoto and Dr.Shigetaka Nakamura for their technical support in measurement of fluorescence using microplate reader.

Moreover, I would like to express my appreciation to my referees, Prof. Takahiro Hohsaka, Prof.Shinya Maenosono, Assoc. Prof.Tsutomu Hamada and Prof.Yasuhiko Iwasaki for their assistance to complete my thesis.

My appreciation is also extended to all current and former lab members who helped me either directly or indirectly during my research work. Also, their critical comments during our group meetings were of great help.

Finally, I am truly grateful to my parents, whose continuous encouragement and emotional support always kept my sights firmly set on my research. This work would not have been completed without them. So, I would like to dedicate this work to them.